Proceedings of the I·R·E

A Journal of Communications and Electronic Engineering

(Including the WAVES AND ELECTRONS Section)

Collins Radio Company and I.R.E. Cedar Rapids Section

DEVELOPMENT OF DIRECTION-FINDING EQUIPMENT

Novel forms and arrangements appear in long-term engineering studies

March, 1947

Volume 35 Number 3

The Institute of Radio Engineers

THE OPERATION

Induction hardening of 17" five-blade lawn mower reel assemblies at **REO MOTORS INC.**, Lansing, Michigan. Discarded method: 15 per hour. New method: one a minute or 300% gain in production. Problems of scale formation and warpage, formerly costly and unpredictable, now negligible. Additional savings in other departments such as complete assembly of blades, spiders and shaft up to finished grind.

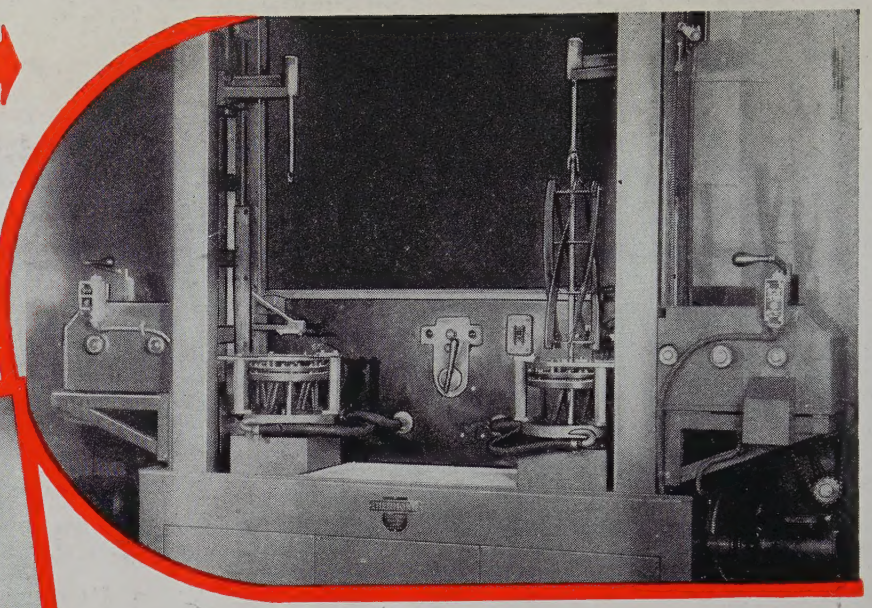

THE EQUIPMENT

Model "1070" **THER-MONIC** high frequency induction generator with an output of 1070 BTU's per minute or approximately 20 KW at a frequency of 375,000 cycles per second. A two-position automatic work table, with simple press-the-button control, speeds the work. All equipment designed and manufactured by **INDUCTION HEATING CORPORATION, NEW YORK 3, N. Y.**

THE AMPEREX TUBES THAT DO THE JOB!

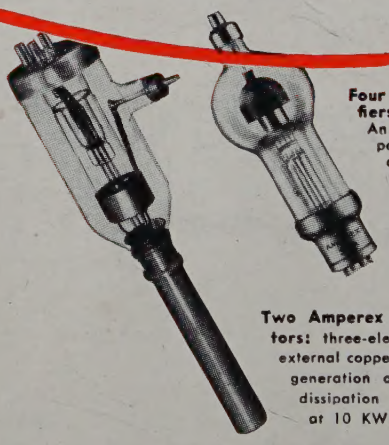

Four Amperex TYPE 575A Rectifiers: Mercury Vapor, High Voltage. An original Amperex contribution particularly noted for reliability and long life. Peak inverse voltage, rating, 15,000; Plate current rating, 1.5 Amps.

Two Amperex TYPE 892 Oscillators: three-electrode, water-cooled external copper anode; standard for generation of HF power. Anode dissipation conservatively rated at 10 KW.

Induction heating may be the answer to your hardening, brazing, melting, forging and annealing problems. In induction heating as in all Industrial, communication, rectification, electro-medical, special purpose and experimental equipment, AMPEREX TUBES are vital for performance, long life and economy. As tube specialists concerned with all electronic developments Amperex engineers are in a position to give detached counsel and information.

Write Amperex Application Engineering Department

POWER TUBE SPECIALISTS SINCE 1925

COMMUNICATION
RECTIFICATION
INDUSTRIAL
ELECTRO-MEDICAL
SPECIAL PURPOSE

AMPEREX

AMPEREX ELECTRONIC CORPORATION

25 WASHINGTON STREET, BROOKLYN 1, N. Y., CABLES: "ARLAB"

In Canada and Newfoundland: ROGERS MAJESTIC LIMITED, 622 Fleet Street West, Toronto 28, Canada

PROCEEDINGS OF THE I.R.E.

(Including the WAVES AND ELECTRONS Section)

Published Monthly by

The Institute of Radio Engineers, Inc.

VOLUME 35 — *March, 1947* — NUMBER 3

PROCEEDINGS OF THE I.R.E.

INSTITUTE NEWS AND RADIO NOTES SECTION

WAVES AND ELECTRONS SECTION

Responsibility for the contents of papers published in the PROCEEDINGS OF THE I.R.E. rests upon the authors. Statements made in papers are not binding on the Institute or its members.

Changes of address (with advance notice of fifteen days) and communications regarding subscriptions and payments should be mailed to the Secretary of the Institute, at 450 Ahnaip St., Menasha, Wisconsin, or 1 East 79 Street, New York 21, N. Y.

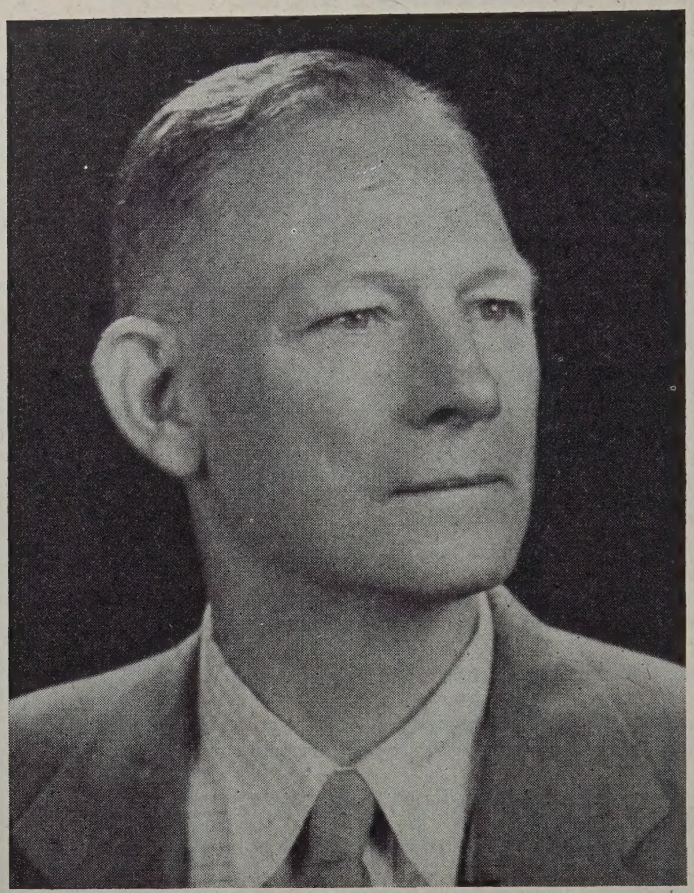

George T. Royden

Board of Directors, 1946

George Taylor Royden was born at an army post, Fort Clark, in Texas on June 20, 1895. As a boy he experimented with electrical devices and constructed several amateur wireless telegraph sets during the years from 1909 to 1917. He attended Stanford University, receiving the B.A. degree in 1917 and the degree of Engineer in 1924.

While employed by the Federal Telegraph Company at Palo Alto, California, in 1916, he assisted with the design of arc transmitters having ratings from 2 to 1000 kilowatts for the Shipping Board and the Navy.

From 1919 until 1925, he worked for the Navy in the radio laboratory at Mare Island Navy Yard with occasional trips to Navy radio stations in San Diego, Hawaii, and Alaska. His assignments included the development of the frequency-measurement technique described in the PROCEEDINGS OF THE I.R.E. for April, 1927.

In 1925, he returned to the Federal Telegraph Company to develop, in the research laboratory of Dr. F. A. Kolster, a radio receiver for operation on alternating current and suitable for reception of broadcast stations.

When the Mackay Radio and Telegraph Company was organized in 1927 to operate Federal's network of radiotelegraph stations serving the principal cities on the Pacific Coast, Mr. Royden became division engineer with offices at San Francisco. He constructed new stations to serve Honolulu and Seattle and installed additional equipment in the stations serving Los Angeles, Portland, and San Francisco.

In 1936 he returned to the Federal Telegraph Company in Newark, N. J. There he was concerned with the engineering development of some radio transmitters for export, several radio-range equipments and a low-frequency telegraph equipment.

In 1946 he transferred to the engineering department of the Mackay Radio and Telegraph Company. A considerable number of patents have been applied for in his name. Those issued are in the fields of radio receivers, direction finders, antennas, modulators, and quartz-crystal-controlled oscillators.

Mr. Royden joined the Institute of Radio Engineers as an Associate in 1919, was transferred to Member in 1927, and elected a Fellow in 1933. He was chairman of the San Francisco Section for the 1933–1934 term. He saw service on the following I.R.E. committees: Admissions 1941 to date, being chairman from 1943 to date; Awards, 1946; Constitution and Laws, 1944; New York Program, 1938–1942; Sections, 1941–1945; and the 1946 Winter Technical Meeting. He is a Member of the American Institute of Electrical Engineers and Sigma Xi.

It is well known that the benefit gained by a group of engineers from a paper presented before them depends not only on the correctness, clarity, and utility of its contents, but also to a considerable extent on its mode of presentation. There is accordingly presented, as a helpful guide to the authors of papers and to those planning technical meetings, the following guest editorial by Mr. A. C. Downes, editorial vice-president of the Society of Motion Picture Engineers, 1941–1946.—*The Editor*

Proper Presentation of Papers Before Technical Meetings

ARTHUR C. DOWNES

It is the purpose of this little editorial to point out the great increase in interest which can be created in any paper by a good presentation to a technical meeting.

Looking back over the many conventions the writer has attended, the papers which are most vividly remembered as those which were presented as though the author were talking to a few friends.

It is true that not every one can present a subject apparently without any notes but proper preparation of an abbreviated version of a paper and notes will enable anyone to give a "good show."

It is of course necessary first to write a good paper, and authors will be wise to consult the very fine article by W. L. Everitt which appeared in the PROCEEDINGS for July, 1946. Too many technical papers are poorly written; this detracts from their value much more than many authors realize.

Most people seem to think that after a paper is written all that is necessary in presenting the subject in a technical meeting is to read the paper word for word, in a soporific monotone, with an occasional interruption to point to some figures or curves on a screen.

It seems probable that the programs of all the technical society conventions for the next few years will be crowded with good material and a presentation such as described above in most cases is boring to a majority of the audience.

Such a presentation ignores the fact that in most audiences only a minority of the attendants will be sufficiently interested in any given subject to listen to a dull reading of the whole paper, but everyone would be interested in an abbreviated version giving the more important facts. The presentation of a well-prepared abbreviated version will not in any degree detract from the value to those in the audience more familiar with the general subject of the paper, since they can study it in detail on publication, and will hold the interest of the entire audience.

If authors will follow this suggestion they will be very much surprised at the greater interest which will be shown when they will talk about their subject rather than read it.

A High-Intensity Source of Long-Wavelength X Rays*

T. H. ROGERS†

It is the policy of The Institute of Radio Engineers to publish in its PROCEEDINGS papers dealing with subject matter in the communications and electronic field, and also in *allied* fields. Wherever theories, techniques, equipment, and applications in such allied fields appear likely to prove useful to communications and electronic engineers, the Institute will accordingly endeavor to make the corresponding material available to its members. The following paper, aside from its intrinsic interest and importance, may well prove helpful to tube engineers and others among the I.R.E. membership.

—*The Editor*

Summary—**Earlier reports on investigations of bactericidal effects and photochemical effects of X rays indicate a need for much higher intensity of radiation for such investigations. This paper discusses the design of an X-ray tube which combines high input energy, the X-ray transparency of beryllium, and close proximity to the target to make available radiation intensities of several million roentgens per minute. An experimental tube which makes such intensities available over a 180-degree solid angle is described. Methods of application to bactericidal and X-ray photochemical research are suggested.**

Introduction

A SURVEY of the 50-year history of the development of the X-ray art reveals that during most of that period the principal advances were made in the field of medicine, with applications in two broad categories, namely, diagnosis and therapy. However, at the present time an important proportion of the X-ray apparatus in existence is devoted to industrial applications.

In comparing industrial and medical applications of X rays, it becomes apparent that by far the greater proportion of industrial applications are "diagnostic" in nature; that is, the discovery of certain information about the internal structure of the material being irradiated is the object of the operation. In many cases, differential absorption, detected by film, fluorescent screen, or ionization device, is utilized to reveal the desired information just as in the case of medical diagnosis. In other cases, the diffraction of the rays into definite patterns, recorded by similar means, provides the information. In both types of cases, the application is one in which the X-ray beam is acted upon by the material involved, and the modifications in the beam are utilized to accomplish the objective. Applications in which the converse effect is utilized, that is, the production of changes in the material by the action of the radiation, as is done in the case of X-ray therapy in the medical field, are strikingly few in the industrial field. In view of the penetrating power and energy of X rays, one is prompted to inquire into the reasons for this lack of development of industrial processes utilizing the power of X rays to modify materials.

Possible applications in this catetory which immediately suggest themselves are bactericidal (for sterilization of food products, etc.), and photochemical. A great number of experiments[1-3] on bactericidal properties of X rays have been made which show logarithmic death rates for very large doses. The dosages required for complete sterilization are so large as to seem to preclude utilization of the method on an industrial basis.

The photochemical reactions produced by X rays have received little study up to this time. Clark[4] enumerates those few cases of such chemical action which have been discovered by various workers. With the well-known exception of the action on silver halides in the photographic emulsion, all such reactions have occurred in extremely minute quantities, and have pointed to the need for much greater intensities of radiation for worth-while experimentation.[5]

Hence, it seems evident that the sparseness of investigations into the field of industrial "therapy" has not been due to a lack of interest but to physical limitations on the intensity of radiation obtainable from available sources of X radiation. The obvious possibilities for further investigation into this field, provided a greatly intensified X ray source could be made available, have led to an investigation of the possibility of the development of such a source as described below.

Factors Affecting X-ray Output

The principal factors which affect the intensity of the X-ray beam issuing from an X-ray tube are: (1) target material; (2) anode voltage; (3) anode current;

* Decimal classification: 621.327.7. Original manuscript received by the Institute, April 16, 1946; revised manuscript received, September 17, 1946.

† Machlett Laboratories, Incorporated, Springdale, Connecticut.

[1] G. T. Lyon, letters to the London *Lancet*, January 29, 1896, and February 17, 1896

[2] G. L. Clark, "Applied X-rays," third edition, pp. 199–200, McGraw-Hill Book Co., New York, N. Y.; 1940.

[3] R. W. G. Wycoff, "The killing of certain bacteria by X-rays," *Jour. Exp. Med.*, vol. 52, pp. 435–446; September, 1930.

[4] G. L. Clark, "Applied X-rays," third edition, pp. 185–197, McGraw-Hill Book Co., New York, N. Y.; 1940.

[5] W. Stenstrom and I. Vigness, "Some effects of radiation on oil," *Amer. Jour. Roent.*, vol. 40, pp. 427–433; September, 1938.

(4) absorption by intervening material; and (5) distance from focal spot to point of utilization.

The manner in which intensity of the emitted radiation varies with the first three factors is given by the formula:[6]

$$\frac{\text{X-ray energy}}{\text{cathode-ray energy}} = kZV,$$

where

k = an experimentally determined constant
Z = atomic number of target material
V = anode voltage.

Tungsten is the target material usually chosen when intensity is the determining factor because of its relatively high atomic number and its thermal and mechanical properties which permit the highest value of cathode-ray energy of any material. For a constant amount of cathode-ray energy, the X-ray intensity is proportional to the anode voltage. The practical limit on voltage in a tube designed for such applications will be determined by many considerations, including complexity of apparatus, desired wavelength characteristics, etc., which are to be discussed in more detail in this paper. The maximum voltage range considered in this paper is below the value of 70 kilovolts, in which range absorption of the radiation is largely by photoelectron production, on which the photochemical effect depends. The intensity is, of course, proportional to the anode current, all other factors remaining unchanged, and the design of a tube for high intensity radiation should provide for the use of as high a value of anode current as possible.

The effect of the factor of "inherent filtration" of the tube, that is, the absorption of a portion of the X-ray energy by the material composing the tube wall at the point of egress, on the issuing beam is next to be considered. In order to evaluate this effect thoroughly, it is necessary first to consider the wave length distribution of the energy in the beam. The X radiation consists of a continuous spectrum of wavelengths extending from the minimum wavelength defined by the relation $\lambda_0 = (12.354/V_0)$ where V_0 is the anode voltage, rising rapidly to a maximum intensity value at a point near $\lambda = 3/2\,\lambda_0$, then gradually decreasing in intensity with increasing wavelength. Superposed on this continuous spectrum are the characteristic lines of the target material if the anode voltage is sufficient to excite the characteristic radiation. These lines, being very narrow, contribute little to the total energy and for the purpose of this discussion may be disregarded. The general form of the energy-wavelength distribution is illustrated by the familiar curves published by Ulrey[7] (Fig. 1), based on intensity measurements of radiation given off by a tungsten target tube, after separation into various

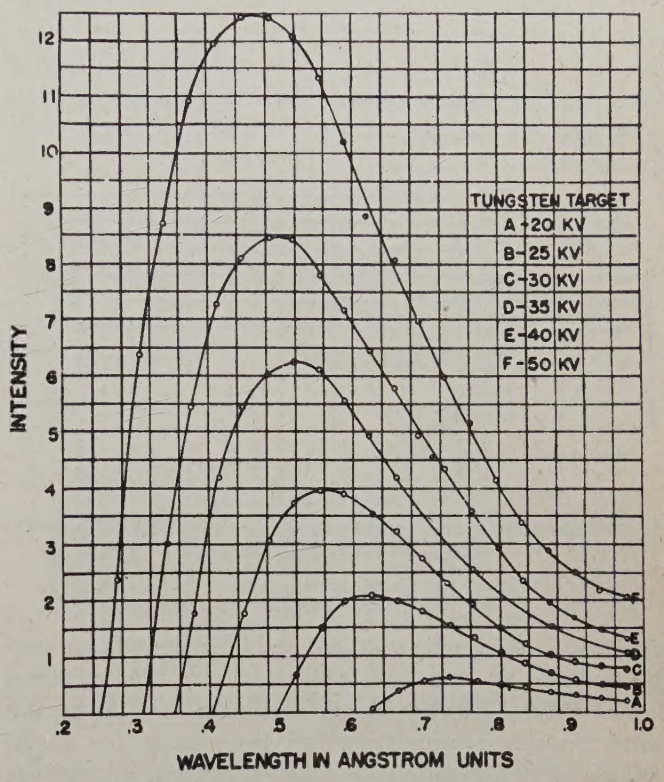

Fig. 1—Intensity versus wavelength relationship of X radiation from tungsten target, after filtration through glass tube wall, measured by ionization effect; wavelength separation by calcite crystal spectrometer.

wavelength components by means of a calcite crystal spectrometer. However, these curves do not accurately represent the true energy-wavelength relationships of the radiation emitted by the target, for reasons which will be apparent from the following discussions.

Inasmuch as the different wavelength components are absorbed to different extents, the inherent filtration of the tube will not only reduce the total energy in the X-ray beam as emitted by the target, but also change the energy-wavelength distribution. In the design of a tube for maximum photochemical effect, it is necessary to consider the wavelength of the radiation as well as its total intensity, since the photochemical effect depends on the amount of ionization produced, which in turn depends on the amount of energy *absorbed* in the material treated. The proportion of the total energy absorbed is very definitely dependent on the wavelength. In this connection it should be pointed out that the usual measure of X-ray intensity, the *roentgen*,[8] is based not on the actual energy in the beam but on its power to ionize air. Hence, in consideration of intensities, it will in many cases be pertinent to the

[6] A. H. Compton and S. K. Allison, "X-Rays in Theory and Experiment," second edition, pp. 89–90, D. Van Nostrand, New York, N. Y.; 1935.

[7] C. T. Ulrey, "An experimental investigation of the energy in the continuous X-ray spectra of certain elements," *Phys. Rev.*, vol. 11, pp. 401–410; May, 1918.

[8] The *roentgen* is defined as the quantity of X radiation such that the associated corpuscular emission per 0.001293 gram of air products, in air, ions carrying 1 electrostatic unit of quantity of electricity of either sign.

problem at hand to convert energy relationships into terms of roentgens.

In order to ascertain the effect of any given inherent filter on the radiation output of a tube, it is necessary to know the energy-wavelength distribution of the radiation, as it originates at the target, before any filtration whatever has taken place. This distribution can be computed by means of the formula, derived from Kramer's law[9–11]

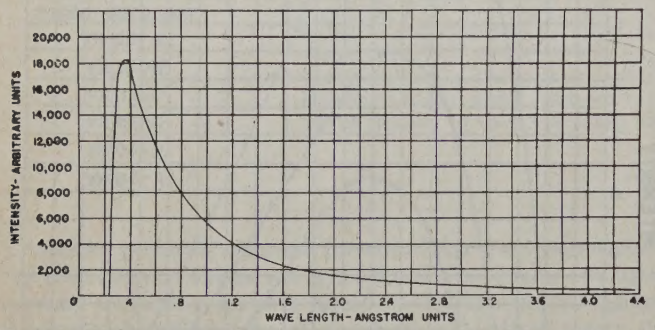

Fig. 2—Calculated energy versus wavelength distribution of X radiation at 50 kilovolts unfiltered.

$$I_\lambda \propto V^2(V_0 - V)d\lambda$$

where V_0 is the anode voltage, and V is the voltage corresponding to the wavelength λ in the relation $V=12.354/\lambda$, V being in kilovolts and λ in Angstrom units. Such a computation has been made for anode voltage of 50 kilovolts (see Table I, column 3), and the resulting distribution is plotted in Fig. 2.

portional to the mass absorption coefficient of air at that wavelength. This coefficient for any given wavelength can be computed from the published[12] values for oxygen and nitrogen. The energy distribution of Fig. 2 can be converted into an intensity-wavelength relationship in which the intensity is in terms of ionizing power, by applying this coefficient to the energy value corresponding to each wavelength (see Table I, column

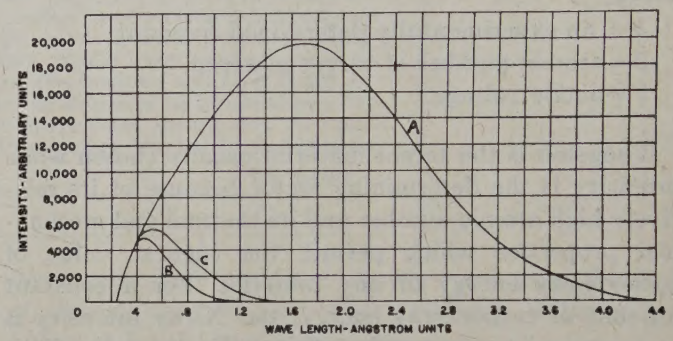

Fig. 3—Calculated intensity versus wavelength distribution of X radiation at 50 kilovolts, intensity expressed in terms of ionizing power: A. filtered by 1-millimeter beryllium; B. filtered by 1-millimeter aluminum; C. filtered by 1 millimeter Pyrex glass.

5). It is, of course, understood that this ionizing power refers to air, and is proportional to the intensity in terms of roentgens per unit of time. The ionizing power for other substances would be proportional to their respective mass absorption coefficients.

The values calculated thus far have taken into account no inherent filtration whatever. Tubes are commonly built with an envelope of Pyrex glass, and a 50-kilovolt tube of this kind, designed for good mechanical and electrical ruggedness, would present a thickness in the order of 1 millimeter to the passage of the X-ray beam. Another possibility for the window would be aluminum. Undoubtedly, however, the least-absorbing window material that could be employed would be beryllium, provided a sufficiently large window could

TABLE I

1 λ	2 V	3 $V^2(V_0-V)$	4 μ/ρ air	5 3×4	6 $\mu(Be)$	7 I(Be)	8 μ(Al)	9 I(Al)	10 μ(PG)	11 I(PG)
0.2475	50.0	00000								
0.417	29.6	17322	0.358	6201	0.340	5999	3.16	4713	1.95	5030
0.631	19.5	11597	0.796	9200	0.469	8770	10.1	3376	5.56	5276.2
0.880	14.0	7056	1.95	13740	0.782	12490	26.3	989	14.4	3255.0
1.00	12.35	5742	2.76	15849	1.012	14330	38.1	355	20.8	1974.8
1.235	10.0	4000	5.12	20452	1.748	17139	71.0	16	37.8	466.3
1.539	8.0	2688	9.68	26000	2.944	19400	132.0	00	72.0	19.5
1.93	6.39	1781	18.65	33200	5.612	18940			135.2	0.03
2.50	4.9	1083	39.53	42800	12.21	12626			278.0	000
3.03	4.0	736	73.9	54300	21.5	6353.1				
3.59	3.4	539	123.1	66300	33.8	2254.2				
4.15	2.9	396	162.5	64300	51.8	360				
4.36	2.8	370	187.8	69400	60.8	163				
5.17	2.38	269	306.14	82300	101.0	3.7				
5.39	2.28	248	350.6	86900	114.0	1.0				
6.97	1.77	151	723.1	109200	276.0	00000				

[9] H. A. Kramers, "On the theory of X-ray absorption and of the continuous X-ray spectrum," *Phil. Mag.*, vol. xlvi, pp. 836–871; November, 1923.

[10] L. Silberstein, "Synthesis of X-ray filtration curves from Kramers' emission law," *Phil. Mag.*, vol. xix, pp. 1042–1054; May, 1935.

[11] G. W. S. Kaye and W. Binks, "The emission and transmission of X and gamma radiation," *Brit. Jour. Rad.*, vol. xiii, pp. 193–212; June, 1940.

[12] "Handbook of Chemistry and Physics," 28th edition, pp. 1925, Chemical Rubber Publishing Co., Cleveland, Ohio; January, 1944.

be constructed of this rather hard-to-fabricate material. The process of rolling thin, vacuum-tight sheets of substantially pure beryllium described by Claussen and Skehan[13] does make possible such windows in a thickness of 1 millimeter or less.[14]

In order to make a comparison among Pyrex glass, aluminum, and beryllium as window materials, from the standpoint of reduction in intensity of the radiation output, the reduced intensity after filtration by a thickness of 1 millimeter of each of these materials is calculated for each incremental value of λ (see Table I, columns 7, 9, and 11). This calculation is made by applying the formula $I = I_0 e^{-\mu x}$ to the values previously obtained for the unfiltered condition, μ being the linear absorption coefficient for each material, respectively, at each value of λ.

These intensity-wavelength distributions are plotted in Fig. 3. By integrating the area under each of the three curves, the total intensity for each kind of window is obtained. The comparative figures, in percentages, are:

Beryllium	100.0 per cent
Pyrex glass	7.9 per cent
Aluminum	4.9 per cent

These figures indicate that the use of beryllium for the window becomes a major factor in the design of our high-intensity X-ray source.

Referring back to our listing of the factors affecting the intensity of the X-ray beam, we find that the distance from the focal spot, or point of generation, to the point of utilization is, of course, a very important factor, since the intensity varies inversely as the square of this distance. A tube design which permits the material to be treated to be placed as near as possible to the focal spot thus provides maximum intensity, other factors being equal. This end can be most readily achieved likewise by employing beryllium as the window material, for it is a relatively good electrical and heat conductor, permitting the window to be positioned very close to the focal spot without becoming overheated or electrically charged, and is mechanically strong and resistant to chemical action, so that a wide variety of materials may be brought directly adjacent to it without danger of mechanical injury or corrosion.

Design of Tube for High Output

Beryllium-window tubes have been described heretofore[15,16] in which the low absorption factor and the proximity to the focal spot have been utilized to provide a maximum intensity of characteristic radiation from a special target material for X-ray diffraction work, for example. These tubes have been provided with very small-diameter windows, admitting only a narrow pencil of radiation, which is entirely suitable for diffraction analysis. For photochemical experiments or processes, however, it is desirable to irradiate as large an area as possible, so as to increase the volume of reaction accomplished. The Machlett AEG-50 tube, originally designed for low-voltage radiography, provides, in addition to the beryllium window and a distance of only 2 centimeters from focal spot to window, a cone of radiation including a 40-degree solid angle, which represents a covered area more than ten times that covered by the 12-degree cone issuing from the diffraction tubes mentioned above. A tube of this type, shown schematically in Fig. 4, was employed for the purpose of making

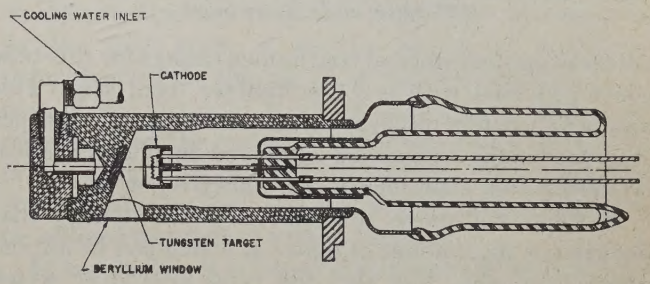

Fig. 4—Schematic view (in section) of beryllium-window tube with 40-degree solid-angle X-ray beam.

quantitative determinations of the intensity of the radiation issuing therefrom. Results of these determinations are given in Table II.

The values given in Table II are based on measurements made by Braestrup,[17] employing the type of ionization chamber described by Taylor and Stoneburner[18] for the measurement of low-voltage X-ray intensities. The tube was operated with a constant-potential anode voltage of 50 kilovolts and both anode and filament voltages were carefully stabilized throughout the measurements. The measurements were made at a distance of 10 centimeters from the target; the intensity at the outer surface of the window, 2 centimeters from the focal spot, was obtained by applying the inverse-square

Table II
Measurements of X-ray Output Intensity from EG-50 Tube

Kilovolts (C.P.)	Distance from Target	Added Filter	Roentgens per minute per milliampere	Per cent transmission	HVL millimeters Al
50	10 centimeters	0	1555	100	0.07
50	10 centimeters	0.05 millimeter Al	903	58	0.09
50	10 centimeters	0.1 millimeter Al	605	39	0.11
50	10 centimeters	0.5 millimeter Al	104	6.7	0.55
50	10 centimeters	1.0 millimeter Al	53	3.4	0.94
50	10 centimeters	2.0 millimeter Al	25.7	1.65	1.50
50	10 centimeters	3.0 millimeter Al	16.1	1.03	1.71
50	10 centimeters	5.0 millimeter Al	7.2	0.46	
50	10 centimeters	0.5 millimeter Be		71.0	
50	10 centimeters	1.0 millimeter Be		52.0	
50	10 centimeters	2.0 millimeter Be		32.5	
50	2 centimeters	0	46,600		

[13] G. E. Claussen and J. W. Skehan, "Malleable beryllium," *Metals and Alloys*, vol. 15, pp. 599–603; April, 1942.

[14] Tubes with low-absorption windows of Lindeman glass, aluminum foil, glass "bubbles," even cellophane, have been built, but such windows are very small and of such fragility as to be impractical for industrial applications as contemplated.

[15] R. R. Machlett, "An improved X-ray tube for diffraction analysis," *Jour. Appl. Phys.*, vol. 13, pp. 398–401; June, 1942.

[16] Z. J. Atlee, "Beryllium windows," *Gen. Elec. Rev.*, vol. 46, pp. 233–236; April, 1943.

[17] C. B. Braestrup, New York City, unpublished private communication to the author.

[18] L. S. Taylor and C. F. Stoneburner, "The measurement of low voltage X-ray intensities," *Bur. Stand. Jour. Res.* (RP 505), vol. 9, pp. 769–780; December, 1932.

laws and a correction factor to compensate for absorption in the intervening air space. A tube current of 2 milliamperes was used; values in the table are expressed in terms of roentgens per minute per milliampere.

These measurements indicate an intensity of 2,330,000 roentgens per minute at a distance of 2 centimeters from the center of the focal spot, when the tube is operated at 50 kilovolts, and 50 milliamperes, which

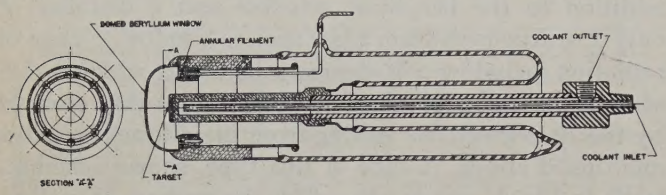

Fig. 5—Schematic view (in section) of beryllium-window tube with 180-degree-angle X-ray beam.

values constitute normal continuous ratings for this tube when provided with a 5.0-millimeter focal spot. This number of roentgens per minute is several hundred times as great as the intensities employed in photochemical or sterilization experiments previously reported.

As suggested above, it is not only the intensity that determines the amount of material which can be altered photochemically, but also the total area over which such intensity is effective. The area covered at any given

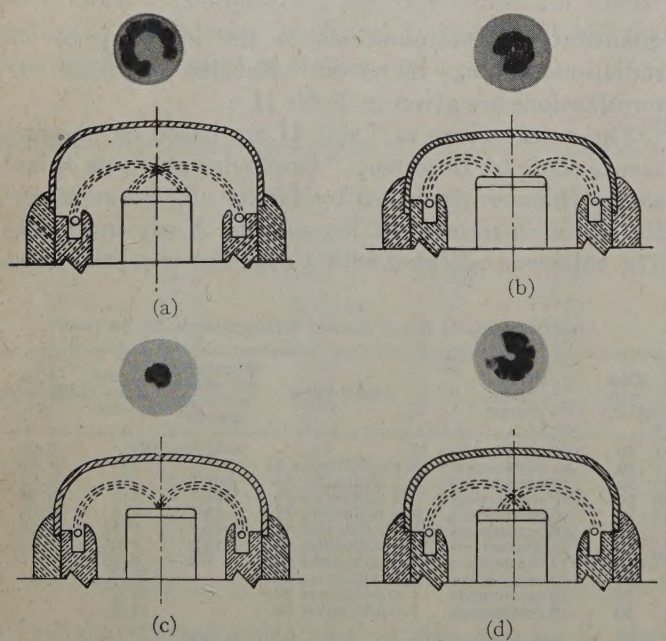

Fig. 6—Diagrams of focusing obtained with domed window tube at various positions of the windows with reference to the anode. (Actual pin-hole focalgrams compared with schematic diagrams of electron trajectories.) (a) Maximum spacing produces "ring" focus. (b) Somewhat closer spacing produces circular focus of large size. (c) Spacing adjusted to produce minimum-size focus. (d) Still closer spacing again results in a "ring" focus.

distance is approximately proportional to the square of the solid angle included by the cone of radiation. At anode voltages in the order of 50 kilovolts or less, the radiation issues from the target with substantially uniform intensity throughout the 180-degree solid angle subtended by the target face. In the case of beryllium-window tubes described heretofore, the cone of radiation has been limited to a very much smaller extent by the size of the window. More than one such window has been provided in some tubes, but even then only a small fraction of the total radiation has been utilized.

The desire to make the entire 180-degree solid angle of radiation available for such applications has led to the invention of a new type of X-ray tube, employing an entirely new principle of focusing the electron stream on the target, so that the cathode structure is entirely out-

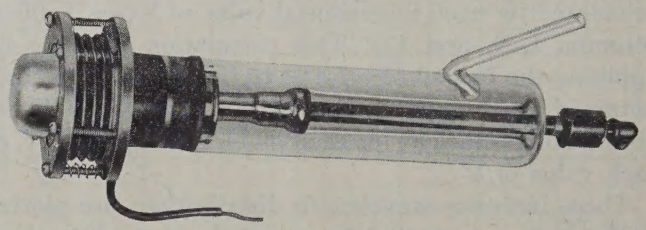

Fig. 7—Photograph of experimental tube with domed window permitting 180-degree solid-angle X-ray beam.

side the hemisphere subtended by the target face and thus does not eclipse any part of the radiation generated. The structure of this tube is shown diagramatically in Fig. 5. The window is in the form of a generally hemispherical dome into which the anode protrudes with the target face parallel to the base of the hemisphere. The cathode consists of an incandescent filament of annular form surrounding the anode, and located within the

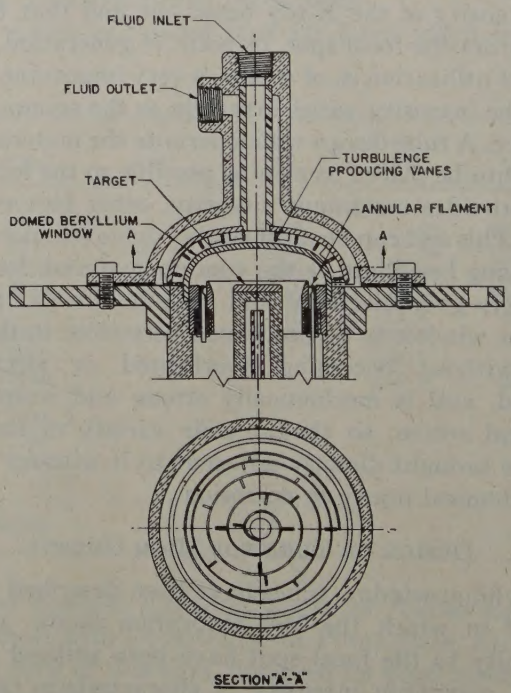

Fig. 8—Arrangement for uniform X-ray treatment of fluids, applied to cone-window tube.

dome in a plane below the plane of the target face so that it does not cast a shadow in the hemisphere of radiation. The dome is at cathode potential, and the resultant electric field in the space between dome and anode is such that the electrons from the filament describe trajectories which terminate on the face of the target, approximately as indicated in Fig. 6. Such a

dome can be formed of the malleable beryllium referred to above.[13]

Such a tube has been constructed experimentally at Machlett Laboratories, in which a dome 2 inches in diameter was employed. The cathode and dome were operated at ground potential; the anode, being at high positive potential, was cooled by water circulating through a long column of insulating plastic tubing. The tube was operated at a maximum load of 100 milliamperes at 60 kilovolts. On the basis of the intensity measurements made on the AEG-50 tube described above, it is estimated that the intensity would be approximately 5 million roentgens per minute, over an area of approximately 25 square centimeters.

This experimental tube (pictured in Fig. 7) was made with the position of the dome adjustable with respect to the target, by means of being mounted on a metal bellows. The effects of various positions on the focusing of electrons on the target are shown by the pinhole photographs of the focal spots reproduced in Fig. 6. The diagrams adjacent to each focalgram show the probable electron trajectories in each case.

In a tube of this sort, the window is not subject to electron bombardment, by either primary or secondary electrons, since it is at cathode potential. Hence, the problem of cooling the window does not arise as in the case of a window at anode potential, which receives considerable bombardment by secondary electrons if located near the focal spot.

In the processing of materials by X-ray treatment with such tubes, an arrangement to permit continuous processing at any required rate would, of course, be desirable. For materials which are in gaseous or fluid form, or can be reduced to such a form, the dome-shaped window lends itself readily to an arrangement in which the fluid is fed in through a pipe to the center of the window and then caused to spread uniformly over the dome in a film of controllable thickness by a hemispherical baffle conforming to the contour of the window with the required spacing therefrom. The treated material returns through an outer pipe concentric with the incoming one. The optimum thickness of film would depend on the coefficient of absorption of the material and the necessary degree of uniformity of treatment of the entire body of the material. The layer of the film adjacent to the window would receive more intense treatment than layers farther away, due to absorption by the first layer. A greater degree of uniformity throughout with thicker films can be obtained if the flow of the material is accompanied by a turbulence which causes the material to become thoroughly intermixed during its passage through the treatment field. An arrangement such as that illustrated by Fig. 8 can be utilized to produce such turbulence.

In conclusion, it is hoped that the availability of these sources of X radiation of utilizable ionizing power several hundred times more intense than those heretofore available will lead to more thorough investigations into this promising field of physical, chemical, and biological research.

The Maximum Efficiency of Reflex-Klystron Oscillators*

ERNEST G. LINDER†, ASSOCIATE, I.R.E. AND ROBERT L. SPROULL*

Summary—**The theory of reflex-klystron oscillators is given in detail. It includes a discussion of relations in a loaded oscillator. It is shown that maximum efficiency for small amplitudes is given by**

$$\eta_0 = 0.169 M^2 i_1 / G_e V_0,$$

where M is the coefficient of modulation of the gap, i_1 is the effective current, G_e is the shunt conductance of the unloaded resonator, and V_0 is the beam voltage. Possibilities of increasing efficiency are considered, including effects of grid transmission on effective current and on space charge, and effects of multiple electron transits.

THE THEORY presented in this paper is based mainly on the previous investigation of D. L. Webster,[1] but it embodies considerable modification and extension of his original treatment. The work was done several years ago but could not previously be made public because of wartime secrecy restrictions. The theory is a small-amplitude one, that is, the oscillatory voltage is assumed small in comparison with the steady voltages. This assumption is most applicable in the case of short wavelengths, such as below 10 centimeters, since there the efficiencies are seldom greater than a few per cent.

* Decimal classification: R355.912.3. Original manuscript received by the Institute, April 5, 1946; revised manuscript received, August 21, 1946.

† RCA Laboratories Division, Radio Corporation of America, Princeton, N. J.

[1] D. L. Webster, "Cathode-ray bunching," *Jour. Appl. Phys.*, vol. 10, pp. 501–508; July, 1939.

I. Energy Relations

The essential phenomenon in bunching in klystrons is that an electron beam, initially uniform with respect to velocity and charge distribution, is velocity modulated; so that, after an interval during which the beam travels in a drift space, the charge distribution in the beam is no longer uniform, and hence the beam contains components of alternating current.

The expression for this current is

$$i_2 = -i_1\left[1 + 2\sum_0^\infty J_n(nr)\cos n\left(\omega t_2 - \theta - \frac{\pi}{2}\right)\right]. \quad (1)$$

The term containing the fundamental frequency ω is

$$i = -2i_1 J_1(r) \cos\left(\omega t_2 - \theta - \frac{\pi}{2}\right). \quad (2)$$

Here i_1 is the value of the current during the first passage of the beam through the gap at time t_1, and i_2 is its value during the second passage at time t_2. $J_n(nr)$ is the Bessell function of order n. The quantity r is called the bunching parameter and is given by $r = \theta M V_m / 2V_0$, where θ is the transit angle of the bunch centers between the first and second transits, M is the coefficient of modulation of the gap, V_m is the amplitude of the oscillatory voltage, and V_0 is the beam voltage.

These expressions were originally derived by D. L. Webster[1] for the case of the two-cavity, single-transit klystron. It can be shown[2] that they are unaltered for the reflex case, except for a change of sign due to the reversal of the current.

In the present treatment the phase angle $\pi/2$ also is introduced to represent a phase shift inherent in the bunching process. This occurs since bunches form about those electrons traversing the gap when the voltage is zero and changing from accelerating to decelerating.[3] Thus the current maxima (bunch centers) are formed out of phase by angle of $\pi/2$ with respect to the voltage maxima. The gap voltage corresponding to the current given by (2) is

$$V = V_m \cos \omega t_2,$$

and the total phase angle between current and voltage is therefore $\theta + (\pi/2)$.

From (1) it is seen that the current resulting from the bunching process contains components of direct current, and alternating currents of the fundamental frequency and all harmonics. To obtain an expression for the power derivable from such a beam, consider its passage across a gap or between grids across which there is the voltage $V_m \cos \omega t_2$. The energy absorbed from the beam during one cycle will then be given by the integral of the product of the instantaneous current and the effective voltage which acts upon the beam during its passage. Thus the energy is

$$W' = -\int_0^{2\pi/\omega} i_2 M V_m \cos \omega t_2 dt. \quad (3)$$

In this integration, all terms will vanish except the one containing the frequency ω.

Hence,

$$W' = 2i_1 M V_m J_1(r) \int_0^{2\pi/\omega} \cos\left(\omega t_2 - \theta - \frac{\pi}{2}\right) \cos \omega t_2 dt$$

$$= \frac{2\pi}{\omega} i_1 M V_m J_1(r) \cos\left(\theta + \frac{\pi}{2}\right).$$

Thus the energy absorbed per second, or the power, will be

$$W = \frac{\omega}{2\pi} W' = i_1 M V_m J_1(r) \cos\left(\theta + \frac{\pi}{2}\right). \quad (4)$$

This is a maximum for

$$\theta + \frac{\pi}{2} = 2m\pi$$

or

$$\theta = 2\pi(m - \tfrac{1}{4})$$

where m is any positive integer. Each integer corresponds to a mode of oscillation.

These values of θ giving maximum power correspond to the passage of the bunch center through the grids when the field has its maximum retarding effect. It is convenient to use the angle.

$$\gamma = \theta - 2\pi(m - \tfrac{1}{4}), \quad (5)$$

which indicates the departure from the power maximum or from a mode center. In terms of this

$$i = -2i_1 J_1(r) \cos(\omega t_2 - \gamma), \quad (6)$$

and

$$W = i_1 M V_m J_1(r) \cos \gamma. \quad (7)$$

The voltage between the grids may now be determined by considering that, if the shunt resistance between them is R, then

$$V_m^2 = 2RP,$$

or from (7), putting $\cos \gamma = 1$ to get the amplitude,

$$V_m^2 = 2Ri_1 M V_m J_1(r), \quad \text{or}$$

$$V_m = 2Ri_1 M J_1(r). \quad (8)$$

The factor M which occurs above, and which will be frequently used also in what follows, may be defined by the expression

$$M = \frac{V_m \text{ (effective)}}{V_m}.$$

An equivalent definition is

$$M = \frac{P}{eV_m},$$

where P is the actual maximum energy lost by an electron in traversing the gap. It would be equal to unity only in the case of an ideal gridded gap and zero transit time. It is a function of the variation of the field across the gap, but here it will be computed only for the case of parallel plane grids of sufficiently fine mesh so that the field may be considered uniform in intensity and normal to the grids at all points. The voltage across the gap is then given by $V_m \cos(\omega t_2 + \gamma)$.

The energy transferred to an electron traversing the gap is

$$P = \int_0^\tau F ds,$$

where τ is the transit time, F the force, and s the position co-ordinate.

[1] E. L. Gintzon, and A. E. Harrison, "Reflex-klystron oscillators," Proc. I.R.E, vol. 34, pp. 97–113; March, 1946.

[2] For discussions of the bunching process see also D. M. Tombs, "Velocity-modulated beams," *Wireless Eng.*, vol. 17, pp. 55–60; February, 1940; and L. J. Black and P. L. Morton, "Current and power in velocity-modulated tubes," Proc. I.R.E., vol. 32, pp. 477–482; August, 1944.

Therefore,

$$P = e\int_0^\tau E\frac{ds}{dt_2}dt_2$$

$$= e\int_0^\tau \frac{V_m}{d}\cos(\omega t_2+\gamma)\frac{ds}{dt_2}dt_2,$$

where E is the field and d the gap spacing.

Because of the assumption of small field, i.e., $V_m \ll V_0$, the velocity ds/dt_2 may be taken as constant and equal to v_0, the entrance velocity. Thus,

$$P = \frac{ev_0V_m}{d} = \int_0^\tau \cos(\omega t_2+\gamma)dt_2$$

$$\frac{P}{eV_m} = \frac{1}{\tau}\int_0^\tau \cos(\omega t_2+\gamma)dt_2$$

$$= \frac{1}{\omega\tau}[\sin(\omega\tau+\gamma)-\sin\gamma]$$

$$= \frac{2}{\omega\tau}\cos\left(\frac{\omega\tau+2\gamma}{2}\right)\sin\frac{\omega\tau}{2}.$$

Therefore,

$$\frac{P}{eV_m} = \frac{2}{\omega\tau}\cos\left(\frac{\omega\tau+2\gamma}{2}\right)\sin\frac{\omega\tau}{2}.$$

The maximum value of this gives M, and evidently occurs when

$$\frac{\omega\tau+2\gamma}{2} = 2n\pi, \quad \text{or} \quad \gamma = 2n\pi - \frac{\omega\tau}{2}.$$

Hence

$$M = \frac{2}{\omega\tau}\sin\frac{\omega\tau}{2}. \tag{9}$$

II. Efficiency of a Loaded Oscillator

The power given by (7) represents the total amount available from the beam. However, this cannot all be exploited in a useful load, except for the hypothetical case in which the oscillator circuit, e.g., cavity resonator, is totally loss-free, so that it has infinite shunt resistance. In general, the power in the load may be determined as follows. The loaded resonator circuit is represented by a lumped-constant circuit in which the capacitance and inductance of the cavity, denoted by C and L, are in parallel. These are shunted by the unloaded shunt resistance[4] R_C, and also by the resistance of the load as reflected across the resonator gap, denoted by R_L.

Hence the total shunt resistance R of the circuit or the gap due to both the load and the cavity losses is given by

$$\frac{1}{R} = \frac{1}{R_C}+\frac{1}{R_L},$$

or in terms of the respective conductances

$$G = G_C + G_L. \tag{10}$$

[4] For methods of measuring R_C see R. L. Sproull and E. G. Linder, "Resonant-cavity measurements," Proc. I.R.E., vol. 34, pp. 305–312; May, 1946.

In the following, resistances and conductances will be used interchangeably to facilitate simplification of equation writing.

The power dissipated in the load is

$$W_L = \tfrac{1}{2}G_L{V_m}^2, \tag{11}$$

and that dissipated in the cavity is

$$W_C = \tfrac{1}{2}G_C{V_m}^2. \tag{12}$$

By use of (10), (11) may be written

$$W_L = \frac{G_L{V_m}^2}{2} = \frac{{V_m}^2}{2}(G-G_C), \tag{13}$$

and by use of (8)

$$\eta = \frac{W_L}{V_0 i_1} = \frac{1}{V_0}\left[MV_mJ_1(\theta MV_m/2V_0) - \frac{G_C{V_m}^2}{2i_1}\right]. \tag{14}$$

In this expression the first term represents the contribution due to the total energy delivered by the beam to the oscillating circuit. The second term represents the effect of the losses in the cavity.

From (14) the condition for the start of oscillation may be simply derived, since it corresponds to $\eta=0$. Thus

$$MV_mJ_1(\theta MV_m/2V_0) = \frac{G_C{V_m}^2}{2i_1}.$$

But since the amplitude of oscillation is infinitesimal at the inception of oscillation, the Bessell function may be replaced by an approximation valid for small arguments. Thus

$$J_1(\theta MV_m/2V_0) = \frac{\theta MV_m}{4V_0}$$

and

$$\frac{\theta M^2{V_m}^2}{4V_0} = \frac{G_C{V_m}^2}{2i_1}$$

or

$$\beta \equiv \frac{\theta M^2 i_1}{2G_CV_0} = 1. \tag{15}$$

This defines β and gives the lowest value for which oscillations may occur. The value $\beta=1$ corresponds to no loading of the cavity, i.e., $G_L=0$. This is evident from (14), since the two right-hand terms represent the total power generated and the power dissipated in the cavity, respectively. If these are equal, then no power can be supplied to a useful load. The starting condition for a loaded cavity will require $\beta>1$, its actual value depending upon the value of G_L.

To derive the conditions for maximum efficiency, consider that with a given oscillator for which V_0, ω, M, G_C, and i_1 are fixed, the efficiency may be varied by changing θ and V_m. The drift angle θ may be varied by altering the reflector voltage V_R. The quantity V_m is affected by varying the load resistance. Hence, to find the maximum efficiency obtainable from a given tube, it is necessary to maximize with respect to both of these two independent variables θ and V_m. Take first,

$$\frac{\partial \eta}{\partial \theta} = \frac{MV_m}{V_0} J_1'\left(\frac{\theta MV_m}{2V_0}\right)\frac{MV_m}{2V_0} = 0,$$

i.e.,

$$J_1'\left(\frac{\theta MV_m}{2V_0}\right) = J_1'(r) = 0, \tag{16}$$

or

$$r_0 = 1.84, \quad \text{and} \quad J_1(r_0) = 0.582. \tag{17}$$

This condition makes $J_1(r)$ a maximum, and hence means that the bunching is such that the alternating component of frequency ω of the beam has its greatest value.

Now maximize with respect to V_m, i.e.,

$$\frac{\partial \eta}{\partial V_m} = \frac{1}{V_0}\left[MV_m J_1'\left(\frac{\theta MV_m}{2V_0}\right)\frac{\theta M}{2V_0} + MJ_1\left(\frac{\theta MV_m}{2V_0}\right) - \frac{G_C V_m}{i_1}\right] = 0$$

or

$$rJ_1'(r) + J_1(r) = \frac{G_C V_m}{Mi_1},$$

or, since

$$J_1'(r_0) = 0,$$

$$J_1(r_0) = \frac{G_C V_m}{Mi_1}. \tag{18}$$

Since, from the theory of Bessell functions,

$$rJ_1'(r) + J_1(r) = rJ_0(r), \tag{19}$$

this condition may be written,

$$J_0(r) = \frac{2G_C V_0}{\theta M^2 i_1} \equiv \frac{1}{\beta}. \tag{20}$$

Since, with a given tube, V_m is a function of the loading, (20) is the condition for optimum loading. That this condition represents a maximum, and not a minimum or a point of inflection, may be shown by investigating the usual conditions involving second-order derivatives. It should be noted that (18) holds only when η is maximized with respect to both θ and V_m, whereas (20) requires only maximization with respect to V_m and hence is valid for all values of r.

The meaning in terms of load conductance of the maximization with respect to V_m may be seen from the following. The general expression for the voltage across the cavity is given by (8). Apply to this the condition for maximum efficiency (18). This gives

$$V_m = \frac{2i_1 MG_C V_m}{GMi_1},$$

from which

$$G = 2G_C.$$

or

$$G_L = G_C. \tag{21}$$

This indicates that equal amounts of power are dissipated in the oscillator resonator and in the load.

It is now possible to derive an expression for the maximum efficiency with respect to both θ and V_m. Let the two conditions for maxima, (16) and (20), be solved simultaneously, giving

$$J_0(1.84) = \frac{1}{\beta_0}, \tag{22}$$

or

$$\beta_0 = 3.17.$$

Then the maximum efficiency for a given tube is obtained by rewriting (14),

$$\eta = \frac{M^2 i_1}{G_C V_0}\left[\frac{r}{\beta} J_1(r) - \frac{r^2}{2\beta^2}\right], \tag{23}$$

and introducing the above optimum values of r and β. This yields

$$\eta_0 = \frac{M^2 i_1}{G_C V_0}\left[\frac{r_0}{\beta_0} J_1(r_0) - \frac{r_0^2}{2\beta_0^2}\right],$$

or

$$\eta_0 = 0.169\,\frac{M^2 i_1}{G_C V_0}. \tag{24}$$

This is valid only if $MV_m \ll \frac{1}{2}V_0$, since this was assumed in the derivation of (1); also, if $MV_m > \frac{1}{2}V_0$, some electrons will be reversed between the grids. Such reversal introduces conditions not covered by the present theory and which moreover clearly would result in a decrease in efficiency.

It is instructive to apply the above small-signal theory to the region where MV_m approaches the limiting value, $\frac{1}{2}V_0$, since, although it is inaccurate there, it nevertheless gives some idea of the ultimate values to be expected for the efficiency.

If it is assumed that the conditions are always such as to give maximum bunching, i.e., (16) is always satisfied, then (14) may be written

$$\eta = \frac{1}{V_0}\left[0.58MV_m - \frac{G_C V_m^2}{2i_1}\right], \tag{25}$$

which expresses efficiency in terms of the amplitude V_m.

A set of curves of efficiency versus MV_m, for the following conditions

$$V_0 = 300 \text{ volts}$$

$$M = 1/\sqrt{2}$$

$$i_1 = 0.01 \text{ ampere}$$

$$MV_{m\,\max} = 150 \text{ volts}$$

is given in Fig. 1 for values of R_C from 5000 to ∞ ohms. These curves are all terminated at the line $MV_m = 150$, since beyond that point electrons will be reversed by the alternating field.

The efficiencies given by (24) correspond to the maxima of curves such as a, b, c, and d, and also to e, the maximum of which occurs just at $MV_m = 150$. However, for curves such as f, (24) does not apply since its maximum occurs in the forbidden region $MV_m > 150$. The correct maximum efficiency in this case is given by the intersection of the curve with the line $MV_m = 150$,

and may be computed from (25). Hence, on this basis, the maximum attainable efficiency for reflex tubes is 29 per cent, corresponding to curve g for $MV_m=150$. It is of interest to compare this with the case of single-transit tubes. Here the restriction on MV_m is $MV_m \leqq V_0$. In this case it is seen from (25) that an ultimate efficiency of 58 per cent might be attained.

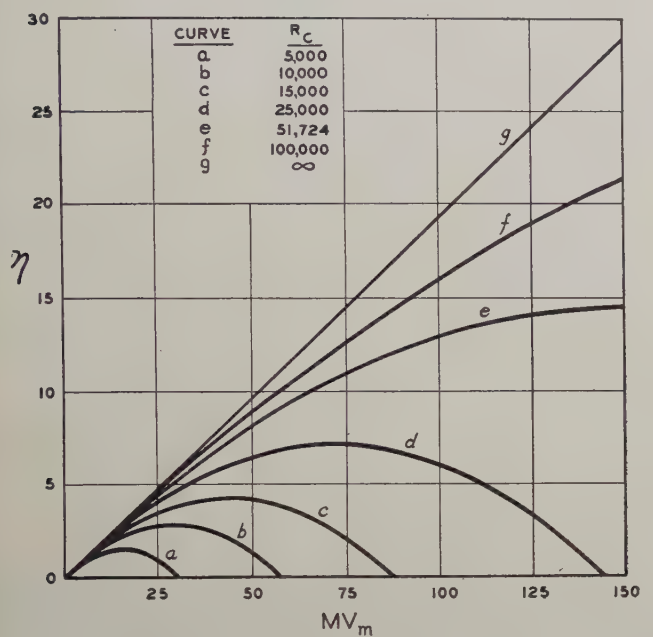

Fig. 1—Efficiency in per cent η versus effective oscillatory voltage MV_m for various values of unloaded cavity shunt resistance R_C.

However, in most actual cases where the efficiency is of the order of a few per cent, MV_m is always much less than its limiting value of $V_0/2$, and the typical curve resembles that of case a, Fig. 1. In all such cases (24) gives the correct maximum efficiency.

To get an expression for V_m, under conditions for maximum η, rewrite (14) and substitute from (18). This yields

$$\eta_0 = \frac{MV_m}{V_0}\left[J_1(r_0) - \frac{G_C V_m}{2Mi_1}\right]$$

$$= \frac{MV_m}{V_0}\,\frac{J_1(r_0)}{2} = 0.29\,\frac{MV_m}{V_0}. \qquad (26)$$

Since this expression and (23) must be equivalent they may be equated and solved for V_m. Thus,

$$V_{m0} = 0.58MR_C i_1. \qquad (27)$$

This formula, like those from which it is derived, is valid only for $MV_m \ll \frac{1}{2}V_0$.

III. Possibility of Increasing the Efficiency

In the expression for maximum efficiency,

$$\eta_0 = 0.169\,\frac{M^2 i_1}{G_C V_0},$$

there does not seem to be much of a possibility of greatly increasing η_0 by attaining more favorable values of M, G_C, or V_0. In general, these factors are not independent, and changes which improve one frequently result in a compensating change in the others. Consider the case where the resonator is a simple cylindrical cavity, of height d and radius a, in which $d \ll a$. Then

$$G_C = \frac{a\delta}{189d^2}$$

where δ is the skin thickness. M may be expressed in terms of V_0 and d by making use of (9) in conjunction with the formula for transit angle.

$$\omega\tau = 1.07\cdot 10^{-7}\,\frac{fd}{\sqrt{V_0}},$$

and that for wavelength,

$$\lambda = 2.61a.$$

These relations give

$$\frac{M^2}{G_C V_0} = \frac{5.77\cdot 10^6}{f\delta}\sin^2\frac{\omega\tau}{2}.$$

Therefore, for a fixed frequency, it is evident that the above quantity depends upon the sine term only, and is greatest when its argument is $\pi/2$, i.e., when the transit angle is π radians. Hence, so long as $\omega\tau=\pi$, variations of M, G_C, and V_0 do not affect the efficiency, and no further increase of efficiency in this particular case is obtained by varying these quantities.

Since the efficiency is directly proportional to i_1, and the power to i_1^2, possibilities of increasing the current are of importance. It is of significance that i_1 is the effective current and not the cathode emission current which will be denoted by i_e. The former is obtained from the latter by subtracting losses principally to the grids and aperture edges.

The losses to the grids may be expressed in terms of the grid transmission coefficient α, which is taken as the ratio of open area to total area over the grid surface. This is a somewhat idealized definition since it assumes no component of lateral velocity to be introduced by the grid wires, and assumes that the shadows cast by previous grids do not affect the transmission coefficient. The area ratio may be shown to be

$$\alpha = \left(\frac{l-b}{l}\right)^2$$

where l is the distance between wire centers, and b is the wire diameter.

If the beam passes through one grid, the transmitted current will be

$$i_1 = \alpha i_e.$$

For two grids it is

$$i_1 = \alpha \cdot \alpha i_e.$$

and for u grids

$$i_1 = \alpha^u i_e. \tag{28}$$

For passage through u grids of transmission α_1, and u' grids of transmission α_2, the resulting current is

$$i_1 = \alpha_1{}^u \alpha_2{}^{u'} i_e.$$

It is obvious that i_1 can be increased by increasing α and decreasing u. The transmission α can be increased by using finer wire and larger spacings. But the fineness of the wire is limited by its temperature rise, and the largeness of the spacing is limited by its effect on M. Large spacings permit fringing electric fields and decrease M. The number u of grids depends upon the design of the beam electron-optical system. It is usually either two or three in reflex tubes, but the beam passes through some of the grids more than once.

Another important consideration that determines i_1 is is that of multiple transits of electrons through the resonator. In the above theory only two transits are considered, first the modulating transit, and second the driving transit which occurs after the electrons have been bunched in the reflection space. Obviously there must be additional transits, since the cathode will act as a reflector. However, because of debunching and improper phasing these additional transits contribute little one way or the other to the oscillations of the resonator except in special cases. Nevertheless, they may contribute substantially to the space charge and thus decrease the cathode current i_e so that in some cases the beam current may be limited by space charge rather than by grid temperature.

The magnitude of this effect may be evaluated by considering a simple structure consisting of a plane cathode, grid, and reflector, with the cathode and reflector at zero potential and the grid positive. Let the grid have a coefficient of transmission α. Then for every N electrons emitted from the cathode, a fraction $N\alpha^2$ will return after one round trip. At the start of the second trip, the fraction $N\alpha^2$ will be joined by a new group of N electrons, making a total of $(1+\alpha^2)N$. After q round trips the number will be

$$(1 + \alpha^2 + \alpha^4 + \cdots + \alpha^{2q})\, N.$$

After equilibrium has been reached, i.e., $q = \infty$, this becomes $N/(1-\alpha^2)$, which is the sum of this infinite series. Hence, if electrons are emitted from the cathode at a rate of N per second, the number moving through the space will be $N/(1-\alpha^2)$. Or, if the emission current is i_e, the space current i_s will be

$$i_s = \frac{i_e}{1 - \alpha^2}. \tag{29}$$

Thus space-charge limitation would occur with a cathode emission current $1-\alpha^2$ times that given by the Child-Langmuir law. If there are u grids, the factor becomes $1-\alpha^{2u}$.

Thus it is evident that there are two distinct grid transmission effects: (1) losses to the grids which decrease the effective current, and (2) transmission by the grids which allows multiple transits, resulting in greater space charge and consequent decrease in cathode emission. These effects are opposed to each other; large α increases (2) while small α increases (1). Hence there is an optimum α.

This is clarified by reference to Fig. 2. A structure having three grids is shown: a is an accelerating grid, whereas b and c are radio-frequency grids. The effective current driving the oscillator is i_1, which is the current remaining after four grid transits. The remaining transits are assumed to contribute only to space charge. The sum of currents due to all transits, regardless of direction of flow, gives the space current i_s.

For the usual reflex-tube case with u grids, i_1 is given by

$$i_1 = \alpha^{u+1} i_e.$$

Then, from (29),

$$i_1 = \alpha^{u+1}(1 - \alpha^{2u}) i_s.$$

Here i_s is a constant determined by the Child-Langmuir law. By differentiating with respect to α, and equating to zero, the maximum for α is found to be

$$\alpha_0 = \left(\frac{u+1}{3u+1}\right)\frac{1}{2u}. \tag{30}$$

Hence, if

$$u = 2, \quad \alpha_0 = 0.810, \quad i_1 = 0.30 i_s,$$

and if

$$u = 3, \quad \alpha_0 = 0.858, \quad i_1 = 0.29 i_s.$$

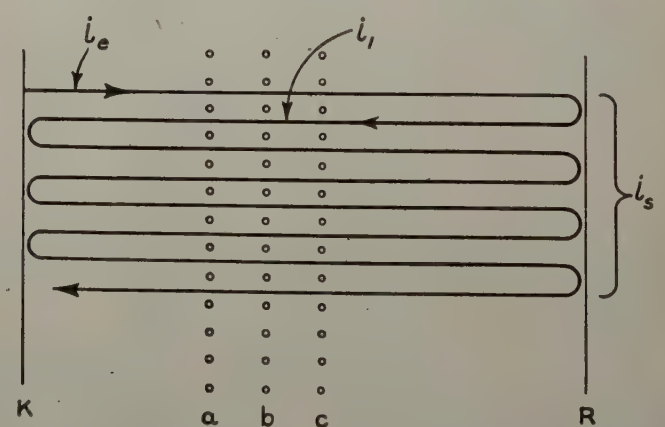

Fig. 2—Schematic electron paths in a triple-grid reflex oscillator, showing the effective current i_1 and the built-up space current i_s due to multiple transits, between cathode K and reflector R.

These results represent a case in which the beam electrons continue to oscillate until all are captured by the grids. If there is any divergence of the beam so that electrons are captured elsewhere, corrections to the above

are required. In some tubes all electrons are collected after two transits by an electrode which does not permit them again to approach the cathode after having once left it. Then space-charge effects are reduced to a minimum, and the grids may be designed for higher transmission limited only by considerations of heat dissipation and effect on M. Also it should be noted that i_1 can be increased by increasing i_s, as for example by diminishing the spacing from the cathode to the firts grid. Here again heat dissipation is a limiting factor. The above maximization of α would usually be most useful in making best use of an i_s already at its highest value.

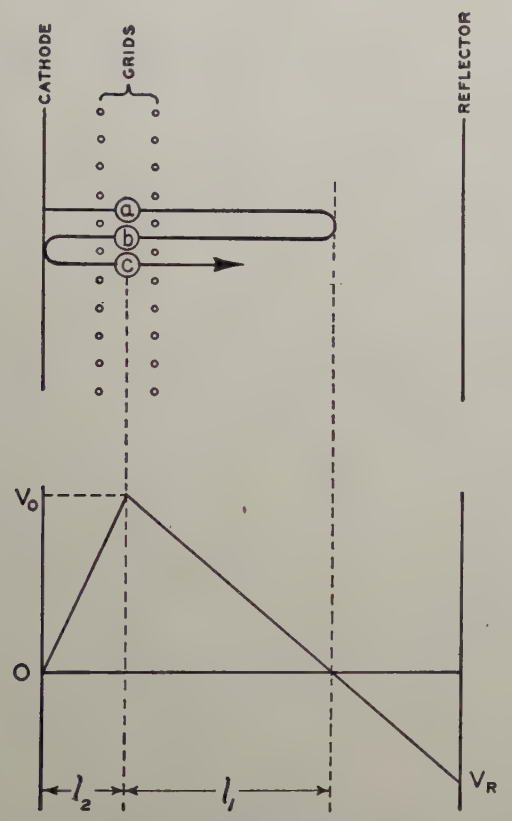

Fig. 3—Schematic diagrams of reflex klystron utilizing three electron transits.

Another method of increasing efficiency lies in the possibility of utilizing electron transits after the second one. As has just been pointed out, multiple transits usually occur, but they are usually ineffective because of debunching and improper phasing. However, it is possible to design a tube so that the third transit will cause a considerable increase in efficiency. This is especially true in the case of low-amplitude (i.e., $V_m \ll V_0$) oscillators, since the velocity spread in the beam is small, and when once bunched the electrons stay sufficiently bunched long enough to permit a third transit with considerable effectiveness.

Referring to Fig. 3, we see that the power developed by the beam during the second transit, i.e., transit b, will be, according to (7),

$$W_1 = i_1 M V_m J_1(r_1) \cos \gamma_1.$$

During the third transit, i.e., transit c, it will be

$$W_1 = i_2 M V_m J_1(r_2) \cos \gamma_2.$$

This assumes that the bunch shape is affected by the second transit only to the extent that r changes between the second and third transits. The fact that various electrons in the bunch are subjected to different action of the radio-frequency field and the bunch thus distorted is ignored. The deceleration of the bunch as a whole during transit b also is neglected, and the bunch therefore is assumed to be reflected at the cathode surface between transits two and three. Both of the above assumptions are justified on the basis of a small-signal theory.

Thus the total will be

$$W = W_1 + W_2 = M V_m (i_1 J_1(r_1) \cos \gamma_1 + i_2 J_1(r_2) \cos \gamma_2) = \tfrac{1}{2} G V_m^2.$$

Introducing this in (13) yields

$$W_L = \frac{V_m^2}{2}(G - G_C) = M V_m [i_1 J_1(r_1) \cos \gamma_1 + i_2 J_1(r_2) \cos \gamma_2] - \frac{G_C V_m^2}{2}.$$

Therefore,

$$\eta = \frac{1}{V_0}\left[M V_m J_1\left(\frac{M V_m \theta_1}{2V_0}\right) - \frac{G_C V_m^2}{2 i_1} + \alpha^2 M V_m J_1\left(\frac{M V_m \theta_2}{2V_0}\right)\right], \qquad (31)$$

where the cosine factors have been given their maximum value of unity. This maximum value may be attained by varying the two voltages V_0 and V_R by small amounts. It is of interest that this exhausts the available parameters which can be adjusted for maximizing the phase angles γ_1 and γ_2. In attempting to utilize still more transits this maximization would not be possible.

These expressions are now similar to those for the double-transit case except for the addition of an extra term which represents the contribution of the third transit. The factor θ_2 which occurs in this added term is similar to θ_1 which has been discussed above and represents the transit angle of the bunch center from the first to the third transit, that is, it is equal to θ_1 plus the added angle caused by l_2.

As before, to maximize (31) with respect to the loading, the derivative of η with respect to V_m is equated to zero. This yields

$$J_0\left(\frac{M V_m \theta_1}{2V_0}\right) + \alpha^2 \frac{\theta_2}{\theta_1} J_0\left(\frac{M V_m \theta_2}{2V_0}\right) = \frac{1}{\beta}. \qquad (32)$$

From the tube geometry and operating voltages, the quantities θ_1, θ_2, α_1 and β are known. Thus V_m may be determined from (32) and then η from (31).

As a specific example a case has been computed[5] for the following numerical values:

$\omega = 5.89 \cdot 10^{10}$ cycles per second ($\lambda = 3.2$ centimeters)

$M = 0.64$

$\alpha = 0.81$

$V_0 = 300$ volts

$i_1 = 0.010$ ampere

$R_C = 5000$ ohms.

The results are plotted in Fig. 4, where contour lines for η are plotted against l_1 and l_2. For a complete picture the factors cos γ_1 and cos γ_2, which were dropped to obtain (31), must now be considered. These are seen to be rapidly varying functions, compared to η, when l_1 and l_2 are varied, since it may be shown that γ changes by 2π radians for a change in l of only 0.274 millimeter.

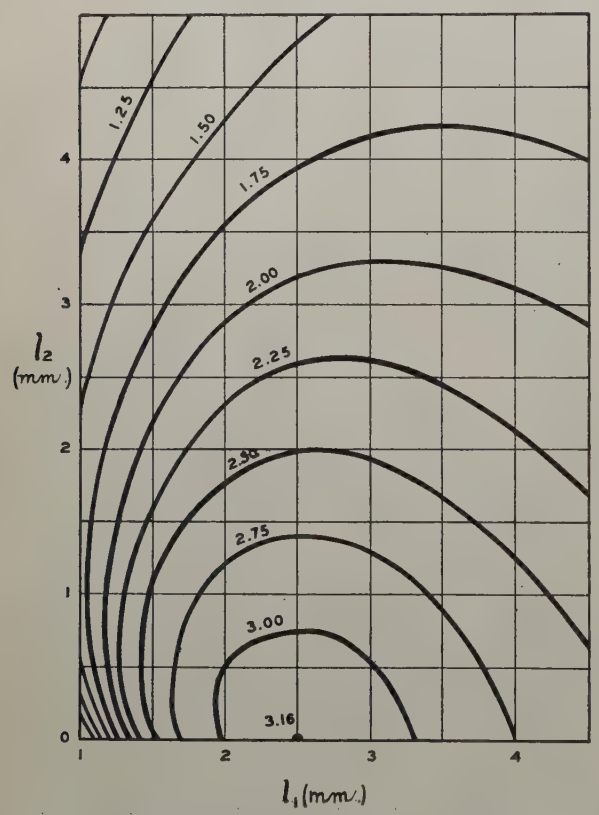

Fig. 4—Constant-efficiency contours (in per cent) versus drift distance in the reflector space l_1, and in the cathode space l_2, for a triple-transit reflex-klystron oscillator.

Thus the surface of Fig. 4, may be considered as an envelope of an array of individual maxima spaced 0.274 millimeter along each axial direction. Any value there plotted hence can be approached closely, if not actually realized.

For the above numerical case, but with only the usual two transits through the resonator, the maximum efficiency as computed from (24) is 1.16 per cent, whereas for three transits it is 3.16 per cent, an increase of 2.7 times. Somewhat greater values than this might theoretically be realized, since the figures for R_C and i_1 used above are conservatively low.

However, in practice, it is doubtful that increases as great as this could be obtained for several reasons. In the first place, the problem of the electron optics has been disregarded. It has been assumed that the beam was ideally collimated. Actually, this condition would be difficult to realize. With the increased path length, control of the beam becomes more difficult. There would likely be more divergence and consequent loss of current to the aperture edges.

Closely associated with the beam control is the shape of the grids, since this is a primary factor in determining the shape of the electron wave fronts which form in the beam due to bunching. For a homogeneous, perfectly collimated beam, and with flat grids, flat wave fronts will form. The reflecting field should then be such as to return flat wave fronts to the grids. However, with curved grids, curved wave fronts are formed and the reflecting field must then be such as to return wave fronts having the same curvature as that of the grids. Otherwise all parts of the wave front or bunch will not pass through the grids at the optimum phase. With two driving transits this problem becomes considerably more difficult, since the wave front shape must conform to the grid shape on both transits. On the first driving transit the shape of the reflector can be varied to produce the correct wave front shape, but on the second driving transit the cathode acts as the reflector, and it probably would be difficult to shape it so as to fulfill simultaneously its function both as cathode and reflector. A possible solution is to use parallel plane grids with a closely spaced parallel plane cathode. The construction of grids which will remain flat when raised to the usual high operating temperatures is a considerable problem that has not yet been solved, but this does not seem to be a difficulty which could not be overcome in a practical fashion.

The question of space charge must also be considered. It is highly desirable to operate with space-charge-limited current for the sake of stability. However, with a cathode closely spaced to the first grid, as it must be to act efficiently as a reflector, space-charge limitation may not always be obtained. In designing a multiple-transit tube this factor should be considered, and the cathode-grid spacing should be chosen to give space-charge limitation, if possible.

[5] The writers are indebted to Mrs. L. A. Hartig for valuable assistance in making these computations.

Electronic Collisional Frequency in the Upper Atmosphere*

E. F. GEORGE†

Summary—The collisional frequency of free electrons with neutral air molecules and atoms in the earth's atmosphere is calculated on the basis of contemporary ideas concerning temperature, pressure, composition, and dissociation of atmospheric gases. Expressions are developed for these calculations.

Since contemporary ideas on the state of the upper atmosphere are markedly different from those held ten years ago, this new determination of collisional frequency yields values different from those found earlier.

Two sets of values are worked out, one for night and the other for day conditions. It is believed that these two cases represent maximum and minimum values. The effective molecular diameter is discussed.

It is pointed out that more exact knowledge of the collisional frequency in the ionospheric regions is important in connection with theories of radio wave propagation.

IN ANY investigation of the propagation of radio waves through the ionosphere, the frequency of collisions between free electrons and molecules or atoms plays an important role. Collisions of this kind result in the absorption of energy from the electromagnetic waves. The refractive index of the ionosphere is influenced also by friction, as shown by the general dispersion equation. Friction, in turn, depends upon the collisional frequency. In view of the importance of the subject, therefore, and in view of the fact that no computed values of the collisional frequency exist which are not based more or less upon discarded ideas as to the conditions prevailing in the ionosphere, it seemed worth while to undertake the following investigation.

In this paper the collisional frequency is computed from the following formula[1]

$$f = nD^2\sqrt{\frac{K\pi T}{2m}} \qquad (1)$$

where f is the collisional frequency, n the number of molecules per cubic centimeter, D the molecular diameter in centimeters, K Boltzmann's constant, T the temperature in degrees Kelvin, and m the mass in grams of the electron. Assuming this formula to be correct, it would not be difficult (though quite tedious) to compute the collisional frequency if the quantities n, D, and T were known. Such, however, is far from being the case. The value of n, for instance, depends upon the temperature and pressure. The pressure, in turn, depends upon the temperature, the relative distribution of the components of the atmosphere, and of the dissociation of the oxygen and nitrogen molecules into atoms. All these factors are unknown, and the results obtained must necessarily depend upon the assumptions which are made regarding these quantities.

Various authorities in this field have assumed temperatures in the upper regions of the atmosphere which vary all the way from 200 to 3000 degrees Kelvin. An increase in temperature causes the air to expand upward, thus decreasing the concentration in the lower regions and increasing it in the upper regions.

All estimates of the temperature in the ionosphere are based on theoretical considerations or upon indirect evidence. Some general methods of estimating the temperature are:

(a) computations from the amount of the sun's radiant energy known or believed to be absorbed in the atmosphere;
(b) sound ranging;
(c) spectroscopy.

According to Hulbert[2] the temperature in the region between 160 and 300 kilometers rises 50 degrees Kelvin per hour during daylight. Wulf and Deming[3] favor a temperature of about 700 degrees Kelvin in the region above 100 kilometers. This conclusion is based on the assumed absorption of the sun's energy by nitrogen.

In this paper, an attempt has been made to distinguish between conditions during the daytime and at night. The temperature at night is assumed to be 220 degrees Kelvin from an altitude of 10 to 400 kilometers. This is in line with the conclusions reached by Vegard and Tonsberg[4] from a study of the Tromso spectrograms. They find the night temperature to be about 225 degrees Kelvin. During the day the temperature is assumed to range from 220 degrees Kelvin at 50 kilometers to 1000 degrees Kelvin at 400 kilometers. The temperatures assumed at the various elevations are shown in Fig. 1 and in column 2 of Tables I and II.

In regard to the distribution of the various components of the atmosphere, Hulburt[2] assumes complete mixing (and therefore the same relative concentrations as at sea level) to an elevation of 150 kilometers. In this paper, complete mixing has been assumed to a height of 90 kilometers, above which a gravitational separation is supposed to exist. This assumption has made it necessary to compute the pressures and molecular

* Decimal classification: R113.502. Original manuscript received by the Institute, June 10, 1946.

† Department of Physics, University of Alaska, College, Alaska.

[1] A. Hund, "Phenomena in High-Frequency Systems," McGraw-Hill Book Co., Inc., New York, N. Y., 1936; p. 385.

[2] E. O. Hulbert, "Physics of the Earth, VIII, Terrestrial Magnetism and Electricity," McGraw-Hill Book Co., New York, N. Y., 1939; pp. 492–500.

[3] O. R. Wulf and L. S. Deming, *Terr. Mag. and Atmos. Elec.*, September, 1938; pp. 283–297.

[4] L. Vegard and E. Tonsberg, "Results of auroral spectrograms obtained at Tromso observatory during the winters 1941–1942 and 1942–1943," *Geofysiske Publikasjoner*, vol. 16, Utgitt Av Det Norske Videnskaps-Akademi 1 Oslo, Sweden, pp. 1–10.

concentrations above 90 kilometers for each component separately. The concentration at great elevations depends quite markedly upon the height at which gravitational separation begins.

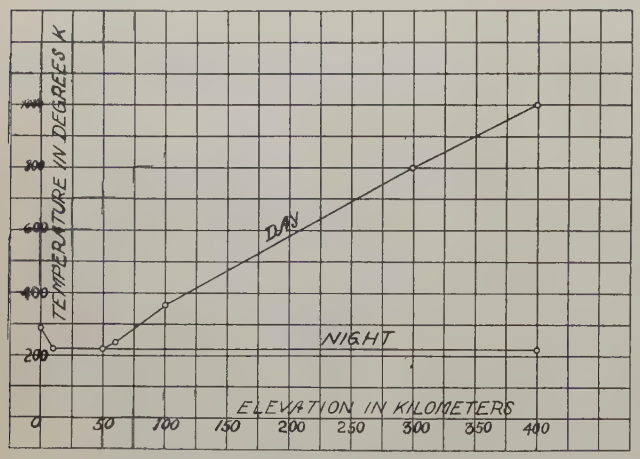

Fig. 1—Assumed relation between temperature and elevation. From sea level to 50 kilometers the same temperatures are assumed for day and night.

The molecular density in the upper atmosphere depends to a very great extent upon dissociation, or the separation of the diatomic molecules into atoms. Wulf and Deming[3] assume complete dissociation of oxygen above 100 kilometers, and the dissociation of nitrogen at higher levels to some unknown extent. In this paper it is assumed that partial dissociation of oxygen begins at about 90 kilometers, and partial dissociation of nitrogen at about 160 kilometers. The percentage dissociation of these elements at the various elevations is shown in columns 4 and 5 of Tables I and II.

Another factor whose value is uncertain within wide limits is the molecular diameter. Since, according to (1), the collisional frequency varies as the square of this factor, it is easily seen that precise results are difficult to obtain. It might be pertinent to inquire at this point what is meant by the diameter of a molecule as the term is used in this connection. In other words, how close must an electron come to the center of a molecule for a "collision" to occur; that is, how close must it come in order to be appreciably deflected one way or the other? Both Hund[1] and Hulburt[2] suggest a diameter of 3×10^{-8} centimeters. A careful check of Hund's results appears to indicate, however, that in his computations of the collisional frequency he actually employed a value of the molecular diameter of about 7×10^{-8} centimeter. In the present paper, the rather shaky assumption has been made that an electron suffers a deflection when it comes within a distance D of the center of the molecule. The *actual* diameter of the molecule is taken as $3.5(10^{-8})$ centimeters and the *effective* diameter as $7.0(10^{-8})$ centimeter. This would appear to be, in effect, what Hund actually did. Fortunately, whatever variations there may be in the assumed values of the molecular diameter, the result, in so far as the collisional frequency is concerned, is not cumulative. In this respect it differs markedly from the other factors above. A comparatively small change in any one of them accumulates in such a way that the result at an altitude of 400 kilometers, amounts to several orders of magnitude.

The atmospheric pressure at the various elevations was computed from

$$p = p_0 e^{-Mg/K\int_0^z dz/T} \tag{2}$$

$$\frac{p}{p_0} = e^{-Mg/K\int_0^z dz/T} \tag{3}$$

where p is the pressure at the elevation z, p_0 the pressure at sea level, M the average mass in grams of the molecule, and g the acceleration due to gravity.[5]

In computing pressures the step-by-step method was used. The first step extends from sea level to a height of 10 kilometers, the second from 10 to 20 kilometers, · · · the last from 350 to 400 kilometers. (See Table I.)

TABLE I-A

Z Kilometers	T Kelvin	g Centimeters Per Second	0% / O O	N% / N N	P Oxygen	P Nitrogen	P Argon	P Helium
0	287	980	0%	0%	2.14×10^{5}	7.93×10^{5}	9.53×10^{3}	4.06×10^{0}
10	220	977	0	0	5.49×10^{4}	2.04×10^{5}	2.48×10^{3}	1.04×10^{0}
20	220	974	0	0	1.17×10^{4}	4.36×10^{4}	5.25×10^{2}	2.23×10^{-1}
40	220	968	0	0	5.40×10^{2}	2.01×10^{3}	2.41×10^{1}	1.03×10^{-2}
50	220	965	0	0	1.17×10^{2}	4.35×10^{2}	5.23×10^{0}	2.23×10^{-3}
60	240	962	0	0	2.71×10^{1}	1.01×10^{2}	1.21×10^{0}	5.17×10^{-4}
80	300	957	0	0	2.25×10^{0}	8.39×10^{0}	1.01×10^{-1}	4.29×10^{-5}
90	330	954	50	0	7.80×10^{-1}	2.91×10^{0}	3.50×10^{-2}	1.49×10^{-5}
100	360	952	70	0	3.51×10^{-1}	1.15×10^{0}	9.26×10^{-3}	1.30×10^{-5}
120	404	946	70	0	1.01×10^{-1}	2.15×10^{-1}	8.46×10^{-4}	1.03×10^{-5}
140	448	940	70	0	3.33×10^{-2}	4.82×10^{-2}	1.00×10^{-4}	8.30×10^{-6}
160	492	934	75	10	1.23×10^{-2}	1.26×10^{-2}	1.47×10^{-5}	6.85×10^{-6}
180	536	930	75	20	5.13×10^{-3}	3.93×10^{-3}	2.57×10^{-6}	5.75×50^{-6}
200	580	923	80	30	2.31×10^{-3}	1.44×10^{-3}	5.20×10^{-7}	4.90×10^{-6}
220	624	917	80	40	1.14×10^{-3}	5.97×10^{-4}	1.19×10^{-7}	4.23×10^{-6}
250	690	909	85	60	4.34×10^{-4}	2.08×10^{-4}	1.60×10^{-8}	3.46×10^{-6}
280	756	900	85	60	1.89×10^{-4}	8.59×10^{-5}	2.63×10^{-9}	2.89×10^{-6}
300	800	894	90	70	1.13×10^{-4}	4.98×10^{-5}		2.59×10^{-6}
350	900	879	90	70	3.76×10^{-5}	1.59×10^{-5}		2.01×10^{-6}
400	1000	864	90	80	1.45×10^{-5}	5.82×10^{-6}		1.61×10^{-6}

TABLE II-B

Z Kilometers	n Oxygen Particles	n Nitrogen Particles	n Argon	n Helium	n Total	Collisional Frequency
0	5.43×10^{18}	2.02×10^{19}	2.43×10^{17}	1.03×10^{14}	2.58×10^{19}	1.04×10^{12}
10	1.83×10^{18}	6.79×10^{18}	8.25×10^{16}	3.46×10^{13}	8.70×10^{18}	3.08×10^{11}
20	3.88×10^{17}	1.45×10^{18}	1.74×10^{16}	7.34×10^{12}	1.85×10^{18}	6.54×10^{10}
40	1.79×10^{16}	6.65×10^{16}	8.01×10^{14}	3.42×10^{11}	8.53×10^{16}	3.01×10^{9}
50	3.87×10^{15}	1.44×10^{16}	1.73×10^{14}	7.41×10^{10}	1.85×10^{16}	6.54×10^{8}
60	8.25×10^{14}	3.06×10^{15}	3.67×10^{13}	1.57×10^{10}	3.93×10^{15}	1.45×10^{8}
80	5.48×10^{13}	2.04×10^{14}	2.46×10^{12}	1.04×10^{9}	2.61×10^{14}	1.08×10^{7}
90	1.73×10^{13}	6.45×10^{13}	7.76×10^{11}	3.30×10^{8}	$8.25\times q0^{13}$	3.58×10^{6}
100	7.13×10^{12}	2.32×10^{13}	1.88×10^{11}	2.64×10^{8}	3.06×10^{13}	1.38×10^{6}
120	1.83×10^{12}	3.88×10^{12}	1.53×10^{10}	1.86×10^{8}	5.72×10^{12}	2.74×10^{5}
140	5.43×10^{11}	7.85×10^{11}	1.63×10^{9}	1.35×10^{8}	1.33×10^{12}	6.72×10^{4}
160	1.82×10^{11}	1.85×10^{11}	2.18×10^{8}	1.02×10^{8}	3.68×10^{11}	1.95×10^{4}
180	7.00×10^{10}	5.36×10^{10}	3.50×10^{7}	7.84×10^{7}	1.24×10^{11}	6.86×10^{3}
200	2.91×10^{10}	1.81×10^{10}	6.55×10^{6}	6.17×10^{7}	4.73×10^{10}	2.71×10^{3}
220	1.33×10^{10}	6.98×10^{9}	1.39×10^{6}	4.94×10^{-17}	2.04×10^{10}	1.21×10^{3}
250	4.59×10^{9}	2.20×10^{9}	1.70×10^{5}	3.66×0^{17}	6.83×10^{9}	4.28×10^{2}
280	1.83×10^{9}	8.40×10^{8}	2.54×10^{4}	2.79×10^{7}	2.69×10^{9}	1.76×10^{2}
300	1.04×10^{9}	4.55×10^{8}		2.37×10^{7}	1.52×10^{9}	1.02×10^{2}
350	3.05×10^{8}	1.29×10^{8}		1.63×10^{7}	4.51×10^{8}	3.22×10^{1}
400	1.06×10^{8}	4.25×10^{7}		1.18×10^{7}	1.60×10^{8}	1.21×10^{1}

Consider, for instance, the ninth step: from 100 to 120 kilometers. Since the change in g is small, the

[5] B. Haurwitz, "Dynamic Meteorology," McGraw-Hill Book Co., New York, N. Y.; 1941, p. 11.

average value ($g=952+946/2=949$) is used. For this particular step we let $z'=z-100$; i.e., $z'=0$ when $z=100$ kilometers and $z'=20$ when $z=120$ kilometers. The value of T, then, for any elevation between 100 and 120 kilometers, is

$$T = 360 + \frac{(404 - 360)z'}{20} = 360 + 2.2z'.$$

Equation (2) then becomes

$$p = p_0 e^{-(949M)/K\int_0^{20}(dz'/360+2.2z')}. \quad (4)$$

Equation (4) is integrated to find p at 120 kilometers.

The rate at which the pressure changes with the elevation is given by

$$\frac{dp}{dz} = -nMg \quad (5)^6$$

or

$$dp = -nMg(dz) \quad (6)$$

But

$$p = nKT \quad (7)$$

Differentiating (7) we get

$$dp = KTdn + Kndt \quad (8)$$

Substituting (8) in (6) we obtain

$$KTdn + Kndt = -nMgdz \quad (9)$$

or

$$\frac{dn}{n} + \frac{dT}{T} = -\frac{Mg}{KT}dz. \quad (10)$$

Integrating (10) we get

$$\ln n + \ln T = -\frac{Mg}{K}\int_0^z \frac{dz}{T} + \ln n_0 + \ln T_0 \quad (11)$$

or

$$\ln\left[\frac{n}{n_0}\frac{T}{T_0}\right] = -\frac{Mg}{K}\int_0^z \frac{dz}{T} \quad (12)$$

or

$$\frac{n}{n_0}\frac{T}{T_0} = \text{antilog of}\left(\frac{-Mg}{K}\int_0^z \frac{dz}{T}\right) = e^{-Mg/K\int_0^z dz/T} \quad (13)$$

$$n = n_0 \frac{T_0}{T} e^{-Mg/K\int_0^z dz/T}. \quad (14)$$

If we now substitute (3) in (14) we get

$$n = n_0 \frac{T_0}{T}\frac{p}{p_0}. \quad (15)$$

[6] G. P. Harnwell and J. J. Livingood, "Experimental Atomic Physics," first edition, McGraw-Hill Book Co., New York, N. Y., 1933; pp. 86–88.

TABLE II-A

Z Kilometers	T Kelvin	ζ Centimeters Per Second	0% / O O_2	N% / N N_2	P Oxygen	P Nitrogen	P Argon	P Helium
0	287	980	0%	0%	2.14×10^{5}	7.93×10^{5}	9.53×10^{3}	4.06×10^{0}
10	220	977	0	0	5.49×10^{4}	2.04×10^{5}	2.48×10^{3}	1.04×10^{0}
20	220	974	0	0	1.17×10^{4}	4.36×10^{4}	5.25×10^{2}	2.23×10^{-1}
40	220	968	0	0	5.40×10^{2}	2.01×10^{3}	2.41×10^{1}	1.03×10^{-2}
50	220	965	0	0	1.17×10^{2}	4.35×10^{2}	5.23×10^{0}	2.23×10^{-3}
60	220	962	0	0	2.56×10^{1}	9.57×10^{1}	1.15×10^{0}	4.90×10^{-4}
80	220	957	0	0	1.25×10^{0}	4.65×10^{0}	5.60×10^{-2}	1.49×10^{-5}
90	220	954	25	0	2.78×10^{-1}	1.03×10^{0}	1.24×10^{-2}	5.30×10^{-6}
100	220	952	35	0	6.45×10^{-2}	2.40×10^{-1}	1.55×10^{-3}	4.30×10^{-6}
120	220	946	35	0	3.83×10^{-3}	1.31×10^{-2}	2.44×10^{-5}	2.84×10^{-6}
140	220	940	35	0	2.52×10^{-4}	7.32×10^{-4}	3.94×10^{-7}	1.88×10^{-6}
160	220	934	35	5	1.68×10^{-5}	4.16×10^{-5}	6.53×10^{-9}	1.25×10^{-6}
180	220	930	40	5	1.14×10^{-6}	2.57×10^{-6}	1.11×10^{-10}	8.30×10^{-7}
200	220	923	40	10	8.50×10^{-9}	1.62×10^{-7}	1.93×10^{-13}	5.54×10^{-7}
220	220	917	40	10	6.48×10^{-8}	1.11×10^{-8}	3.44×10^{-14}	3.70×10^{-7}
250	220	909	45	10	1.40×10^{-10}	2.07×10^{-10}		2.03×10^{-7}
280	220	900	45	10	3.53×10^{-12}	4.01×10^{-12}		1.12×10^{-7}
300	220	894	45	15	3.10×10^{-13}	2.95×10^{-13}		7.59×10^{-8}
350	220	879	50	15	7.83×10^{-16}	5.54×10^{-16}		2.88×10^{-8}
400	220	864	50	15	2.57×10^{-18}	1.16×10^{-18}		1.11×10^{-8}

TABLE II-B

Z Kilometers	n Oxygen	n Nitrogen	n Argon	n Helium	n Total per cubic centimeter	Collisional Frequency
0	5.43×10^{18}	2.02×10^{19}	2.43×10^{17}	1.03×10^{14}	2.58×10^{19}	1.04×10^{12}
10	1.83×10^{18}	6.79×10^{18}	8.25×10^{16}	3.46×10^{13}	8.70×10^{18}	3.08×10^{11}
20	3.88×10^{17}	1.45×10^{18}	1.74×10^{16}	7.34×10^{12}	1.85×10^{18}	6.56×10^{10}
40	1.79×10^{16}	6.65×10^{16}	8.01×10^{14}	3.42×10^{11}	8.53×10^{16}	3.02×10^{9}
50	3.87×10^{15}	1.44×10^{16}	1.73×10^{14}	7.41×10^{10}	1.85×10^{16}	6.55×10^{8}
60	8.50×10^{14}	3.17×10^{15}	3.81×10^{13}	1.62×10^{10}	4.06×10^{15}	1.43×10^{8}
80	4.14×10^{13}	1.54×10^{14}	1.86×10^{12}	7.90×10^{8}	1.98×10^{14}	7.00×10^{6}
90	9.22×10^{12}	3.44×10^{13}	4.13×10^{11}	1.76×10^{8}	4.39×10^{13}	1.56×10^{6}
100	2.14×10^{12}	7.97×10^{12}	5.13×10^{10}	1.43×10^{8}	1.02×10^{13}	3.60×10^{5}
120	1.27×10^{11}	4.36×10^{11}	8.09×10^{8}	9.44×10^{7}	5.65×10^{11}	1.99×10^{4}
140	8.37×10^{9}	2.43×10^{10}	1.31×10^{7}	6.25×10^{7}	3.27×10^{10}	1.16×10^{3}
160	5.59×10^{8}	1.38×10^{9}	2.17×10^{6}	4.13×10^{7}	1.98×10^{9}	7.00×10^{1}
180	3.78×10^{7}	8.53×10^{7}	3.68×10^{5}	2.76×10^{7}	1.51×10^{8}	5.34×10^{0}
200	2.82×10^{6}	5.37×10^{6}	6.40×10^{4}	1.84×10^{7}	2.66×10^{7}	9.43×10^{-1}
220	2.15×10^{5}	3.77×10^{5}	1.14×10^{3}	1.23×10^{7}	1.29×10^{7}	4.55×10^{-1}
250	4.65×10^{3}	6.88×10^{3}		6.76×10^{6}	6.77×10^{6}	2.40×10^{-1}
280	1.17×10^{2}	1.33×10^{2}		3.74×10^{6}	3.74×10^{6}	1.32×10^{-1}
300	1.03×10^{1}	9.80×10^{0}		2.52×10^{6}	2.52×10^{6}	8.93×10^{-2}
350	2.60×10^{-3}	1.84×10^{-3}		9.54×10^{5}	9.54×10^{5}	3.39×10^{-2}
400	8.55×10^{-5}	3.84×10^{-5}		3.69×10^{5}	3.69×10^{5}	1.36×10^{-2}

After the pressures (Fig. 2) were computed from (2), the molecular concentrations (Fig. 3) were obtained from (15) and then the collisional frequency (Fig. 4) from (1).

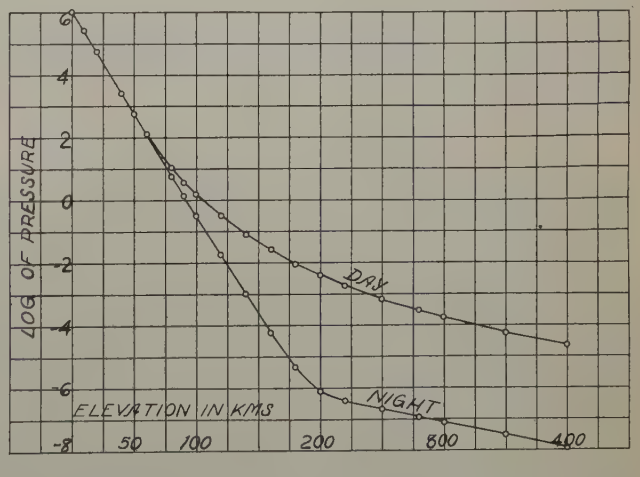

Fig. 2—The logarithm of atmospheric pressure, in dynes per square centimeter, plotted against the elevation in kilometers.

It might be worth while to point out here that, in view of (15), Hulburt's equation $n=n_0\ e^{-(Mgz/KT)}$ is without foundation, and that values of the molecular

concentration computed by his formula are necessarily wrong.

On the basis of assumptions that appear to be consistent with recent developments in the theory of the ionosphere, two sets of collisional frequencies have been computed. These extend from sea level to an altitude of 400 kilometers. One set, shown in Table I, is for conditions which are supposed to exist during daylight hours. The other, shown in Table II, is for night.

The author expresses his gratitude to S. L. Seaton, physicist-in-charge of the College Observatory, Carnegie Institution of Washington, for suggesting the problem and for encouragement and helpful criticism throughout.

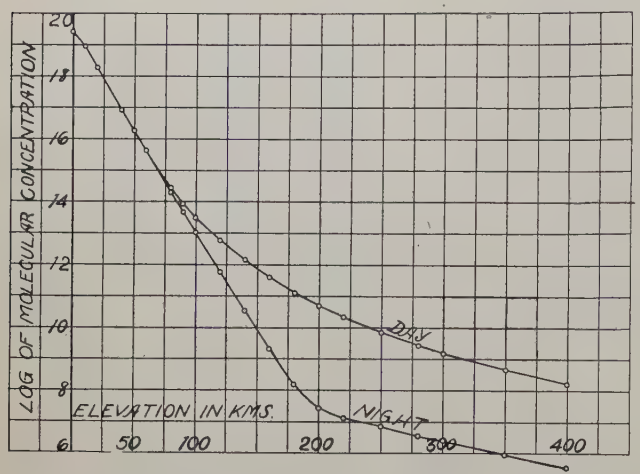

Fig. 3—The logarithm of the molecular concentration plotted against the elevation in kilometers.

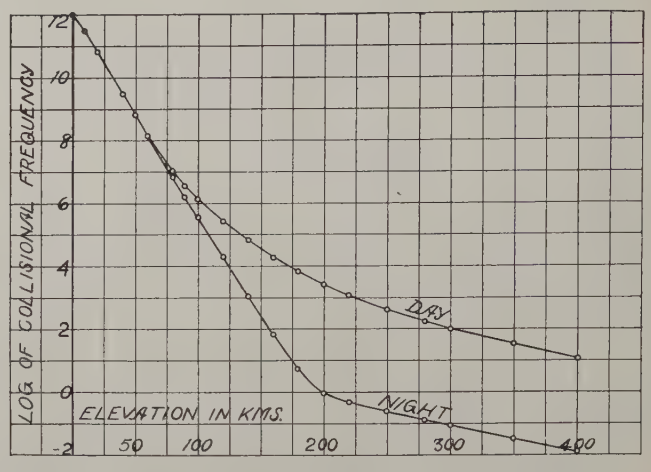

Fig. 4—The logarithm of the collisional frequency plotted against the elevation in kilometers.

Noise Spectrum of Crystal Rectifiers*

P. H. MILLER, Jr.†

***Summary*—Studies of the noise spectrum of crystal rectifiers were made over a frequency range of 50 cycles to 1 megacycle. The circuits used in the analysis are described. It was found throughout the range that, regardless of the type of power applied to the crystal, the noise temperature varies inversely with the frequency. The noise in the audio range is always large; a noise temperature ratio of 10^6 is not uncommon. A mechanism responsible for the observed noise has not yet been suggested.**

Introduction

THE MECHANISMS responsible for extra noise in crystal rectifiers are at present little understood. Extra noise is the difference between the noise actually observed and the noise to be expected from diode (shot) and Johnson noise in the rectifying barrier and spreading resistance. Extra noise in production crystals at 30 megacycles is not large, but at audio frequencies it may be many orders of magnitude larger. Rough whisker tips[1] and imperfectly soldered back contacts have been blamed as sources of extra noise. Etch[2] and tapping have been found to influence noise, but the temperature effect has been found to be small.[3]

Several papers[4–6] have been written to elucidate noise and several mechanisms have been proposed to explain extra noise. The experiments herein described examined the characteristics of this noise under various conditions to ascertain if the predictions of various proposed

* Decimal classification: R362.1. Original manuscript received by the Institute, March 14, 1946; revised manuscript received May 17, 1946; second revision received July 22, 1946. Presented 1945 Winter Technical Meeting, New York, N.Y., January 25, 1946. This work was done in part under Contract No. OEMsr-388 with the Trustees of the University of Pennsylvania under the auspices of the Office of Scientific Research and Development which assumes no responsibility for the accuracy of the statements contained herein.

† Randal Morgan Laboratory of Physics, University of Pennsylvania, Philadelphia 4, Pennsylvania.

[1] A. H. White and W. G. Pfann, "Correlation of noise with geometry point contact in silicon rectifiers," Bell Laboratories Memorandum, 42–120–96; August 24, 1942.

[2] A. W. Lawson and W. E. Stephens, "Effect of etch on crystal rectifiers," University of Pennsylvania, National Defense Research Council Division 14, no. 126; March 10, 1943.

[3] A. W. Lawson, P. H. Miller, and W. E. Stephens, "Noise in silicon rectifiers at low temperatures," University of Pennsylvania, National Defense Research Council, Division 14, no. 189; October 1, 1943.

[4] V. Weisskopf, "The theory of noise in crystal rectifiers," National Defense Research Council, Massachusetts Institute of Technology, no. 133; May 12, 1943.

[5] L. I. Schiff, "Noise in crystal rectifiers," University of Pennsylvania, National Defense Research Council, Division 14, no. 126; March 10, 1943.

[6] C. J. Christensen and G. L. Pearson, "Spontaneous resistance fluctuations in carbon microphones and other granular resistances," *Bell Sys. Tech. Jour.*, vol. 15, pp. 197–223; April, 1936.

mechanisms agreed with experiments. In these experiments the extra noise in different frequency ranges from 50 cycles to 1 megacycle was investigated in a variety of applications.

Apparatus

The block diagrams of the three schemes used in the analysis of the frequency spectrum are shown in Fig. 1. In all cases an input circuit, preamplifier, selective amplifier, and output meter were connected in series.

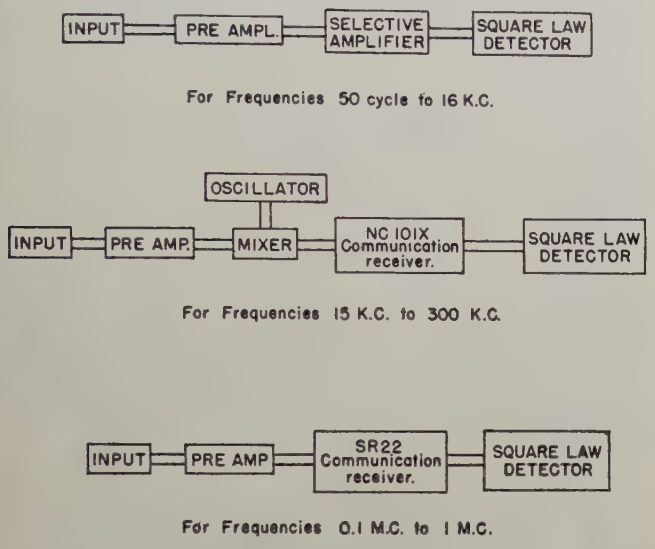

Fig. 1—Block diagrams of apparatus for investigation of frequency dependence of noise.

The noise temperature t of a crystal is defined as the ratio of the output noise power of an amplifier which is completely noiseless (grid resistance at zero temperature), with the crystal rectifier across the input, to that of the same amplifier with a passive circuit element of the equivalent resistance (and reactance) of the crystal rectifier at room temperature. The output power with the crystal is $1/R_L\int_0^\infty V_g^2\,Gd\nu$ where V_g^2 is the square of the voltage on the grid of the amplifier which is a result of crystal noise, G the voltage gain squared of the amplifier, and R_L the output load resistance of the amplifier.

The contributions of the grid resistor to the output noise is always negligible, since the noise voltage generated by the crystal rectifier with power applied under our conditions of measurement is much larger. For the input circuit shown in Fig. 2, the output noise power

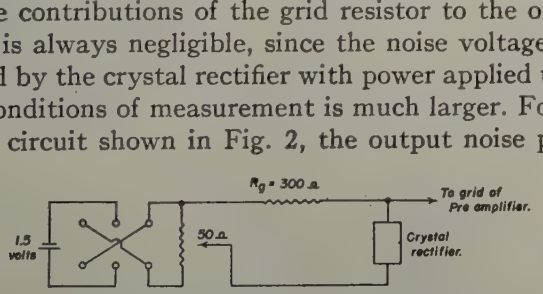

Fig. 2—Input circuit for applying bias to crystal rectifiers.

with the passive resistor replacing the crystal rectifier would be

$$\frac{1}{R_L}\int_0^\infty \frac{4kTRR_g^2}{(R+R_g)^2}Gd\nu$$

where R is the resistance of the passive resistor and R_g is the grid resistance which is assumed noiseless. This assumption is permissible since the above quantity is not experimentally measured but is merely an aid in expressing the problem. Thus

$$t = \frac{\int_0^\infty V_g^2Gd\nu}{\frac{4kTRR_g^2}{(R+R_g)^2}\int_0^\infty Gd\nu} = \frac{(R+R_g)^2}{4kTRR_g^2}\,\frac{D}{\int_0^\infty Gd\nu}$$

where D is the square of the output voltage as measured by a square-law detector. If V_g is a function of frequency, it is clear that the noise temperature will be sensitive to the frequency-response characteristic of the amplifier. There is always present at the output a background consisting of tube noise and discrete frequency pickup which must be subtracted from the observed output.

The value of the integral $\int_0^\infty Gd\nu$ can be established in two ways. The first is to measure the over-all gain of the preamplifier and selective amplifier point by point and graphically integrate the curve. An alternate method is to replace the crystal with a diode noise source whose dynamic resistance is large compared with R_g. The output voltage-squared deflection produced by the shot effect is

$$D_0 = 2eIR_g^2\int_0^\infty Gd\nu$$

where e is the electronic charge and I the diode current. The diode current is made large enough so that the contribution of the grid resistor to the noise can be neglected in comparison with that of the shot noise. The values of $\int_0^\infty Gd\nu$ found in these two manners were found to agree within 25 per cent. Since absolute values for the noise temperatures were not desired, no further refinement in experimental technique was thought worthwhile.

In the audio-frequency range the use of a diode is open to question, for in most diodes the noise depends in an exponential manner on the current rather than in a linear manner. The cause of this extra noise is presumably "flicker" effect.

A square-law output meter must be used when reliable estimates of noise temperatures are to be made. There are two fundamental difficulties in using a diode rectifier in the output circuit. The allowance for background is very uncertain. For instance, there is no simple formula for the average value of the positive part of the sum of two sinusoidal voltages of different amplitudes and frequency, and, furthermore, most diode circuits take a complicated average. If the ratio of amplitudes is large, then only the larger amplitude contributes to the average value. When the noise is comparable with or smaller than the background, only a very qualitative indication of the amount of noise can be obtained. When

square-law detection is employed the increase in deflection is a measure of the average of the square or the applied voltage, regardless of the nature of the applied voltage or background.

The second difficulty encountered in using a diode is that the relationship between the average value of the positive part of the noise voltage and the average value of the square of the noise voltage is not known except for some special noise sources. The error made by taking the square of the average to be the same as the average of the square is not believed to be more than 50 per cent.

An electronic square-law detector using a 6V6 biased to −22 volts was developed. The circuit diagram is shown in Fig. 3. This device was sufficiently accurate and at the same time more rugged than the sensitive element of a bolometer, thermister, or thermocouple.

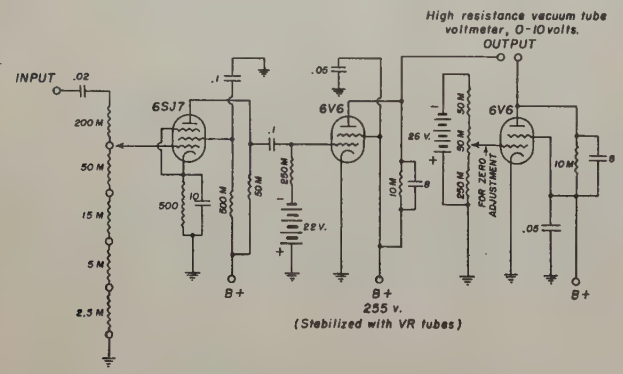

Fig. 3. Square-law detector for measurement of noise voltage squared.

The input circuit when direct-current bias is applied is shown in Fig. 2. The 300-ohm resistance in series with the bias acts as the grid resistor. This value was chosen because it is typical of that found in 30-megacycle intermediate-frequency amplifiers. In calculating the noise temperatures it was arbitrarily assumed that the resistance of the crystal was also 300 ohms. This is not true at all if direct-current bias in the back direction is applied. However, the noise temperature so obtained is a measure of the amount of noise power delivered to the output circuit and this is the important quantity in any application. A crystal rectifier with large true noise temperature may present only a small noise voltage to the grid, since the noise generator may have an internal resistance which is very large in comparison with the grid resistance.

In the audio range the preamplifier is battery operated to avoid 60-cycle pickup. The selective amplifier is of the Twin T type. Actually, too narrow a bandwidth is a disadvantage, since for a bandwidth of $\Delta\nu$ the beat frequency between different components in the transmitted band have periods larger than $1/\Delta\nu$, and these fluctuations may be troublesome and difficult to average. In the present form with 10 per cent tolerance components in the filter the $\int_0^\infty G d\nu$ is different for each band and must be evaluated experimentally.

The apparatus used in the frequency range of 15 to 400 kilocycles is indicated in Fig. 1. The preamplifier has a maximum voltage gain of about 10^4 and is flat up to 1 megacycle. The amplified noise voltage is fed into the mixer circuit, which consists of a mixer crystal, especially selected for negligible harmonics, and a 7-megacycle crystal-controlled local oscillator. A noise frequency ν from the input circuit mixed with the local oscillator to give $7 \pm \nu$ megacycles. If the communications receiver (NC101X)is tuned to $7+\nu$ megacycles, then all the noise in the range $\nu-\Delta\nu/2$ to $\nu+\Delta\nu/2$ will be measured on the output meter where $\Delta\nu$ is the bandwidth of the amplifier.

For frequencies higher than 100 kilocycles, frequency conversion is unnecessary and the output of the preamplifier can be coupled directly to a communication receiver and output meter.

Results

The major part of the studies was concerned with the behavior of noise as a function of the direct-current bias, but a limited number of experiments on the characteristics of the noise with the application of microwave power were carried out.

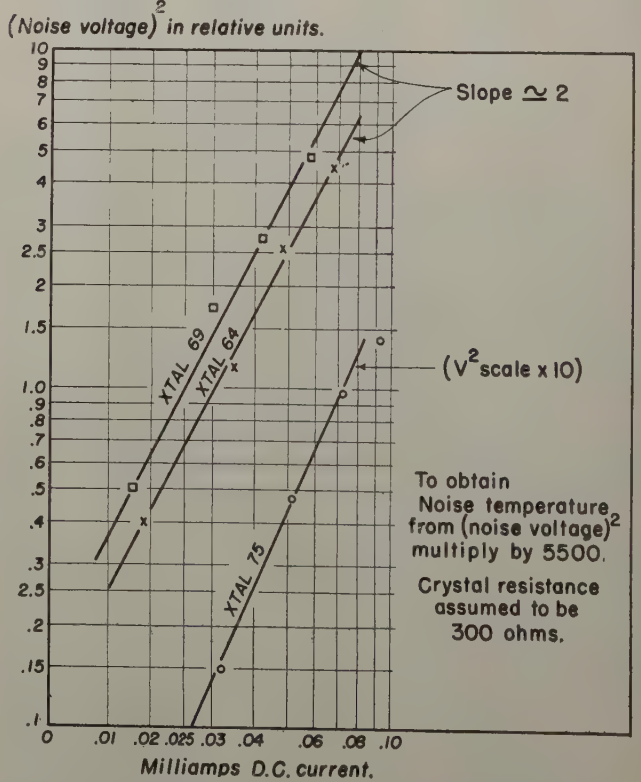

Fig. 4—Noise voltage squared in silicon-crystal rectifiers as a function of reverse current. Frequency range centered about 2400 cycles. A temperature t produces at the input terminals a noise voltage squared per cycle bandwidth of $4\times10^{-21}t$.

At all frequencies between 50 cycles and 1 megacycle, the extra noise was found to be approximately proportional to the square of the current, provided the resistance of the crystal rectifier was large in comparison with

the 300-ohm grid resistance. Typical results are shown in Fig. 4. Noise of the shot type varies linearly with current. A fluctuating resistance at the contact between the metal and semiconductor would produce noise with the observed dependence upon current.

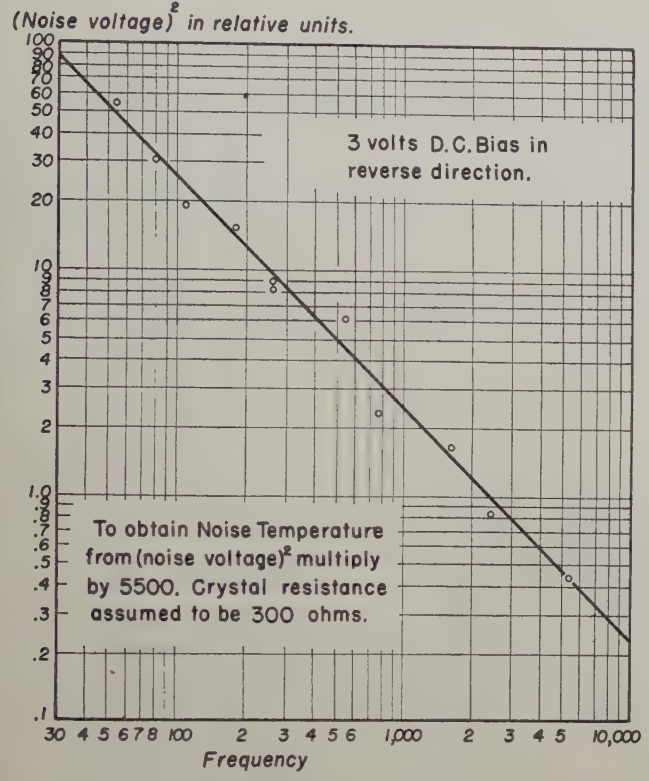

Fig. 5—Noise temperature of silicon-crystal rectifiers as a function of frequency. A temperature t produces at the input terminals a noise voltage squared per cycle bandwidth of $4\times10^{-21}t$.

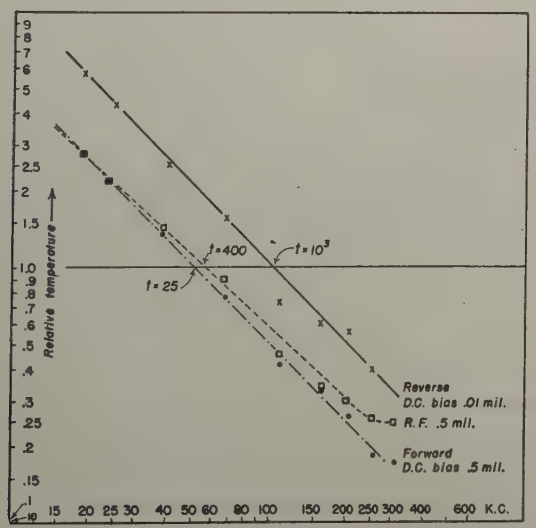

Fig. 6—Noise temperature of silicon-crystal rectifiers as a function of frequency. A temperature t produces at the input terminals a noise voltage squared per cycle bandwidth of $4\times10^{-21}t$.

The noise temperature of the crystal rectifiers was found to vary inversely with frequency in the range between 50 cycles and 1 megacycle. Typical experimental results for silicon-crystal rectifiers in different frequency ranges are shown in Figs. 5 and 6. For the frequency range from 50 to 10,000 cycles the mean slope of log temperature versus log frequency plots for ten different crystals with direct-current bias was -1.01, with the extreme values being -1.11 and -0.92. These results are typical of the manner in which the inverse-frequency behavior was followed. Measurements were also made on germanium-crystal rectifiers with both mechanical and welded contacts. The noise generated was of the same order of magnitude and exhibited the same frequency characteristics. In the welded units the platinum whisker formed an alloy at the germanium surface, so it is not likely that mechanical movement is responsible for the noise.

Some measurements were made on the noise generated when the silicon-crystal rectifier was cooled to liquid-air temperature and direct-current bias applied. It was found that the order of magnitude of the noise power was not changed. Only a limited number of experiments were conducted because stability of contact was difficult to maintain under such large temperature changes. These results indicate that if the mechanism responsible for the noise depends on thermal activation the energy required is less than 0.01 volt.

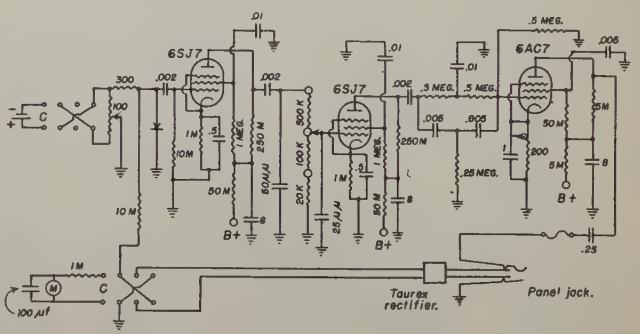

Fig. 7—Self-contained apparatus for measuring audio noise.

Attempts were made to study the variation in audio noise with variations in the preparation and assembly of the silicon surface and metal whisker and, while large variations in the noise were observed, no classification of the results can be made because the influence of extraneous factors was larger than that of those which were controlled.

Since the noise voltage in the audio range is large and can be easily measured, the correlations between this noise and that generated at 30 megacycles when the crystal is used as a crystal mixer was investigated. For this purpose the audio noise tester with a band pass from 1 to 15 kilocycles shown in Fig. 7 was constructed. The output could be measured with either an external square-law detector or, when only empirical information is desired, with a built-in copper-oxide rectifier and meter. The sensitivity is such that a grid voltage of 2×10^{-6} volt doubles the background.

To simulate radio-frequency conditions the potentiometer is adjusted to give ±0.4 volt, open-circuited. This results in a bias voltage in the reverse direction of

nearly 0.4 volt and in the forward direction of about 0.2 volt. These values were found to be typical of the average noise behavior in the forward and reverse directions. In making the correlation the noise-voltage reading in the reverse direction was divided by two, since when radio-frequency power is applied the impedance presented to an audio-current pulse is the intermediate-frequency load resistance in parallel with the intermediate-frequency impedance of the crystal. In contrast, an audio-current pulse with direct-current bias in the reverse direction develops a voltage across about twice this impedance, since only the load resistance is present. The correlation was found to be comparatively insensitive to the exact values chosen for bias voltage.

Fig. 8 shows the correlation between 30-megacycle noise temperature and the number obtained from the audio noise tester. The numbers are proportional to the audio noise voltage. Twenty commercial mixer crystals of a single manufacturer were measured before and after mistreatment by successive applications of 75- and 150-volt pulses in a 50-ohm concentric line having a time constant of the order of 10^{-8} second. From the experimental results it appears that the intermediate-frequency noise temperature can be predicted from the

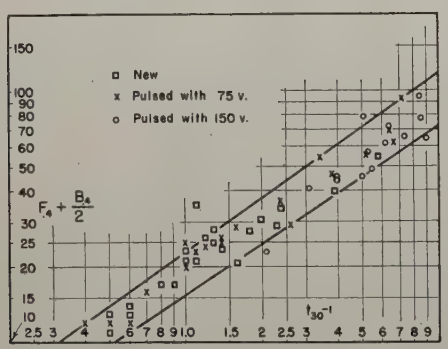

Fig. 8—Correlation between audio noise voltage generated by direct-current power and 30-megacycle noise power (expressed as temperature ratio) generated by microwave power applied to the crystal rectifier. Twenty 1N21 units were mistreated by the applications of power in a Torrey line and remeasured. The ordinates represent the sum in arbitrary units of the noise voltage generated in the circuit of Fig. 2 by the application of 0.4 volt in the forward direction plus one half of that generated by the applications of 0.4 volt in the reverse direction. $t_{30}-1$ represents the noise temperature minus unity of the crystal rectifiers at an intermediate frequency of 30 megacycles when employed in a microwave mixer under typical operating conditions.

audio measurement to about 25 per cent. The same sort of correlation was obtained for other crystal types and manufacturers, but somewhat different constants apply.

If crystal rectifiers are to be used in continuous-wave systems their audio noise will limit their performance. The production crystals of several manufacturers were investigated to see if reasonable numbers of crystals with low audio noise could be selected. Some yield curves are shown in Fig. 9. Approximately 5 per cent of production crystals have a noise temperature less than 1000 at 1 kilocycle. As the audio noise varies roughly as the square of the rectified current, an improvement in the signal-to-noise ratio of about 25 appears possible by reducing the local oscillator power.

There is as yet no hint of a mechanism which will give the observed frequency law. Any model will require relaxation times larger than one fiftieth of a second. The motion of individul molecules forming absorbed gas layers or mechanical changes at the contact which are a result of lattice vibrations will have relaxation times shorter than 10^{-6} second. No one has yet invented a suitable mechanism. Studies of surface characteristics

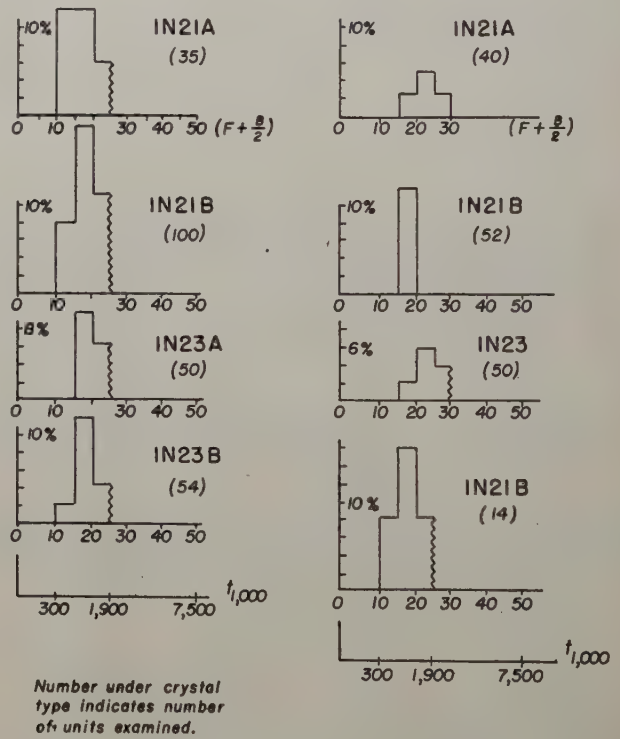

Fig. 9—Yield of low audio noise crystal rectifiers from various production lines. The abscissas are proportional to the audio noise voltage (see Fig. 9) and the ordinates represent the percentage of crystal rectifiers having an audio noise voltage between 0–5, 5–10, 10–15, 15–20 units, etc. The units not shown generate noise voltages to the right of the wavy vertical line. The nonlinear scale at the bottom gives the noise temperature at 1000 cycles.

have been made in a rectilinear electron microscope in which variation in field emission from the point of a silicon needle can be studied. The pattern formed on the fluorescent screen consisted of small spots which were continually moving around. The time constant of their motion was of the order of one-tenth second, and this suggests there may be a relation between this phenomenon and the generation of noise pulses. The relationship between the spots and work function of the surface is not clear, inasmuch as local geometrical condition of the surface exerts a strong influence on the field emission.

Some Considerations Governing Noise Measurements on Crystal Mixers*

SHEPARD ROBERTS†, MEMBER I.R.E.

Summary—The general principles of analysis and measurement of noise in radio receivers are discussed starting with basic definitions and following with a derivation of the fundamental equations for noise and noise figures of single and cascaded networks. A treatment of the noise generated in a crystal rectifier, when used as the first detector in a superheterodyne receiver, is given in which the "noise temperature" of the crystal is defined and the contribution by virtue of this noise temperature to the over-all noise figure of the receiver is indicated. The problem of designing a noise-measuring set is treated in sufficient detail to show how the noise temperature of a crystal rectifier can be measured independently of its other properties.

I. Introduction

RECEIVERS employing the superheterodyne circuit with a crystal rectifier as first detector, or mixer, are widely used in the microwave frequency range. The signal input and the power from a local oscillator of slightly different frequency are mixed in the crystal rectifier. The resultant beat or intermediate frequency is but a small fraction, usually one per cent or less, of the high-frequency signal, which may be thousands of megacycles. The intermediate frequency is therefore low enough to be amplified by more or less conventional vacuum-tube amplifier circuits.

It is clear that the crystal mixer, because it comes first in the receiver, has a major effect on the noise factor,[1] or over-all noise figure. It is also unfortunate but true that crystal rectifiers of widely different quality are, or can be, manufactured by similar processes. Therefore it is necessary to consider carefully what tests should be performed in order to select crystals of superior quality only. The tests have to be simple enough to be made by unskilled personnel on every crystal unit, and yet rigorous enough to prevent acceptance of any inferior units.

The most obvious and simple test that can be made on a crystal rectifier is the determination of its static volt-ampere characteristic, or its forward and inverse resistances. However, attempts to rely on these characteristics in factory testing have ended in failure, because a crystal does not necessarily rectify as well at microwave frequencies as it does at lower frequencies. It has been found necessary to make tests at or near the signal frequency to prevent acceptance of inferior units. On the other hand, if a crystal unit is known originally to have passed radio-frequency tests at the factory, then the static measurements can be and are used successfully to determine when the unit is burned out in service. It is not within the scope of this paper to describe measurements of this type.

One of the radio-frequency tests which needs to be made is the determination of the gain or efficiency with which the crystal converts power from signal frequency to intermediate frequency. "Gain" is a general term applicable to any linear device; an amplifier, for example. A precise definition of gain will be given later. In the case of crystal converters the power gain is almost always less than unity, often being in the range $\frac{1}{4}$ to $\frac{1}{3}$, so that it is more realistic to speak of the "conversion loss" of the crystal, loss being the reciprocal of gain. Instead of expressing loss as a direct power ratio one may alternatively give the loss in decibels, which is ten times the logarithm of this ratio.

The crystal mixer is a linear device in that the radio-frequency signal input and intermediate-frequency output are linearly related even though they are at different frequencies. This linear relation between the input and output currents and voltages is expressible in a set of simultaneous linear equations in exactly the same form as is done for any linear network. From these equations one can predict how the impedance measured at the intermediate frequency should depend on the signal-frequency impedance to which the crystal is connected, or vice versa. Knowledge of the existence of these linear equations is a great help in formulating methods of measuring the conversion loss of the crystal. This general problem of the application of linear network theory in conversion-loss measurements has been discussed in detail by Peterson and Llewellyn.[2]

In addition to making a test of conversion loss, one needs to check the noise-generating ability of each crystal. This may be regarded a radio-frequency test in that the high-frequency local oscillator power is applied to the crystal, and furthermore, the noise-power output depends, among other things, upon the radio-frequency tuning.

In the following sections considerable attention will be given to the general principles of the analysis and measurement of noise in receivers, starting with basic definitions and continuing with the derivation of equations for noise and noise figures of single and cascaded networks. This analysis follows very closely, but with significant modifications, the methods of H. T. Friis.[3] A

* Decimal classification: R261.51×R362.1. Original manuscript received by the Institute, March 6, 1946; revised manuscript received September 12, 1946. This paper is based on work done for the Office of Scientific Research and Development under Contract No. OEMsr-262 with the Massachusetts Institute of Technology.

† Formerly, Radiation Laboratory, Massachusetts Institute of Technology, Cambridge, Massachusetts; now, Research Laboratory, General Electric Company, Schenectady, New York.

[1] D. O. North, "The absolute sensitivity of radio receivers," *RCA Rev.*, vol. 6, pp. 332–344; January, 1942.

[2] L. C. Peterson and F. B. Llewellyn, "The performance and measurement of mixers in terms of linear-network theory." PROC. I.R.E., vol. 33, pp. 458–476; July, 1945.

[3] H. T. Friis, "Noise figures of radio receivers," PROC. I.R.E., vol. 32, pp. 419–422; July, 1944.

discussion of noise in crystal rectifiers is given in which the "noise temperature" is defined and the contribution of crystal noise to the over-all noise figure of the receiver is indicated. The general problem of designing a noise-measuring set is treated in sufficient detail to show how the noise temperature of a crystal rectifier can be measured independently of its other properties.

II. General Theory of Noise Measurements

1. *Available Power*

The term "available power" will be used frequently in the analysis of gain and noise. This term is used in reference to a signal generator or any other device that can be represented according to Thévenin's theorem as a constant-voltage source e_g, in series with an impedance R_g+jX_g. An antenna or the output of a low-level amplifier stage may be taken as examples. The available power is, just as the name implies, the maximum power that can be delivered to a load if the load impedance is suitably adjusted. The optimum load impedance is evidently R_g-jX_g, and the available power is then $e_g^2/4R_g$. If e_g is the voltage corresponding to the desired signal and S_g is the available signal power, then

$$S_g = e_g^2/4R_g. \tag{1}$$

2. *Gain of a Linear Amplifier*

Linear amplification is an important function of the input stages of any radio receiver. In a superheterodyne receiver the input stages may combine the functions of amplification and frequency conversion. The input stages of a superheterodyne receiver are nevertheless linear in

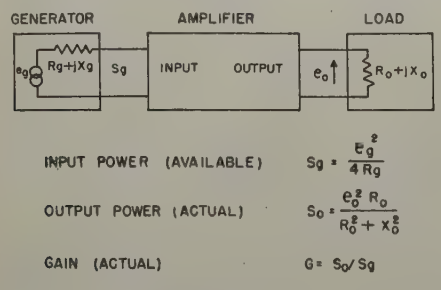

Fig. 1—Circuit showing how input and output power are determined.

that the output is proportional to the input even though it may be at a different frequency. We are primarily interested in the amplification of signal and noise power, and shall therefore use the term "linear amplifier" in a general sense to mean any circuit that amplifies an electrical signal in such a manner that the output is proportional to the input, whether or not the output has the same carrier frequency.

The power gain G of an amplifier is by definition the ratio of output to input signal power. In applying this definition the amplifier is assumed to operate between a generator and a load, each having a specified impedance. This is shown in Fig. 1. The input power which will be considered is that available from the signal generator. One may argue that all of the available power can be utilized with suitable impedance-matching networks between the generator and the amplifier, and that if this is done the maximum gain will be reached and there will be no distinction between available and actual power. However, as will be shown later, one generally strives for minimum noise figure rather than maximum gain, so that the above method of operation is usually not the best. The available power is of primary significance because it characterizes the generator and is unaffected by the usual impedance-matching networks. On the other hand, the output power S_0 is that actually delivered to the load from the amplifier. The reason for considering actual power at this point rather than available power is that an output meter measures actual power and it is intended to express the results of the theory in terms of measurable quantities. The ratio of actual output power to available input power is called "actual" gain to distinguish it from "available" gain, which will be defined later.

From the above definition it is seen that the actual gain of an amplifier depends not only on the amplifier itself but also on the impedances of the generator and load to which it is connected. At first glance this may seem surprising, but on second thought it should not appear at all unreasonable that an amplifier should be rated with reference to the circuits with which it actually has to operate.

3. *Gain of Networks in Cascade*

For a more detailed analysis it may be desirable to divide the amplifier into sections, or separate four-terminal networks connected in tandem. From the discussion leading up to the definition of actual gain of an amplifier it should be clear that, at a junction of two sections, one should consider the available power from the first section rather than the actual power delivered to the second. Accordingly, the gain of any section of the amplifier, except the last one, may be defined as the ratio of the available power output to the available power at its input terminals. This is called "available" gain. The available gain is seen to depend on the impedance of the preceding section but not on the load impedance provided by the following section. The gain to be specified for the last section is "actual" gain, which has already been defined. The actual gain of the entire amplifier is thus equal to the product of the gains of its separate sections.

4. *Noise Originating in the Signal Generator*

It is customary to use a standard-signal generator connected in place of the antenna for testing the performance of a receiver. To make noise measurements one should consider the noise generating characteristics of such a generator as well as its signal-generating characteristics. The noise generated in the output attenuator

of a signal generator is for all practical purposes the same as that which would be generated by thermal agitation in any equivalent resistor. The mean-square noise voltage, in a narrow frequency band df, developed across a resistor R_g on open circuit as a result of thermal agitation alone is given by the well-known thermal-agitation-noise formula

$$d\bar{e}^2 = 4kTR_g df \tag{2}$$

where

k = Boltzmann's constant = 1.38×10^{-23} joule per degree Kelvin

T = absolute temperature, Kelvin.

Inasmuch as the noise voltage depends on the temperature of the resistor, it is evident that one must specify a standard temperature if the test conditions are to be uniform. It is convenient to specify a temperature T_0 of 290 degrees Kelvin, both because this is often a reasonable approximation to the ambient temperature at which measurements are made and because, for this value of temperature, one obtains the following simple result

$$kT_0/\epsilon = V_s = 1/40 \text{ volt}, \tag{3}$$

where

ϵ = electronic charge = 1.60×10^{-19} coulomb.

The available noise power from a resistor at temperature T_0 in a frequency band df is equal to the mean-square noise voltage divided by $4R_g$.

$$dN_g = kT_0 df. \tag{4}$$

This equation shows the important fact that noise power is independent of the resistance of the signal generator. For this reason it is possible to use an analysis based on the comparison between signal and noise power without any explicit consideration of impedance. To be sure, specific impedances are implied in the definitions of gain and other quantities, but these impedances do not appear in the calculations.

5. *Noise Figure*

If dN_0 is the noise output (actual) in a narrow frequency band df which includes the frequency of the output signal S_0, and if dN_g is the noise input (available) in a frequency band of the same width df, but including the frequency of the input signal S_g, one finds that the ratio dN_0/S_0 is greater than dN_g/S_g by a factor F, called the noise figure of the amplifier.

$$\frac{dN_0}{S_0} = F\frac{dN_g}{S_g}, \tag{5}$$

or, remembering that $S_0/S_g = G$,

$$dN_0 = FGkT_0 df. \tag{6}$$

This definition takes account of the possibility that S_g and S_0 may have different carrier frequencies.

A complication arises in the case of "image-frequency" response of a superheterodyne receiver, for which there may be more than one possible input signal frequency that will give the same output frequency. This can be an important matter in a microwave receiver because the signal and image frequencies are relatively close together. However, an analysis that takes account of image-frequency response will not be attempted in this paper. For simplicity, we shall assume that there is only one possible input frequency corresponding to a given output frequency, and vice versa. It turns out that the noise figure of a receiver can actually be improved by suppressing image response but this is a separate problem.[4]

An alternate expression for noise output is

$$dN_0 = dN_0' + dN_0'' \tag{7}$$

where dN_0' represents Johnson noise which originates in the generator and dN_0'' represents noise which originates in the amplifier. From the definition of gain we have

$$dN_0' = GkT_0 df. \tag{8}$$

Then from (6)

$$F = dN_0/dN_0', \tag{9}$$

or

$$F = 1 + \frac{1}{GkT_0}\frac{dN_0''}{df}. \tag{10}$$

In this way the noise figure is determined by the spurious noise which originates in the amplifier itself. This formula also indicates that if a different standard had been chosen for T_0, the resulting value of F minus one would have been inversely proportional to this temperature.

6. *Integrated Noise Output and Noise Figure*

The noise output dN_0 and noise figure F resemble the gain G in that they are variables depending on the output frequency[5] and, in general, on the impedances of the generator and load. An exception to this rule is that, in the case of a high-gain amplifier, the dependence of noise figure on the load impedance may be so small as to be quite negligible. The total noise output is obtained by integrating (6) with respect to output frequency.

$$N_0 = kT_0\int_0^\infty FG df. \tag{11}$$

There is no question about the convergence of (11) because it represents actual power in a physical system.

Similarly, that part of the output noise power that originates in the generator can be found by integrating (8).

[4] D. O. North, Discussion on "Noise figures of radio receivers," by H. T. Friis, Proc. I.R.E., vol. 33, pp. 125–126; February, 1945.

[5] This interpretation was proposed by the author in Radiation Laboratory Report 61-11, January 30, 1943, listed as report no. PB12126 by the Office of Technical Services, Department of commerce.

$$N_0' = kT_0 \int_0^\infty G df. \tag{12}$$

In a manner quite analogous to (9) one can define the integrated noise figure F' as the ratio of N_0 to N_0', or

$$F' = \frac{N_0}{N_0'} = \frac{\int FG df}{\int G df}. \tag{13}$$

If the bandwidth B of the amplifier is defined in the following manner

$$B = \frac{1}{G_{\max}} \int G df, \tag{14}$$

where $G_{\max}$ is the maximum of the gain versus frequency characteristic, then (13) reduces to

$$F' = \frac{N_0}{kT_0 B G_{\max}}. \tag{15}$$

This gives F' in terms of measurable quantities and agrees with the definition of noise figure by Friis.

7. *Noise Diode Theory*

Now suppose that the signal generator is not actually at the temperature T_0 but at some other temperature equal to t_a times T_0, where t_a is a dimensionless quantity which may be either greater or less than unity. That part of the noise output which originates in the amplifier is unaffected by the value of t_a and is thus equal to dN_0''. The total integrated noise output may be expressed in a form analogous to (7).

$$N_{0a} = N_{0a}' + N_0'', \tag{16}$$

where

$$N_{0a}' = kT_0 \int t_a G df,$$

$$N_0'' = N_0 - N_0' = kT_0 \int (F - 1) G df.$$

Then

$$N_{0a} = kT_0 \int (F - 1 + t_a) G df. \tag{17}$$

The noise-power output of the generator can be changed by changing its physical temperature or, artificially, by passing current through it from an emission-saturated diode.[6] Such a generator has an effective or "noise" temperature greater than its physical temperature. To show this, we shall consider that the signal generator resistance is R_g with a physical temperature T_a and with a current I from an emission limited diode passing through it.

The mean-square noise current from the diode in a frequency band df is given in theory by the Schottky formula:

$$d\overline{i^2} = 2\epsilon I df, \tag{18}$$

and the mean-square voltage across the resistor is

$$d\overline{e^2} = (4kt_a T_0 R_g + 2\epsilon I R_g^2) df. \tag{19}$$

The available noise power is the mean-square voltage divided by $4R_g$. This is

$$\begin{aligned} dN_g &= kT_0 \left(t_a + \frac{\epsilon I R_g}{2kT_0} \right) df \\ &= kT_0 \left(t_a + \frac{IR_g}{2V_e} \right) df = kT_b df. \end{aligned} \tag{20}$$

The last equality is taken as a definition of T_b, which is called the noise temperature of the generator. The value of T_b may be normalized by dividing by T_0 and the resulting dimensionless ratio is called the noise temperature ratio, designated by the symbol t_b. The noise temperature ratio of the resistor with diode current is

$$t_b = t_a + \frac{IR_g}{2V_e} = t_a + 20IR_g. \tag{21}$$

If the noise output from the amplifier is N_{0b} when the diode current is turned on and N_{0a} when it is turned off, we have, from (17), assuming constant t_a and t_b,

$$\frac{N_{0b} - N_{0a}}{t_b - t_a} = kT_0 \int G df. \tag{22}$$

Solving (17) for $\int FG df$ and substituting in (13), we have

$$\begin{aligned} F' &= \frac{(1 - t_a) \int G df + \dfrac{N_{0a}}{kT_0}}{\int G df} \\ &= 1 - t_a + (t_b - t_a) \frac{N_{0a}}{N_{0b} - N_{0a}}, \end{aligned} \tag{23}$$

or

$$F' = 1 - t_a + 20IR_g \frac{N_{0a}}{N_{0b} - N_{0a}}. \tag{24}$$

If the current I is adjusted so that N_{0b} is twice N_{0a}, and if t_a may be taken equal to unity, then (24) reduces to

$$F' = 20IR_g. \tag{25}$$

Equations (23) and (24) provide a method of measuring noise figure without determining bandwidth or gain, and without restricting the physical temperature of the generator. For example, a noise generator whose resistance R_g is adjusted to equal that of the signal source is connected in place of the latter. Some device capable of indicating the relative noise output power is

[6] The use of diodes for measuring receiver noise figures and crystal noise was demonstrated by E. J. Schremp in December, 1942. For earlier noise measurements with diodes see D. O. North, "Fluctuations in space-charge-limited currents at moderately high frequencies; Part II—Diodes and negative-grid triodes (continued)," *RCA Rev.*, vol. 5, pp. 106–124; July, 1940.

connected to the output of the receiver. First, with the diode plate voltage turned off, the output power N_{0a} is observed. Then the plate voltage is turned on, the filament current is adjusted to a convenient value, and a noise output N_{0b} is observed with a plate current I flowing in the diode. The noise figure can be found by substituting these values into (24). Inasmuch as only the ratio of N_{0a} to $N_{0b}-N_{0a}$ appears, it is not necessary to measure the absolute values of N_{0a} or N_{0b} but only their ratio. The only other requirement is that the noise temperature of the generator be uniform and predictable over the frequency band of the amplifier. This means that the resistance R_g in (24) should be constant over this band of frequency and that the diode should be connected to this resistance in such a way as to minimize lead impedances. When these conditions are met, the diode method of noise-figure measurements has advantages over the method indicated in (15) with respect to accuracy, simplicity, and economy.

Various other schemes, based principally on (25), have been devised for using the noise diode in making noise-figure measurements. Some of these require an accurate power-output meter. Other methods relax on the accuracy of the output meter but require an accurate 3-decibel attenuator. Still others require merely a variable uncalibrated attenuator or volume control with any sort of output meter. These schemes will not be treated in detail here.

The noise diode is, therefore, a very useful device for absolute measurements of effective noise figure of an amplifier at frequencies up to about 300 megacycles. Above this frequency the lead impedances of existing tubes become large enough so that an accurate absolute calibration is difficult. Diodes and other kinds of noise generators are nevertheless useful for measurement at the higher frequencies when an absolute calibration is not required.

Even at lower frequencies the noise output of the diode may not be given accurately by (18) unless the plate current is entirely temperature-limited, in which case the current is nearly independent of the plate voltage. In this respect diodes with tungsten cathodes are generally superior to those with oxide-coated cathodes.

8. *Noise in Cascaded Networks*

The next step in the analysis of noise in a linear amplifier is to treat the amplifier as a cascade of sections, or four-terminal networks, in exactly the same manner as was done for the analysis of gain. An amplifier with two sections, taken as an illustration, is shown in Fig. 2. The available noise and signal power from the output of the first section are dN_1 and S_1, respectively. The available input power to the first section and the actual output power from the second section are designated by the same notation as heretofore. The gain G_1 of the first section, the gain G_2 of the second section, and the over-all gain G are given as follows:

$$G_1 = \frac{S_1}{S_g}; \qquad G_2 = \frac{S_0}{S_1}; \qquad G = G_1G_2 = \frac{S_0}{S_g}. \tag{26}$$

The noise output dN_0 may be resolved in two components dN_2'' and dN_2', originating respectively in the second section and in circuits preceding this section. From the definition of gain we have

$$dN_2' = G_2 d\,N_1. \tag{27}$$

Then

$$dN_2'' = dN_0 - G_2 dN_1. \tag{28}$$

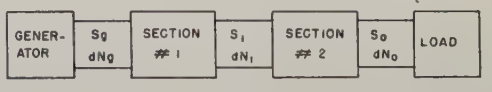

S_g, S_i, dN_g AND dN_i ARE AVAILABLE SIGNAL AND NOISE POWER

S_0 AND dN_0 ARE ACTUAL POWER.

Fig. 2—Circuit showing division of amplifier into two sections.

The noise figure of the second section may be expressed in terms of the noise originating in that section as indicated by (10).

$$F_2 = 1 + \frac{1}{G_2 kT_0}\left(\frac{dN_0}{df} - G_2\frac{dN_1}{df}\right). \tag{29}$$

Making use of (6) we obtain

$$\left.\begin{aligned} \frac{dN_0}{df} &= FG_1G_2kT_0 \\ \frac{dN_1}{df} &= F_1G_1kT_0 \end{aligned}\right\}. \tag{30}$$

Then

$$F_2 = 1 + FG_1 - F_1G_1. \tag{31}$$

Or, if F_2 is given and one wants to determine the over-all noise figure,

$$F = F_1 + \frac{F_2 - 1}{G_1}. \tag{32}$$

Substituting this value of F in (13) gives

$$F' = \frac{\int G_2(F_1G_1 + F_2 - 1)df}{\int G_1G_2 df}. \tag{33}$$

If the second section has a narrow pass band relative to the first section, then F_1 and G_1 may be assumed constant over the significant part of the range of integration and (33) reduces to

$$F' = F_1 + \frac{F_2' - 1}{G_1}. \tag{34}$$

Equation (34) should not be confused with (32). The similarity in form should not obscure the fact that the integrated noise figures in (34) have an entirely different interpretation from the frequency-dependent noise figures in (32). Furthermore, the derivation of (34) indicates that this equation is not generally valid. It fails when the bandwidth of the first section is comparable to or less than that of the rest of the amplifier, in which case the correct noise figure can only be obtained by performing the integrations indicated in (33).

Solving (34) for F_1 gives

$$F_1 = F' - \frac{F_2' - 1}{G_1}. \tag{35}$$

This expresses F_1 in terms of measurable quantities and provides a method of determining the noise figure of the first section of the amplifier. An integrated noise figure for any section but the last can not be obtained, because the integral indicated in (11) does not converge if applied to available power instead of actual power.

III. Crystal Noise and its Measurement

1. *Sources of Noise*

The sources of noise in crystal rectifiers are not completely understood. It is fairly well established, however, that noise can originate in a crystal in a manner very similar to shot noise in a thermionic diode. But in some cases the noise originating in the crystal greatly exceeds that which can be accounted for by shot noise. The primary purpose of testing the noise of each crystal unit in the factory is to eliminate these noisy units.

The local oscillator also generates noise at the signal frequency, thereby contributing to the noise output of the crystal. This source of noise cannot be blamed on the crystal, but has to be considered in the design of a testing apparatus or in the design of a microwave receiver. Several schemes have been devised for suppressing noise from this source, a filter commonly being used in the crystal-testing apparatus.

Regardless of its origin, the noise output of a crystal depends to a great extent on the nature of the circuit in which the crystal is incorporated. The dependence of noise on the circuit parameters has not been studied in detail, nor is it within the scope of this paper to do so. Instead, we shall show how the noise power can be measured, once the operating conditions have been specified.

2. *Noise-Temperature Ratio of a Crystal*

The noise-temperature ratio of the crystal, designated by the symbol t_c, is defined as the ratio of the available noise-power output at the intermediate frequency to that from a resistor at the standard temperature T_0. Then, if the crystal mixer is to be the first section in an amplifier, the noise-power output dN_1 is

$$dN_1 = t_c k T_0 df. \tag{36}$$

The value of t_c is, as a rule, greater than unity, although it is not inconceivable that it might be less. The noise temperature ratio of good crystals, of types used as mixers in microwave receivers, is usually quite low, say in the range 1.0 to 2.0. The noise-temperature ratio is alternatively called output-noise ratio.

Equation (6) gives the noise output of an amplifier in terms of its gain and noise figure. The noise output of the first section bears the same relation to the gain and noise figure of that section, and a comparison between (6) and (36) yields t_c in terms of the gain and noise figure of the crystal.

$$t_c = F_1 G_1. \tag{37}$$

Equation (34) may be rewritten showing how the over-all noise figure of the receiver depends on the noise temperature of the crystal.

$$F' = \frac{F_2' + t_c - 1}{G_1}. \tag{38}$$

Equations (34) and (38) indicate that by itself the gain G_1 (or loss $1/G_1$), is not sufficient to determine how a given crystal unit will contribute to the over-all noise figure of a receiver. Neither is the noise figure F_1, nor the noise temperature ratio t_c. Two of these quantities are needed and for this reason the tests customarily made on crystal rectifiers include separate measurements of gain (or loss) and noise temperature.

3. *General Aspects of Crystal Noise Measurements*

If either a crystal or an artificially noisy resistor is connected to the input of an amplifier, the noise-power output is that given by (17), in which the values of F and G are those of the amplifier, and in which the appropriate value of noise temperature ratio, either t_b or t_c, is substituted for t_a. The noise-power output of the amplifier depends as much on the impedance of the crystal as on its noise temperature, inasmuch as F and G are variables themselves depending on this impedance. The diode generator is a noise source whose impedance can be adjusted by exchanging resistors and whose noise temperature can be varied by controlling the cathode emission current. Its noise temperature ratio is given by (21) and thus it can be used to calibrate the amplifier, thereby determining how the noise-power output does depend on both the noise temperature and impedance of the crystal.

It is often desired to determine the noise temperature of the crystal by a single measurement independently of its impedance. This can be done if the amplifier is designed so that the output is not affected by differences in the conductance of the crystal, because the differences in susceptance of different crystal units measured at the intermediate frequency are much smaller than the differences in conductance. A careful analysis of the input circuit indicates that such a design is possible.

4. Analysis of Input Circuit

The analysis of noise in an amplifier will be given primarily from the point of view of the design of an amplifier suitable for noise measurements of crystals. Therefore, we shall start with the simplest possible amplifier, namely one with negligible feedback, or induced grid noise,[7] and shall discuss the design of the desired input circuit for such an amplifier. It will be inferred that similar circuits can be made to work with amplifiers that do have feedback and induced grid noise. Experimentally, this has been found to be true.

Consider a multistage amplifier without feedback or induced grid noise and let the grid and cathode of the first tube be the input terminals. The noise-power output of this amplifier can be represented as the sum of two components, one proportional to the mean-square noise voltage at the input terminals and the other constant and equal to the noise-power output when the input is short-circuited. This representation is possible because, under the assumed conditions, the noise voltage at the grid and the noise generated elsewhere in the amplifier are statistically independent.

It will further be assumed that the amplifier has an input conductance g_2. This conductance may take the form of a physical resistor or of residual circuit losses or both. The noise output may then be expressed as follows:

$$dN_0 = u(g_2\overline{de_1^2} + vkT_0df), \tag{39}$$

where u and v are arbitrary functions of frequency and $\overline{e_1^2}$ is the mean square input noise voltage.

Now assume that the amplifier input is connected to an admittance g_1+jb_1 having a noise-temperature ratio t_c. The noise-temperature ratio of the conductance g_2 is taken to be t_2. In this case the mean-square input noise voltage $\overline{de_1^2}$ can be determined with reference to Fig. 3.

Fig. 3—Simplified circuit for determining input noise voltage.

The noise-current generators i_1 and i_2 in Fig. 3 are given as follows:

$$\left.\begin{aligned}\overline{di_1^2} &= 4kT_0t_cg_1df,\\ \overline{di_2^2} &= 4kT_0t_2g_2df.\end{aligned}\right\} \tag{40}$$

Then

$$\overline{de_1^2} = \frac{\overline{di_1^2} + \overline{di_2^2}}{|y|^2} = \frac{4kT_0(t_cg_1 + t_2g_2)}{(g_1 + g_2)^2 + b_1^2}df. \tag{41}$$

Putting (41) in (39) gives

$$dN_0 = ukT_0\left[\frac{4g_2(t_cg_1 + t_2g_2)}{(g_1 + g_2)^2 + b_1^2} + v\right]df. \tag{42}$$

The integrated noise-power output is then

$$N_0 = kT_0\int_0^\infty u\left[\frac{4g_2(t_cg_1 + t_2g_2)}{(g_1 + g_2)^2 + b_1^2} + v\right]df. \tag{43}$$

The integration may be simplified if the bandwidth of the amplifier is small compared to that of the input circuit. In this case b_1, as well as g_1, g_2, t_1, and t_2, may be assumed to be constant over the range of integration. Then

$$N_0 = kT_0\left[\frac{4g_2(t_cg_1 + t_2g_2)}{(g_1 + g_2)^2 + b_1^2}\int udf + \int uvdf\right]. \tag{44}$$

This can be expressed in simpler form if we define U and V so that

$$U = kT_0\int udf; \qquad UV = kT_0\int uvdf. \tag{45}$$

Then

$$N_0 = U\left[\frac{4g_2(t_cg_1 + t_2g_2)}{(g_1 + g_2)^2 + b_1^2} + V\right]. \tag{46}$$

This equation shows specifically how the output noise depends on the admittance g_1+jb_1 as implied in (17).

In a crystal-testing apparatus it may be desirable to connect a nondissipative coupling network between the crystal and the input to the amplifier. In this case the impedance g_1+jb_1 will take the general form shown in Fig. 4.

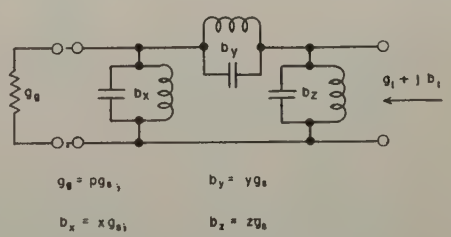

Fig. 4—Input coupling circuit.

The most probable or standard value of crystal conductance is designated g_s, and all the elements in the circuit are normalized with respect to g_s. The factors of proportionality are p, x, y, and z as indicated in Fig. 4. From analysis of this circuit we obtain the following values for g_1 and b_1.

$$g_1 = g_s\frac{py^2}{p^2 + (x + y)^2}, \tag{47}$$

$$b_1 = g_s\left[\frac{xy(x + y) + p^2y}{p^2 + (x + y)^2} + z\right]. \tag{48}$$

The derivative of (46) with respect to p may be put in the following form:

[7] D. O. North and W. R. Ferris, "Fluctuations induced in vacuum-tube grids at high frequencies," Proc. I.R.E., vol. 29, pp. 49–50; February, 1941.

$$\frac{dN_0}{dp} = \frac{\partial N_0}{\partial g_1}\frac{dg_1}{dp} + \frac{\partial N_0}{\partial b_1}\frac{db_1}{dp}. \tag{49}$$

In order to make the noise output insensitive to differences in conductance one may choose values for x, y, and z such that this derivative is zero for all values of t_c when the crystal conductance equals g_s, or $p=1$.

Because only the square of b_1 appears in (46), the noise output is an even function of b_1 and if $b_1=0$, then $\partial N_0/\partial b_1=0$. Setting (48) equal to zero, we have

$$z = -\frac{y + xy(x+y)}{1+(x+y)^2}. \tag{50}$$

By differentiating (47) one obtains

$$\frac{dg_1}{dp} = \frac{y^2[(x+y)^2 - p^2]}{[p^2+(x+y)^2]^2} = \frac{y^2[(x+y)^2-1]}{[1+(x+y)^2]^2}. \tag{51}$$

This is zero when

$$x + y = \pm 1. \tag{52}$$

Therefore, by choosing x, y, and z so as to satisfy (50) and (52), one can make both parts of the derivative indicated by equation (49) equal to zero. The values of x, y, and z can also be chosen so as to satisfy a third condition; namely, that $g_1=ng_s$ when $p=1$. In this case (47) becomes

$$n = \frac{y^2}{1+(x+y)^2}. \tag{53}$$

By simplifying and solving equations (50), (52), and (53) and assuming all possible combinations of plus and minus signs, one obtains the following four solutions:

$$x = +\sqrt{2n} - 1;\ y = -\sqrt{2n};\ z = +\sqrt{2n} - n, \tag{54a}$$
$$x = +\sqrt{2n} + 1;\ y = -\sqrt{2n};\ z = +\sqrt{2n} + n, \tag{54b}$$
$$x = -\sqrt{2n} + 1;\ y = +\sqrt{2n};\ z = -\sqrt{2n} + n, \tag{54c}$$
$$x = -\sqrt{2n} - 1;\ y = +\sqrt{2n};\ z = -\sqrt{2n} - n. \tag{54d}$$

The networks represented by (54a) and (54b) are analogous in some respects to transmission lines of $\frac{1}{8}$ and $\frac{3}{8}$ wavelength, respectively. Solutions (54c) and (54d) are negatives of the first two, obtained by reversing the sign of all susceptances.

If (54b) is selected as an example, and if the values of x, y, and z are substituted in (47) and (48), the result is

$$g_1 = ng_s\frac{2p}{p^2+1}, \qquad b_1 = ng_s\frac{p^2-1}{p^2+1}. \tag{55}$$

If one lets $g_2=mng_s$ and substitutes these values in (46), one obtains

$$N_0 = U\left[\frac{4m(p^2+1)[2pt_c + m(p^2+1)t_2]}{[2p+m(p^2+1)]^2 + (p^2-1)^2} + V\right]. \tag{56}$$

If the crystal admittance is matched to the amplifier, i.e., if $g_1=g_2$ when $p=1$, then $m=1$ and (56) reduces to

$$N_0 = U\left[\frac{4p}{(p+1)^2}(t_c - t_2) + 2t_2 + V\right]. \tag{57}$$

The noise output given by (57) is plotted as a function of p for different values of t_c in Fig. 5. In this figure the

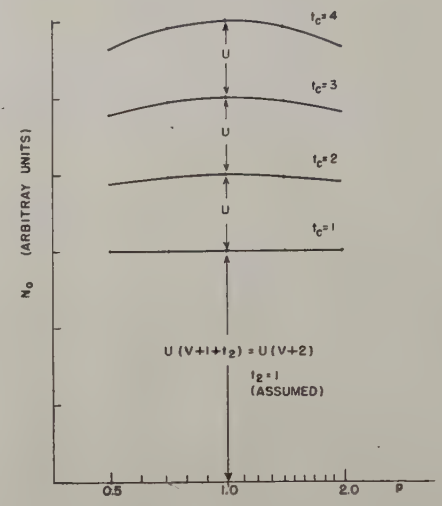

Fig. 5—Output noise power as given by equation (57).

value $t_2=1$ is assumed. The noise output is completely independent of the conductance, pg_s, of the crystal for only one value of t_c, namely $t_c=t_2$. For other values of t_c the fraction $4p/(p+1)^2$ has to be considered. This fraction has the value unity when $p=1$ and is almost unity in a relatively wide range of p. For example, if $p=\frac{1}{2}$ or 2, the ratio is just 8/9. Therefore, if p is assumed to be within this range, it is a fair approximation to set the fraction involving p equal to unity and (57) becomes

$$N_0 \cong U(t_c + t_2 + V). \tag{58}$$

Inasmuch as U, t_2, and V are constants, (58) indicates that the output meter can be directly calibrated with respect to noise temperature of the crystal independently of the crystal conductance. This calibration is made by connecting in place of the crystal the noise-diode generator with a resistance R_g equal to $1/g_s$ and determining the output reading for different values of t_b as given by (21). This method is equally accurate for any sort of output meter, regardless of whether it indicates something proportional to output power or to any arbitrary function of power.

As a check on the adjustment of the input-coupling circuit one can also make similar calibrations using different values of R_g, say, $R_g=1/pg_s$, where p is greater or less than unity. When the data so obtained are plotted in a manner similar to Fig. 5, the resulting curves should be symmetrical about the line $p=1$, assuming that a logarithmic scale is chosen for p. If the curves are not symmetrical, the values of b_x, b_y, and b_z have not been correctly adjusted. The final adjustment of these reactances is made by a trial-and-error method until the resulting curves are symmetrical about $p=1$.

We have shown that in principle it is possible to design a measuring circuit such that the noise-power output is unaffected by small differences in crystal conductance. But we have assumed the use of an amplifier without feedback or induced grid noise. In practice both these effects are encountered; therefore, the design which has been derived is not strictly appropriate. However, it has been demonstrated experimentally that the trial-and-error method of tuning the coupling network does work successfully even when feedback and induced grid noise are present. Noise-measuring sets based on this circuit and using the diode for calibration are widely used for factory testing of crystal-rectifier units suitable for microwave mixers.

In the circuit which we have considered, the noise output still depends to a certain extent on the susceptance of the crystal but, as previously pointed out, the differences in the susceptance are not as great as the differences in conductance. Feedback in the intermediate-frequency amplifier has been used with success to reduce the variations of output noise resulting from susceptance differences while retaining the other desirable features, but an analysis of this problem will not be given here.

In writing this paper the author has made free use of both published and unpublished work of a number of individuals in the Radiation Laboratory and in other laboratories. The earliest work on crystal measurements (as distinguished from measurements of the complete receiver) at the Radiation Laboratory was done by W. M. Breazeale, who had a prominent part in formulating some of the basic techniques.

Graphical Analysis of Cathode-Biased Degenerative Amplifiers*

WILLIAM. A. HUBER†, MEMBER, I.R.E.

Summary—**A method of graphical analysis by which it is possible to predict the performance of cathode-follower and plate-resistance-loaded, cathode-degenerative triode amplifiers is given. The method is based on data supplied by the average plate characteristic curves. Several numerical examples are given illustrating various points of the text. It is shown that the graphical method may be advantageously used in design problems requiring the selection of the correct cathode resistor for a given signal input and bias condition.**

Introduction

AFTER design theory has been applied to a resistance-loaded, cathode-degenerative triode amplifier and the circuit constants determined, it is generally desirable to analyze the circuit design. For this purpose graphical analysis can be used to an advantage because it is possible to determine the static operating potentials and the dynamic signal swings by reference to the plate characteristic curves. It is the purpose of this paper to describe a graphical method of analysis based on data supplied by the average plate characteristic curves for predicting the performance of resistance-loaded, cathode-degenerative triode amplifiers.

Cathode-Follower Amplifier

The cathode-follower amplifier has been treated in the literature[1-5] on various occasions, so it is assumed that the reader is familiar with its operation and purpose Fig. 1 shows the basic cathode-follower circuit. The input voltage e_s is fed to the control grid and the output voltage e_k is taken off the cathode. The total output load is assumed to be resistive and is represented in Fig. 1 as R_k. The input voltage equals

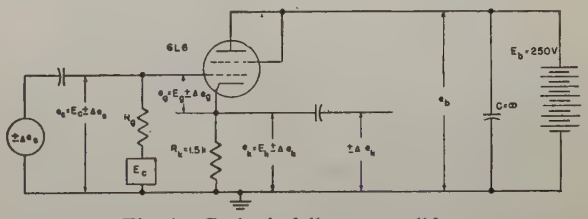

Fig. 1—Cathode-follower amplifier.

$$e_s = e_g + e_k. \tag{1}$$

If voltages e_g and e_k of (1) are plotted as functions of plate current on the plate characteristic curves, the solution of (1) over the current range recorded on the plate characteristics can be obtained directly from these curves. To construct the required curves for the solution of (1) when the effects of circuit reactances and electron transit time are not considered, the following data

* Decimal classification: R363.23. Original manuscript received by the Institute April 8, 1946; revised manuscript received, August 23, 1946.

† Signal Corps Engineering Laboratories, Bradley Beach, N. J.

[1] A. Preisman, "Some notes on video-amplifier design," *RCA Rev.*, pp. 430–432; April, 1938.

[2] C. E. Lockhart, "The cathode follower," *Electronic Eng.* (London), pp. 287–293, December, 1942; pp. 375–382; February, 1943; pp. 21–24; June, 1943; pp. 145–147; September, 1943.

[3] D. L. Shapiro, "The graphical design of cathode-output amplifiers," PROC. I.R.E., vol. 32, pp. 263–268; May, 1944.

[4] Kurt Schlesinger, "Cathode-follower circuits," PROC. I.R.E., vol. 33, pp. 843–855; December, 1945.

[5] Sidney Moskowitz, "Cathode followers and low-impedance plate loaded amplifiers," *Communications*, vol. 25, pp. 51; March, 1945.

should be known: (1) type of tube to be used; (2) circuit connections; (3) plate voltage E_b applied to the tube; and (4) ohmic value of the cathode load resistor R_k.

A procedure for constructing the required curves, which are identified in Fig. 2 as curves 1, 2, and 3, is tabulated below.

Curve 1: The load line is a straight line constructed by joining point $e_b = E_b$ on the voltage axis with point $i_p = E_b/R_k$ on the current axis.

Curve 2: The dynamic plate-current line is a plot of plate current i_p versus grid voltage $-e_g$. The values of plate current plotted are those corresponding to the intersection of load line, curve 1, and the $-E_g$ family of curves. The current scale used is that of the plate characteristics, while any convenient grid-voltage $-e_g$ scale can be chosen for abscissa; the only requirement is that zero grid voltage must correspond to zero plate voltage.

Curve 3: The cathode load line is a linear plot of plate current i_p versus output voltage e_k and is constructed by drawing a straight line from the origin through any point on the characteristics satisfying the relationship $i_p = e_k/R_k$. The current scale used is that of the plate characteristics, while the voltage scale is the same as that chosen for the grid voltage $-e_g$ except for a change in sign.

Before illustrating the application of (1) to Fig. 2, it will be convenient to express the instantaneous total voltages as each consisting of a quiescent voltage on

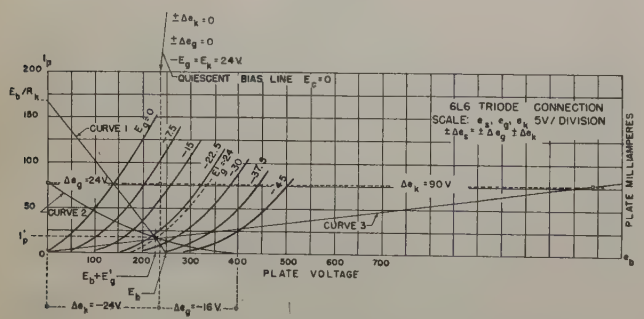

Fig. 2—Graphical calculation with zero applied bias.

which the signal voltage is superimposed. The instantaneous total voltages between the various elements are as follows:

Between grid and ground

$$(e_s = E_c \pm \Delta e_s). \tag{2}$$

Between grid and cathode

$$(e_g = E_g \pm \Delta e_g). \tag{3}$$

Between cathode and ground

$$(e_k = E_k \pm \Delta e_k). \tag{4}$$

Substituting (2), (3), and (4) in (1), we obtain

$$E_c \pm \Delta e_s = (E_g \pm \Delta e_g) + (E_k \pm \Delta e_k). \tag{5}$$

The first step in the application of (5) to Fig. 2 is to determine the quiescent voltage of the grid and cathode by assuming the signal voltages equal to zero. For this condition (5) reduces to

$$E_c = E_g + E_k. \tag{6}$$

In general there are three values of E_c in (6) which are of interest. They are $E_c = 0$, $E_c =$ negative value, and $E_c =$ positive value. When $E_c = 0$ the operation of the stage is referred to as the zero applied bias condition, in which case (6) reduces to

$$-E_g = E_k. \tag{7}$$

Referring to Fig. 2 it will be seen that (7) is satisfied for a plate-current and bias-voltage condition corresponding to the intersection of curves 2 and 3. A line drawn perpendicular to the voltage axis through the intersection point of curves 2 and 3 is referred to as the quiescent bias line when $E_c = 0$. Signal voltages $\pm\Delta e_g$ and $\pm\Delta e_k$ are determined by reference to the quiescent bias line and curves 2 and 3. The instantaneous value of grid voltage $\pm\Delta e_g$ is measured between the quiescent bias line and curve 2, the instantaneous value of output voltage $\pm\Delta e_k$ is measured between the quiescent bias line and curve 3, and the instantaneous value of input voltage $\pm\Delta e_s$ is measured between curves 2 and 3 and is equal to

$$\pm \Delta e_s = \pm \Delta e_g \pm \Delta e_k. \tag{8}$$

Values of input voltage above the intersection point of curves 2 and 3 are positive, i.e.,

$$\Delta e_s = \Delta e_g + \Delta e_k \tag{9}$$

while values of input voltage below the intersection of curves 2 and 3 are negative, i.e.,

$$-\Delta e_s = -\Delta e_g - \Delta e_k. \tag{10}$$

An example of the calculated performance of a cathode-follower amplifier operated with zero applied bias is given in the Appendix, example 1.

If a negative bias voltage $-E_c$ is applied to the grid of the tube shown in Fig. 1 it will alter its quiecsent bias voltage. To account for this quiescent bias change in the graphical analysis diagram, it will be necessary to alter the position of the quiescent bias line shown in Fig. 2. Referring to (6) it can be seen that if the applied bias voltage $\pm E_c$ is not equal to zero, quiescent grid voltage $-E_g$ can never equal quiescent cathode voltage E_k, therefore, it will be necessary to construct two quiescent bias lines for analytical purposes when dealing with an applied bias condition. An illustration of this type of graphical construction is shown in Fig. 3. It will be noted that the quiescent cathode-voltage and quiescent grid-voltage lines are positioned on the voltage axis so as to effect a voltage scale separation equal to the applied grid-bias voltage $-E_c$. The value of the applied

grid bias $-E_c$ is measured between curves 2 and 3 below the intersection point. An example of the calculated performance of a cathode-follower amplifier operated with negative applied bias is given in the Appendix, example 2.

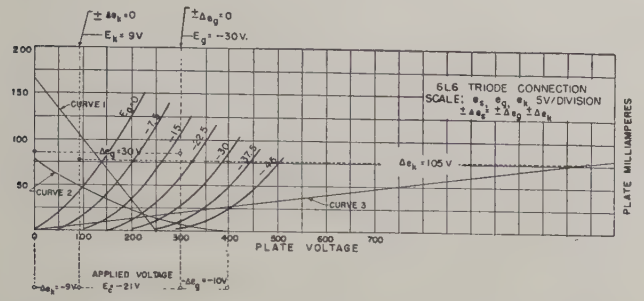

Fig. 3—Graphical calculation with a negative applied bias.

If a positive bias voltage E_c is applied to the grid of the tube shown in Fig. 1, it will alter the position of the quiescent voltage line. Referring to Fig. 4, the quiescent cathode-voltage and quiescent grid-voltage lines are positioned on the voltage axis so as to effect a voltage scale separation equal to the applied grid-bias voltage E_c which for this condition is measured between curves 2 and 3 above their intersection point. An example of the calculated performance of a cathode-follower amplifier operated with positive applied bias is given in the Appendix, example 3.

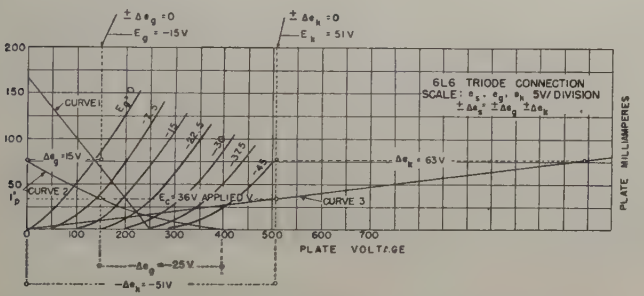

Fig. 4—Graphical calculation with a positive applied bias.

If it is found desirable to alter the quiescent grid bias, and other considerations do not dictate the ohmic value of the cathode resistor, it is convenient to alter the bias by the proper selection of this resistor. A numerical example illustrating the selection of the required cathode resistor to obtain a given bias is given in the Appendix, example 4.

If it is desired to decrease the bias on a cathode follower by returning the grid to a tap on the cathode resistor, the position of the tap to obtain this bias can be determined as illustrated in the Appendix, example 5.

Graphical Analysis of Plate-Resistance-Loaded, Cathode-Degenerative Triode Amplifier

To predict the performance of a plate-resistance-loaded, cathode-degenerative triode amplifier, as shown in Fig. 5, by graphical analysis when the effects of circuit reactances and electron transit time are not considered, the following data should be known: (1) type of tube to be used; (2) circuit connections; (3) plate voltage E_b applied to the tube; (4) ohmic value of the plate load resistor R_L; and (5) ohmic value of the cathode load resistor R_k.

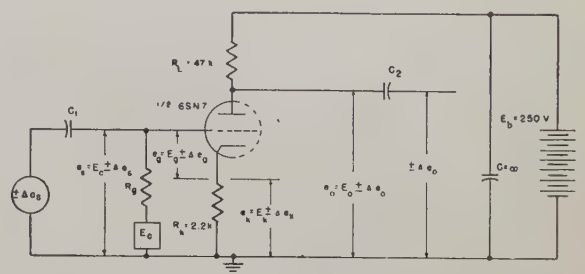

Fig. 5—Resistance-loaded amplifier.

To proceed with the graphical analysis of the plate-resistance-loaded, cathode-degenerative triode amplifier it is necessary to draw four curves on the plate characteristics, which are identified in Fig. 6 as curves 1, 2, 3, and 4.

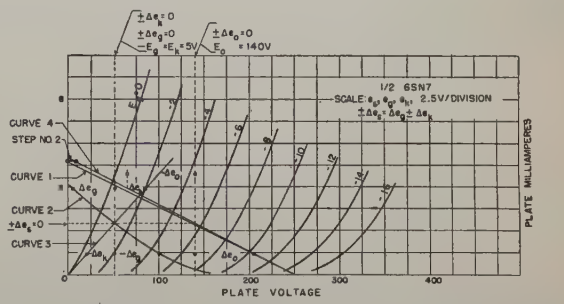

Fig. 6—Graphical calculation of a resistance-loaded amplifier.

Curve 1: The load line is a straight line constructed by joining point $e_b = E_b$ on the voltage axis with point $i_p = E_b/R_L + R_k$ on the current axis.

Curve 2: The dynamic plate current line is plotted by following the procedure illustrated for curve No. 2 under the cathode follower amplifier.

Curve 3: The cathode load line is plotted by following the procedure illustrated for curve No. 3 under the cathode follower amplifier.

Curve 4: The plate load line is a straight line constructed by joining point $e_b = E_b$ on the voltage axis with point $i_p = E_b/R_L$ on the current axis.

The four curves listed above are similar to those used for determining the performance of the cathode-follower amplifier, with the exception that the effect of the plate load resistor must now be accounted for when constructing load-line curve 1 illustrated in Fig. 6. Data is obtained from the constructed curves in much the same way as indicated for the cathode-follower amplifier. Plate output voltage data is obtained by projecting the plate-current data to the plate load-line curve 4. The plate output voltage equals

$$e_0 = E_0 \pm \Delta e_0 \qquad (11)$$

where E_0 equals the quiescent plate voltage and $\pm\Delta e_0$ equals the change in plate voltage due to an impressed signal voltage $\pm\Delta e_s$ on the grid of the tube. An example of the calculated performance of a plate-resistance-loaded, cathode-degenerative triode amplifier is given in the Appendix, example 6.

Graphical analysis can be conveniently used for the purpose of selecting the correct value of cathode resistor for a resistance-loaded amplifier when it is required that the self bias developed by this degenerative resistance have a given value with respect to the positive peak-input voltage. A numerical example illustrating this form of bias selection is given in the Appendix, example 7.

Appendix

Example 1: If circuit constants are as shown in Fig. 1, then to determine the quiescent bias and corresponding output signal for a given input signal with zero applied bias, construct curves 1, 2, and 3 on the plate characteristic curves as shown in Fig. 2. The following data can be read directly from the curves of Fig. 2. As indicated by (7) the quiescent grid-bias voltage is read corresponding to the intersection of curves 2 and 3 when $E_c = 0$; therefore $E_g = -24$ volts. The output voltage equals

$$\Delta e_k = \quad 90 \text{ volts}$$

$$-\Delta e_k = -\ 24 \text{ volts}$$

$$\pm\Delta e_k = \quad 114 \text{ volts.}$$

The maximum allowable peak-to-peak voltage swing when $E_c = 0$ can be determined by substituting data obtained from Fig. 2 in (9) and (10) and adding the peak values to obtain the peak-to-peak result.

$$\Delta e_s = \Delta e_g + \Delta e_k = 24 + 90 = 114 \text{ volts} \qquad (9)$$

$$-\Delta e_s = -\Delta e_g - \Delta e_k = -\ 16 - 24 = -\ 40 \text{ volts} \qquad (10)$$

$$\pm\Delta e_s = 154 \text{ volts.}$$

From the above data it is possible to calculate the voltage gain for a given input voltage swing.

$$\text{Voltage gain} = \frac{\pm\Delta e_k}{\pm\Delta e_s} = \frac{114 \text{ volts}}{154 \text{ volts}} = 0.74.$$

Example 2: If it is desired to alter the value of the quiescent grid bias used in example 1 from -24 volts to an assumed value of -30 volts, construct curves 1, 2, and 3 on the plate characteristic curves, as shown in Fig. 3. The quiescent grid-voltage line is drawn through curve 2 at point $E_g = -30$ volts. Through corresponding current point and curve 3 draw the quiescent cathode-voltage line. The following data can be read directly from Fig. 3.

$$E_c = E_g + E_k = -\ 30 + 9 = -\ 21 \text{ volts} \qquad (6)$$

$$\Delta e_k = 105 \text{ volts}$$

$$-\Delta e_k = -\ 9 \text{ volts}$$

$$\Delta e_s = \Delta e_g + \Delta e_k = 30 + 105 = 135 \text{ volts} \qquad (9)$$

$$-\Delta e_s = -\Delta e_g - \Delta e_k = -\ 10 - 9 = -\ 19 \text{ volts.} \qquad (10)$$

Example 3: If it is desired to alter the value of the quiescent grid bias used in example 1 from -24 volts to an assumed value of -15 volts, construct curves 1, 2, and 3 on the plate characteristic curves as shown in Fig. 4. The quiescent grid-voltage line is drawn through curve 2 at point $E_g = -15$ volts. Through the corresponding current point and curve 3, draw the quiescent cathode-voltage line. The following data can be read directly from Fig. 4.

$$E_c = E_g + E_k = -\ 15 + 51 = 36 \text{ volts} \qquad (6)$$

$$\Delta e_k = 63 \text{ volts}$$

$$-\Delta e_k = -\ 51 \text{ volts}$$

$$\Delta e_s = \Delta e_g + \Delta e_k = 15 + 63 = 78 \text{ volts} \qquad (9)$$

$$-\Delta e_s = -\Delta e_g - \Delta e_k = -\ 25 - 51 = -\ 76 \text{ volts.} \qquad (10)$$

Example 4: The method of obtaining a given quiescent grid bias by selection of the correct ohmic value of the cathode resistor is illustrated with the aid of Fig. 2. If the plate voltage $E_b = 250$ volts and the desired quiescent grid voltage $E_g' = -24$ volts, then substituting these values in the following equation results in

$$e_b = E_b + E_g' = 250 - 24 = 226 \text{ volts.} \qquad (12)$$

From point $e_b = 226$ volts on the voltage axis draw a perpendicular line through grid curve $E_g' = -24$ volts. Corresponding to this intersection point of curve $E_g' = -24$ volts and the constructed perpendicular line, read $I_p' = 16$ milliamperes on the current axis. Substituting these values in the following equation results in the selection of the following value for the cathode resistor:

$$R_k = \frac{E_g'}{I_p'} = \frac{-\ 24}{0.016} = 1500 \text{ ohms.} \qquad (13)$$

If it is desired to graphically analyze this cathode-follower circuit, construct curve 1 by drawing a straight line from point $E_b = 250$ volts on the voltage axis to the grid-voltage curve $E_g = 0$. The slope of curve 1 should be such that it passes through the intersection point of grid-voltage curve $E_g' = -24$ volts and the previously constructed perpendicular line. From data obtained from curve 1, curves 2 and 3 can be constructed.

Example 5: The positive bias required in example 3 can be obtained from an external supply or by connecting the grid return to a tap on the cathode resistor. The position of the tap can be determined with the aid of Fig. 4. At a point on curve 2 corresponding to the desired bias $E_g = -15$ volts, read corresponding current $I_p'' = 34$ milliamperes. This results in the following value of resistance between cathode and tap.

$$R_{k_1} = \frac{E_g}{I_p''} = \frac{-15}{0.034} = 440 \text{ ohms.} \quad (14)$$

Example 6: From the circuit data given in Fig. 5 the performance characteristics of the plate-resistance-loaded, cathode-degenerative triode amplifier can be determined by constructing curves 1, 2, 3, and 4 on the plate characteristic curves as shown in Fig. 6. In this example the grid swing is assumed to be sinusoidal and equal to 16 volts peak to peak. It is desired to determine the output voltage corresponding to three input voltage points on the sine wave, namely $\Delta e_s = 0$, $\Delta e_s = 8$ volts, and $-\Delta e_s = -8$ volts. The following data was obtained from Fig. 6 at the above-named input signal points.

Zero signal condition: $\Delta e_s = 0$; $E_g = -5$ volts; $E_k = 5$ volts; $E_0 = 140$ volts.

Input signal at maximum: $\Delta e_s = 8$ volts; $e_{g\max} = E_g + \Delta e_g = -5 + 4.5 = -0.5$ volts; $e_{k\max} = E_k + \Delta e_k = 5 + 3.5 = 8.5$ volts; $e_{0\min} = E_0 - \Delta e_0 = 140 - 75 = 65$ volts.

Input signal at minimum: $-\Delta e_s = -8$ volts; $e_{g\min} = E_g - \Delta e_g = -5 - 5 = -10$ volts; $e_{k\min} = E_k - \Delta e_k = 5 - 3 = 2$ volts; $e_{0\max} = E_0 + \Delta e_0 = 140 + 65 = 205$ volts.

Output signal equals: $\pm\Delta e_0 = 75 + 65 = 140$ volts.

Voltage gain equals: $\pm\Delta e_0 / \pm\Delta e_s = 140/16 = 8.75$.

Example 7: The requirement is to determine the correct value of cathode resistance for a resistance-loaded amplifier when it is required that the self bias developed by this degenerative resistor have a given value with respect to the positive peak input voltage. Circuit constants for this problem are given in Fig. 5, except that the value of the cathode resistor is unknown, and is to be determined for a grid swing which is assumed to be sinusoidal and equal to 16 volts peak to peak. Inasmuch as the value of the cathode resistor is unknown it is not possible to construct the load line by the method given under curve 1, but it can be constructed by the following procedure, which makes reference to Fig. 6.

Step 1: Draw plate load-line curve 4 by connecting with a straight-line point $e_b = E_b = 250$ volts on the voltage axis and point $i_p = E_b/R_L = 250/47{,}000 = 5.3$ milliamperes on the current axis.

Step 2: Draw a line parallel to the voltage axis between the current axis and curve 4 whose magnitude is equal to the positive peak input-signal voltage plus a safety factor. In the example under consideration a convenient value is 9 volts. The voltage scale used is that of the plate voltage e_b.

Step 3: Draw load-line curve 1 by connecting with a straight-line point ($E_b = 250$ volts) on the voltage axis and the intercept point of the line constructed in step 2 and the current axis. The current at this point on the axis is equal to

$$i_p \text{ (curve 1 intercept)} = E_b/R_L + R_k. \quad (15)$$

Therefore, the load plus cathode resistor equals

$$(R_L + R_k) = E_b/i_p \text{ (curve 1 intercept)} = 250/5.1$$

$$= 49{,}200 \text{ ohms.}$$

The cathode resistor equals

$$R_k = 49{,}200 - 47{,}000 = 2200 \text{ ohms.}$$

If it is required that other points on the input-voltage curve be determined, construct curves 2 and 3 and proceed as outlined in appendix, example 6.

Correction

Joseph M. Pettit has drawn to the attention of the editors the following corrections to the paper, "The Compensated-Loop Direction Finder," by F. E. Terman and J. M. Pettit, which appeared on pages 307–318 of the May, 1945, issue of the PROCEEDINGS OF THE I.R.E.

1. On page 307, the term in the right-hand column, line 13, should read: $(2\pi a \cos\alpha)/\lambda$ (radians)

2. Equation (1) should read:

$$|E_1 - E_2| = 2E_1 \sin \tfrac{1}{2}((2\pi a \cos\alpha)/\lambda).$$

3. Equation (2) should read:

$$|E_1 - E_2| = 2E_1(\pi a \cos\alpha)/\lambda.$$

4. On page 309, equation (6) should read:

$$\tau_H \epsilon^{-j\gamma H} = \frac{\sqrt{K' - \sin^2\theta} - \cos\theta}{\sqrt{K' - \sin^2\theta} + \cos\theta}.$$

5. Lines 13 and 14, right-hand column, should read
λ = wavelength, centimeters
$c = 3 \times 10^{10}$

6. Equation (7) should read:

horizontally polarized: $E_H(1 - r_H \epsilon^{-j(\gamma H + \beta)})$

7. On page 310, equation (8) should read:

$$e_{b_2} - e_{b_2} = (E_v \sin\theta)(bN)(1 + r_v \epsilon^{-j(\gamma v + \beta_0)}) \cdot j2 \sin((\pi a \cos\alpha \sin\theta)/\lambda).$$

8. Equation (9) should read:

$$e_{a1} - e_{a_2} = (E_v \cos\theta \cos\alpha)(aN)(1 + r_v \epsilon^{-j(\gamma v + \beta_0)}) \cdot j2 \sin((\pi b \cos\theta)/\lambda).$$

9. On page 311, equation (11) should read:

$$e_1 - e_2 = (E_H \sin\alpha)(aN)(1 + r_H \epsilon^{-j(\gamma H + \beta_0)}) \cdot j2 \sin \tfrac{1}{2}((2\pi b \cos\theta)/\lambda).$$

An Approximate Theory of Eddy-Current Loss in Transformer Cores Excited by Sine Wave or by Random Noise*

DAVID MIDDLETON†, MEMBER, I.R.E.

Summary—**An approximate theory is developed for the eddy-current loss in transformer cores excited by high-frequency (megacycle) sine waves and by broad-band (video) random noise. The boundary conditions are established, subject to which the field equations governing the distribution of the electric and magnetic fields in thin rectangular laminae are solved, and from which in turn are determined the skin depth δ_0 and mean eddy-current loss $\overline{W}$ for current and voltage-fed transformers. The voltage-fed case is considered in greater detail, as it is the more general analytically and the more common in practice. From it the constant-current or current-fed case is readily derived. Curves and formulas are given showing the variation of δ_0 and $\overline{W}$ with frequency and lamination thickness for a sine wave and for a uniform band of noise (f_2-f_1) cycles wide. Among the results it is found that the skin depth decreases, as one would expect physically, with increasing lamination thickness, frequency, core conductivity, and effective permeability. The mean eddy-current loss in the constant-voltage transformer diminishes with increasing frequency or spectral width, because of skin effect, and increases with the thickness of the laminae. For voltage-fed transformers $\overline{W}$ varies approximately as the inverse square root of the bandwidth. On the other hand, $\overline{W}$ in the constant-current cases is found to vary about as (bandwidth$^{1/2}$). A short discussion of the advantages and limitations of the theory, of the approximations made, and of some of the considerations involved in reducing eddy-current loss is included.**

I. Introduction

GENERALLY, the principal problem in the design of transformers is to achieve a given performance with as little power loss as possible. The losses that do occur are chiefly of three kinds: (a), loss in the windings, or "copper" losses; (b), losses due to hysteresis effects; and (c) loss due to eddy currents flowing in the core. The first, depending on skin and proximity effects, as well as on the easily-measured quantities of wire size and conductivity, and the second, largely a function of the operating conditions and the magnetic behavior of the core, are both difficult to measure and to predict theoretically. We shall not attempt to deal with either (a) or (b) here. The third kind of loss arises from the currents induced in the core because of the failure of the applied magnetic field to penetrate the core material uniformly. Although (a) may be obtained with only moderate accuracy and (b) but approximately with the help of the Steinmetz formula, a knowledge of the eddy-current losses and of their dependence on the various parameters, such as permeability, conductivity, frequency, lamination thickness, etc., is helpful in putting the transformer design on a somewhat more predictable basis. Accordingly, the purpose of this paper is to develop at least an approximate theory for these losses and for such auxiliary quantities of interest as the skin depth associated with the induced currents.

Specifically we are concerned with current- and voltage-fed[1] transformers, of a rectangular cross section, when a high-frequency sine wave (megacycle) or broad-band noise (in the video-range), is the primary current or voltage. Voltage-fed transformers are of principal interest here, although current-fed cores are also considered briefly. For sinusoidal excitation the treatment of the latter is already classic, but for the former apparently little has been done. The results for random-noise excitation in either case are believed to be new. This work was originally undertaken to supplement the experiments of Cobine, Curry, Gallagher, and Ruthberg,[2] but the analysis is equally applicable to general noise problems, and may be of use in the case of television signals, which are broadband and to a first approximation exhibit the characteristics of random noise.

Our problem, then, requires first the distribution of the magnetic field in the core of a transformer when a sine wave or random noise is applied across the primary terminals. The core is formed of a large number of laminations consisting of thin metal sheets, each insulated from the other by a very thin dielectric layer, assumed negligibly thick in the present analysis.[3] In a region containing no sources or sinks, Maxwell's equations take the form (in rationalized meter-kilogram-second units)

* Decimal classification: R382.1. Original manuscript received by the Institute, February 28, 1946; revised manuscript received, June 4, 1946.

† Harvard University, Cambridge, Massachusetts. This work was done at the Radio Research Laboratory under Contract No. OEM-sr-411 in connection with Harvard University and the Office of Scientific Research and Development, which assumes no responsibility for the accuracy of the statements contained herein.

[1] By current-fed or "constant" current, we mean that the source has an infinite, or very large impedance relative to that of the transformer, and that the root-mean-square current flowing in the windings is maintained independent of frequency. On the other hand, voltage-fed, or "constant"-voltage transformers, are those for which the source has negligible relative impedance and a root-mean-square voltage output which is similarly maintained independent of frequency.

[2] Cobine, Curry, Gallagher, and Ruthberg, "Video Transformers for Noise Voltage," Harvard Radio Research Laboratory Report OEMsr-411-244, October 30, 1945. (This report is available for inspection at the Office of War Archives, Littauer Center, Harvard University and contains some information on uses of noise voltages and currents in transformers as well as technical details concerning the design and operation of such apparatus. Copies of the above report are also expected to be available on request from the United States Department of Commerce.)

[3] An attempt partially to account for lamination thickness is made in Section II; see the discussion following equation 10.

$$\nabla \times E + \partial B/\partial t = 0_1, \qquad \nabla \cdot B = 0_1 \tag{1}$$

$$\nabla \times H - \partial D/\partial t = \sigma E = J, \quad \nabla \cdot D = 0_1 \tag{2}$$

where $D = \epsilon E$ and the medium supports no fixed distribution of charge, since the conductivity σ exceeds zero. Here E and H are the familiar field vectors, J is the volume density of current (ampere/meter^2), and the medium is homogeneous and isotropic, so that the ratio D/E is constant. For good conductors the conduction current is extremely large compared to the displacement current provided $\sigma/\omega\epsilon \gg 1$ where $\omega = 2\pi f$ is the angular frequency of the current, or of its lowest spectral component. Equation (2) may then be modified to give

$$\nabla \times H \doteq \sigma E, \qquad \nabla \cdot E = 0. \tag{3}$$

Now, for ferromagnetic materials, of which transformer cores are generally made, the flux density B is a nonlinear, multivalued function of the field strength H. The simultaneous solution of (1) and (2), even for the simplest geometrics, presents formidable mathematical difficulties.[4,5] To reduce the problem to one within the power of our analysis we must make the usual and important assumption that B and H are proportional. This further implies that hysteresis and eddy-current loss are independent effects. It is also clear that a reduction of the nonlinear problem to one that is linear precludes any information concerning hysteresis losses.

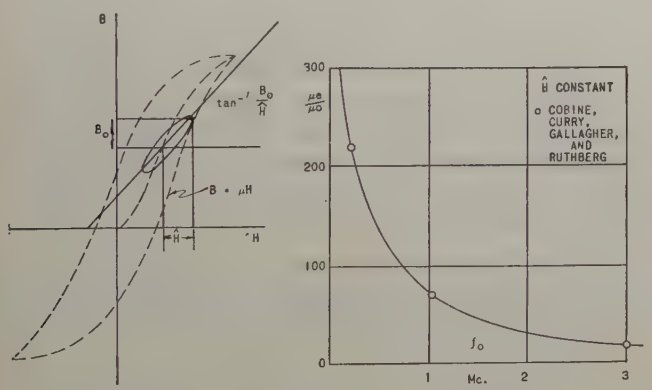

(a) (b)

Fig. 1(a)—Variational B–H loop, (b) Effective permeability as a function of frequency.

We approximate the physical problem in terms of a linear model by selecting an adjusted, or "effective" value μ_e of μ so that $B \doteq \mu_e H$. For sine waves we define μ_e as the slope of the major axis of the variational $B-H$ loop, which is nearly elliptical for small variations, as shown in Figs. 1(a) and 2. Fig. 1(a) applies equally well when there is no direct-current H field; the loop is then merely shifted to a similar position about the origin. Analytically this is equivalent to the relation $\mu_e \doteq \tan^{-1} B_0/\hat{H}$. A similar definition applies for random noise, where now the loop is filled in, in the manner of Fig. 3. The lower frequencies are the ones chiefly responsible for the loop envelope. When the applied field is large, the variational B–H loops are only roughly elliptical, but the above procedure may still be used. Figs. 1(b) and 2 for sinusoidal excitation, obtained experimentally from the data of footnote 2, illustrate the change in μ_e with frequency for zero direct-current H fields.

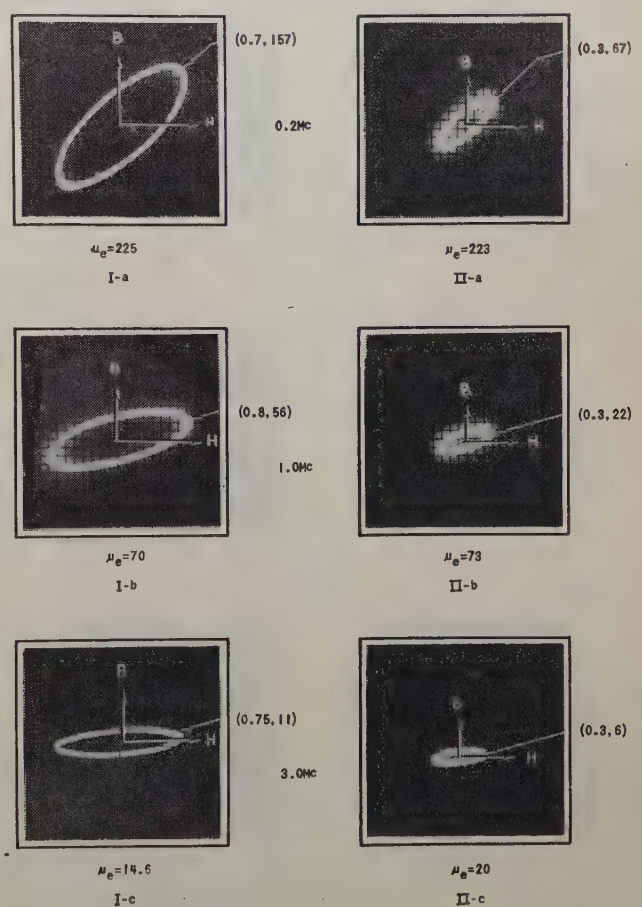

Fig. 2—Variational B–H loops, for sinusoidal excitation at different frequencies (0.002-inch Hypersil). (,) H in oersteds, B in gauss.

Because of the many other parameters whose effects we wish to examine, and because of the general lack of data, we assume in most of our calculations that μ_e remains independent of frequency. For sinusoidal excitation it is a simple matter to take the varying $\mu_e(f_0)$ into account, once data of the kind shown in Figs. 1(b) and 2 are available. Sample curves based on Figs. (1b) and 2, and illustrating the modification in skin depth and eddy-current loss, are shown in the appropriate figures following. For any particular calculation, and this holds also for noise excitation, the results are quite applicable, always provided the proper value of μ_e is chosen. In

[4] W. Cauer, *Arch. für Elektrotech.*, vol. 15, pp. 310; 1925 solves the nonlinear, current-fed problem for sine waves of small amplitudes. The author is indebted to Dr. R. W. Hickman for this reference.

[5] V. E. Legg, "Magnetic measurements at low-flux densities using the alternating-current bridge," *Bell Sys. Tech. Jour.*, vol. 15, pp. 39–62; January, 1936.

the case of noise the value of μ_e selected in the manner described above is a "lumped" value, based on the composite effects of all components in the disturbance, and

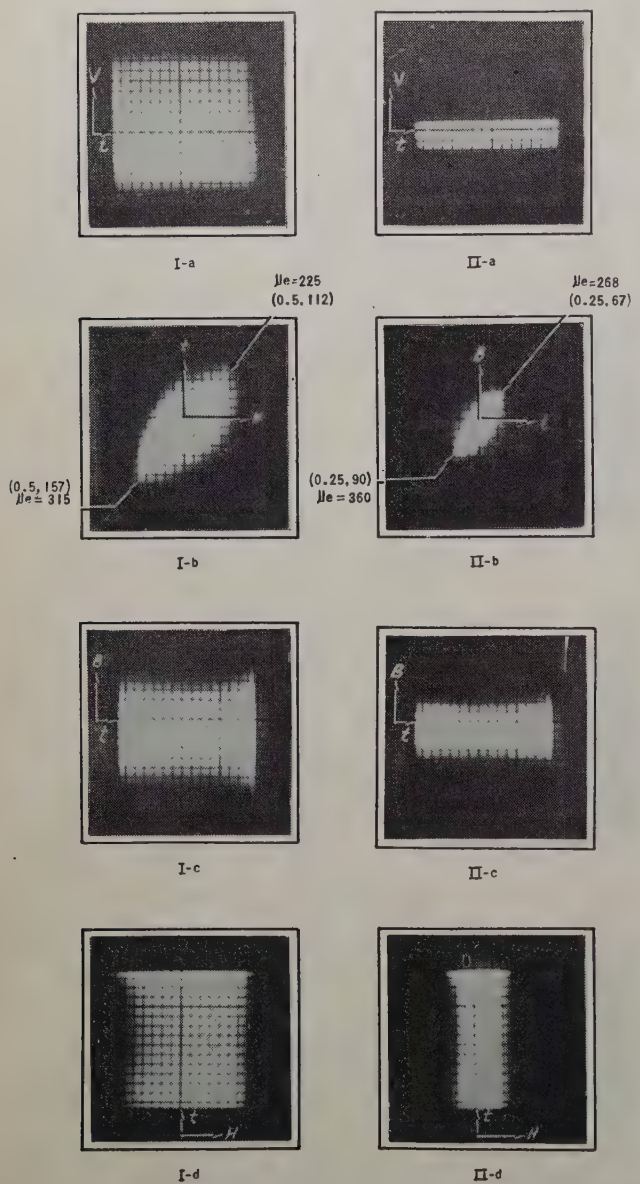

Fig. 3—Variational B–H loops for a fixed bandwidth of random noise. (,) H in oersteds, B in gauss. Exciting current, I—66 milliamperes root-mean-square II—20 milliamperes root-mean-square: peak-to-peak voltage, I—307; II—72. $N=30$, $A=0.605$ centimeter^2, $L=8.85$ centimeters.

in our simplified theory depends only on the upper and lower spectral limits f_2 and f_1. Unfortunately, here, even the limited data corresponding to Figs. 1(b) and 2 are not at present available. Such evidence as there is, however, seems to indicate that μ_e is some function of f_1 and f_2, where the low-frequency components at, and in the spectral vicinity of, f_1 are of primary importance.

The field equations (1) and (3) take the form

$$\nabla^2 \boldsymbol{H} = \mu_e \sigma \partial \boldsymbol{H}/\partial t \quad \text{and} \quad \nabla^2 \boldsymbol{E} = \mu_e \sigma \partial \boldsymbol{E}/\partial t, \qquad (4)$$

which are examples of the familiar diffusion equation. Let us consider a sample lamination, illustrated in Fig. 4. By definition, the metal slab is insulated over all bounding surfaces. An important consequence of this is that no current flows into or out of the slab. (We recall

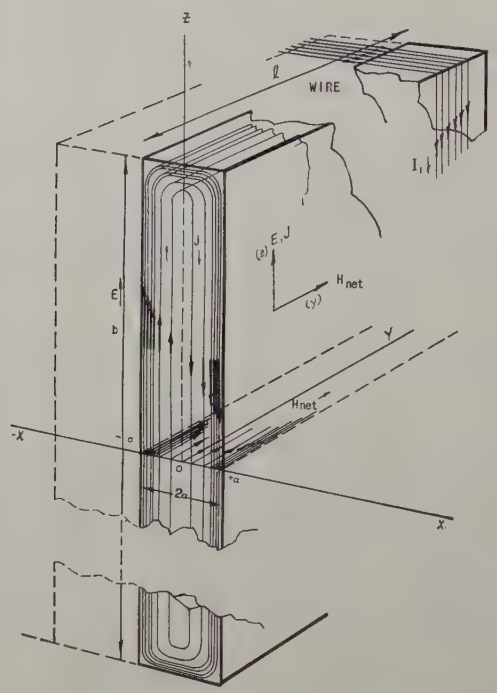

Fig. 4—Sample laminae, showing distribution of E and H fields.

that displacement currents $J_{dis}=\partial \boldsymbol{D}/\partial t$, although in general different from zero, have been neglected because $\sigma \gg \omega \epsilon$; for sufficiently high frequencies, well above those considered in this paper, the displacement currents must be considered, with a consequent modification of (5).) If I_w is the current flowing into, or out of, the walls, we then have

$$I_w = \iint_{\text{walls}} \boldsymbol{J} \cdot \boldsymbol{n} ds = \sigma \iint_{\text{walls}} \boldsymbol{E} \cdot \boldsymbol{n} ds = 0, \qquad (5)$$

where $\boldsymbol{n}$ is a unit vector normal to the surface of the particular wall in question. We require the lamination thickness $2a$ to be small compared to the length l_0 and width b, so that the effects of the ends and edges are negligible. The fields may be considered uniform in the yz plane, varying only in the x direction. In effect, we have an infinite slab, with $\boldsymbol{n}=\pm \boldsymbol{i}$. Equation (5) indicates that there can be no x-component of the E field, and if the impressed H field consists of but one component, the E field will likewise, by virtue of (3). Taking $\boldsymbol{H}=j H_y(x,t)$ gives from (4)

$$\frac{\partial^2 H_y}{\partial x^2}(x,t) \quad \mu_e \sigma \frac{\partial H_y}{dt} x, t);$$

$$\frac{\partial^2 E_z}{\partial x^2}(x,t) = \mu_e \sigma \frac{\partial E_z}{\partial t}(x,t), \qquad (6)$$

and from (3) it follows that

$$E_z = \frac{1}{\sigma}\frac{\partial H_y}{\partial x}, \tag{7}$$

determining E_z once H_y has been found. Similar formulas may be deduced for other geometries under the above conditions, a very common one in experimental practice being the toroid.[6]

II. Boundary Conditions and the Solution of the Differential Equation

The boundary conditions at the surface of the laminae are determined from the method of exciting the field in the metal. The transformer core is (ideally) wrapped with a large number of turns of wire, consisting of separate primary and secondary circuits. If $V_{01}(t)$ and $V_{02}(t)$ are the applied voltages and R_{01} and R_{02} are the resistances, including any loads, of the primary and secondary respectively, the circuit equations become

$$\begin{aligned} V_{01}(t) - \left(L_1\frac{dI_1}{dt} + M\frac{dI_2}{dt}\right) &= I_1R_{01}; \\ V_{02}(t) - \left(L_2\frac{dI_2}{dt} + M\frac{dI_1}{dt}\right) &= I_2R_{02}, \end{aligned} \tag{8}$$

with L_1 and L_2 self-inductances and M the mutual inductance between primary and secondary circuits. We neglect the effects of capacitance, and we assume that the leakage flux is negligible in comparison with the total flux. This will be the case for even a moderate air gap between windings or between windings and the core, since the flux is predominantly confined to the high-permeability regions of the metal. The principal effect, which again ignores capacitive phenomena, is to reduce the current because of the increase in length of wire in each turn, i.e., because of the increased resistance of the windings.

The quantities within the parentheses of (8) represent the induced voltage in the primary and secondary. These are

$$\begin{aligned} V_{in}(t)_1 &= -\left(L_1\frac{dI_1}{dt} + M\frac{dI_2}{dt}\right) \\ &= -N_1\iint_{S_1}\frac{\partial B}{\partial t}\cdot n\,dS_1, \end{aligned} \tag{9}$$

and

$$\begin{aligned} V_{in}(t)_2 &= -\left(L_2\frac{dI_2}{dt} + M\frac{dI_1}{dt}\right) \\ &= -N_2\iint_{S_2}\frac{\partial B}{\partial t}\cdot n\,dS_2, \end{aligned} \tag{10}$$

where S_1 and S_2 are the cross sections of the windings, and N_1 and N_2 are the total number of primary and secondary turns. Since there is little leakage, for all practical purposes $S_1 = S_2 = As$, with $A = 2abq$, and q the number of laminations. We have introduced the "stacking" factor s, defined as the ratio of the thickness of the core metal alone to the total thickness, including the interlaminar insulation. Numerically s lies in the range $0.8 < s < 1.0$ in most cases. Equation (9) is easily evaluated with the help of (6) to give

$$\begin{aligned} (V_m)_1 &= -\frac{2N_1bqs}{\sigma}\left.\frac{\partial H_y}{\partial x}\right|_{x=a}; \\ (V_m)_2 &= -\frac{2N_2bqs}{\sigma}\left.\frac{\partial H_y}{\partial x}\right|_{x=a}. \end{aligned} \tag{11}$$

[Note that N_2 does not appear explicitly in the first equation of (11), nor does N_1 in the second, as we might expect at first glance from (9) and (10), because of the presence of the mutual term $M(N_1, N_2)$. They are, however, contained in $\partial H_y/\partial x|_{x=a}$.]

If l is the mean length of the magnetic circuit, and the cross section of the core is essentially uniform, the net magnetic field at the boundaries $x = \pm a, \pm 2a, \pm \cdots \pm qa$ is

$$H_y(a, t) = [N_1I_1(t) + N_2I_2(t)]/l. \tag{12}$$

Solving (8) for I_1 and I_2 with the help of (9) and (10) allows us to write this as

$$\begin{aligned} H_y(a, t) = \frac{1}{l}&(N_1V_{01}(t)/R_{01} + N_2V_{02}(t)/R_{02}) \\ &+ N_1V_{in}(t)_1/lR_{01} + N_2V_{in}(t)_2/lR_{02}, \end{aligned} \tag{12a}$$

which may be expressed in the more compact form

$$H_y(a, t) = H_0(a, t) - \beta_0\left.\frac{\partial H_y}{\partial x}\right|_{x=a}, \tag{13}$$

where $H_0(a, t)$ is formally identified as the *applied* field, independent of any inductive or capacitive effects in the transformer circuit, and $-\beta_0\partial H_y/\partial x|_{x=a}$ as the *induced* field. Comparison of (12a) and (13) shows that, for the *applied* field,

$$H_0(a, t) = N_1V_{01}(t)/R_{01}l + N_2V_{02}(t)/R_{02}l, \tag{14a}$$

and for the induced field

$$H_{in}(a, t) = -\beta_0\left.\frac{\partial H_y}{\partial x}\right|_{x=a}, \tag{14b}$$

where

$$\begin{aligned} \beta_0 &= \frac{2bqas}{\sigma al}\left(\frac{N_1^2}{R_{01}} + \frac{N_2^2}{R_{02}}\right) = \frac{As}{\sigma al}\left(\frac{N_1^2}{R_{01}} + \frac{N_2^2}{R_{02}}\right) \\ &= \frac{1}{a\mu_e\sigma}\left(\frac{L_1}{R_{01}} + \frac{L_2}{R_{02}}\right) \end{aligned} \tag{15}$$

from the expression for self-inductance, in this instance $L = (As)N^2/\mu_e/l$. Observe from (15) that $\beta_0\alpha\mu_e\sigma$ is

[6] N. W. McLachlan, "Bessel Functions for Engineers," Oxford University Press, New York, N. Y., 1941; p. 142.

independent of α, μ_e, and σ, provided the over-all cross section of the core is unaltered.

The exciting magnetic field is impressed on the pair of faces $x=\pm a, \cdots, \pm qa$, so that $H_y(a,t)=-H_y(-a,t)$ etc., and thus, because of (7), the electric field is antisymmetric.

We may then use

$$\left.\frac{\partial H_y}{\partial x}\right|_{x=0} = 0 \tag{16}$$

as one boundary condition, while (13) is the other.

We seek first the steady-state solution when the primary voltage consists of but one frequency, and the *applied* secondary voltage $V_{02}(t)$ is zero, a usual condition in practice. The extension to the case of random noise will follow (see Section IV).

The solution of (6), where now

$$H_0(a,t) = H_0 e^{i\omega_0 t}, \qquad \omega_0 = 2\pi f_0;$$
$$H_0 \equiv N_1 V_{01}/R_{01} l, \qquad i=\sqrt{-1}, \tag{17}$$

and where V_{01} is the peak amplitude of the sine wave, is

$$H_y(x,t) = (A_1 e^{-\gamma x} + B_1 e^{\gamma x}) e^{i\omega_0 t},$$
$$\gamma = (i\omega_0 \mu_e \sigma)^{1/2} = (1+i)(\omega_0 \mu_e \sigma/2)^{1/2}. \tag{18}$$

We may eliminate the constants A_1 and B_1 with the help of the boundary conditions (13) and (16), obtaining finally

$$H_y(x,t) = \frac{H_0 e^{i\omega_0 t} \cosh (1+i)\alpha_0 x}{\cosh (1+i)\alpha_0 a + \beta_0 \alpha_0 (1+i) \sinh (1+i)\alpha_0 a},$$
$$\alpha_0 \equiv (\omega_0 \mu_e \sigma/2)^{1/2}, \quad -a \leqq x \leqq a. \tag{19}$$

Either the real or the imaginary part of H_y yields the distribution of the H field, depending on whether we choose $H_0(a,t)=H_0 \cos \omega_0 t$ or $H_0 \sin \omega_0 t$. Note also that (19) is analytically equivalent to the distribution of temperature in an infinite slab of width $2a$ from each side of which there is radiation into a medium whose temperature varies harmonically with time.

The complex-current distribution obtained from (7) and (19) is

$$J_z(x,t) = \sigma E_z(x,t)$$
$$= \frac{H_0 \alpha_0 (1+i) \sinh (1+i)\alpha_0 x \, e^{+i\omega_0 t}}{\cosh (1+i)\alpha_0 a + \beta_0 (1+i)\alpha_0 \sinh (1+i)\alpha_0 a}. \tag{20}$$

The usual solution[7,8,9] assumes a *net* field at the boundary whose amplitude is maintained independent of frequency. Physically this corresponds to the "constant"-current, or current-fed, source, rather than to the "constant"-voltage source considered above. Then the boundary condition (13) is modified to $H_y(a,t)=H_0' e^{i\omega_0 t}$, and the solutions corresponding to (19) and (20) are

$$H_y(x,t) = H_0' e^{i\omega_0 t} \frac{\cosh (1+i)\alpha_0 x}{\cosh (1+i)\alpha_0 a};$$
$$J_z(x,t) = H_0' e^{i\omega_0 t} \alpha_0 (1+i) \frac{\sinh (1+i)\alpha_0 x}{\cosh (1+i)\alpha_0 a}. \tag{21}$$

Observe that (21) may be obtained from (19) and (20) on setting $\beta_0=0$.

A quantity giving some indication of the uniformity or nonuniformity of the magnetic field and, hence, of the effective H-field penetration is the skin depth $\delta_0 \equiv a - x_0$ (where x_0 is measured from the center of the lamina). Our definition of δ_0 differs somewhat from the more usual one in that it is the depth at which the eddy-current *losses*, due to the induced currents, are a fraction C of their total value, instead of being the depth at which the amplitude $|J|$ of the (volume) current density is $(1-C)$ of its value at the surface. Analytically δ_0 may be determined from

$$1 - \int\int dy dz \int_{-x_0}^{x=x_0=a-\delta_0} \overline{J \cdot E^*} dx \Big/ \int\int dy dz \int_{-a}^{a} \overline{J \cdot E^*}\, dx = C, \qquad 0 < C < 1, \tag{22}$$

where C has some value between zero and unity, and (*) denotes the complex conjugate. It is clear that the value of δ_0 depends on our choice of C.

Of principal interest is the mean power loss per unit volume $\overline{W}$ arising from eddy currents. With the help of (6) we have

$$\overline{W} = \frac{1}{V} \int\int\int \overline{J \cdot E^*}\, dV$$
$$= \frac{1}{2\sigma a} \int_0^a \left|\frac{\partial H_y}{\partial x}\right|^2 dx, \tag{23a}$$

or

$$= \frac{1}{2\sigma a} \lim_{T\to\infty} \frac{1}{T} \int_0^T dt \int_0^a \overline{\left|\frac{\partial H_y}{\partial x}\right|^2} dx, \text{ watts/meter}^3. \tag{23b}$$

with $V[=(As)l]$ the volume of the magnetic circuit. Equation (23a) applies for a sinusoidal voltage of the form $V_{01} e^{i\omega_0 t}$ and (23b) is used when there is a noise voltage, $V_0(t)=\sum_n (a_n - ib_n) e^{i\omega_n t}$ in the primary circuit. The bar indicates the statistical average over the random variables a_n and b_n.

Still another quantity that is sometimes considered in the study of the skin-effect problem involving ferromagnetic materials is the apparent permeability μ_a, discussed, for example, in footnote 8. However, the definition of this quantity appears to have been made only for sine-wave excitation in current-fed ($\beta_0=0$) cases. We

[7] J. J. Thompson, *Electrician*, vol. 28, p. 599; 1891.
[8] M. Latour, "Note on losses in sheet iron at radio frequencies," Proc. I.R.E., vol. 7, pp. 61–70; February, 1919.
[9] C. Dannatt, *Jour. I.E.E.* (London), vol. 79, p. 667; 1936.

can show that μ_a takes the same values under voltage-fed ($\beta_0>0$) conditions, but because it is lengthy and difficult to extend the definition in the instance of noise excitation, and because μ_a itself is not essential to our analysis, we have omitted it in this paper.

III. Sinusoidal Excitation

(a) *Skin depth.*

If we introduce the definition

$$\lambda_0 \equiv 2\alpha_0 a = (2\omega_0\mu_e\sigma a^2)^{1/2}, \tag{24}$$

and write

$$\Delta(\lambda_0) = [1 + (2a/\beta_0)\sin\lambda_0/\lambda_0 + 2a^2/\beta_0^2\lambda_0^2]\cosh\lambda_0 - [1 + 2a\sinh\lambda_0/\beta_0\lambda_0 - 2a^2/\beta_0^2\lambda_0^2]\cos\lambda_0, \tag{25}$$

we obtain from (20)

$$\boldsymbol{J}\cdot\boldsymbol{E}^* = (H_0^2/2)\frac{a^2\sigma}{(\beta_0 a\sigma)^2}\left\{\frac{\cosh(\lambda_0 x/a)-\cos(\lambda_0 x/a)}{\Delta(\lambda_0)}\right\}. \tag{26}$$

Here the following relations have proved useful:

$$\sinh(1+i)z/2\ \sinh(1-i)z/2 = (\cosh z-\cos z)/2, \tag{27a}$$

$$\cosh(1+i)z/2\ \cosh(1-i)z/2 = (\cosh z+\cos z)/2. \tag{27b}$$

When the result (26) is inserted into (22), the relative skin depth δ_0/a is determined from

$$1-C = \frac{\sinh\lambda_0(1-\delta_0/a)-\sin\lambda_0(1-\delta_0/a)}{\sinh\lambda_0-\sin\lambda_0},\quad 0<C<1. \tag{28}$$

We observe that δ_0/a is independent of β_0. When $\lambda_0<0.1$, we find that

$$\delta_0/a = 1-(1-C)^{1/3} = 0.535 \text{ if } C = 0.90, \tag{29a}$$

and the skin depth δ_0 is proportional to the lamination thickness. However, when λ_0 is large, say 10 or greater, we have

$$\delta_0/a = -[\log(1-C)]/\lambda_0 \leqq 0.230,\ C=0.90,\ \lambda_0>10, \tag{29b}$$

and δ_0 is seen to be independent of a by virtue of (24). This agrees with what we would expect physically, namely that, as λ_0 becomes larger, the eddy currents are crowded progressively nearer the surface, with a consequent bunching of flux in that region. Figs. 5 and 6 show the variation of δ_0/a and δ_0 with lamination thickness and frequency.

(b) *Eddy-Current Loss.*

From (20) and (23a) we obtain the mean eddy-current loss per unit volume

$$\overline{W} = \frac{a^2\sigma}{(\beta_0 a\sigma)^2}\left(\frac{N_1V_{01}}{2^{1/2}R_{01}l}\right)^2\left\{\frac{1}{\lambda_0}\frac{\sinh\lambda_0-\sin\lambda_0}{\Delta(\lambda_0)}\right\}\ \text{watts/meter}^3. \tag{30}$$

When λ_0 is large we have a simpler result, namely,

$$\overline{W} = \frac{a^2\sigma}{(\beta_0 a\sigma)^2}\left(\frac{N_1V_{01}}{2^{1/2}R_{01}l}\right)^2\frac{[\tanh\lambda_0-\sin\lambda_0/\cosh\lambda_0]}{\lambda_0\{[1+2a\sin\lambda_0/\beta_0\lambda_0+2a^2/\beta_0^2\lambda_0^2]-\cos\lambda_0[1/\cosh\lambda_0-2a^2/\beta_0^2\lambda_0^2+2a\tanh\lambda_0/\beta_0\lambda_0]\}} \tag{31}$$

$$\rightarrow \frac{1}{(\beta_0 a\sigma)^2}\left(\frac{N_1V_{01}}{2^{1/2}R_{01}l}\right)^2 a\left(\frac{\sigma}{2\omega_0\mu_e}\right)^{1/2}, \tag{32}$$

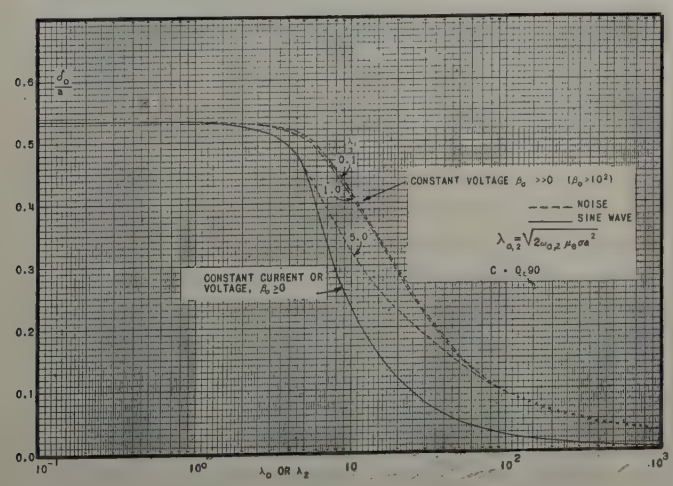

Fig. 5—Skin depth, sinusoidal and random noise excitation; λ_1 is held constant while λ_2 varies in the case of noise.

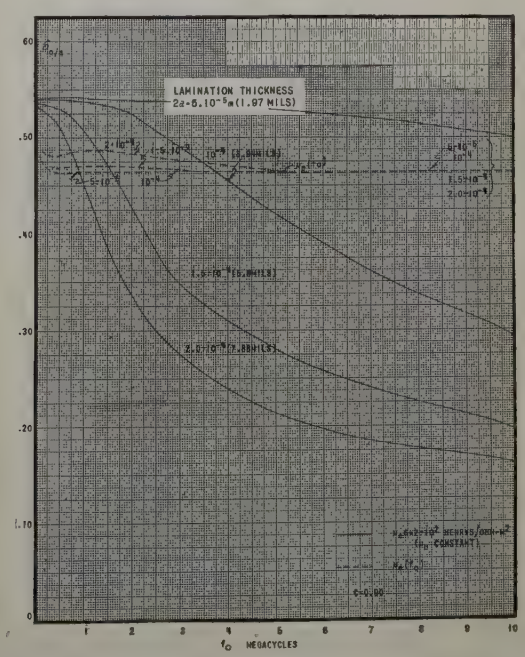

Fig. 6—Skin depth, sinusoidal excitation, for various lamination thicknesses. The dotted curves apply for μ_e as a function of frequency.

provided $\beta_0/a > 40, \lambda_0 > 5.3$. Now in many practical cases $\beta_0/a \sim 10^3$, or larger. Then (30) may be split into two parts, each of which is applicable for a range of λ_0. In region I, when $\lambda_0^2 \ll 1$, say $\lambda_0 \leqq 0.10$, we have

$$\overline{W}_I = \frac{a^2\sigma}{(\beta_0 a\sigma)^2}\left(\frac{N_1V_{01}}{2^{1/2}R_{01}l}\right)^2 \frac{1}{3}\,\frac{(\beta_0 a\mu_e\sigma\omega_0)^2}{1+(\beta_0 a\mu_e\sigma\omega_0)^2},$$
$$\beta_0/a \geqq 10^2,\ \lambda_0 < 0.10. \qquad (33)$$

From this we observe that the losses at constant total width are proportional to the *square* of the lamination thickness, and to the first power of the conductivity σ, when we recall from (15) that $(\beta_0 a\sigma)$ is independent of a, μ_e, σ. In this region the losses also increase with frequency, leveling out when $(\beta_0 a\mu_e\sigma)^2 \gg 1$. These results are in qualitative agreement with the simpler theories.[10]

The second interval II obtains when $\lambda_0 > 0.10$, $\beta_0/a \geqq 10^2$, and from (30) we have accordingly[11]

$$\overline{W}_{II} = \frac{a^2\sigma}{(\beta_0 a\sigma)^2}\left(\frac{N_1V_{01}}{2^{1/2}R_{01}l}\right)^2 \left\{\frac{1}{\lambda_0}\left[\frac{\sinh\lambda_0 - \sin\lambda_0}{\cosh\lambda_0 - \cos\lambda_0}\right]\right\},$$
$$\beta_0/a \geqq 10^2,\ \lambda_0 > 0.1. \qquad (34)$$

We see that when λ_0 exceeds 0.10 the losses cease to be proportional to the square of the lamination thickness, but vary in a fashion which becomes more nearly linear.

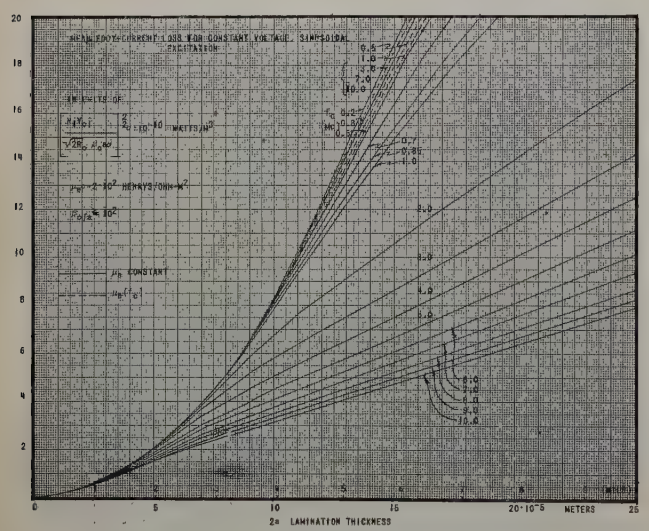

Fig. 7—Mean eddy-current loss per unit volume as a function of lamination thickness for voltage-fed transformers and sinusoidal excitation.

Similarly, the dependence of the losses on conductivity changes from a linear to a square-root relation, while an increase in frequency ultimately results in vanishingly small losses. This occurs because there is a considerable increase in the effective resistance of the laminations arising from the very incomplete penetration of the magnetic field and consequent small skin depth. Fig. 7 illustrates the variation of the mean power loss per unit volume as a function of lamination thickness, whereas Fig. 8 shows the loss as it depends on frequency. Observe from Fig. 8 that there is a frequency for which the losses are a maximum, in the neighborhood of 0.10 megacycle or below; this frequency may be quite low for the thicker laminations.

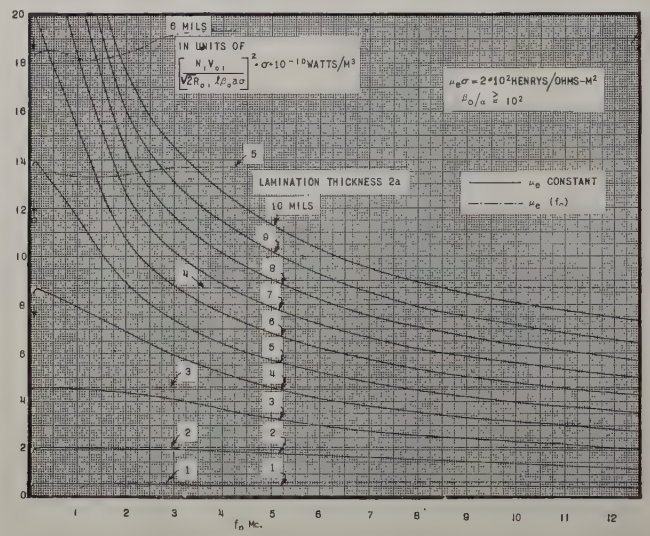

Fig. 8—The same as Fig. 7, where now frequency is the independent variable.

For constant-current transformers ($\beta_0 = 0$) the expression of the eddy-current loss takes the more familiar and simpler form

$$\overline{W} = (H_0'^2/2)\,\frac{\lambda_0}{2a^2\sigma}\left(\frac{\sinh\lambda_0 - \sin\lambda_0}{\cosh\lambda_0 + \cos\lambda_0}\right) \text{watts/meter}^3, \qquad (35)$$

cf. (5), footnote 9. Here $H_0'^2/2 = [N_1^2\bar{I}_1^2 + N_2^2\bar{I}_2^2]/l^2 = \text{constant}$. Fig. 9 indicates the frequency-dependent nature of $\overline{W}$ for various thicknesses of lamination. In this instance $\overline{W}$ is seen to *decrease* with increasing a and to *increase* with increasing frequency, beyond certain values of a and f_0. We may offer as a partial explanation of the phenomenon the fact that, since the primary and secondary currents are maintained constant in magnitude, the *net* field, $H_0' = H_{\text{applied}} - H_{\text{induced}}$ (vide (12) through (14)), must also remain fixed. However, an increasing frequency leads to greater applied magnetic fields (and applied voltages) and consequently to larger induced fields, whose spatial distribution becomes progressively less uniform. The result is larger currents induced in the core, and greater eddy-current losses. On the other hand, for thicker laminations, which also yield very nonlinear H-field distributions, the net fields are established with smaller applied voltages. This means smaller induced fields and currents, so that the losses

[10] Electrical Engineering Staff, Massachusetts Institute of Technology, "Magnetic Circuits and Transformers," John Wiley and Sons, New York, N. Y., 1943; chap. 5, sec. 2.

[11] At first glance (34) appears to be valid only in the range $0.1 < \lambda_0 < 5.3$ (with about 1 per cent error at $\lambda_0 = 5.3$), and with β_0/a large compared to unity. However, we note from (31) that when $\lambda_0 \geqq 5.3$, $\cosh\lambda_0$ is equal to or greater than 10^2, and $\tanh\lambda_0 = 1.00$, so that the denominators of (30), (31), and (34) are numerically almost identical although different analytically. Equation (34) may then be used with negligible error in place of the more general results (30). But if β_0/a is much less than 40 the simpler form, (34), ceases to be adequate, and (30) must serve.

decrease. The above two effects oppose each other in varying degrees, as can be seen from Fig. 9.

IV. Random Noise Excitation (Voltage-Fed Transformers; $\beta_0 > 0$)

A random noise voltage, here the potential applied across the primary terminals, may be represented by[12–14]

$$V_{01}(t) = \sum_{n=0}^{N} (a_n - ib_n)e^{i\omega_n t}, \tag{36}$$

where the quantities a_n and b_n are random variables, subject to a normal, or Gaussian, distribution law; N is a number much greater than unity. The random variables a_n and b_n obey the following conditions:

$$\overline{a_n b_k} = 0; \qquad \overline{a_n} = \overline{b_n} = 0;$$
$$\overline{a_n a_k} = \overline{b_n b_k} = W(f_n)\delta_n{}^k/T = W(f_n)\Delta f \delta_n{}^k. \tag{37}$$

$\delta_n{}^k = 0$, $n \neq k$; $\delta_n{}^k = 1$; $n = k$. The first relation in (37) states that a_n and b_n are independent; the second, that their mean value is zero; and the third gives the value of the mean square. Here $W(f_0)\Delta f$ is the mean-square voltage in the frequency interval $\Delta f = 1/T$. We may write this as

$$\sigma_n{}^2 = W(f_n)\Delta f = \overline{a_n{}^2} = \overline{b_n{}^2}; \quad \omega_n = 2\pi n/T = 2\pi f_n. \tag{38}$$

In the steady state the sinusoidal solution (19) may be used for each component f_n. Accordingly, with the help of (36), the complex H field is

$$H_y(x,t) = \frac{N_1}{R_{01}l} \sum_{n=1}^{N} \frac{(a_n - ib_n)e^{i\omega_n t}\cosh(1+i)\alpha_n x}{\cosh(1+i)\alpha_n a + \beta_0\alpha_n(1+i)\sinh(1+i)\alpha_n a}, \qquad \alpha_n = (\omega_n \mu_e \sigma/2)^{1/2} \tag{39}$$

with an analogous expression for $J_z(x,t)$ based on (20). Now the significant form of solution here is the mean-square or root-mean-square value. We find, then, for $\overline{H_y{}^2}$:

$$\overline{H_y(x,t)^2} = \overline{|H_y|^2}/2$$
$$= \left(\frac{N_1}{R_{01}l}\right)^2 \sum_{n=1}^{N} \frac{(\overline{a_n{}^2}+\overline{b_n{}^2})/2 \cosh(1+i)\alpha_n x \cosh(1-i)\alpha_n x}{[\cosh(1+i)\alpha_n a+\beta_0\alpha_n(1+i)\sinh(1+i)\alpha_n a][\cosh(1-i)\alpha_n a+\beta_0\alpha_n(1-i)\sinh(1-i)\alpha_n a]} \tag{40}$$

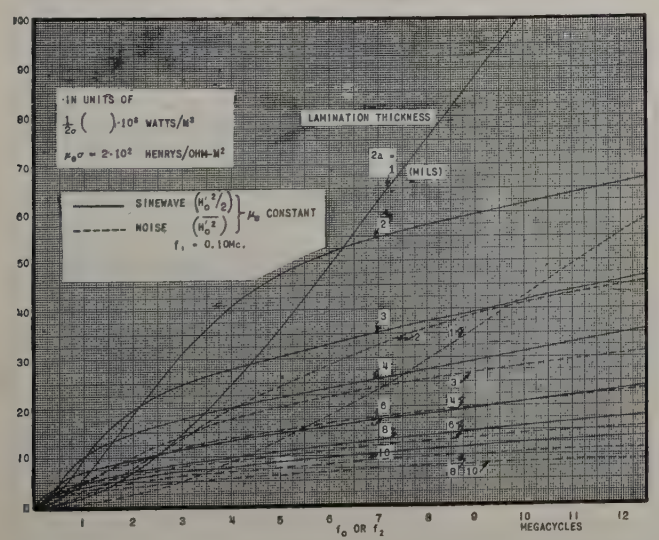

Fig. 9—Mean eddy-current loss for current-fed transformers, excited by sine wave or by random noise.

The bars indicate that an ensemble average is taken,[13] and here $\delta_n{}^k$ is the usual Kronecker delta, such that since the cross terms vanish by virtue of (37). If we allow N and n to become infinite in such a way that $f_n = nf_1 = f \neq 0$, (corresponding to the infinite time average), and that $\Delta f(=1/T)$ hence becomes the infinitesimal df, the sum in (40) may be replaced by an integral to give

$$\overline{H_y{}^2} = \left(\frac{N_1}{R_{01}l}\right)^2 \int_0^\infty \frac{\cos(\lambda x/a)+\cos(\lambda x/a)}{2(\beta_0/2a)^2\lambda^2\Delta(\lambda)} W(f)df,$$
$$\lambda = (2\omega\mu_e\sigma a^2)^{1/2}, \tag{41}$$

with the aid of (27b) and (37). In (41), $W(f)$ is the mean-square input *voltage spectrum*, in volts squared per unit band-width, and λ is a variable analogous to λ_0; $\Delta(\lambda)$ is given by (25) when λ is substituted for λ_0. We note that

$$\lambda = 2\alpha a = (2\omega\mu_e\sigma a^2)^{1/2},$$
$$\therefore \quad f = \lambda^2/4\pi a^2\mu_e\sigma, \qquad df = \lambda d\lambda/2\pi a^2\mu_e\sigma. \tag{42}$$

From (36) it is evident that

$$\overline{V_{01}{}^2} = \sum_{n=1}^{N} (\overline{a_n{}^2} + \overline{b_n{}^2})/2 \to \int_0^\infty W(f)df. \tag{43}$$

We shall find it helpful to represent the mean-square applied voltage by

$$\overline{V_{01}{}^2} = W_0 \int_0^\infty w(f)df = gW_0; \qquad g \equiv \int_0^\infty w(f)df; \tag{44}$$

W_0 is the maximum spectral density in (volts²/frequency), and $w(f)$ gives the functional dependence of spectral shape on frequency, with maximum value unity.

[12] S. O. Rice, "Mathematical analysis of random noise," *Bell Sys. Tech. Jour*, vol. 23, p. 282; 1944; vol. 24, p. 46; 1945.
[13] M. C. Wang and G. E. Uhlenbeck, "On the theory of the brownian motion II," *Rev. Mod. Phys.*, vol. 17, p. 323, 1945.
[14] D. Middleton, "Calculation of the Effect of Rectification and Clipping on Spectra of the Output of the 6D4, 884, and 2D21 Noise Sources," Harvard Radio Research Laboratory Report No. OEMsr 411-90, June 23, 1944. See footnote 2, concerning availability of copies. Also, D. Middleton, "The response of biased saturated linear and quadratic rectifiers to random noise," *Jour. Appl. Phys.*, vol. 17, pp. 778–801; October, 1946.

The relation (44) enables us to express our results on a comparative basis with those obtained for sinusoidal excitation, provided we set $(\overline{V_{01}^2})_{\text{noise}} = (V_{01}^2/2)_{\text{sine wave}}$. Equation (41) becomes finally

$$\overline{H_y(x,t)^2} = \frac{a^2\sigma}{(\beta_0 a\sigma)^2}\left(\frac{N_1^2\overline{V_{01}^2}}{R_{01}^2 l^2}\right)\left[\frac{1}{\pi\mu_e g}\int_0^\infty \frac{[\cosh(\lambda x/a)+\cos(\lambda x/a)]w(\lambda^2/4\pi a^2\mu_e\sigma)d\lambda}{\lambda\Delta(\lambda)}\right]. \quad (45)$$

Starting with (20) and applying the above analysis, we obtain in a similar fashion

$$\overline{J_z(x,t)^2} = \frac{\sigma}{(\beta_0 a\sigma)^2}\left(\frac{N_1^2\overline{V_{01}^2}}{R_{01}^2 l^2}\right)\left[\frac{1}{2\pi\mu_e g}\int_0^\infty \frac{[\cosh(\lambda x/a)-\cos(\lambda x/a)]w(\lambda^2/4\pi a^2\mu_e\sigma)d\lambda}{\Delta(\lambda)}\right]. \quad (46)$$

Finally, we have the following general results for the skin depth δ_0, cf. (22)

$$1-C = \int_0^\infty [\sinh\lambda(1-\delta_0/a)-\sin\lambda(1-\delta_0/a)]wd\lambda/\Delta(\lambda) \Big/ \int_0^\infty [\sinh\lambda-\sin\lambda]wd\lambda/\Delta(\lambda), \quad 0<C<1, \quad (47)$$

and of chief interest, the mean eddy-current loss per unit volume

$$\overline{W} = \frac{a^2\sigma}{(\beta_0 a\sigma)^2}\left(\frac{N_1^2\overline{V_{01}^2}}{R_{01}^2 l^2}\right)\left[\frac{1}{2\pi\mu_e\sigma a^2 g}\int_0^\infty [\sinh\lambda-\sin\lambda]wd\lambda/\Delta(\lambda)\right] \text{watts/meter}^3. \quad (48)$$

It is possible to simplify the quantity $\Delta(\lambda)$ defined by (25) if we observe that when λ is less than about 0.10, $\Delta(\lambda)$ may be written

$$\Delta(\lambda) \doteq \lambda^{-2}\{4a^2/\beta_0^2 + \lambda^4(1+4a/\beta_0+a^2/6\beta_0^2)\}. \quad (49a)$$

In many practical cases $\beta_0/a \geqq 10^2$; then (49a) reduces to

$$\Delta(\lambda) \doteq \lambda^{-2}(4a^2/\beta_0^2+\lambda^4). \quad (49b)$$

On the other hand, when λ exceeds 0.10, and β_0/a is large compared with unity, we may write with less than a per cent of error:

$$\Delta(\lambda) \doteq \cosh\lambda - \cos\lambda,$$

from the same argument as that justifying (34).

In this paper we are specifically interested in random noise having a uniform mean-square current or voltage spectrum, extending from f_1 to f_2. From (44) it is clear that now $g=f_2-f_1$, and further, that w is unity.

(a) Skin Depth

Here, as before, we take $C=0.90$, and when λ_1 exceeds 0.10, (47) assumes the following form for a uniform band of noise:

$$0.10 = \int_{\lambda_1}^{\lambda_2} \frac{\sinh\lambda(1-\delta_0/a)-\sin\lambda(1-\delta_0/a)}{\cosh\lambda-\cos\lambda}d\lambda \Big/ \int_{\lambda_1}^{\lambda_2}\frac{\sinh\lambda-\sin\lambda}{\cosh\lambda-\cos\lambda}d\lambda, \quad \beta_0/a \geqq 10^2. \quad (50)$$

The first integral is obtained by graphical means; see Fig. 12. The second integral, however, can be evaluated in closed form for all (positive) values of λ_1 and λ_2 with the help of the relations

$$(1+i)\coth(1-i)\lambda/2 + (1-i)\coth(1+i)\lambda/2 = 2(\sinh\lambda-\sin\lambda)/(\cosh\lambda-\cos\lambda), \quad (51)$$

and

$$\int(1+i)\coth(1\mp i)\frac{\lambda}{2}d\lambda = \pm i\log\left(\frac{\cosh\lambda-\cos\lambda}{2}\right) + 2\tan^{-1}(\tan\lambda/2/\tanh\lambda/2)\mp 4\pi n + G, n=0,1,2,\cdots, \quad (52)$$

with G an additive constant. We have finally

$$\int_{\lambda_1}^{\lambda_2}\frac{\sinh\lambda-\sin\lambda}{\cosh\lambda-\cos\lambda}d\lambda = 2\{\tan^{-1}[\tan\lambda_2/2/\tanh\lambda_2/2] - \tan^{-1}[\tan\lambda_1/2/\tanh\lambda_1/2]\} \quad \lambda_2>\lambda_1\geqq 0. \quad (53)$$

Again, when $\lambda_2<0.1$ we observe from (49b), (50), and (53) that δ_0/a is the same as for the case of the sine wave, cf. (29a). But for λ_1 large, say 10 or greater, we have

$$(1-C)(\lambda_2-\lambda_1) \doteq \int_{\lambda_1}^{\lambda_2} e^{-\delta_0\lambda/a}d\lambda = (a/\delta_0)[e^{-\lambda_1\delta_0/a} - e^{-\lambda_2\delta_0}/a]. \quad (54)$$

A rough calculation for the case $\lambda_2=13$, $\lambda_1=10$ gives $\delta_0/a \doteq 0.20$, showing that the skin depth decreases, as previously observed, when λ is increased, because of the failure of the H field to penetrate the laminations. As Fig. 5 indicates, it is the high-frequency components that most affect δ_0. This we would expect because the crowding of flux and eddy currents near the surface is more pronounced for such frequencies. Equation (54) shows further that for large values of λ_1 and λ_2, δ_0 is independent of lamination thickness (2a).

(b) Eddy-Current Loss

By virtue of (53) substituted in (48), we are able to write a closed expression for the eddy-current loss in the instance of a uniform noise band:

$$\overline{W} = \frac{a^2\sigma}{(\beta_0 a\sigma)^2}\left(\frac{N_1^2\overline{V_{01}^2}}{R_{01}^2 l^2}\right)\left[\frac{4}{\lambda_2^2-\lambda_1^2}\left\{\tan^{-1}\left[\tan\lambda_2/2/\tanh\lambda_2/2\right]-\tan^{-1}\left[\tan\lambda_1/2/\tanh\lambda_1/2\right]\right\}\right]$$

$$\lambda_2 > \lambda_1 \geqq 0.10,\ \beta_0/a \geqq 10^2. \qquad (55)$$

Here it can be verified, for small values of λ_1 and λ_2, that the quantity within the brackets has approximately the value 2/3 and is independent of a. Again we find qualitative agreement with the result for the sine wave, in the voltage-fed case, specifically for low frequencies, or more generally, for small values of λ_1, λ_2. The mean loss per unit volume varies as the square of the lamination thickness and directly with the conductivity, and is, to a first approximation, independent of μ_e. When $\lambda_2 \leqq 0.10$, (48) may be modified with the help of (49b) to read

V. Excitation by Random Noise (Current-Fed Transformers, $\beta_0 = 0$)

For primary and secondary currents maintained independent of the frequency ($\beta_0 = 0$), the transformer is current-fed, as previously explained. In the case of noise the requirement is that $\overline{I_1^2}$ and $\overline{I_2^2}$ are not functions of frequency. The general results (47) and (48) are accordingly modified to

$$\overline{W} = \frac{a^2\sigma}{(\beta_0 a\sigma)^2}\left(\frac{N_1^2\overline{V_{01}^2}}{R_{01}^2 l^2}\right)\frac{1}{3}\left\{1-\frac{\tan^{-1}(\beta_0 a\mu_e\sigma\omega_2)-\tan^{-1}(\beta_0 a\mu_e\sigma\omega_1)}{\beta_0 a\mu_e\sigma(\omega_2-\omega_1)}\right\},\quad \beta_0/a > 10^2,\ \lambda_2 \leqq 0.10. \qquad (56)$$

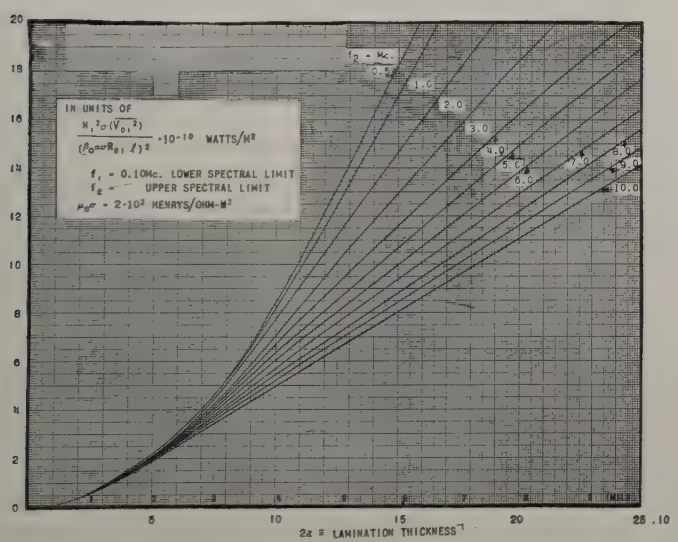

Fig. 10—Mean eddy-current loss for a uniform band of random noise as a function of lamination thickness, voltage-fed transformer.

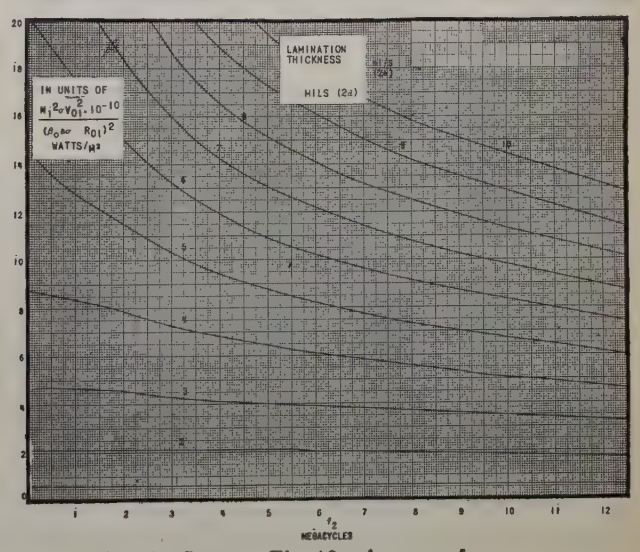

Fig. 11—Same as Fig. 10, when now frequency is the independent variable.

Note that when $f_2 \to f_1$, i.e., when the noise band becomes "monochromatic," we obtain precisely (33). For high frequencies such that λ_1 is in excess of 5.3, (55) takes the form

$$W = \frac{a^2\sigma}{(\beta_0 a\sigma)^2}\left(\frac{N_1^2\overline{V_{01}^2}}{R_{01}^2 l^2}\right)\frac{2}{\lambda_1+\lambda_2} = \frac{1}{(\beta_0 a\sigma)^2}\left(\frac{N_1^2\overline{V_{01}^2}}{R_{01}^2 l^2}\right)a\left(\frac{\sigma}{\pi\mu_e}\right)^{1/2}\frac{1}{f_2^{1/2}+f_1^{1/2}}, \qquad (57)$$

showing clearly that the losses are now proportional to the lamination thickness, and nearly inversely proportional to the square root of the bandwidth, particularly if $f_1 \ll f_2$. Figs. 10 and 11, analogous to Figs. 7 and 8, show the variation of eddy-current loss with frequency (f_2) and lamination thickness ($2a$).

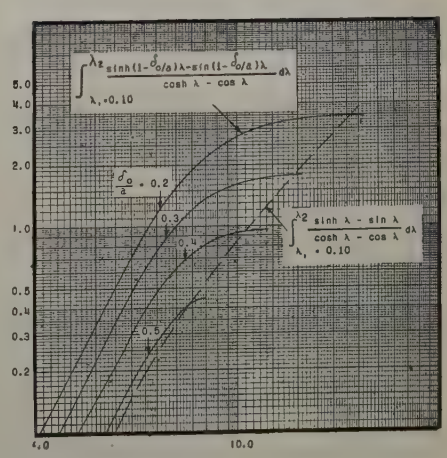

Fig. 12—The solution of (50) when $C = 0.90$.

$$1 - C = \int_0^\infty \lambda^2 \left[\frac{\sinh \lambda(1 - \delta_0/a) - \sin \lambda(1 - \delta_0/a)}{\cosh \lambda + \cos \lambda}\right] w d\lambda \Big/ \int_0^\infty \lambda^2 \left(\frac{\sinh \lambda - \sin \lambda}{\cosh \lambda + \cos \lambda}\right) w d\lambda, \quad 0 < C < 1, \tag{58}$$

and

$$\overline{W} = \frac{1}{2a^2\sigma l^2}(N_1^2\overline{I_1^2} + N_2^2\overline{I_2^2})\left[\frac{1}{2\pi\mu_e\sigma a^2 g}\int_0^\infty \lambda^2 \left(\frac{\sinh \lambda - \sin \lambda}{\cosh \lambda + \cos \lambda}\right) w d\lambda\right] \text{watts/}m^3, \tag{59}$$

where $w(\lambda^2/4\pi a^2\mu_e\sigma)$ now gives the functional dependence of the spectral shape of the *mean-square current* on frequency, and has as before the maximum value unity; g is still given by (44), and W_0 is the maximum spectral density, but with the units (ampere^2/frequency). $\overline{I_1^2}$ and $\overline{I_2^2}$ are respectively the mean-square primary and secondary currents. In making measurements it is often expedient to have an open-circuited secondary, so that $I_2=0$. We give below a brief outline of the principal results for a uniform noise-*current* spectrum extending from f_1 to f_2.

(*a*) *Skin Depth*

Here δ_0/a may be obtained from (58) and Table I, when w is set equal to unity. Again, for small λ, such that $\lambda \leqq 0.10$, we observe that (29a) applies equally well here. Large values of λ_1, (and λ_2), however, lead to

$$\begin{aligned}(1 - C)(\lambda_2^3 - \lambda_1^3)/3 &= \int_{\lambda_1}^{\lambda_2} \lambda^2 e^{-\delta_0\lambda/a} d\lambda \\ &= -(a/\delta_0)e^{-\delta_0\lambda/a}\{\lambda^2 + 2a^2(\delta_0\lambda/a + 1)/\delta_0^2\}\Big|_{\lambda_1}^{\lambda_2}.\end{aligned} \tag{60}$$

A calculation for $\lambda_2=13$, $\lambda_1=10$ gives $\delta_0/a=0.20$, in qualitative agreement with previous results, (29b) and (54). Note that here also δ_0 is independent of lamination thickness when λ is large. The variation of δ_0/α with λ_2, ($\beta_0=0$), although not explicitly calculated, appears to be qualitatively similar to the more common case shown in Fig. 5 for which β_0 is very much larger than zero, and for the same reason.

(*b*) *Eddy-Current Loss*

When $g=(f_2-f_1)$ and $w=1$, (59) yields the mean power loss per unit volume. Table I in the Appendix gives values of the integral in (59). For λ less than about a tenth, $\overline{W}$ takes the simple form (open-circuited secondary, $I_2=0$),

$$\overline{W} = \overline{2I_1^2}\left(\frac{2N_1 a\mu_e\sigma\pi}{3l}\right)^2 (f_2^2 + f_1f_2 + f_1^2), \lambda \leqq 0.10, \tag{61}$$

showing that the losses are again proportional to the square of the lamination thickness, but unlike the voltage-fed transformer, they vary as the square of σ and μ_e, vide (56). When λ_1 is large, $\overline{W}$ becomes

$$\begin{aligned}\overline{W} &= \frac{1}{3a^2\sigma}\left(\frac{N_1^2\overline{I_1^2}}{l^2}\right)\frac{\lambda_2^2 + \lambda_2\lambda_1 + \lambda_1^2}{\lambda_2 + \lambda_1} \\ &= \frac{2\pi}{3a}\left(\frac{2\mu_e}{\sigma}\right)^{1/2}\left(\frac{N_1^2\overline{I_1^2}}{l^2}\right)\frac{f_2 + (f_1f_2)^{1/2} + f_1}{f_1^{1/2} + f_2^{1/2}}, \\ &\qquad \lambda_2 > \lambda_1 > 5.3.\end{aligned} \tag{62}$$

Now $\overline{W}$ depends on a^{-1} and approximately on the square root of the bandwidth, which is a variation that is the reciprocal of that for the constant-voltage case; vide (57). The dotted curves in Fig. 9 show the change in $\overline{W}$ with frequency (f_2). Behavior similar to that of the sine wave ($\beta_0=0$) is indicated, except that the losses are not generally so great. The explanation of the shape of these curves follows the reasoning behind (35). Fig. 27(a) in footnote reference 2, obtained experimentally, is seen to be in qualitative agreement with Fig. 9 of the text, for the range indicated.

VI. Conclusion

In the preceding sections we have attempted to construct a theory for the eddy-current loss in transformer cores when the exciting voltage (or current) is a high-frequency sine wave, or high-frequency broad-band noise. As explained more fully in Sections I through V, our analysis has been based on a number of approximations, which apply with a varying degree of accuracy, depending on the conditions of operation. The most important, perhaps, is that the nonlinear physical problem has been replaced by a linear mathematical one, after a "suitable" choice of permeability. The second significant approximation appears in the boundary conditions, where capacitive effects have been ignored. This may lead to a considerable error, particularly at the higher frequencies. The other approximations, negligible leakage and edge effects, uniformity of cross section, etc., are easily justified in the light of the practical problems involved, and lead to no appreciable discrepancies. An important limitation of the theory, however, is its inability to give us any information concerning hysteresis losses. Further, it indicates that the eddy-current loss is directly proportional to the mean-square applied voltage (or current), which is certainly not altogether true, since harmonics of the applied wave are generated because of the nonlinear relation between B and H. From the experimental evidence[15] this departure from the mean square does not appear to be serious.

There are two cases of interest, the current-fed ($\beta_0=0$), and the voltage-fed ($\beta_0>0$) transformer. We are concerned primarily with the latter, for it is the more general and occurs more often in practice. Let us summarize some of the more important results with respect to minimizing the eddy-current losses, when $\beta_0>0$:

1. Make the laminations as thin as possible;
2. Use core materials with as low an intrinsic conductivity (σ) as is practicable and compatible with the required magnetic properties of the metal, so that
3. μ, and hence μ_e, may have values even at the high frequencies. For the latter (μ_e) this is quite important if we wish to keep the losses down (see Figs. 7 and 8).

[15] See Figs. 17–23 (omit 21a) of footnote 2.

4. Operate at high frequencies (f_0), or in the case of noise, with wide spectral bands whose lower limits are themselves reasonably high frequencies. The losses are less because the effective resistance of the core is noticeably increased due to the appreciable skin effect in the laminae, which arises from the preponderant number of high-frequency components. We must bear in mind, however, that the effective permeability μ_e for noise is chiefly determined by the low-frequency components (see Section I), and hence, if the lower spectral limit is too high, μ_e may be small enough to offset the skin effect in reducing the eddy-current losses. See the dotted curves in Fig. 8, for example where $\mu_e=\mu_e(f_0)$; and

5. Cut down the excitation, if possible (chiefly to lessen hysteresis).

While the above are not entirely new observations, the extent to which they apply may be seen in a quantitative fashion from the figures for a range of design-parameter values it is believed has not hitherto been covered. The curves have all been computed on the assumption of constant μ_e,[16] except as otherwise indicated, in order to show the variation of the losses $\overline{W}$, and δ_0, as functions of the parameters $2a$, f_0, f_2. We observe from Fig. 5 that in the case of a uniform noise band (f_2-f_1) cycles wide, it is the high-frequency components that are important in determining the skin-depth δ_0, as defined in Section II. For voltage-fed transformers the eddy-current loss varies about as the inverse square root of the bandwidth, an observation which seems to be borne out by the evidence of date.[17]

Because of the dearth of experimental data and the attendant difficulty of separating the losses, i.e., distinguishing between hysteresis and eddy-current phenomena, we are not able to test the theory. What evidence there is[17] seems to indicate that the theory is qualitatively correct with the exceptions noted above and gives results of the right order of magnitude. Further work is clearly needed, both experimental and theoretical. It is hoped that the present effort will stimulate investigation and at the same time provide moderately reliable numerical answers. We are greatly indebted to J. H. Van Vleck, Harvard University, and J. D. Cobine, General Electric Research Laboratory, Schenectady, N. Y., for suggestions and much encouragement in the preparation of this paper, and to Dr. Cobine for Figs. 2 and 3. We also wish to thank Miss Eleanor Pressly, who did much of the computation.

Appendix

A Partial Glossary of Technical Symbols:

σ = conductivity (mhos/meter)

μ_e = effective, or adjusted permeability (henry/meter)

V_{01} = peak primary-voltage amplitude (volts)

V_{02} = peak secondary-voltage amplitude (volts)

R_{01} = resistance of primary circuit (direct- or alternating current) (ohms)

R_{02} = resistance of secondary circuit (direct- or altering current) (ohms)

L_1 = primary inductance

L_2 = secondary inductance

I_1 = peak primary current (amperes)

I_2 = peak secondary current (amperes)

M = mutual inductance

N_1 = number of primary turns

N_2 = number of secondary turns

$\overline{W}$ = mean eddy-current power loss per unit volume. (watts/meter^3)

W_0 = maximum spectral density (volts^2/frequency), (amperes^2/frequency)

δ_0 = skin depth (meters)

l = mean length of magnetic circuit (meters)

l_0 = length of lamination (meters)

A = cross-sectional area of core (meters^2)

$2a$ = thickness of lamination (meters)

b = width of lamination (meters)

q = number of laminations

s = stacking factor

$\alpha_0=(\omega_0\mu_e\sigma/2)^{1/2}$, (m^{-1})

$\alpha=(\omega\mu_e\sigma/2)^{1/2}$, (m^{-1})

$\lambda_0=(2a^2\mu_e\sigma\omega_0)^{1/2}$

$\lambda=(2a^2\mu_e\sigma\omega)^{1/2}$

$\omega_0=2\pi f_0=2\pi\times$frequency of sine wave (second^{-1})

$\omega=2\pi f=2\pi\times$frequency (second^{-1})

f_1 = lower spectral limit to uniform noise band (sec^{-1})

f_2 = upper spectral limit to uniform noise band (sec^{-1})

$\lambda_1=(2a^2\mu_e\sigma\omega_1)^{1/2}$, corresponding to lower spectral limit

$\lambda_2=(2a^2\mu_e\sigma\omega_2)^{1/2}$, corresponding to upper spectral limit

$\mu_e(f_0)$ = effective permeability as a function of sinusoidal frequency (f_0).

Table 1

$$\Phi(\lambda)=\int_0^{\lambda}\lambda^2\left[\frac{\sinh\lambda-\sin\lambda}{\cosh\lambda+\cos\lambda}\right]d\lambda$$

λ	Φ	λ	Φ	λ	Φ	λ	Φ
0	0	1.0	0.02495	3.0	7.724	5.0	41.83
0.05	$1.30\cdot10^{-9}$	1.1	0.04425	3.1	8.73	5.1	44.39
0.10	$4.41\cdot10^{-8}$	1.2	0.0759	3.2	9.81	5.2	47.05
0.15	$4.01\cdot10^{-7}$	1.3	0.124	3.3	10.95	5.3	49.81
0.20	$2.04\cdot10^{-6}$	1.4	0.192	3.4	12.17	5.4	52.73
0.25	$7.44\cdot10^{-6}$	1.5	0.286	3.5	13.45	5.5	55.70
0.30	$2.16\cdot10^{-5}$	1.6	0.409	3.6	14.81	5.6	58.77
0.35	$5.36\cdot10^{-5}$	1.7	0.567	3.7	16.23	5.7	61.96
0.40	$1.18\cdot10^{-4}$	1.8	0.767	3.8	17.73	5.8	65.26
0.45	$2.36\cdot10^{-4}$	1.9	1.013	3.9	19.30	5.9	68.67
0.50	$4.41\cdot10^{-4}$	2.0	1.311	4.0	20.95	6.0	72.20
0.55	0.00078	2.1	1.664	4.1	22.67		
0.60	0.00131	2.2	2.077	4.2	24.47		
0.65	0.00211	2.3	2.551	4.3	26.34		
0.70	0.00328	2.4	3.087	4.4	28.30		
0.75	0.00495	2.5	3.689	4.5	30.34		
0.80	0.00727	2.6	4.357	4.6	32.47		
0.85	0.0104	2.7	5.094	4.7	34.68		
0.90	0.0142	2.8	5.904	4.8	36.98		
0.95	0.0189	2.9	6.781	4.9	39.36		
1.0	0.02495	3.0	7.724	5.0	41.83		

[16] Because of the very limited data for μ_e as a function of frequency (and excitation), we have shown only briefly the effects of changing μ_e in Figs. 6, 7, and 8. These appear particularly noticeable for the higher frequencies and the thicker laminae, resulting in increased losses. There also seems to be little reduction in δ_0, vide Figs. 5 and 6.

[17] See footnote reference 1, Fig. 21(a).

Discussion on

"Concerning Hallén's Integral Equation for Cylindrical Antennas"*

S. A. SCHELKUNOFF

Sanford Hershfield:[1] These commments refer only to resonant and antiresonant lengths of cylindrical antennas. Referring to discussions of antenna theories evolving from Hallén's integral-equation approach used by Professor King and from the Maxwell's-equations approach used by Dr. Schelkunoff, Fig. 1 presents the notation and terminology of both contributors so as to avoid any misunderstanding in the interpretation of quantities involved in the discussion of a comparison of antenna lengths by these theories.

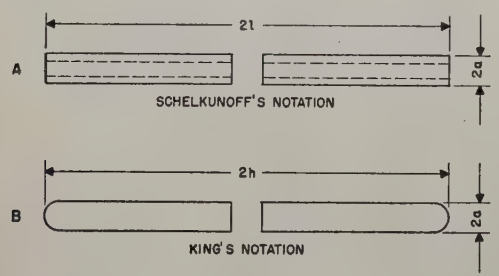

Fig. 1—Antenna terminology.

The equations and curves plotted in Schelkunoff's original paper[2] are for hollow cylindrical antennas. The equations and curves plotted in the King-Middleton paper[3] are for antennas with rounded ends. Hence, the King-Middleton approach (or any approach evolving from Hallén's integral equation) requires no correction for the ends as long as the ends are rounded. The antenna length $2h$ is measured along the axis. However, the approach of Schelkunoff excludes electric lines of force from the interior of the cylinder. Hence, antenna A, Fig. 1, must be corrected for any end capacitance resulting from a concentration of charge on the sharp edges.

Antenna A of Fig. 1 is reproduced again as antenna A of Fig. 2. Let us discuss antennas A and B of Fig. 2. The cylindrical surface area $x-x'$ of antenna A is $2\pi a^2$. The hemispherical surface area $y-y'$ of antenna B is also $2\pi a^2$. Hence, because of this equality it seems reasonable to assume that antenna B is equivalent to antenna A and can replace it for computation purposes. Both antennas A and B of Fig. 2 are uncorrected for the capacitance resulting from the concentration of charge on the sharp edges of antenna A or the charge on the hemispheres of antenna B.

The shortening of the resonant length obtained by Schelkunoff's equations and curves is due to size (diameter) and shape (cylindrical) only. For a cylindrical cross section an additional shortening due to the end capacitance is obtained by using the following equation:[4]

$$\text{per cent shortening} = 100\,\frac{K}{30\pi}\,\exp\left(-\frac{K}{120}-1\right). \qquad (1)$$

The experimental work of D. D. King quoted in the paper under discussion has been compiled for antennas with hemispherical ends. Hence, the correction factor (1) rightfully applies to this case. As tabulated in Table II of the paper under discussion, the uncorrected value for $\pi-\beta l_{\text{antires}}$ estimated by Professor King from Dr. Schelkunoff's curves is 0.47, while the uncorrected value for $(\pi/2)-\beta l_{\text{res}}$ is 0.094 for $K=480$ $(\Omega=10)$. The correction for antiresonance is, according to (1),

$$\text{per cent shortening} = 100\,\frac{480}{30\pi}\,\exp\left(-\frac{480}{120}-1\right)=3.45.$$

Hence the antiresonant length $\beta l_{\text{antires}}=(\pi-0.47)(1-0.0345)$, or $\pi-\beta l_{\text{antires}}=0.564$.

Similarly, for resonance, $(\pi/2=-\beta l_{\text{res}}=0.145$.

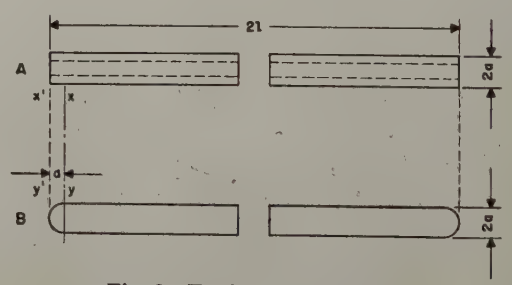

Fig. 2—Equivalent antennas.

Brown and Woodward[5] in a recent paper give experimental data for a hollow cylindrical antenna. Their antenna half-length is expressed in electrical degrees A; while their antenna diameter is expressed in electrical degrees D.

Since $\Omega=2\log_e(2h/a)$ (King's notation) and $K=120\log_e[(2l/a)-1]$ (Schelkunoff's notation) $2h/a=148$ for $\Omega=10$ and $(2l/a)\times 0.9655=148$ for $K=480$. But

* Proc. I.R.E., vol. 33, pp. 872–878; December, 1945. Discussion, vol. 34, pp. 265–269; May, 1946.

[1] Federal Telephone and Radio Corporation, Newark, N. J.

[2] S. A. Schelkunoff, "Theory of antennas of arbitrary size and shape," Proc. I.R.E., vol. 29, pp. 493–520; September, 1941 (Figs. 23, 24, 25, 26, and 27).

[3] R. King and D. Middleton, "The cylindrical antenna; current and impedance," *Quart. Appl. Math.*, vol. 3, January, 1946.

[4] S. A. Schelkunoff, "Electromagnetic Waves," D. Van Nostrand Co., Inc., New York, N. Y.; p. 465.

[5] G. H. Brown and O. M. Woodward, Jr., "Experimentally determined impedance characteristics of cylindrical antennas," Proc. I.R.E., vol. 33, pp. 257–262; April, 1945.

$2l=2A$ and $a=D/2$ in Brown and Woodward's notation. Hence, $A/D=37$ for $\Omega=10$, or $A/D=38.3$ for $K=480$. These two ratios cause negligible difference in the value of A. Using Fig. 5 of Brown and Woodward's paper (the dotted curve, base reactance removed) we find that $A=147.5$ degrees falls on this curve. This gives $\pi-\beta l_{\text{antires}}=(32.5/180)\pi=0.566$.

For the resonant condition, Fig. 11 of Brown and Woodward's paper yields a shortening of 8.5 per cent. This gives $(\pi/2)-\beta l_{\text{res}}=0.085(\pi/2)=0.1335$.

In Table I are tabulated some data from Table II of the paper under discussion to which have been added data obtained by using the curves of Brown and Woodward's paper as well as the results obtained by employing the end correction to Schelkunoff's uncorrected theory in the manner described above.

TABLE I

	$\pi-\beta l_{\text{antires}}$	$\pi/2-\beta l_{\text{res}}$
D. D. King (experimental)	0.60	0.098
Brown and Woodward (experimental)	0.566	0.1335
King-Middleton (2nd order)	0.614	0.094
Schelkunoff (estimated by King)	0.47	0.094
Schelkunoff (corrected for end capacitance)	0.564	0.145

Hence, with cap-capacitance correction, it appears that the discrepancy between the King-Middleton and the Schelkunoff resonant and antiresonant lengths is in the region of 1st resonance more so than in the region of 2nd resonance.

Ronold King:[6] It would seem that antennas A and B in Mr. Hershfield's Fig. 2 are approximately equivalent electrically only in the idealized and physically unrealizable case in which antenna A has *no* chargeable surface except the outer surface of the cylinder. That is, it has no flat ends as has a solid cylinder, and it has no sharp edges or chargeable interior surface near the open ends as has a tube. (It is this idealized situation which is assumed in the Hallén analysis when the boundary condition $I_h=0$ is imposed.) On the other hand, if antenna A is a solid cylinder or a tube, it is not equivalent to B as postulated by Mr. Hershfield. The hemisphere $y'-y$ in B is approximately equivalent to the end $x'-x$ of the cylinder A; it can not in addition compensate for the flat end of a solid cylinder or the edges and inner surface of a tube. If it is desired to approximate either a flat end or edges and interior of a tube by a hemisphere, then antenna B must be increased in half length by the radius of the hemisphere so that its half length measured along the *axis* is $h=l+a$, where l is measured to the *base* of the hemisphere.

Dr. Schelkunoff's correction for hemispherical ends appears to be calculated for a cylinder of half length l measured to the *base* of the hemisphere. If this is true, the half length along the axis is again $h=l+a$. The reference value from which the shortening is measured is the length of an infinitely thin antenna for which $a=0$. For this, at resonance, $\beta l_0=\beta h_0=\pi/2$; at antiresonance, $\beta l_0=\beta h_0=\pi$. The shortening measured by D. D. King and calculated by King and Middleton is, at resonance, $\pi/2-\beta h_{\text{res}}=\pi/2-\beta(l_{\text{res}}+a)$; at antiresonance, $\pi-\beta h_{\text{antires}}=\pi-\beta(l_{\text{antires}}+a)$. The values presumably calculated by Schelkunoff are $\pi/2\beta l_{\text{res}}$ and $\pi-\beta l_{\text{antires}}$. Hence, in order to compare values calculated from Schelkunoff's theory for a cylinder with hemispherical ends for which correction is made, it would appear necessary to *subtract* βa from both $\pi/2-\beta l_{\text{res}}$ and $\pi-\beta l_{\text{antires}}$ in order to obtain $\pi/2-\beta h_{\text{res}}$ and $\pi-\beta h_{\text{antires}}$. The values to be subtracted are approximately 0.020 and 0.035, so that the corrected Schelkunoff values in the tables become 0.125 and 0.529.

It is to be noted that the experimental values quoted from Brown and Woodward apply to a tube, not to a cylinder with hemispherical ends. Brown and Woodward appear to have measured the impedance terminating a flexible coaxial line which presumably contained dielectric material, while the slotted section of line probably did not. Unless the dielectric in the cable was made exactly an integral multiple of a half wavelength long, it could make considerable difference in the measured reactance and, hence, affect the conditions for resonance and antiresonance. Since Brown and Woodward were concerned primarily with determining impedances encountered in practice, and since no reference is made by them to methods used to eliminate or compensate for the effect of the dielectric material in the cable, it is probably fair to assume that their impedances are the values apparently terminating the coaxial cable, and not the corrected true impedances of the antenna as measured by D. D. King. Without more precise knowledge of the apparatus and of the precautions taken, it is difficult to compare intelligently the Brown and Woodward results with those of D. D. King and the several theories.

[6] Cruft Laboratory, Harvard University, Cambridge 38, Mass.

Correspondence

A New Source of Systematic Error in Radio Navigation Systems Requiring the Measurement of the Relative Phases of the Propagated Waves

In recent years various schemes have been proposed for the accurate location of a radio station. The methods under consideration in this note involve the measurement of the relative phases of the radio waves transmitted between the unknown station and two or more other radio stations, the locations of which are known. Let r_1 and r_2 be the distances along the propagation paths between the unknown station and two of the known stations, c the velocity of propagation, and f the radio frequency. The phase difference between the waves at the unknown station may be expressed

$$\Delta\phi = \frac{2\pi f}{c}(r_2 - r_1) + \theta + \phi(r_2) - \phi(r_1) \quad (1)$$

where θ is the difference in the phases of the radio waves at the two known stations and $\phi(r_2)$ and $\phi(r_1)$ are phase terms which vary with the distance and which, so far as the writer knows, have been overlooked in past studies of this problem. Most navigational systems dependent on phase measurements have been developed at comparatively low frequencies, say less than 500 kilocycles, and those which require a high degree of accuracy for their success depend upon the use of the ground wave. when the transmitting and receiving antennas are near the ground, the ground wave consists essentially of a surface wave only at these lower frequencies and then $\phi(r)$ is simply the phase of the surface-wave attenuation function which has been discussed in detail in a recent paper by the author.[1] Thus the surface wave value of $\phi(r)$ was shown in that paper to increase from 0 to $(\pi - b)$ as the "numerical distance" p increases from 0 to 100. The angle b is less than $\pi/2$ for vertical polarization and approaches zero for very low frequencies or high ground conductivities. The value of $\phi(r)$ for the surface wave depends upon the value of the "numerical distance," which in turn depends upon the frequency and the ground constants. Thus the value of $\phi(r)$ will depend upon the ground constants, and we see by the above formula that accurate navigational fixes can be obtained only when accurate data are available relative to the effective values of the ground constants along the propagation paths. To the extent that the ground constants do not vary with time, the navigational fixes can be corrected for this systematic variation of phase with distance by an appropriate calibration. However, one application of these accurate navigation systems is in connection with surveying, and in that case calibration is obviously impracticable. From the above discussion we see that the maximum possible value of $[\phi(r_2) - \phi(r_1)]$ for the surface wave will be equal to π, and thus the maximum possible error in determining the difference in distance $(r_2 - r_1)$ will be equal to a half wavelength at the operating frequency when this term is ignored; errors of this magnitude would be considered intolerable for some applications. When the ground constants are accurately known and are uniform, as in propagation over sea water, the theoretical formulas in the reference cited can probably be used to calculate the value of $[\phi(r_2) - \phi(r_1)]$ for the surface wave within a degree or two, but this solution to this problem would be quite difficult to use over paths with inhomogeneities in the ground constants.

Two other methods of eliminating this error are (1) the use of horizontal polarization for which the surface wave is negligible, but this would be practicable over extended distances only at very-high-frequencies and higher; or (2) the use of very low frequencies at sufficiently short distances such that $p < 0.0001$ since, in this case, $\phi(r)$ for the surface wave is less than one degree; this would often involve propagation at distances less than one wavelength and in that case $\phi(r)$, although practically independent of the ground constants, would still be variable with distance because of the presence of the "induction" and "electrostatic" field components.

The phase term $\phi(r)$ will also vary with the height of the radio antennas in a manner that can be determined by calculating the phase of the vector sum of the three components of the ground wave: the direct wave, the ground-reflected wave, and the surface wave; the appropriate formula is given in the reference cited, equation (1). Within the line of sight, at antenna heights sufficiently large that the surface wave can be neglected, the field oscillates with increasing height between values corresponding to the sum and difference of the direct and ground-reflected waves, while the phase term $\phi(r)$ changes slowly except for abrupt changes which take place each time the field passes through a null; these abrupt phase changes are equal to π radians in the limiting case when the direct and ground-reflected waves have equal intensities but are correspondingly smaller when these two components of the ground wave have much different intensities. In general, when more than one propagation path exists, the resultant phase will oscillate around the expected value for the path along which the strongest wave is propagated. This will, of course, be true also in the case of paths traversing the ionosphere or the troposphere as well as for waves reflected from objects near the direct path.

When convenient methods become available for the accurate measurement of $\Delta\phi$, it may turn out that the dependence on the ground constants of the surface-wave value of $\phi(r)$ may provide a new and feasible means for determining the effective values of these ground constants over the propagation paths.

The need for corrections to distance determinations dependent upon phase measurements was called to my attention by measurements made with the "Raydist" system for accurate distance and position determination, developed by Charles E. Hastings of the Hastings Instrument Company. This system is essentially the radio analogue of Michelson's optical interferometer. Using this system on a frequency of approximately 12.8 megacycles, measurements made every 100 feet up to about one mile indicated a random error of ± 3 feet and a cumulative error over the entire distance of from +10 to +25 feet, depending upon the path chosen. This cumulative error was initially attributed to an error in the velocity of propagation but is readily explained qualitatively by the above theory of the propagation of phase. It is, of course, equally correct to consider that the phase velocity is variable for waves propagated near the surface of the earth, but this would require a velocity of propagation variable with the distance and it seems more natural to use the above theory of phase variations and a constant velocity of propagation, especially in view of the fact that theoretical formulas for $\phi(r)$ are already available in the literature.

KENNETH A. NORTON
Central Radio Propagation Laboratory
National Bureau of Standards
Washington 25, D. C.

[1] K. A. Norton, "The calculation of ground-wave field intensity over a finitely conducting spherical earth," PROC. I.R.E., vol. 29, pp. 623–639; December, 1941.

On the Resonant Frequencies of n-Meshed Tuned Circuits

We shall prove the following theorem, which we shall later apply to the predimensioning of quartz crystals.

In an n-meshed coupled tuned circuit, (Fig. 1) multiplying all the inductances, both self and coupled, by a factor A^2, and all the capacitances, both self and coupled, by a factor B^2, the resonant frequencies of the circuit are multiplied by a factor $1/AB$. Thus the circuit may be scaled.

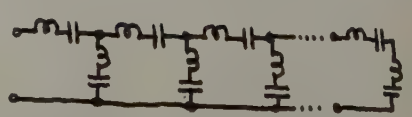

Fig. 1

Let Q_i be the charge in the ith mesh.
I_i be the current in the ith mesh.
L_{ii} and L_{ij} be the total series inductance in the ith mesh, and the coupled inductance between the ith and the jth mesh, respectively.

C_{ii} and C_{ij} be similarly defined quantities for the self and coupled capacitances.

$$S_{ij} = 1/C_{ij}.$$

Then

$$\text{magnetic energy} = \frac{1}{2}\sum_{i}^{n}\sum_{j}^{n} L_{ij}I_iI_j^1 \quad (1)$$

$$\text{electric energy} = \frac{1}{2}\sum_{i}^{n}\sum_{j}^{n} S_{ij}Q_iQ_j. \quad (2)$$

Hence the frequency determinant is

$$\begin{vmatrix} S_{11}-uL_{11} & S_{12}-uL_{12} & \cdots & S_{1n}-uL_{1n} \\ S_{12}-uL_{12} & S_{22}-uL_{22} & \cdots & S_{2n}-uL_{2n} \\ \cdots & \cdots & \cdots & \cdots \\ S_{1n}-uL_{1n} & S_{2n}-uL_{2n} & \cdots & S_{nn}-uL_{nn} \end{vmatrix} = 0 \quad (3)$$

where

$$u = \omega^2$$

ω = angular frequency.

This determinant can of course be derived from the mesh-circuit equations. They are written here in this manner because of their similarity to the equations for mechanical systems. Now expanding the determinant in powers of u, we have

$$a_nu^n + a_{n-1}u^{n-1} + a_iu^i + a_0 = 0 \quad (4)$$

where a_i is a sum of terms, each one of which is a product of i factors chosen from the L_{ij} and $n-i$ factors chosen from the S_{ij}. From this we deduce the following: if we multiple every L_{ij} by a factor A and every S_{ij} by a factor B, the a_i are multiplied by a factor A^iB^{n-i}. Hence by a well-known theorem in the theory of equations, the roots of (4), that is u, are multiplied by B/A. This proves the theorem stated above.

This theorem, when translated into mechanical terms wherein electric and magnetic energy correspond to potential and kinetic energy respectively, is of some use in the predimensioning of quartz oscillating crystals. In this case capacitance coupling corresponds to that due to the elastic constants c_{rs}, r not equal to s, and inductance which is a measure of the kinetic energy, depends mainly upon the density and dimensions of the crystal. Thus, if one obtains a good crystal at one frequency which may be due to fortunate coupling, both inductive and capacitative, between various modes of vibrations, one can obtain a similarly good crystal of the same type by simply scaling the dimensions.

For example, the high-frequency shear ($Y'X$) mode in an AT crystal is coupled capacitatively to the $Z'X$ shear via the elastic constant c_{56}, and is coupled kinetically or inductively to flexure in the $Y'X$ and $Z'X$ planes. The coupling to flexure is inductive because it is solely a function of dimensions, since this coupling vanishes when the ratio of the Y' and Z' dimensions to that of the X is small. Hence by the theorem proven above, one can transfer to another frequency by simply scaling dimensions.

PHILIP PARZEN
Demornay Budd
New York, N. Y.

[1] J. Carson, "Electric Circuit Theory and Operational Calculus." McGraw Hill Publishing Company, New York, N. Y., 1926; page 6.

Contributors to Proceedings of the I.R.E.

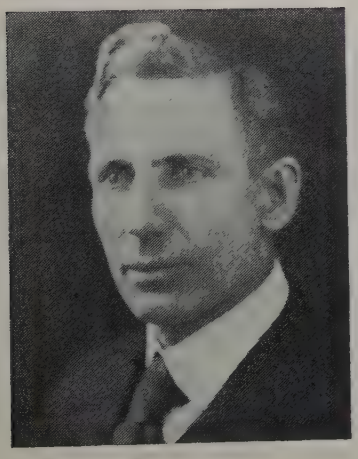

E. F. GEORGE

E. F. George was born in West Virginia in 1878. He attended West Virginia Wesleyan, Valparaiso University, West Virginia University, the University of Illinois, the University of Chicago, and in 1920 received his Ph.D. degree from Ohio State University.

From 1902 to 1906 he served as a railroad surveyor, and in 1918 became a first lieutenant in the United States Field Artillery. Dr. George taught physics at West Virginia University from 1920 to 1925. He served as the head of the physics department at Texas Technological College from 1925 to 1942. In 1942 he became affiliated with the Radar Laboratory, United States Signal Corps, and from 1943 to 1944 he was a professor of physics at Hamilton College, Clinton, New York. Since 1944 he has been head of the physics department at the University of Alaska, College, Alaska.

Dr. George has served as a Captain in the United States Army Reserve and in the Texas National Guard. He has also worked with the Ionospheric Observatory, College, Alaska, and the Watson Laboratories, Red Bank, New Jersey, and Ottawa, Canada.

❖

William A. Huber (A'44–M'46) was born at Blackwood, New Jersey, on August 25, 1910. He was graduated in electrical engineering from Drexel Institute of Technology, Philadelphia, Pennsylvania, in 1937. After graduation he joined the RCA Manufacturing Company at Camden, New Jersey, where he was employed in the radio receiver department.

In February, 1941, Mr. Huber became associated with the War Department (Signal Corps) as a civilian radio engineer and was

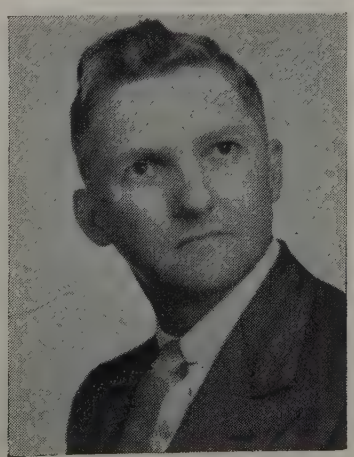

WILLIAM A. HUBER

ERNEST G. LINDER

❖

stationed at Fort Monmouth, New Jersey. He was assigned to the radio position finding section, Fort Hancock, Sandy Hook, New Jersey, doing pioneer work in radar research and development. In June, 1942, Mr. Huber was transferred to the Evans Signal Laboratory, Belmar, New Jersey, as engineer in charge of the oscilloscope section, and was responsible for the development of much original radar indicating and ranging equipment.

Mr. Huber has on file with the U. S. Patent Office several patent applications pertaining to radar systems.

❖

Ernest G. Linder (A'40) was born in 1902 at Waltham, Massachusetts. He received the B.A. degree from the University of Iowa in

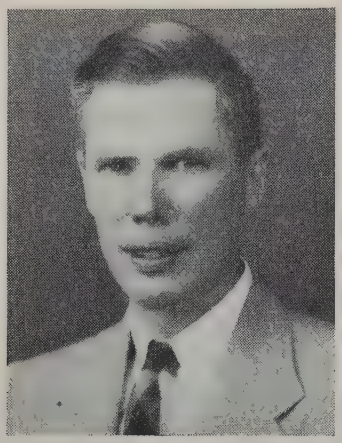

P. H. Miller, Jr.

1925, and the M.S. degree in 1927. He was an instructor in physics at the State University of Iowa from 1925 to 1927; an instructor at California Institute of Technology from 1927 to 1928; and a Detroit Edison Fellow at Cornell University from 1928 to 1932, where he received his Ph.D. degree in 1931. Dr. Linder was employed in the Research Division of the RCA Victor Company from 1932 to 1935, and the RCA Manufacturing Company, RCA Victor Division, from 1935 to 1942. At present he is with the RCA Laboratories at Princeton, New Jersey. He is a member of the American Physical Society.

❖

David Middleton (S'42–A'44–M'45) was born on April 19, 1920, in New York City. In 1942 he received the B.A. degree in physics from Harvard University, followed by the M.A. degree in 1945. During the last half of 1942 he was employed as a teaching fellow in electronics in the preradar training program carried on at that institution during the war. From December of 1942 through 1945, he was engaged as a research associate in the Theory Group of the Harvard Radio Research Laboratory, where much of his work dealt with noise and problems encountered in its use as a radar and communication countermeasure.

Mr. Middleton is at present completing his Ph.D. degree at Harvard University, as a National Research Council predoctoral fellow in physics. He is a member of Phi Beta Kappa, Sigma Xi, and the American Physical Society.

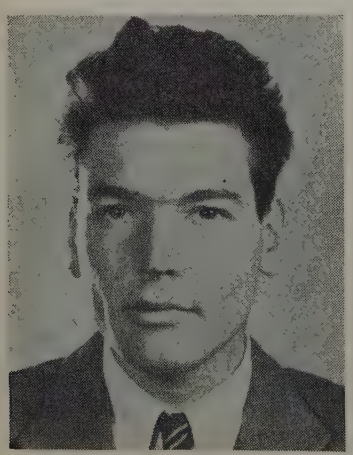

David Middleton

❖

P. H. Miller, Jr., was born at Philadelphia, Pennsylvania, on January 22, 1916. He received his B.S. degree from Haverford College in 1935, and the Ph.D. degree in physics from California Institute of Technology in 1940.

Since 1939 he has been with the physics department of the University of Pennsylvania, serving as instructor from 1939 to 1942, and as assistant professor until 1946, when he was made associate professor. He served as acting chairman of the department from May, 1945, to March, 1946.

Dr. Miller has worked on the physics of solids, and during the war was active in the Office of Scientific Research and Development project at the University of Pennsylvania for development of crystal rectifiers. He is a member of Sigma Xi, Phi Beta Kappa, and a Fellow of the American Physical Society.

❖

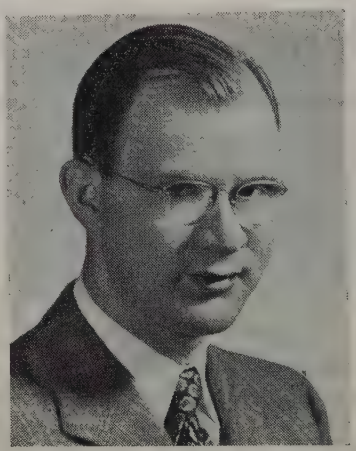

Shepard Roberts

Shepard Roberts (S'38–A'41–M'45) was born in New Rochelle, New York, on April 12, 1915. He received the S.B. degree in 1938, the S.M. degree in 1939, and the Sc.D. degree in 1946 from the Massachusetts Institute of Technology. From 1939 to 1940, he was a research assistant in the Laboratory for Insulation Research at the Massachusetts Institute of Technology, where he worked on dielectric measurements in the range of microwaves. In 1940 he was made a staff member of the M.I.T. Radiation Laboratory and in 1941 he participated in the early experiments with 3-centimeter radar and wave-guide techniques. A major part of his subsequent work in this laboratory was concerned with testing and standardizing crystal rectifiers for radar receivers. From 1945 to 1946 he was a graduate student and research associate in the Laboratory for Insulation Research, where he studied the nonlinear dielectric properties of barium titanate. He is now employed at the General Electric Research Laboratory in Schenectady. Mr. Roberts is a member of Sigma Xi.

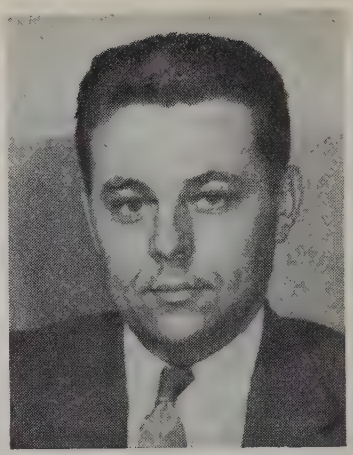

T. H. Rogers

T. H. Rogers was born in 1906 at White, Arkansas. He received the B.S. degree in electrical engineering from Mississippi State College in 1928, and the M.E.E. degree from the Polytechnic Institute of Brooklyn in 1933. From 1928 to 1929 Mr. Rogers was employed as a test engineer by the General Electric Company, Schenectady, N. Y. He served as a member of the technical staff at the Bell Telephone Laboratories, New York, N. Y., from 1929 to 1932. Since 1934 he has been employed by the Machlett Laboratories, Inc., Springdale, Conn., and was appointed manager of engineering in 1944. Mr. Rogers is a member of Tau Beta Pi.

❖

Robert L. Sproull was born in 1918 at Lacon, Illinois. He received the B.A. degree from Cornell University in 1940. He was successively President White Fellow, Charles A. Coffin Fellow, and a research assistant in physics at Cornell University, where he received the Ph.D. degree in 1943. He was employed in the summer of 1940 by the development department of Eastman Kodak Company and in the summer of 1941 by the electronics research department of Bell Telephone Laboratories. From 1943 to 1946 he was with RCA Laboratories at Princeton, New Jersey. He is now professor of physics at Cornell University. He is a member of the American Physical Society and is president of The Telluride Association, an endowed educational foundation.

Robert L. Sproull

Institute News and Radio Notes

Fiscal Matters of Interest to I.R.E. Membership

From time to time situations arise which the Board of Directors feel should be called to the attention of all members of the Institute. Such a situation now confronts us. It concerns fiscal and budgetary problems.

All members are aware of the recent increasing costs of salaries, wages, services, and materials. Your Institute has been unavoidably subject to such increased costs as has every individual and organization. Since its income is derived solely from dues and advertising revenue, rising costs can be met only through increasing dues or by reducing the services and benefits to members.

The Institute is the technical society of your profession. It belongs to you. It exists only to serve you and your profession. It is now serving you in four ways:

1. Through publishing the PROCEEDINGS which keeps you in touch with the latest technical advances.
2. Through Sectional activities with their technical meetings.
3. Through technical committees which establish the standards that guide your profession, in which work you collaborate with other members in your own fields of activity.
4. Through conventions, where by technical meetings and social gatherings you meet members of your profession and learn from them of technical achievements.

The Institute's income goes primarily into the publishing of the PROCEEDINGS and secondarily into supporting Sectional activities and the expenses of the work of technical committees. Conventions are usually made self-sustaining through revenue secured from industry exhibitors.

These services are expensive and at the present time cost about twice the amount of receipts from membership dues. These dues are, incidentally, the lowest of any of the larger engineering societies. How then does the Institute make ends meet? Through the income from advertising. However, costs are rising faster than the increases in income from both growth in number of members and from advertising.

Some years ago your Board of Directors presaw the mass of technical information that the end of the war would release and accumulated a fund of $20,000 to pay for the extra PROCEEDINGS pages needed to publish it. You have been enjoying an enlarged PROCEEDINGS recently but the cost of a PROCEEDINGS page has doubled since 1939 and the $20,000 fund was entirely consumed in 1946. Gifts make it possible to continue an enlarged PROCEEDINGS through March of this year but in order to balance its accounts the number of pages of technical and editorial material must be reduced from over 100 pages to 72 pages per issue commencing in May. Your Board of Directors greatly deplores this situation because it means that it is impossible to catch up with the large backlog of papers on hand awaiting publication. In fact it means that the backlog will increase. This condition creates a disservice both to you and to the authors who wish to publish the results of their work promptly and in your PROCEEDINGS, not in other publications to which they must seek recourse if we cannot accommodate them.

Your Board of Directors does not intend to permit this condition to continue unchallenged. Nor does it propose to ask for gifts to finance a continuing deficit. The problem is being intensively studied and a further report will soon be submitted to you.

Additional data of interest concerning the Institute's fiscal situation are given below.

Before the war there were published in the PROCEEDINGS about fifty-six pages of technical and editorial material each month. Since 1943 the volume of material available for publication has been rising at a rapid rate until, at the present time, it would take between 150 and 175 pages to keep abreast of the inflow of technical papers. To make the Institute's budget for 1947 balance, only 72 pages of technical and editorial material per issue can be financed. Although this is more than the average prewar publication, it is still much below the amount needed to keep abreast of our expanding technical field. The condition is unusual because the expansion of radio communication and allied electronic fields in the last eight years has been unparalleled among the technical arts. The large increase in our membership testifies to this growth. These conditions mean that the PROCEEDINGS, to serve the profession properly, must expect to continue permanently with more pages per issue than for prewar. This requirement combined with a doubling of unit production costs and a large backlog of unpublished papers creates the existing emergency conditions.

Full advantage has been taken of advertising revenue promotion. During the past five years the income from advertising has risen at a greater rate than dues income but there is no assurance that this revenue will continue to increase. It may decrease. A reduced technical content is not the way to inspire confidence in the prestige of the PROCEEDINGS.

To meet the problem of increasing requirements in office space and rental rates, the Building Campaign was inaugurated. Your Institute is now housed in its own permanent and fully owned home, and the charges against current income to maintain and operate it are much less than those that would now be required for the occupancy of rented quarters. Without the saving thus effected, your 1947 PROCEEDINGS would be still smaller.

Advertising net revenue has increased 8.9 times. Income from dues and subscriptions has increased 4.3 times. Surplus has increased 2.5 times. Total income has increased 5.1 times. Surplus which in 1940 amounted to a bit more than the income for that year, now is only 52 per cent of the current annual income. Advertising income has been increasing at a lesser rate than other income since 1943.

There has been an astonishing change in the cost of running the Institute per member (regardless of grade) over a period of years. This amount has increased, so that it now costs almost $20.00 per member, although dues are only $10, $7, and $3 for different categories of membership grade.

From 1940 through 1946

Membership has increased	3.3 times
Total salaries have increased	4.8 times
Editorial salaries have increased	3.5 times
PROCEEDINGS total printing costs have increased	5.3 times
PROCEEDINGS printing cost per member has increased	1.6 times

I.R.E. dues compared to those of other leading societies

Society	DUES OF PROFESSIONAL SOCIETIES					
	Student	Junior Member	Associate or Technical Member	Active Member and Member	Senior Member and Associate Fellow	Fellow
Institute of Radio Engineers	$ 3.00		$7.00, $10.00	$10.00	$10.00	$10.00
American Institute of Electrical Engineers	3.00		10.00	15.00		20.00
American Society of Civil Engineers	15.00	$15.00	25.00	25.00		
American Society of Mechanical Engineers	3.00	10.00, 15.00		20.00		
American Society of Chemical Engineers		10.00	15.00	15.00		
*Institute of Aeronautical Sciences			10.00	14.00	16.00	20.00
Society of Motion Picture Engineers	5.00		10.00	15.00		
American Institute of Mining and Metallurgical Engineers	2.00	10.00	15.00	15.00		

* Includes subscription to Journal.

I.R.E. People

W. R. G. Baker

W. R. G. Baker, president of the Institute of Radio Engineers, recently was presented the Certificate of Appreciation by Brigadier General Calvert H. Arnold, chief of Procurement and Distribution, Office of the Chief Signal Officer, at a ceremony in Schenectady, N. Y. Dr. Baker, General Electric vice-president in charge of the company's Electronics Department, was cited for "patriotic services in a position of trust and responsibility . . . for outstanding contribution to the war effort by the development, design and production of complex Signal Corps radio and radar equipment."

❖

Frederick R. Lack

At the annual meeting of the American Standards Association, Frederick R. Lack (A'20–F'37) was elected president for the ensuing year. Mr. Lack is vice-president and a director of the Western Electric Company and was formerly vice-president of the American Standards Association.

After a career with the Bell Telephone System, which he began as an assembler in 1911, Mr. Lack became vice-president and a director of Western Electric in 1942. Following service in World War II, where he was for a time director of the Army and Navy Electronics Production Agency, he resumed his duties in 1943 as director of Western Electric's radio division in New York.

Mr. Lack is a director of The Institute of Radio Engineers, the Radio Manufacturers Association, and the Smith-Winchester Manufacturing Company. He is president of the Harvard Engineering Society, and a member of the American Institute of Electrical Engineers and the American Physical Society.

❖

B. J. Miller

Dr. Baker Receives Certificate of Appreciation from Brigadier General Calvert H. Arnold

❖

B. J. Miller

The appointment of B. J. Miller (A'46) as chief of the recently organized Guided Missile Electronics Section of the National Bureau of Standards, was announced recently by E. U. Condon (M'42–SM'43), director of the Bureau.

The new section is concerned with the electronic and servomechanism phases of guided missiles, research and development of which is the primary responsibility of the Bureau's guided-missile section. Scientists of these sections are presently engaged in research stages of the "Kingfisher Project," advance development of the now famous BAT, a radar-guided bomb developed by the Bureau and used extensively in the latter part of the war against the Japanese. Harry Diamond (A'26–M'30–SM'43–F'43), chief of the ordnance development division, is deputy chief of this project.

Dr. Miller received the B.S. degree from St. Ambrose College in 1933, and the master and doctor of physics degrees from the University of Iowa in 1936 and 1939. He was an instructor of physics at St. Ambrose College and of applied mathematics at St. Louis University prior to joining the staff of the National Bureau of Standards in 1943. Since 1945 he has been engaged in work on electronics for guided missiles. As a physicist in the ordnance development division of the Bureau, Dr. Miller played an active part in research phases of the radio proximity fuze.

Dr. Miller is a member of the American Physical Society and of Sigma Xi.

❖

J. H. Boekhoff

J. H. Boekhoff (A'45), formerly director of sales and service engineering for the Collins Radio Company, was recently appointed manager of broadcast sales. He will devote full time to the co-ordination of sales of both amplitude- and frequency-modulation broadcast transmitters, accessories, and studio speech equipment.

Mr. Boekhoff received the B.S.E.E. degree from the University of Minnesota. He became associated with Collins in 1941, was rapidly advanced through test engineering and design engineering, and in 1943 joined the sales department.

J. H. Boekhoff

I.R.E. People

ROY WENSLEY

ROY WENSLEY

Roy Wensley (A'46) was recently appointed general manager of the Wilcox-Gay Corporation. He became affiliated with the Westinghouse Electric Corporation as a switchboard-design engineer in 1916. In 1921 he was advanced to section head of the switchboard department where his progress was marked by pioneering developments in supervisory and automatic controls for hydrogenerator and electric substations.

From 1929 to 1931 Mr. Wensley served as a correlator of the Domestic Refrigeration program, and then became chief engineer of the Westinghouse Protective Relay Section. He joined the ITE Circuit Breaker Company of Philadelphia in 1935 as assistant general manager, and in 1941 was made general manager, which position he held up to the time of new affiliation.

Mr. Wensley is a member of the American Institute of Electrical Engineers.

❖

LOUIS KAHN

Louis Kahn (A'31), assistant chief engineer of the Aerovox Corporation, has been awarded a Certification of Appreciation for his activity in the war committee work of the American Standards Association for his contributions to the joint engineering studies and recommendations dealing with wartime capacitor problems.

In commenting on the award, the ASA stated: "You are one of those who volunteered your time and experience in the War Committee Work of our Association. By developing standards for Army and Navy equipment and procedure, such committees rendered a most valuable service to our Armed Forces. Simplification of products, interchangeability of repair parts, better procedures for subcontracting, higher standards of manufacture, resulted in the saving of time, money and material, and covtributed to Victory. . . . The contribution made to the country by ASA War Committees has been signally honored by Army and Navy, and the ASA feels it only right to pass this honor along to you and to the others who actually did the work."

SECTIONS

Chairman		Secretary
	ATLANTA March 21	M. S. Alexander 2289 Memorial Dr., S.E. Atlanta, Ga.
H. L. Spencer Associated Consultants 18 E. Lexington Baltimore 2, Md.	BALTIMORE	G. P. Houston, 3rd 3000 Manhattan Ave. Baltimore 15, Md.
Glenn Browning Browning Laboratories 750 Main St. Winchester, Mass.	BOSTON March 20	A. G. Bousquet General Radio Co. 275 Massachusetts Ave. Cambridge 39, Mass.
I. C. Grant San Martin 379 Buenos Aires, Argentina	BUENOS AIRES	Raymond Hastings San Martin 379 Buenos Aires, Argentina
H. W. Staderman 264 Loring Ave. Buffalo, N. Y.	BUFFALO-NIAGARA March 19	J. F. Myers Colonial Radio Corp. 1280 Main St. Buffalo 9, N. Y.
J. A. Green Collins Radio Co. Cedar Rapids, Iowa	CEDAR RAPIDS	Arthur Wulfsburg Collins Radio Co. Cedar Rapids, Iowa
A. W. Graf 160 N. La Salle St. Chicago 1, Ill.	CHICAGO March 21	D. G. Haines Hytron Radio and Electronic Corp. 4000 W. North Ave. Chicago 39, Ill.
J. D. Reid Box 67 Cincinnati 31, Ohio	CINCINNATI March 18	P. J. Konkle 5524 Hamilton Ave. Cincinnati 24, Ohio
H. C. Williams 2636 Milton Rd. University Heights Cleveland 21, Ohio	CLEVELAND March 27	A. J. Kres 16911 Valleyview Ave. Cleveland 11, Ohio
E. M. Boone Ohio State University Columbus, Ohio	COLUMBUS March 14	C. J. Emmons 158 E. Como Ave. Columbus 2, Ohio
Dale Pollack 352 Pequot Ave. New London, Conn.	CONNECTICUT VALLEY March 20	R. F. Blackburn 62 Salem Rd. Manchester, Conn.
Robert Broding 292 Kingston Dallas, Texas	DALLAS-FT. WORTH	A. S LeVelle 308 S. Akard St. Dallas 2, Texas
J. E. Keto Aircraft Radio Laboratory Wright Field Dayton, Ohio	DAYTON March 20	Joseph General 411 E. Bruce Ave. Dayton 5, Ohio
P. O. Frincke 219 S. Kenwood St. Royal Oak, Mich.	DETROIT March 21	Charles Kocher 17186 Sioux Rd. Detroit 24, Mich.
N. J. Reitz Sylvania Electric Products, Inc. Emporium, Pa.	EMPORIUM	A. W. Peterson Sylvania Electric Products, Inc. Emporium, Pa.
E. M. Dupree 1702 Main Houston, Texas	HOUSTON	L. G. Cowles Box 425 Bellaire, Texas
H. I. Metz Civil Aeronautics Authority Experimental Station Indianapolis, Ind.	INDIANAPOLIS	M. G. Beier 3930 Guilford Ave. Indianapolis 5, Ind.
R. N. White 4800 Jefferson St. Kansas City, Mo.	KANSAS CITY	Mrs. G. L. Curtis 6003 El Monte Mission, Kansas
J. R. Bach Bach-Simpson Ltd. London, Ont., Canada	LONDON, ONTARIO	G. L. Foster Sparton of Canada, Ltd. London, Ont., Canada
C. W. Mason 141 N. Vermont Ave. Los Angeles 4, Calif.	LOS ANGELES March 18	Bernard Walley RCA Victor Division 420 S. San Pedro St. Los Angeles 13, Calif.
L. W. Butler 3019 N. 90 St. Milwaukee 13, Wis.	MILWAUKEE	E. T. Sherwood 9157 N. Tennyson Dr. Milwaukee, Wis.
J. C. R. Punchard Northern Electric Co. 1261 Shearer St. Montreal 22, Que., Canada	MONTREAL, QUEBEC April 9	E. S. Watters Canadian Broadcasting Corp. 1440 St. Catherine St., W. Montreal 25, Que., Canada

	Chairman		Secretary
New York April 2	J. T. Cimorelli RCA Victor Division 415 S. Fifth St. Harrison, N. J.		J. R. Ragazzini Columbia University New York 27, N. Y.
North Carolina-Virginia	L. R. Quarles University of Virginia Charlottesville, Va.		J. T. Orth 4101 Fort Ave. Lynchburg, Va.
Ottawa, Ontario March 20	D. W. R. McKinley 211 Cobourg St. Ottawa, Canada		W. A. Caton 132 Faraday St. Ottawa, Canada
Philadelphia April 3	Samuel Gubin 4417 Pine St. Philadelphia 4, Pa.		A. N. Curtiss RCA Victor Division Bldg. 8–9 Camden, N. J.
Pittsburgh April 14	W. E. Shoupp 911 S. Braddock Ave. Wilkinsburg, Pa.		C. W. Gilbert 52 Hathaway Ct. Pittsburgh 21, Pa.
Portland	Francis McCann 4415 N.E. 81 St. Portland 13, Ore.		A. E. Richmond Box 441 Portland 7, Ore.
Rochester March 20	A. E. Newlon Stromberg-Carlson Co. Rochester 3, N. Y.		K. J. Gardner 111 East Ave. Rochester 4, N. Y.
St. Louis	S. H. Van Wambeck Washington University St. Louis 5, Mo.		N. J. Zehr 1538 Bradford Ave. St. Louis 14, Mo.
San Diego April 1	Rawson Bennett U. S. Navy Electronics Lab. San Diego 52, Calif.		Clyde Tirrell U. S. Navy Elctronics Laboratory San Diego 52, Calif.
San Francisco			F. R. Brace 955 Jones San Francisco, 9, Calif.
Seattle April 10	E. H. Smith 823 E. 78 St. Seattle 5, Wash.		W. R. Hill University of Washington Seattle 5, Wash.
Syracuse	C. A. Priest 314 Hurlburt Rd. Syracuse, N. Y.		R. E. Moe 1633 E. Genesee St. Syracuse 10, N. Y.
Toronto, Ontario	H. S. Dawson Canadian Association of Broadcasters 80 Richmond St., W. Toronto, Ont., Canada		C. J. Bridgland Canadian National Telegraph 347 Bay St. Toronto, Ont., Canada
Twin Cities	M. E. Knox 43—44 Ave., S. Minneapolis, Minn.		Paul Thompson 4602 S. Nicollet Minneapolis, Minn.
Washington April 14	F. W. Albertson Room 1111, Munsey Bldg. Washington 4, D. C.		G. P. Adair Federal Communications Commission Washington 4, D. C.
Williamsport April 2	W. C. Freeman, Jr. 2018 Reed St. Williamsport 39, Pa.		S. R. Bennett Sylvania Electric Products, Inc. Plant No. 1 Williamsport, Pa.

SUBSECTIONS

Fort Wayne (Chicago Subsection)	R. B. Jones City Signal Service 319 E. Main St. Fort Wayne 2, Ind.	S. J. Harris Farnsworth Television and Radio Co. 3702 E. Pontiac Fort Wayne 1, Ind.
Hamilton (Toronto Subsection)	T. S. Farley 74 Hyde Park Ave. Hamilton, Ont., Canada	E. Ruse 195 Ferguson Ave., S. Hamilton, Ont., Canada
Monmouth (New York Subsection)	K. G. Jansky Bell Telephone Laboratories, Box 107 Red Bank, N. J.	L. E. Hunt Bell Telephone Laboratories, Box 107 Deal, N. J.
Princeton (Philadelphia Subsection)	C. W. Mueller RCA Laboratories Princeton, N. J.	A. V. Bedford RCA Laboratories Princeton, N. J.
South Bend (Chicago Subsection) March 20	A. R. Kahn Electro-Voice, Inc. Buchanan, Mich.	A. M. Wiggins Electro-Voice, Inc. Buchanan, Mich.
Winnipeg (Toronto Subsection)	W. A. Cole 323 Broadway Ave. Winnipeg, Manit., Canada	C. E. Trembley Canadian Marconi Co. Main Street Winnipeg, Manit., Canada

I.R.E. People

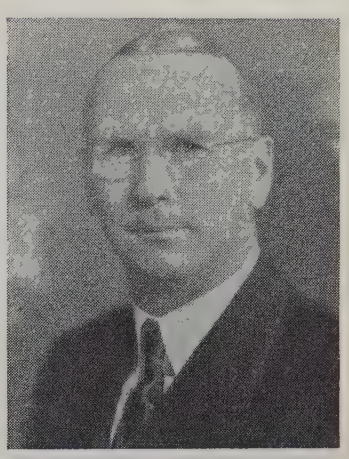

Jerome R. Steen

Jerome R. Steen

The appointment of Jerome R. Steen (A'36–M'36–SM'43) as director of quality control for the lamp, fixture, wire products, tungsten and chemicals, radio tube and electronic divisions of Sylvania Electric Products, Inc., was recently announced by E. Finley Carter (A'23–F'36), vice-president in charge of engineering.

Mr. Steen was graduated from the University of Wisconsin in 1923, and has been associated with the General Electric Company, the Grigsby-Grunow Company, and the Bell Telephone Laboratories. He joined the staff of Sylvania Electric in 1931 as supervisor in charge of finished tube quality control at the radio tube division's Emporium, Pennsylvania, plant, and in 1936 his work was expanded to include similar activities at the Salem, Massachusetts, radio tube plant. In 1942 he was transferred to the commercial engineering department, and in 1944 was appointed manager of the quality control engineering department, radio tube division.

Mr. Steen is a member of the American Society for Quality Control, the Institute of Mathematical Statistics, and the American Statistical Association.

❖

Samuel Lubin

The appointment of Samuel Lubin (M'46) to the field engineering department of the Sprague Electric Company, North Adams, Massachusetts, has been announced by Leon Podolsky (A'30–M'46), manager of this department.

A graduate electrical engineer, Mr. Lubin received his education at the Northwestern School of Engineering, George Washington University, Washington, D. C., and Washington University, St. Louis, Missouri From 1932 to 1939, he was managing director of International Radio, Ltd., at Tel Aviv, Palestine. He later joined the new development section of the Technical Standards Division of R.E.A. On wartime leave from this position, he served as transition engineer of the Radio Research Laboratory at Harvard University.

Mr. Lubin is a member of Tau Beta Pi.

I.R.E. People

B. V. K. French

B. V. K. French

B. V. K. French (M'30–SM'43) has joined the staff of Howard Sams and Company, Inc., Indianapolis, Indiana, as director of field relations.

In 1923 Mr. French joined Federal Telephone and Telegraph of Buffalo as a development engineer. Two years later he became a member of the radio engineering staff of the American Bosch Company. In 1933 he joined the staff of the RCA License Division Laboratory in New York City. During 1935 and 1936 Mr. French was chief engineer for the Case Electric Company, Marion, Indiana. In 1937 he entered the engineering department of the P. R. Mallory Company, of Indianapolis. During the early part of the war, he served on the Joint Army-Navy Standardization Board. In 1944 he became supervisor of the Mallory Research Laboratory, New York City.

Mr. French has served as chairman of the Connecticut and Indianapolis Sections of the I.R.E.

❖

I.R.E. Members of New NAB Committees

Industry leaders who will serve on committees of the National Association of Broadcasters during 1947 include H. W. Slavick (A'28), Program Executive Committee; Orrin Towner (A'24–M'29–SM'43), R. V. Howard (M'41–SM'43), R. C. Hale (A'45), Oscar Hirsch (A'26–M'44), G. P. Houston (A'28), O. B. Hanson (A'18–M'27–F'41), W. B. Lodge (A'34–M'37–SM'43), and E. M. Johnson (S'40–A'41–M'44), Engineering Executive Committee; T. A. M. Craven (F'29), Board Liaison Committee of the Engineering Committee; J. E. Fetzer (A'24–M'28–SM'43) and Frank King (M'43–SM'43), Employer-Employee Relations Committee; and F. W. Borton (A'30), Board Liaison Committee of the Employer-Employee Relations Committee.

Meetings and Conferences are listed on page 336.

James L. Middlebrooks

James L. Middlebrooks (A'45) has been appointed chief facilities engineer for the American Broadcasting Company, succeeding Ben Adler (A'28) who recently resigned to become vice-president in charge of engineering for the Transmitter Equipment Manufacturing Company.

Mr. Middlebrooks attended the George School of Technology and the Alabama Polytechnic Institute, and was graduated in 1927 with a degree in electrical engineering. From 1927 to 1932 he was vice-president of the Middlebrooks Electric and Construction Company, Birmingham, Alabama, and from 1932 to 1936 he was chief engineer of station WAPI in Birmingham. Mr. Middlebrooks served as chief construction engineer of the Columbia Broadcasting System from 1936 to 1942, leaving there to serve in the United States Navy. Prior to his release from the Navy as a Commander in 1945, he was

Harris and Ewing

James L. Middlebrooks

officer-in-charge of the shore electronics installation and maintenance groups, electronics division, Bureau of Ships, Washington, D. C. He resigned as director of engineering for the National Association of Broadcasters to join ABC.

Mr. Middlebrooks is a member of the Society of Motion Picture Engineers and of the American Society of Naval Engineers.

❖

Ralph D. Hultgren

Ralph D. Hultgren (M'46) was recently awarded the Legion of Merit at Wright Field, Ohio, in recognition of his services in directing the design of microwave radar beacons during the period from May, 1943, to March, 1946.

Mr. Hultgren is a graduate of Purdue University. Prior to his release from military service as a Captain, he was project officer in charge of radar-beacon development for the radio and radar subdivision of Air Materiel Command's engineering division. Since leaving the Army Mr. Hultgren has been an electrical engineer for the Procter and Gamble Company at Cincinnati.

Stanford University Scientist in Postwar Research

Stanford University scientists outstanding in wartime research, and presently assigned to postwar research tasks under U. S. Navy contract, include Dr. William W. Hansen (A'39), Dr. Karl Spangenberg (A'34–SM'45), and Dr. Frederick E. Terman (A'25–F'37). The navy program is designed to encourage fundamental research and to assist in the training of men for research rather than for the development of equipment.

Dr. Hansen, noted physicist, will make further studies in nuclear physics concerning principally the measurement of nuclear moments, or the magnetic strength of atomic nuclei, and the behavior of neutrons from the cyclotron. Coinventor of the klystron which made possible modern radar, Dr. Hansen was prominent in wartime electronic developments, and also served as consultant on some aspects of the atomic bomb research.

Dr. Spangenberg, continuing a project begun by him at Harvard's radio research laboratory, will study properties of receiver oscillator tubes and circuits of types used in microwave radio and radar from the point of view of determining characteristics under conditions where operation is over a very wide frequency range.

Dr. Terman, who will serve as consultant on the navy project, is dean of Stanford's school of engineering and wartime director at the radio research laboratory at Harvard.

❖

L. W. Howard

L. W. Howard (A'28) has acquired the inventory and equipment of the Electronic Components Company and, with a partner, has formed the Triad Transformer Manufacturing Company at Los Angeles, California. Mr. Howard, who was formerly vice-president in charge of engineering and sales for a leading west-coast transformer manufacturer, will have charge of engineering and sales.

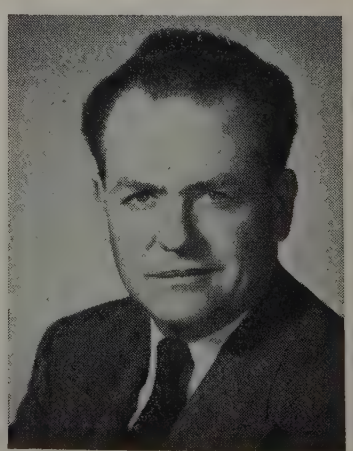

L. W. Howard

Joseph T. Cimorelli

Chairman, New York Section—1947

Joseph T. Cimorelli was born on March 18, 1912, in Catskill, New York. He was graduated from the Massachusetts Institute of Technology with the B.S. degree in 1932, and in 1933 received the M.S. degree in electrical engineering.

In 1935 Mr. Cimorelli joined the Radiotron Division of the RCA Manufacturing Company in Harrison, New Jersey, where he worked on tube-application problems. In 1940 he was transferred to the company's Chicago office. Here he worked as the field engineer of the tube-application section, assisting local receiver manufacturers in their design problems. In 1942 Mr. Cimorelli returned to the Harrison laboratories to continue his field-engineering work with equipment manufacturers, and also with government agencies and laboratories. Since 1944 he has been in charge of the application engineering laboratory of the Tube Department, Radio Corporation of America, at Harrison.

Mr. Cimorelli, who has served on several committees of The Institute of Radio Engineers, was Secretary-Treasurer of the New York Section in 1945 and became Chairman in 1946. He joined the Institute in 1941 as an Associate and became a Senior Member in 1945.

After a new engineering system has been conceived by its inventor and developed in the laboratory, it is found that new problems arise and considerable delays ensue prior to its large-scale practical application. Such difficulties are rarely anticipated by the inventor-engineer and are even less frequently condoned by him. In the following guest editorial, the chairman of the Ottawa Section of the Institute, and a research physicist of the National Research Council of Canada brings an instructive analysis of such situations which should carry understanding of the problems of major commercialization to the development engineer.—*The Editor.*

P.I.C.A.O. and the Radio Engineer

D. W. R. McKinley

Recently a series of demonstrations of radio aids to civil aviation was held in England and the United States for the benefit of delegates to the Special Radiotechnical Division of the Provisional International Civil Aviation Organization. After the demonstrations, the Radiotechnical Division of P.I.C.A.O. met in Montreal to assess the aids now available, to standardize on a selected few if possible, and to encourage the development of future aids by stating the operational requirements and by suggesting how the evolution of the proposed systems might be modified and co-ordinated to meet these requirements. The degree of unanimity reached at the Montreal conference was very marked, especially in view of the large number of nations represented and the profusion of systems proposed. It was interesting to note, however, that most of the constructive work toward achieving the desired objectives was done by technical men sitting in subcommittees; the smaller the subcommittee the better. The "back-room boys," including airline operators as well as radio engineers, gave careful consideration to the technical, engineering, and operational features of the systems and devices under scrutiny. Their findings then went to the full session where the political and economic aspects were threshed out expeditiously and with reasonable harmony.

The results of the P.I.C.A.O. meeting should have a most salutary effect, not only on the radio-engineering fraternity, but on the general public as well. Since the war there has been a considerable outpouring of extravagant and speculative publicity which has erroneously given the impression that it will be but a matter of weeks or months before civil aviation receives the full benefit of the new radio and radar techniques. The experience of the past few years proved that, even under wartime pressure, the consolidation and acceptance of the new devices is not immediate. This observation will apply with even greater emphasis to peacetime civil aviation where the conditions of safety and reliability are so much more stringent and are strongly influenced by economic considerations. P.I.C.A.O. now provides a checkrein on the enthusiast, whether he be an individual, an industrial firm or research establishment, or a government. This function has been served to some extent in the past by the Radio Technical Commission for Aeronautics in the United States and by the Commonwealth and Empire Conferences on Radio for Civil Aviation in the United Kingdom and Dominions, but these organizations have been largely national in scope, and while they may, and should, continue to function, the common proving ground and final court of appeal will be P.I.C.A.O. There is ample evidence to show that governments may separately arrive at plans for systems which are satisfactory internally but which do not fit into the world-wide pattern. It is to be hoped that P.I.C.A.O. will be able to anticipate and avoid much of the duplication and cross-purpose development which has occurred in the past. This can only be achieved if there is first an international fusion of the technical mind.

In particular it should be noted that P.I.C.A.O. has provided, for the first time on record, a complete set of internationally agreed operational requirements for radio aids to navigation. The first test of any proposal or system will be—does it meet the operational requirements? If it does, then the next logical step is to apply the criteria of engineering and production reliability, and lastly the economic test. The economics of a system are by no means the least important of the factors to be considered. For example, it is not feasible, operationally or financially, to tear out the vast network of low-frequency radio ranges now existing in North America, admittedly obsolete and inadequate as they may be, and to replace it with a new system, such as the P.I.C.A.O.-agreed omnidirectional ranges with distance indicators. It is fortuitous that, for economic reasons, the introduction of new systems will have to be gradual, because this slow infiltration of new developments will also provide a valuable opportunity for large-scale operational trials before the systems are "frozen."

It is sometimes hard for the radio engineer to realize that his idea, which works so well in an experimental form and theoretically satisfies the operational requirements, may suffer sadly when it is put into the field and subjected to the test of operational experience. The ultimate judges of radio aids to civil aviation are the airlines. If the device will enable them to provide safer and more expeditious service and at the same time will be economically practical, the airlines will accept it, but not otherwise. Civil aviation provides a vast and fertile field for the radio engineer's talents, but the engineer will have to keep his feet solidly on the ground of practicability. This implies not that his indulgence in technical fantasies should be rigidly restrained, but that his enthusiasm for the application of these new ideas should be tempered with a large dose of common sense.

Electron Tubes in World War II*

JOHN E. GORHAM†, MEMBER, I.R.E.

Summary—Although the military uses of electronics have been well publicized in technical journals, the improvements in electron tubes that made possible these military innovations have not been fully reported. While this information is known in some detail by the technical people who were engaged in various phases of tube research and development, an over-all summary of the work done by industrial laboratories and Federal agencies has not been available to many engineers and students interested in this field. In this paper, the status of electron-tube development at the close of the war is indicated in broad outline; a more comprehensive picture depends upon more detailed reports from the various laboratories engaged in war activities.

This summary of wartime advances in electron tubes is based on the knowledge of the vacuum-tube field gained by the engineers of the thermionics branch of the Signal Corps Engineering Laboratories, Bradley Beach, New Jersey, in developing, standardizing, and giving type approval of all tubes procured for the army during the war.

No effort is made to give specific credit either to individuals or industrial organizations. By and large it is a story of common achievement of many people, with industry working hand in hand with the War and Navy Departments to meet the urgent requirements of an ever-expanding demand for new and improved military electronic equipment.

I. General Research and Miscellaneous Related Tube Problems

Cathodes

AT THE start of World War II it was the practice to use oxide cathodes in low-power and receiving-type tubes, thoriated-tungsten filaments in medium-power tubes, and pure tungsten in high-power tubes. In general there were few power-pulse requirements. During the war, the use of thoriated filaments had been successfully extended to all types of power tubes, including the highest-power pulsed-oscillator tubes designed. In addition, during the last year of the war, oxide cathodes were used in power tubes capable of delivering 500 or 600 kilowatts peak power, and up to several megawatts peak power in magnetrons. The peak emission of thoriated filaments, for design purposes, has been increased from approximately 100 milliamperes per watt to approximately 200 milliamperes per watt. The peak emission from oxide cathodes has been increased to 30 amperes per square centimeter in production tubes, and as high as 80 amperes per square centimeter for several hundred hours in laboratory tubes. The highest peak emission reported is about 140 amperes per square centimeter. Oxide-cathode direct-current emission has been increased to approximately 0.5 ampere per square centimeter under optimum conditions.

* Decimal classification: R330. Original manuscript received by the Institute, March 27, 1946; revised manuscript received, July 31, 1946.

† Evans Signal Laboratory, Belmar, New Jersey.

There was little advance in the efficiency and stability of secondary-electron multipliers during the war. Electron multipliers may be considered to have a nominal multiplication factor of approximately 5 per stage for optimum acceleration voltages of the order of a few hundred volts per stage. After about 200 or 300 hours the performance of these multipliers is seriously reduced.

Except for low-power voltage-regulator and mercury-pool type tubes, relatively few tubes having cold cathodes were used in military equipment during World War II because of the lack of satisfactory life from such cathodes. In one type of pulse-modulator tubes, mercury is held in fine iron powder to permit use in aircraft. Mercury-pool ignitrons were used as pulsed modulator tubes to a limited extent.

It has been generally proved that at least 80 per cent of the total emission from the magnetron cathode is largely due to electrons emitted as a result of back-bombardment by electrons that do not reach the anode. As a result of such back-bombardment, considerable power is sent back to the cathode, with resultant heating and evaporation of the cathode coating and even the base metal. This has been overcome to some extent by appropriate reduction in power after the magnetron reaches stable operation. Some higher-frequency magnetron cathodes actually have radiators. More rugged types of coatings have been developed in which the oxides are pressed into a wire mesh which is sintered to a base cylinder, or in which approximately 50 per cent of the coating consists of 3- or 4-micron nickel powder to increase electron and heat conductivity and also to increase to some extent the binding force holding the barium.

Grids

An outstanding advancement during World War II has been the development of alloys and surfaces which overcome the problem of primary grid emission in thoriated-filament tubes, thereby eliminating the phenomenon of grid blocking, which normally leads to destruction of such tubes. These alloys include 4 per cent tungsten-platinum alloy wire, platinum-coated molybdenum-core grid wire, and "mossy"-surfaced tantalum or molybdenum wire.

It has been found that the presence of secondary emission tends to reduce the driving power of conventional grid tubes. The uniformity and stability of such secondary emission are very poor, however, and the current practice is generally to avoid making use of this factor in service tubes.

It has been discovered that there are certain temperatures at which the emission from grid wires is a minimum, and though it is not generally possible to maintain

the grids at this temperature, at least one tube type has been put into wide production with a fair degree of success using this principle. A second method used in receiving tubes (and, during the last years of the war, in power tubes) consists of the use of heat conduction to maintain grid temperature sufficiently low to minimize the effect of emission. This has been accomplished in some cases, such as in the 7C22, by the use of nickel cylinders with grid straps punched and rotated 90 degrees to reduce their effective cross section to electron flow but at the same time maintain their cross section for heat flow.

In various other power receiving tubes relatively large copper rods have been fastened at appropriate intervals to help remove heat. Another application makes use of very short grid wires to facilitate conduction to end rings. Still another method employed with moderate success in reducing grid emission involves the use of gold-plated molybdenum wire. It has been found that the gold will dissolve barium for at least 1000 hours in tubes such as the 715C. A solid solution is ultimately formed which apparently draws together and exposes the base metal through the resultant cracks.

Anodes

During World War II the problem of anode heat dissipation had not been a major one, except in planar-type lighthouse tubes. A principal problem in connection with anode design, and for that matter with general design of tubes, has been to reduce lead-reactance effects by providing extremely low-impedance paths at radio-frequency connections. The most important advance in anode design has been the development of various different but essentially similar re-entrant anode designs. These employ large-diameter glass-to-metal seals in both copper and kovar, and result in attendant reduction of lead-reactance effects up to at least 700 megacycles.

Zirconium or zirconium compounds have been sprayed on anodes to make them more nearly perfect black-body radiators, and simultaneously serve as getters. The principal requirement in planar-tube anode design at present is to improve heat dissipation and frequency drift due to warm-up.

Gas Reservoirs

Titanium-hydride reservoirs have been developed which are capable of maintaining the pressure at constant value and appreciably extending the life of hydrogen thyratrons under extreme operating conditions.

II. Magnetron Tubes

The development of the magnetron as an efficient microwave generator took place almost entirely during World War II. During the war, the magnetron advanced from the status of the elementary split-anode variety to the highly perfected and complex multiresonant-cavity type. Operating efficiencies were raised from about 10 to over 50 per cent. Tubes were developed and produced in large numbers for wavelengths as short as approximately 1 centimeter. Representative types of magnetrons are shown in Fig. 1.

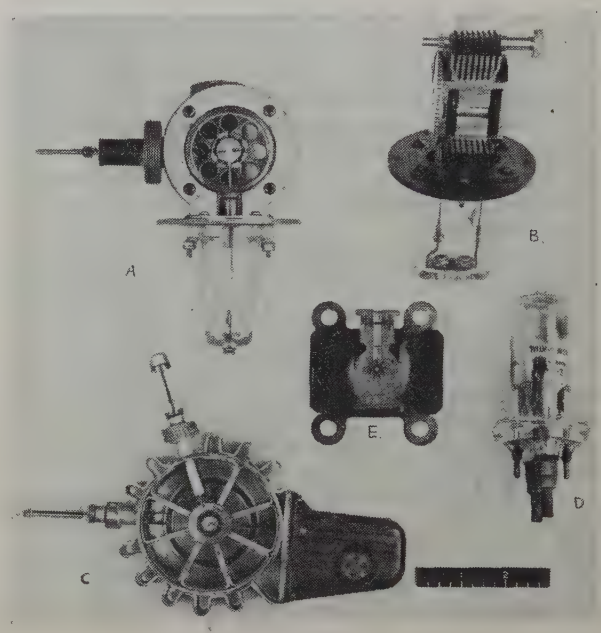

Fig. 1—Representative types of magnetrons: (a) 2J31 hole-and-slot pulse type. (b) 2J54 tunable pulse type. (c) 2J64 vane type for pulse communication. (d) 5J31 split-anode continuous-wave type. (e) 3J21 rising-sun pulse type.

During the course of the war, extensive studies were made of mode separation and the manner and efficiency of operation. Methods of eliminating undesirable modes (arising from multiple degeneracy due to the multiresonator anode blocks) were developed, such as strapping and the use of "rising-sun" alternately long and short cavity construction. The usual technique of strapping consists of electrically connecting alternate cavity vanes near the cathode ends by means of metal straps or wires within the tube. This strapping depends on end effects at the top and bottom of the vanes. The rising-sun anode construction consists of making alternate cavities tuned respectively to frequencies above and below the operating frequency of the magnetron, and was originated to avoid straps in super-high-frequency tubes. Lately, the fact that the rising-sun structure does not depend on end effects has been used in designing higher-power, longer-anode magnetrons.

Several mechanical tuning methods were developed. These include internal tuning by means of moving plungers in the resonant cavities ("crown of thorns"), changing the capacitance of the straps to ground and each other, the addition of an external tunable resonator coupled to an internal resonator or strap, and simultaneous application of strap and plunger tuning.

"Packaging" was also introduced, whereby the

magnetron was produced as a complete unit containing or having attached permanent magnets as an integral part of the magnetron instead of depending on the furnishing of proper magnetic fields as part of the operating equipment.

At present, several 25-centimeter pulsed magnetrons of fixed frequency are available with peak powers as high as 1 megawatt. Development has just been completed on a tunable type capable of 600 kilowatts peak power output and 8 per cent tuning range.

At wavelengths of about 10 centimeters, tubes have been produced in quantity with peak powers ranging up to approximately 2 megawatts. Tunable tubes have been made which have approximately 7 per cent tuning range and 1 megawatt peak power output.

The maximum peak power attainable at about 3 centimeters is approximately 1 megawatt from a fixed-frequency magnetron. A variable-frequency magnetron is also available at this frequency capable of 50 kilowatts peak power and 12 per cent tuning range. At about 1 centimeter only two fixed-frequency pulse magnetron types have been produced in quantity. The tubes are capable of peak powers of the order of 50 kilowatts. In general, the life expectancy of pulsed magnetrons is in the neighborhood of 500 hours, except at extremely short wavelengths where life expectancy is about 250 hours.

Continuous-wave magnetrons using split anodes in the high- and ultra-high-frequency bands, and cavities in the higher frequency bands, have been developed primarily as sources of jamming power of from over 1 kilowatt down to about 50 watts. Due to serious back-bombardment of the cathodes, tube life is usually less than 100 hours, although efficiencies are about 40 per cent. Interdigitated magnetrons, having as anodes two cylindrical sets of interlocking teeth, have been made to give about 15 watts output at 7 centimeters.

During the last part of the war, magnetron modulation was investigated to permit communication at all frequencies. One electronic frequency-modulation method consists of varying the current of an electron beam through one of the magnetron cavities. This method has been used at 4000 megacycles to get 4 megacycles total swing at about 25 watts continuous-wave power output. Preliminary tests show that external magnetrons may be used to modulate the magnetron generator tube by virtue of change of electronic reactance, but at present modulation linearity is not as good as that obtained by the former method. Amplitude modulation is not satisfactory at this date, but there are indications that considerable success may be achieved in the near future. Pulse-time modulation is feasible at any frequency and involves transmission at constant power level.

III. Transmit-Receive Tubes

The transmit-receive (TR) tube (Fig. 2) is a switching tube, usually gas-filled, which is generally used in radio-frequency systems (radar, for example) where a transmitter and receiver make use of a common antenna. Its function is to protect the receiver input-circuit elements during the pulsing of the transmitter and allow the radio-frequency power received by the antenna between pulses to reach the receiver. Antitransmit-receive (ATR) tubes are used in conjunction with TR tubes to reduce the dissipation of receiver signals in the transmitter.

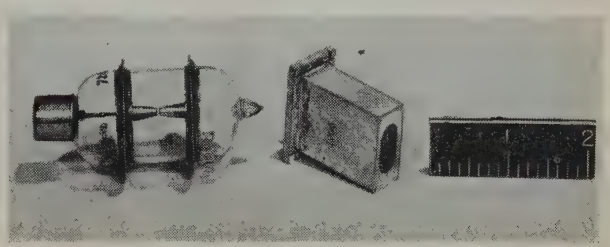

Fig. 2—Transmit-receive tubes; types 721A, 1B37.

Table I
TR-Tube Performance Characteristics

Type	Application	Wavelength	Power level	Insertion loss	Recovery time	Bandwidth
1B23	TR	20–50 centimeters	50 kilowatts	1 decibel	—	high Q
702A, B	TR	20–50 centimeters	50 kilowatts	—	—	—
721B	TR external cavity	10 centimeters	250 kilowatts	1.0–1.5 decibels	<7 microseconds	high Q
1B27	TR external cavity	10 centimeters	250 kilowatts	1.0–1.5 decibels	<5 microseconds	high Q
1B58	TR fixed-tuned	8–11 centimeters	200 kilowatts	1.0–1.5 decibels	15 microseconds	10 per cent
1B55	TR fixed-tuned	8–11 centimeters	200 kilowatts	1.0–1.5 decibels	15 microseconds	10 per cent
PS3S	TR fixed-tuned	8–11 centimeters	200 kilowatts	1.0–1.5 decibels	15 microseconds	10 per cent
1B44	ATR fixed-tuned	8–11 centimeters	1 milliwatts	1 decibel	—	5 per cent
1B52	ATR fixed-tuned	8–11 centimeters	1 milliwatts	1 decibel	—	5 per cent
1B53	ATR fixed-tuned	8–11 centimeters	1 milliwatt	1 decibel	—	5 per cent
1B56	ATR fixed-tuned	8–11 centimeters	1 milliwatt	1 decibel	—	5 per cent
1B57	ATR fixed-tuned	8–11 centimeters	1 milliwatt	1 decibel	—	5 per cent
1B38	Pre-TR for use with low-power TR	10.7 centimeters	1 milliwatt	0.10 decibel	20 microseconds	—
1B54	Pre-TR for use with low-power TR	8.4 centimeters	1 milliwatt	0.10 decibel	20 microseconds	—
1B24	TR tunable self-contained cavity	3 centimeters	60 kilowatts	1.0–1.5 decibels	<3 microseconds	high Q
724B	TR external cavity	3 centimeters	60 kilowatts	1.0–1.5 decibel	<6 microseconds	high Q
1B63	TR broad-band fixed-tuned	3 centimeters	300 kilowatts	<0.8 decibel	<5 microseconds	12 per cent
1B35	ATR fixed-tuned cavity	3 centimeters	60 kilowatts	0.8 decibel	—	6 per cent
1B37	ATR fixed-tuned cavity	3 centimeters	60 kilowatts	0.8 decibel	—	6 per cent
1B26	TR self-contained cavity	1 centimeter	40 kilowatts	0.85–1.5 decibels	<4 microseconds	high Q
1B36	ATR fixed-tuned	1 centimeter	40 kilowatts	0.8 decibel	—	>2 per cent

Pre-TR tubes are used for added receiver protection during transmitter pulses. These last two tube types have general requirements similar to that of TR tubes (see Table I). TR, ATR, and pre-TR tubes should have low leakage power to the receiver during the transmitter pulse, rapid recovery time immediately following the pulse to enable the maximum received energy to reach the receiver for short range echoes, and satisfactory life. Most tubes were filled either with argon or mixtures of hydrogen and water vapor at pressures in the range of 10 to 25 millimeters.

In general, the recovery time of good tubes at power levels of 30 kilowatts peak is in the order of 4 to 7 microseconds. At higher powers, recovery-time figures are progressively larger. For instance, at line powers of 100 kilowatts the recovery time is approximately 50 per cent greater than at 30 kilowatts. As might be expected, leakage power is also a function of line power. At 30 and 100 kilowatts the leakage powers are of the order of 20 and 75 milliwatts peak, respectively. The insertion loss is approximately one decibel. Recently multicavity fixed-tuned tubes have been made with a frequency coverage of about 12 per cent.

IV. Crystal Rectifiers

Crystal rectifiers (Fig. 3) are used in receiver applications for mixers, video detectors, second detectors, and direct-current restorers. In construction they consist of a semi-conductor, either silicon or germanium, in contact with a cat's whisker of metal, usually tungsten. At present, crystal mixers give the lowest noise figures in receivers above about 1000 megacycles.

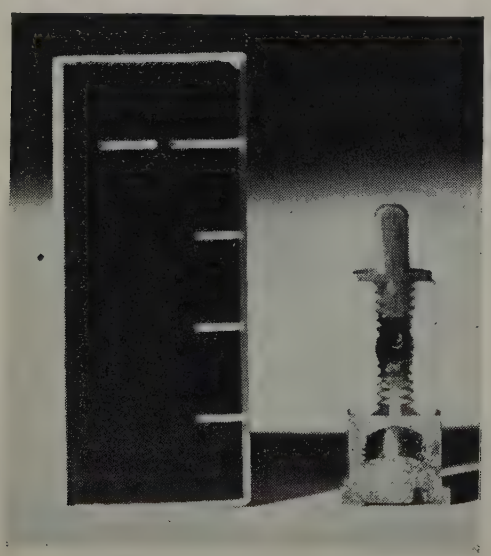

Fig. 3—Crystal detector: 1N21.

In general, microwave crystal converters have conversion losses of the order of about 6.5 to 8.5 decibels, being best at 3000 megacycles and worst at about 30,000 megacycles. They are capable of withstanding pulses ranging from 5 ergs at 3000 megacycles to 0.1 erg at 30,000 megacycles. On the basis of their use with an intermediate-frequency amplifier of 5 decibels noise figure, receiver noise figures are attainable which vary from about 12.7 decibels at 3000 megacycles to 15.2 decibels at 30,000 megacycles.

Germanium crystals, used as second detectors, at present are capable of withstanding 50 or more volts in the back direction, compared with about 5 volts for silicon crystals. In general, they have rectification efficiencies in the same order of magnitude as receiving-type diode tubes. For direct-current restorer applications, germanium crystals have resistances, measured at 1 volt, greater than 0.1 megohm in the back direction and approximately 200 ohms in the forward direction. Germanium crystals are being used at present as second detectors and direct-current restorers for experimental circuit work. Their properties, especially as compared to diodes, are being studied.

V. Klystrons

Development and application of klystrons during World War II has mainly centered about reflex tubes for local-oscillator use, requiring about 20 milliwatts of power output, and signal-generator use, requiring about one watt. Although the theoretical maximum efficiencies are 30 per cent for the reflex klystron and 58 per cent for the two-cavity type, the actual efficiencies thus far attained are only a few per cent for reflex tubes and 5 to 6 per cent for two-cavity types. The best tube in this respect, to date, is the 2K54 for which efficiencies of 10 per cent are obtained under pulsed operating conditions.

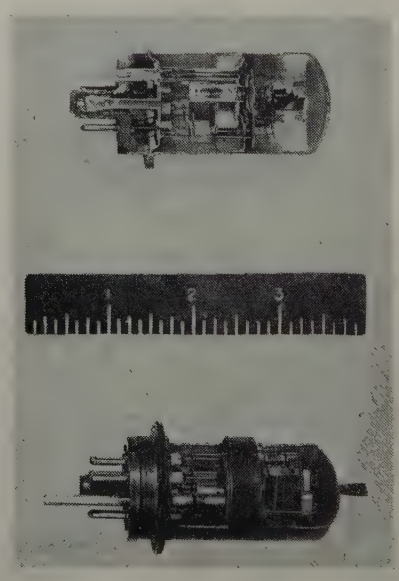

Fig. 4—Thermally tuned reflex klystron, 9000 megacycles: type 2K45.

Tuning of klystrons is generally accomplished by either changing the resonant frequency of the cavity or, in the case of reflex klystrons, by varying the potential of the repeller. Repeller-voltage changes are capable of producing only relatively small frequency changes of the

order of 1 per cent. The degree of frequency change attainable by means of cavity variation depends largely on the cavity construction. Klystrons designed to operate with external cavities may have frequency tuning ranges in the order of 2 to 1. Klystrons constructed with cavities which are an integral part of the tube usually are tuned by the motion of a metal diaphragm, which permits variation in the spacing of the resonator grids. This produces changes in grid-to-grid capacitance and consequent shift in the resonant frequency.

Tuning has also been accomplished in some tube types by electronic control of an auxiliary electron source within the same envelope, which heats a thermally sensitive mechanical element attached to the cavity diaphragm. The thermal time constant of such devices varies between 2 and 10 seconds, depending on the type of tube. Tubes with thermal tuning are available in the regions of 10,000 and 25,000 megacycles (Fig. 4).

The power output of reflex klystrons below 3000 megacycles is of the order of 1 watt. Between 3000 and 10,000 megacycles, $\frac{1}{4}$ watt may be attained. Above 10,000 megacycles, available types exist only in the region of about 25,000 megacycles and are capable of approximately 20 milliwatts output. Two-cavity klystrons have been produced in the 2300- to 4000-megacycle region, capable of delivering between 20 and 40 watts of power.

VI. Planar Tubes

Planar-type tubes (Fig. 5) are suitable for high-frequency operation because of (a) reduction in lead inductances by use of disk seals, (b) reduction in interelectrode capacitances by means of small electrode areas and parallel-plane structure, and (c) essentially complete enclosure of the radio-frequency fields permitted by a tube construction suitable for operation in an inclosed cavity. A number of types, all developed during World War II, are now available. These include the 2C40, a low-power triode with 50 milliwatts output at 3370 megacycles; 2C43, a pulse triode with 750 watts peak output at 3370 megacycles; 3C22, a continuous-wave triode with 25 watts output at 1400 megacycles; 2C38, continuous-wave triode with 10 watts output at 2500 megacycles; and the 2C36 and SB846A, British-type disk-seal triodes for low-power use up to about 4000 megacycles.

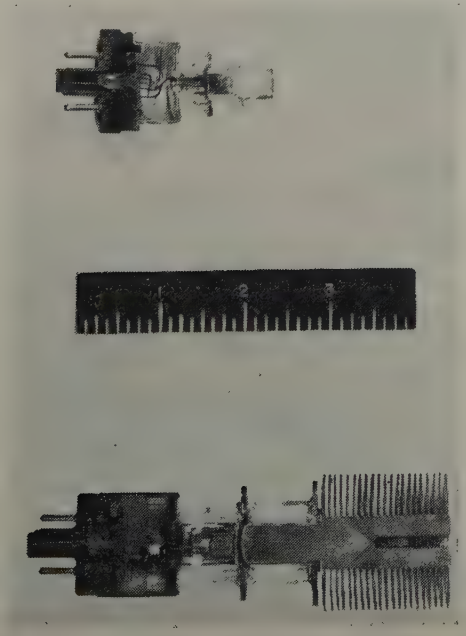

Fig. 5—Cutaway planar tubes: types 2C43, 3C22.

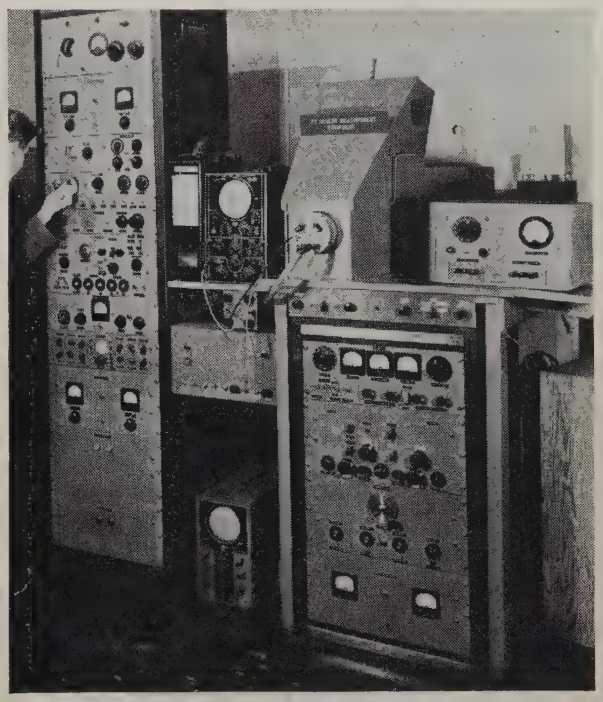

Fig. 6—Cathode-ray-tube screen test.

Present types of planar tubes are constructed with oxide-coated cathodes; tungsten or nickel grids; and steel, molybdenum, or kovar paltes. The glass seals are made to silver-plated steel or kovar. In the case of silver-plated steel, special glass having a thermal-expansion coefficient equal to steel is used. Interelectrode spacings on the 2C40 type are as low as 0.003 inch and 0.010 inch for grid to cathode and grid to plate, respectively. These small spacings, in view of the fact that such tubes are intended for use in accurately machined cavities, require unusually small mechanical tolerances in manufacture.

VII. Indicator and Pickup Tubes

Cathode-ray indicator tubes are used wherever a visible indication of rapidly changing electrical phenomena is required. Because of the almost infinitesimal inertia of the electron beam, these tubes are capable of responses far more rapid than any mechanical indicators.

The transforming of visible or invisible radiation images into electrical signals is accomplished in electronic pickup tubes. Such tubes are designed to have high sensitivity to radiation. By means of very rapid electronic scanning of a photosensitive mosaic, high-resolution electrical transmission of rapidly moving images is accomplished.

During the war, the following improvements were made in electron guns:

(a) In electrostatic-focus types, zero first-anode-current guns were developed in which the first anode did not intercept any beam current, with the result that power-supply requirements were reduced and better focusing control was obtained.

(b) In magnetic-focus types an additional cylinder was added to the high-voltage anode, which aided in alignment of the gun and improved the focus.

(c) Limiting apertures were added in magnetic-focus types to reduce the spot size and improve the focus.

With regard to screens, several new types were developed:

(a) Double-layer screens which have the property of emitting increased intensities of persistent light after successive excitations of the screen. The color of its fluorescent light is different from that of its phosphorescent light.

(b) Dark-trace screens showing a darkening of the normally white screen material, usually potassium chloride, at the point of excitation by the electron beam, were used in projection systems.

(c) Exponential screens having light output which decays at such rate that its instantaneous intensity is proportional to exponential t/t_0, where t_0 is a constant of the screen and t is the time.

Commutator tubes of several varieties were developed during the war for multichannel communication over a single transmission frequency.

Improved tubes suitable for projection purposes were also developed during the war with high light output (6 candle power per watt) and good contrast. Cathode-ray tubes with two or more guns in the same envelope were developed for special applications, eliminating complex switching circuits. Pickup tubes were developed with sensitivities in the infrared. Tubes were also developed capable of converting infrared images directly to visible images by focusing the electron pattern from a photosensitive surface on a fluorescent screen at the opposite end of a cylindrical tube.

At present, cathode-ray tubes with faces from 1 to 12 inches in diameter are available in quantity. These tubes are in some instances focused and deflected by electrostatic methods and in others by magnetic methods.

The various screen types and general information concerning their properties are listed in Table II.

Levels of fluorescent light output vary according to screen types, being about 15 foot-lamberts for tubes of the highest output (nonprojection tubes with P1 screens). Improvements in focusing and line widths were limited and were less than a factor of 2 to 1. Present line widths of from 0.3 millimeter to 1 millimeter are a function of tube size and gun construction (Fig. 6).

Pickup tubes of the orthicon type have been produced with sensitivity in the infrared and in the blue part of the spectrum. Orthicon tubes have been made with a resolution of 1500 lines per frame at the center for high resolution reconnaissance work. For portable systems, tubes have been constructed operating with only a few hundred volts having a sensitivity of 0.03 microamperes per foot-candle.

VIII. Power and Gas Tubes

At the start of World War II radar transmitters were operated at or below about 200 megacycles and used tubes which had thoriated filaments. During the war oxide cathodes came to be used in power-oscillator tubes with a reduction of cathode power by a factor of about five.

Table II

Cathode-Ray-Tube Screen Characteristics

Screen type	Composition	Color	Persistence	Decay time to 1 per cent (seconds)	Applications
P5	$CaWO_4$:(W)	Blue	short	10^{-5}	Photography of rapid transients (to 60 kilocycles).
P11	α*—ZnS:Ag	Blue	short	0.005	Photography of transients (to 9 kilocycles).
P4	α*—ZnS:Ag + $Zn_8BeSi_5O_{19}$:Mn	White	short	0.005+0.06 (B) (Y)	Television.
P1	Zn_2SiO_4:Mn (α)	Green	short	0.05	Most cathode-ray oscilloscopes. Rapid-scan radar cathode-ray tube.
P12	Zn(Mg)F_2:Mn	Orange	long	0.4	Fire-control radars operating at 4 to 16 scans per second.
P2	ZnS:Cu(Ag) (β*)	Green	long	0.3	Prewar long-persistence oscilloscopes.
P14	β*—ZnS:Ag on ZnS(75):CdS:Cu	White ↓ Orange	long	1	Eagle and H2K radars operating at about 1 scan per second.
P7, (P8)	β*—ZnS:Ag on ZnS(86):CdS:Cu	White ↓ Yellow	long	3	Most radars operating slower than 1 scan per second.
P10	KCl	Magenta on White	long	5	Radars operating in high ambient light and slower than 0.2 scan per second.

Several types of $\frac{1}{4}$- to $\frac{1}{2}$-megawatt triode tubes have been developed with the tuned circuits inside the vacuum envelope. By the close of the war, triode oscillator tubes had been developed which gave approximately 0.6 megawatt up to about 700 megacycles. Power-amplifier tubes are available that can handle 100 or 200 watts continuous-wave output up to 700 megacycles with a power gain of about 5 decibels.

Hydrogen thyratrons were originated and put into production during the war to eliminate temperature dependence of mercury tubes. These thyratrons handle powers of from a fraction of a watt to 2 megawatts pulse power. Series and/or parallel operation of thyratrons has been accomplished to allow up to four times the power of a single thyratron. Ignitrons have been used up to 2 megawatts at 20 microseconds pulse width. High-vacuum modulator tubes have been developed to handle a few hundred kilowatts peak power at duty ratios of about 0.0006. Tubes of each of these types are shown in Fig. 7.

Fig. 7—Pulse modulator tubes: 5C22 hydrogen thyratron; 715C high-vacuum type; 1R21 mercury-pool ignitron.

The resnatron, employed during the war in radar countermeasures to jam German radar, is the most powerful ultra-high-frequency oscillator and amplifier now in existence. It supplies over 50 kilowatts in continuous-wave operation at frequencies ranging from 350 to 650 megacycles, with a plate efficiency of the order of 60 to 70 per cent. Features of this tetrode include beam-forming grids, electron bunching, and self-contained resonant cavities which permit phase-shift compensation for transit-time effects without lowering efficiency.

IX. Receiving Tubes

There are so many types of receiving tubes that it is impossible to begin to describe them here. Consequently only a few practices of a general nature that came into considerably wider employment during the war will be mentioned in this section. The use of standard tubes at low plate and screen voltages was accomplished to allow operation directly from a 24-volt storage battery in place of a high-voltage power supply. Subsequently, tubes with 26.5-volt filaments and a design optimized for 28-volt plate and screen operation were developed. Tubes were "ruggedized" to withstand vibration and shock up to 500 times the acceleration of gravity. Subminiature tubes (T-3 bulbs of $\frac{3}{8}$-inch diameter) were in existence before the war for hearing-aid use. During the war, subminiature types for VT fuzes were developed which could withstand being shot from guns. Size and weight limitations of new radar and allied equipment, along with the need for high peak power output, created the need for receiving-type tubes capable of operating in a pulsed condition at potentials and currents far above their rated values. Fig. 8 shows six different types of receiving tubes.

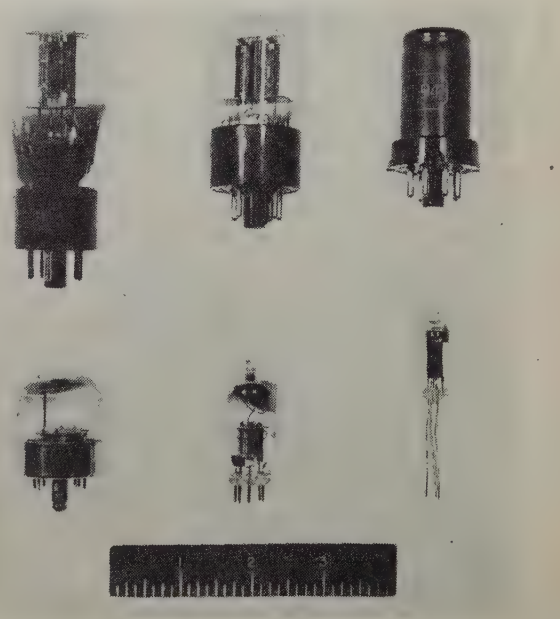

Fig. 8—Receiving tubes having transconductances of 3000 to 5000: G, GT, metal, lockin, miniature, and subminiature tube types 6J5G, 6J5GT, 6J5, 7F8, 6J6, 6K4.

There is now an overabundance of receiving-tube types—one or two thousand, or perhaps more. It is not unusual to find half a dozen or more tubes, substantially equivalent, differing by having several filament voltages, two or three types of bases and bulbs, and different arrangements of pin connections. Almost every metal-tube type is duplicated in a glass version with the same base, and most are also duplicated in lock-in construction under different type designations. Now most of these types are becoming available in miniature bulbs.

X. Acknowledgment

It is a pleasure to acknowledge the aid of my associates in the preparation of this paper: M. E. Crost, K. Garoff, D. R. Gibbons, L. L. Kaplan, B. Kazan, H. L. Ownes, D. E. Ricker, and C. S. Robinson, Jr.

Specification and Measurement of Receiver Sensitivity at the Higher Frequencies*

JOSEPH M. PETTIT†, SENIOR MEMBER, I.R.E.

Summary—The paper discusses the influence of receiver noise on sensitivity performance at higher frequencies. Established I.R.E. standard definitions and test methods do not give proper emphasis to the important factor of noise. A practice recently adopted of specifying sensitivity in terms of *noise figure* is reviewed, and there is introduced a method, not yet commonly used, of measuring this quantity with a diode noise generator.

Noise figure, however, is not an adequate specification of sensitivity, for it ignores over-all gain. To include both factors, a proposed *combined sensitivity figure* is presented.

The alternatives for specifying sensitivity in terms of voltage or power are compared, and the concept of *available power* is explained.

Introduction

THE PRIMARY type of performance test is one which determines the general suitability of a receiver in terms of arbitrary performance standards for a given type of service. An example of this approach is seen in broadcast practice, where the I.R.E. Standards[1] specify completely the type of modulated signal to be supplied to the receiver, the gain and tone-control settings, and an arbitrary "Normal Test Output." No such standardization exists for the diversity of receivers found in the higher-frequency ranges. In fact, there is even lack of agreement upon the methods for comparing two similar receivers with respect to a single performance characteristic such as sensitivity. The discussion to follow will be directed primarily toward outlining the several factors involved in specifying and measuring receiver sensitivity, together with an attempt at evaluating their relative merits.

The subject of the sensitivity of receivers for the ultra-high-frequency and higher ranges has received considerable attention in the current literature,[2] mostly dealing with the influence of thermal agitation noise in the receiver input circuits. This emphasis has resulted from the greater importance which must be assigned to such noise in these frequency ranges, particularly in high-gain, broadband receivers, as compared to those for the broadcast range. In the broadcast range, sensitivity is defined[3] solely in terms of signal input required to produce an arbitrary output power; this is a measure of over-all gain only, and ignores the problem of the noise threshold. The present trend, on the other hand, seems to overemphasize the noise problem, whereas actually it is valueless to build a receiver with a low noise threshold if the over-all gain is inadequate. This rather obvious requirement has at times been overlooked. One example was a receiver intended for aircraft use which, merely because of inadequate audio gain, was incapable of amplifying weak signals, barely above the noise threshold, to a level where they could be heard above the acoustic noise present in the aircraft. Yet in the laboratory this receiver was perfectly capable of detecting exceedingly weak signals. Thus the total gain must also be evaluated in over-all testing of the complete receiver. This gain to be specified depends, in turn, upon the exact service for which the receiver is intended, and hence the heed for arbitrary standards seems unavoidable.

Actually, two values of gain are involved: one a minimum gain required to amplify the receiver noise to a level where the noise output is perceptible above the ambient room noise, and the other an arbitrary gain to provide adequate signal output. To whatever extent the receiver transmits differently the noise and the signal, both of these gains have to be specified and tested independently.

Receiver sensitivity can be described and tested by at least two methods. One is to determine independently the quantities described above; the other is to obtain a single figure which combines all of them.

Noise Figure

The term "noise figure"[4] refers to a figure of merit which compares the actual noise threshold of a receiver with that of a hypothetical noise-free receiver having the same bandwidth. Much has been written on this subject, and only the basic relationships will be summarized here. For purposes of the over-all receiver test it is most convenient to refer all noise to the input terminals of the receiver, since the theoretically perfect receiver is defined as one which does not introduce additional noise beyond that which comes to it from the signal source, i.e., the antenna and transmission circuits. These circuits are treated together, since these tests should regard the receiver as an entity in itself, designed to operate from a specified source impedance. Thus, considerations of antenna and transmission efficiency are excluded from this discussion. Consider, therefore, a receiver designed to operate from a voltage source of internal resistance R_s. The thermal-noise voltage developed in the resistance R_s, which is also the theoretical minimum noise of the receiver, can be

* Decimal classification: R261.2. Original manuscript received by the Institute April 5, 1946; revised manuscript received, September 23, 1946.

† Formerly, Airborne Instruments Laboratory, Inc., Mineola, New York; now, Stanford University, California.

[1] "Standards on Radio Receivers," 1938, pp. 31, 14–15, Institute of Radio Engineers.

[2] D. O. North, "The absolute sensitivity of radio receivers," *RCA Rev.*, vol. 6, pp. 332–343; January, 1942. This paper gives a good bibliography of previous papers on the subject.

[3] See definition 1R36, p. 3, of footnote reference 1.

[4] H. T. Friis, "Noise figures of radio receivers," PROC. I.R.E., vol. 32, pp. 419–422; July, 1944.

regarded as an equivalent constant-voltage generator in series with R_s, as shown in Fig. 1. The voltage E_n of this generator is given by the relation[5,6]

$$E_n^2 = 4kTR_s\Delta f = 1.6 \times 10^{-20} R_s \Delta f \qquad (1)$$

where

k = Boltzman's constant, 1.37×10^{-23} joule (or watt-seconds) per degree Kelvin

T = temperature of the resistance in degrees Kelvin, usually taken to be room temperature; for instance, 292 degrees Kelvin

Δf = receiver noise bandwidth (precise definition to be given later, but it is closely equal to the band between the frequency limits at which the response has fallen off by 3 decibels).

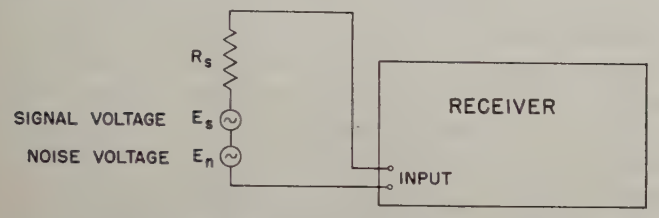

Fig.1—Signal and noise voltages at input of radio receiver.

Let E_n' be the *actual* noise of the receiver, including the theoretical noise, and referred back to the voltage source at the input. This is again an equivalent noise voltage in series with the resistance R_s, replacing E_n in Fig. 1. Then the *noise figure* may be defined as

$$F = (E_n'/E_n)^2. \qquad (2)$$

This is essentially a power ratio, although, of course, the measurement of E_n' can be made from either voltage or power. The ratio is usually expressed in decibels, typical figures for microwave receivers ranging from 8 to 30 decibels.

There are two approaches to the measurement of the voltage E_n'. In either case the test generator must present the specified source impedance for which the receiver is intended. In one case the test generator may be a noise source whose power is adjustable and known, and whose frequency spectrum is uniform over the receiver pass band. Up to about 100 megacycles such a generator can use, as the noise source, a temperature-limited conventional diode wherein the noise component of the plate current is proportional to the direct current through the diode. Special coaxial diodes such as the British CV172 can be used up to 300 megacycles. This relation has been shown to be[7]

$$I_n^2 = 2eI_{dc}\Delta f \qquad (3)$$

where

e = charge on the electron, 1.60×10^{-19} coulomb

I_{dc} = direct current in diode, in amperes

Δf = bandwidth, for which I_n is the root-mean-square noise current.

To measure E_n', the noise generator,[8] an example of which is shown in Fig. 2, is connected to the receiver through the proper source impedance. Noise from the generator is increased from zero until the output noise

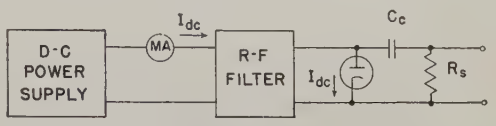

Fig. 2—Simplified schematic diagram of diode noise generator.

power of the receiver is doubled. The added noise must then be equal to the actual receiver noise referred to the input, plus the thermal noise from the source resistance R_s. In measuring the receiver output noise, the principal requirement is that all the significant noise sources be included ahead of the point of measurement. Usually noise generated in the receiver beyond the first intermediate-frequency amplifier stages is ineffective, inasmuch as the signal has assumed large proportions compared to this noise. Hence the output noise can be measured at any point following these first stages. The indicator must add correctly the root-mean-square noise of the receiver and that from the noise generator.

If a 3-decibel attenuator can be inserted just ahead of the detector at the time the noise from the test generator is added, the requirements on the output indicator can be simplified. The noise generator is connected to the input terminals, and the output from the generator set first at zero. The actual receiver output noise, without the attenuator in the circuit, is then observed on the indicator. Next the attenuator is inserted, and the output of the noise generator increased until the indicator gives the same reading as before. The added input noise is then equal to the original noise, provided that insertion of the attenuator in no way influences the band-pass or gain characteristic of the receiver. It is not necessary for the indicating meter to read linearly in root-mean-square values, since the meter receives the same current in both readings. Furthermore, if the receiver has a gain control calibrated with sufficient accuracy, and if changes in the gain do not change the input noise of the receiver (a reasonable approximation if the gain control does not act on a high-gain first intermediate-frequency stage), then the 3-decibel attenuation can be inserted by reducing the gain by 3 decibels. The need for the attenuator is thus obviated, and, further,

[5] J. B. Johnson, "Thermal agitation of electricity in conductors, *Phys. Rev.*, vol. 32, pp. 97–110; July, 1928.

[6] H. Nyquist, "Thermal agitation of electric charge in conductors," *Phys. Rev.*, vol. 32, pp. 110–113; July, 1928.

[7] W. Schottky, "Spontaneous current fluctuations in various conductors," *Ann. Phys.*, vol. 57, pp. 541–567; December 20, 1918. This is rigorously true only for pure metal filaments. Oxide-coated cathodes have additional noise known as flicker effect, although this is a low-frequency phenomenon and would not affect measurements on high-frequency receivers. Temperature-limited operation can be obtained with certainty only with pure metal filaments.

[8] The necessary requirements for use of this type of circuit are that the diode be a high impedance compared to the desired source resistance R_s, and that the connections to the receiver be very short. If these are met, equations (4) and (5) can be used for the measurements. The coupling capacitor C_c must have essentially zero impedance at the desired noise frequencies. The radio-frequency filter is basically a low-pass structure. It must have no shunt paths for the direct current I_{dc}, and must present to the diode a high impedance at the noise frequencies.

the second detector of the receiver can be used directly as the output indicator.

The most useful feature of the noise-generator method arises from the fact that the noise (either power or current squared) produced by the generator is directly proportional to Δf, as indicated by the relation

$$(E_n')^2 = (I_n R_s)^2 = 2eI_{dc}R_s^2\Delta f. \quad (4)$$

Since the receiver noise figure $F=(E_n'/E_n)^2$ and $E_n^2=4kTR_s\Delta f$,

$$F = eI_{dc}R_s/2kT = 20I_{dc}R_s \text{ (if } T = 292 \text{ degrees Kelvin)}. \quad (5)$$

It will be noted that Δf has dropped out of the determination; this is a decided help, for it is not easy to measure Δf. Hence, receivers of differing band-pass characteristics can be compared more readily by means of the noise-generator method.

The alternative approach to the measurement of the actual receiver noise, referred to the input terminals, is to use a continuous-wave signal generator to supply the necessary energy to double the receiver output indication due to the noise voltage E_n'. The basic requirement is that the output indicator respond identically to the summation of continuous-wave plus noise energy as it does to noise alone. This predicates root-mean-square or power types of indicator, including thermocouples, bolometers, etc. The expression for the noise figure is then

$$F = E_s^2/4kTR_s\Delta f \quad (6)$$

where E_s is the continuous-wave signal voltage applied in series with R_s required to double the receiver output indication due to the actual receiver noise E_n'. The quantity Δf is obtained from the selectivity characteristic of the receiver. It is defined by the relation

$$\Delta f = (1/A_0^2)\int_0^\infty A^2 df. \quad (7)$$

where

A = voltage amplification at the frequency f

A_0 = amplification at the reference frequency f_0.

The reference frequency f_0 may be either the center frequency of the pass band or the frequency of maximum gain. In any event A_0 must be the amplification for the frequency at which the continuous-wave signal generator is set during the noise-figure test. It is usually convenient to use the frequency of maximum gain, for it is more easily located in a test. For single-tuned circuits, the noise bandwidth can be taken as that between the 3-decibel points.

One difficulty in using a continuous-wave signal generator lies in the measurement of the low input power required. For instance, a typical microwave receiver may have $F=15$ decibels above the theoretical limit of thermal noise from the signal source, and a bandwidth of 4 megacycles. For this receiver the continuous-wave power to double the output power due to noise alone is about 0.5 micromicrowatt.

Minimum Gain Requirement—Standard Noise Output

As stated earlier, a receiver that is able to detect weak signals to the limit imposed only by noise must be able to amplify this input noise to a readily observable level at the output or display. Where the conditions of service are accurately known, it is possible to require that a specified minimum noise voltage or power shall be delivered to the receiver output with the receiver gain control set at maximum. For every type of service and for each method of presenting the output there can be specified a *standard noise output*[9] which defines this minimum noise. For instance, a useful figure for a receiver intended for aural output in an aircraft installation is 0.5 milliwatt in a 600-ohm noninductive resistor, the power being measured with a root-mean-square meter whose accuracy is good at frequencies up to 10 kilocycles. The 600-ohm load is an arbitrary one, based upon standard military headphones. For cathode-ray display, standard noise level may be defined in terms of the height of the "grass" pattern produced by the noise, such that this height is equal to, say, one half of full deflection. Such a standard is, unfortunately, not completely objective, for, if the noise is not clipped, the grass height is quite random, and can only be estimated. The measurement for intensity-modulated cathode-ray presentations is even more obscure, and will not be considered here.

Signal Amplification—Standard Output

Here we return to the subject of sensitivity in terms of the amount of signal required to produce an arbitrary output (aural power, video deflection, etc.), which may be designated as *standard output*. This corresponds to the I.R.E. "Normal Test Output," and is usually a mean value somewhere between the noise threshold and the maximum output that the receiver is capable of delivering without overloading. The important consideration is that the gain thus measured be strictly a signal gain, free of noise considerations and within the linear range of the receiver. As an example, consider again the airborne receiver, for which it was proposed that 0.5 milliwatt is a suitable standard noise output. A review of tests by the Psychoacoustic Laboratory at Harvard indicates that, for voice communication, an average speech power of 100 milliwatts at the headphones is required in an airplane at an altitude of 35,000 feet; hence, a good airborne receiver should deliver a maximum power of at least this much. A suitable standard output for purposes of sensitivity measurement could then be 10 milliwatts. For military headphone use this power would be measured with a root-mean-square or average meter using a 600-ohm load. If cathode-ray

[9] This concept and those to follow arose from discussions in 1944 at the Radio Research Laboratory, Harvard University, concerning performance standards for wide-tuning-range search receivers.

display only is to be used, the standard output would be defined as some suitable mean deflection.

The proper setting of the receiver gain control is a problem. In broadcast receivers thermal noise is negligible and the gain control is usually set at maximum. For a high-gain noisy receiver it is not possible to do this and still have standard output represent mostly signal with negligible noise. It therefore becomes impossible to dissociate sensitivity related to signal gain and sensitivity related to noise. A proposal for correlating these sensitivities into a combined figure of merit is presented in the next section.

Combined Sensitivity Figure

In order to provide a single figure whereby receivers intended for the same type of service may be directly compared, the concept of *standard gain setting* is introduced. This is the setting of the gain control that provides delivery of *standard noise output.* The test procedure consists first of connecting to the receiver a signal generator of proper source impedance and of specified modulation suitable for the intended service. Then, with zero signal delivered by this generator, the receiver is adjusted for *standard gain setting*, that is, to deliver *standard noise output.* If *standard noise output* is not achieved, even at maximum gain, then maximum gain is used in lieu of standard gain. The output of the signal generator is then advanced until *standard output* is obtained from the receiver. The amount of this signal from the generator is then defined as the sensitivity of the receiver. Thus there is provided a combined figure weighing both gain and noise.

It is interesting to note how the various design variables show up in such a figure for sensitivity. Consider, for instance, two receivers that have the same maximum gain, but one of which has greater noise, due either to unnecessarily large bandwidth or to poor design of the input circuits. Standard gain for the second receiver will be lower, and thus a larger signal will be required to produce standard output. Of course, if greater bandwidth achieves a certain advantage from some other operating standpoint, this must be weighed separately against the poorer sensitivity.

Note, however, that if these two receivers do have equally good input design, the difference being only in bandwidth, they will then be found to have equal noise figures. That is, *when compared to hypothetical noise-free receivers of the same bandwidth*, they are equally good. Yet, from a practical standpoint, they are not equally good when compared for the same type of service because one has a bandwidth unnecessarily large. Thus noise figure alone is not an adequate sensitivity specification.

If one of two receivers having the same input noise has insufficient gain to deliver standard noise output, this receiver will require a larger signal to produce standard output, and will thus properly be rated as a poorer receiver for the intended service.

Conclusion

Receiver sensitivity at the higher frequencies, where noise is a limiting factor, should be specified in terms of both the noise threshold and the over-all signal gain. This can be done by specifying two independent quantities, one, the *noise figure*, and two, the conventional I.R.E. type of sensitivity, involving an arbitrary *normal test output.* Alternatively, the two quantities can be joined in a *combined sensitivity figure.*

Appendix

Voltage Sensitivity Versus Power Sensitivity

Traditionally, at the lower frequencies at least, the sensitivity of a receiver has been specified in volts, or microvolts, rather than in watts. Furthermore, for an established service like standard broadcasting, voltage levels of "distant," "local," etc., signals induced in a typical antenna are well known, and appear in the published standards of The Institute of Radio Engineers. On the other hand, in the microwave radar art which has grown up during the war, power measurements are used almost exclusively.[10] Each has its field of utility; it is believed that no essential value would be gained by attempting to standardize on either voltage or power for the entire frequency range. At the lower frequencies, where propagation is primarily ground-wave transmission, the voltage induced in a receiving antenna is calculated as the product of the electric field strength of the wave and the "effective height" of the antenna. It is convenient to treat the problem in this way, inasmuch as noise figure, antenna gain, transmission-line loss, etc., for the receiver usually do not have to be considered. As one moves to higher frequencies, however, particularly in passing into the ultra-high-frequency range, these other factors do enter, and in such a way as to make it more convenient to handle all the calculations on a power basis.

In discussing the use of power in receiver measurements it is necessary to explain the concept of available power.[11] To begin with, it should be pointed out that in all standard receiver measurements the signal generator is connected, not to the receiver terminals directly, but in series with an impedance so chosen as to typify the normal source impedance presented by the antenna or transmission line. How much of the energy thus provided by the signal generator is actually absorbed by the receiver is not known unless the exact receiver input impedance is known. Since it is considered the problem of the receiver designer to utilize this available energy most efficiently, usually through proper impedance matching, his degree of success will show up in the sensitivity attained. Thus the signal-generator voltage or

[10] L. S. Schwarz, "Specification of receiver sensitivity and transmitter power output at ultra-high frequencies," Proc. I.R.E., vol. 34, p. 663; September, 1946.

[11] See page 419 of footnote reference 4.

power in any receiver test is actually only a measure of the energy *available* to the receiver. It may be expressed either in terms of voltage which is applied in series with the source impedance, or in terms of the maximum power available, i.e., that power which would be delivered to the receiver if it were carefully matched to the source impedance. The relation between applied voltage and available power is the following (see Fig. 1):

$$P_{max} = E_s^2/4R_s \qquad (8)$$

where

P_{max} = available power

E_s = root-mean-square voltage from signal generator

R_s = resistive component of source impedance (including both dummy antenna and signal generator).[12]

In order to illustrate the relative magnitudes of corresponding power and voltage figures, Table I is presented for the familiar broadcast situation.

The first factor pointing to the desirability of a shift from voltage to power definitions, as the higher frequencies are reached, is the types of measuring instruments available. Signal generators up to 50 megacycles may use vacuum-tube voltmeters to measure the radio-frequency voltage, but such voltmeters are generally not usable at higher frequencies. The next step is a crystal-type voltmeter, which has been used in signal generators up to 1000 megacycles. Beyond 1000 megacycles, however, it has proved more expedient to use devices such as thermistors and bolometers, which are basically power devices since their operation depends upon a heating phenomenon. Another factor is that power is the natural measure for noise. If the equation for thermal noise in (1) is converted to express available power, it becomes

$$P_n = E_n^2/4R_s = kT\Delta f. \qquad (9)$$

It is thus seen that the available noise power is independent of the impedance level, Δf being the prime consideration. Finally, high-frequency propagation and transmission are calculated more easily on a power basis. With high-gain antennas, particularly those using reflectors, it is more convenient to talk of intercept areas, rather than effective heights, and thus to talk in terms of watts per square meter, rather than in volts per meter.

TABLE I

	Root-Mean-Square Voltage in Series with Antenna[13] (E_s)	Available Power[14] (P_{max})
Distant signal	50×10^{-6} volts (50 microvolts)	25×10^{-12} watts (25 micromicrowatts)
Mean signa	5×10^{-3} volts (5 millivolts)	0.25×10^{-6} watts (0.25 microwatts)
Local signal	100×10^{-3} volts (100 millivolts)	100×10^{-6} watts (100 microwatts)
Strong signal	2 volts	40×10^{-3} watts (40 milliwatts)

[12] Any reactance which may be in the signal source does not enter in this power equation.

[13] Listed in "Standards on Radio Receivers," 1938, p. 14. Institute of Radio Engineers.

[14] For a frequency of 1 megacycle where R_s for the standard dummy antenna is about 25 ohms.

Balanced Amplifiers*

FRANKLIN F. OFFNER†, SENIOR MEMBER, I.R.E.

Summary—**Push-pull impedance-coupled amplifiers have wide applicability in electronic instrumentation. Four gain factors are required to completely describe their performance. Of these factors, one should be large and the others as small as possible. These characteristics are obtained by in-phase feed-back, applied properly. A number of circuits, suitable for various applications, are described.**

1. Introduction

BALANCED push-pull impedance-coupled[1] amplifiers have a wide applicability in electronic instrumentation. Among their uses are: differential input amplifiers with balanced output for bioelectric and other measurements; differential input stages for single-ended amplifiers; and phase inverters. In addition, such amplifiers frequently have advantages over single-ended amplifiers for low-frequency applications, since cathode and screen-grid by-pass capacitors may be eliminated, and power-supply impedance does not affect the frequency response.

The amplification of a single-ended amplifier is given by a single parameter μ, the ratio of output to input voltage. Generally, μ is complex and a function of frequency. In contrast, four gain factors are required to completely describe the performance of a push-pull amplifier. Of these, the first factor, the conventional differential gain, should be high, while the other factors, the in-phase gain, the inversion gain, and the differential unbalance, should be as low as possible. It will be shown that the desired characteristics are obtained by the use of in-phase feedback.

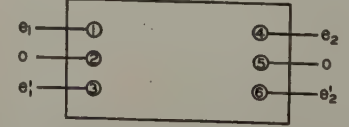

Fig. 1—Generalized push-pull amplifier.

2. Generalized Theory

A push-pull impedance-coupled amplifier is a six-terminal network, with three input and three output terminals (Fig. 1). The input signal voltages e_1 and e_1' are applied between terminals 1, 2 and 3, 2, respectively. The output voltages e_2 and e_2' are developed between

* Decimal classification: R363.23. Original manuscript received by the Institute, March 7, 1946; revised manuscript received, August 9, 1946.

† Offner Electronics Inc., Chicago, Illinois.

[1] Impedance coupling as used here includes resistance, resistance-capacitance, and choke coupling, but not transformer coupling.

terminals 4, 5 and 6, 5. Four gain factors must be considered. These are most directly taken as:

$$\mu = e_2/e_1 \quad \text{for} \quad e_1' = 0 \tag{1a}$$

$$\mu' = e_2'/e_1' \quad \text{for} \quad e_1 = 0 \tag{1b}$$

$$\gamma = -e_2'/e_1 \quad \text{for} \quad e_1' = 0 \tag{1c}$$

$$\gamma' = -e_2/e_1' \quad \text{for} \quad e_1 = 0 \tag{1d}$$

In a truly balanced amplifier, $\mu=\mu'$, and $\gamma=\gamma'$. In any real amplifier, this is never exactly true.

To illustrate the significance of these factors, consider the amplifier of Fig. 2. The amplification of the upper half of the amplifier is μ; that of the lower, μ'. There is no cross-coupling, and a signal applied at 1, 2 will produce no output at 6, 5. Thus $\gamma=\gamma'=0$.

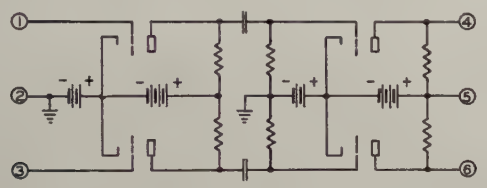

Fig. 2—Push-pull amplifier without cross-coupling.

If in the above amplifier a cathode-resistor bias common to the two tubes of each stage is used, in-phase degeneration will produce cross-coupling, and γ and γ' will no longer be zero.

Assuming a linear amplifier, the principle of superposition gives the total output voltage as

$$e_2 = \mu e_1 - \gamma' e_1' \tag{2}$$

$$e_2' = \mu' e_1' - \gamma e_1. \tag{3}$$

New gain factors derived from those above are more easily interpretable in terms of amplifier performance.

Differential Gain

The differential gain of the amplifier is

$$G_0 = (e_2 - e_2')/(e_1 - e_1') \tag{4}$$

for $e_1'=-e_1$. Substituting (2) and (3),

$$G_0 = \tfrac{1}{2}(\mu + \mu' + \gamma + \gamma'). \tag{5}$$

In-Phase Gain

The in-phase gain of the amplifier is

$$G_c = (e_2 + e_2')/(e_1 + e_1') \tag{6}$$

for $e_1'=e_1$. Substituting,

$$G_c = \tfrac{1}{2}(\mu + \mu' - \gamma - \gamma'). \tag{7}$$

Thus, if $\mu+\mu'=\gamma+\gamma'$, the in-phase gain is zero.

Inversion Gain

In general, if an in-phase signal is applied to the input, a differential output signal will be obtained. This may be termed the *inversion gain* G_i of the amplifier:

$$G_i = (e_2 - e_2')/\tfrac{1}{2}(e_1 + e_1') \tag{8}$$

for $e_1=e_1'$.

$$G_i = \mu - \mu' + \gamma - \gamma'. \tag{9}$$

It is seen, therefore, that even though the in-phase gain is made zero, the inversion gain may be large. This is of importance in many applications of differential amplifiers. It will be shown later, however, that reduction of the in-phase gain by properly applied in-phase feedback will simultaneously reduce the inversion gain.

Differential Unbalance

The fourth gain factor, the differential unbalance G_u, gives the unbalance of the output when a balanced input signal is applied:

$$G_u = (e_2 + e_2')/(e_1 - e_1') \tag{10}$$

for $e_1=-e_1'$.

$$G_u = \tfrac{1}{2}(\mu - \mu' - \gamma + \gamma'). \tag{11}$$

3. Gain Factors With In-Phase Feedback

In the generalized circuit of Fig. 1, in-phase feedback may be introduced.[2] This is shown in Fig. 3, where voltage feedback from the 4, 6 output terminals

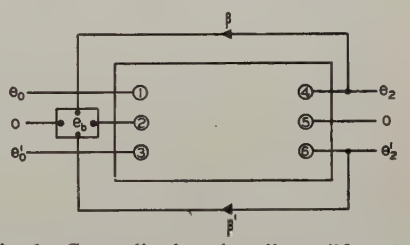

Fig. 3—Generalized push-pull amplifier with in-phase feedback.

is introduced in series with the common input lead, in such phase relationship as to reduce the in-phase gain. The feedback voltage e_b is

$$e_b = \beta e_2 + \beta' e_2'.$$

In general, because of variation in components, β is not necessarily equal to β'. Then

$$e_1 = e_0 - e_b = e_0 - \beta e_2 - \beta' e_2' \tag{12a}$$

$$e_1' = e_0' - e_b = e_0' - \beta e_2 - \beta' e_2', \tag{12b}$$

and by (2) and (3),

$$e_2 = \mu(e_0 - e_b) - \gamma'(e_0' - e_b) \tag{13a}$$

$$e_2' = \mu'(e_0' - e_b) - \gamma(e_0 - e_b), \tag{13b}$$

and

$$e_b = \beta[\mu(e_0 - e_b) - \gamma'(e_0' - e_b)] + \beta'[\mu'(e_0' - e_b) - \gamma(e_0 - e_b)]$$

$$e_b = \frac{\beta(\mu e_0 - \gamma' e_0') + \beta'(\mu' e_0' - \gamma e_0)}{1 + \beta(\mu - \gamma') + \beta'(\mu' - \gamma)}. \tag{14}$$

[2] The generalized amplifier of Fig. 1 may already contain in-phase feedback (as in Section 5 below). In this section the effect of adding in-phase feedback around an amplifier is considered irrespective as to whether it already had feedback of this type.

To calculate the gain factors for in-phase signals, put $e_0=e_0'$:

$$e_b = \frac{\beta(\mu-\gamma')+\beta'(\mu'-\gamma)}{1+\beta(\mu-\gamma')+\beta'(\mu'-\gamma)}\,e_0. \tag{15}$$

In-Phase Gain with Feedback

The in-phase gain with feedback, G_c', is obtained by putting the new input voltage $e_0=e_0'$ for $e_1=e_1'$ in (6); and substituting e_2 and e_2' from (13):

$$G_c' = (\mu+\mu'-\gamma-\gamma')(e_0-e_b)/2e_0$$
$$G_c' = G_c/[1+\beta(\mu-\gamma')+\beta'(\mu'+\gamma)]. \tag{16}$$

For $\beta=\beta'$ this reduces to

$$G_c' = G_c/(1+2\beta G_c) \tag{17}$$

which is similar to the familiar feedback equation.

Inversion Gain with In-Phase Feedback

The inversion gain with in-phase feedback, G_i', may be calculated by a similar procedure, using equation (8):

$$G_i' = (\mu-\mu'+\gamma-\gamma')(e_0-e_b)/e_0$$
$$G_i' = G_i/[1+\beta(\mu-\gamma')+\beta'(\mu'-\gamma)]. \tag{18}$$

For $\beta=\beta'$, this again reduces to

$$G_i' = G_i/(1+2\beta G_c). \tag{19}$$

Differential Gain with Feedback

The differential gain with feedback, G_0', is calculated from (4) by putting $e_0'=-e_0$ for $e_1'=-e_1$; and substituting e_2 and e_2' from (13):

$$G_0' = [(\mu+\gamma)(e_0-e_b)+(\mu'+\gamma')(e_0+e_b)]/2e_0$$
$$G_0' = \tfrac{1}{2}(\mu+\mu'+\gamma+\gamma')-\tfrac{1}{2}(\mu-\mu'+\gamma-\gamma')e_b/e_0$$
$$G_0' = G_0-\tfrac{1}{2}G_i e_b/e_0. \tag{20}$$

Substituting e_b from (14), with $e_0'=-e_0$:

$$G_0' = G_0-\tfrac{1}{2}G_i[\beta(\mu+\gamma')-\beta'(\mu'+\gamma)] \\ /[1+\beta(\mu-\gamma')+\beta'(\mu'-\gamma)]. \tag{21}$$

If $\beta=\beta'$, this reduces to

$$G_0' = G_0-\beta G_u G_i/(1+2\beta G_c) \tag{22}$$

and if $\beta G_c\gg 1$, this becomes

$$G_0' = G_0-\tfrac{1}{2}G_u G_i/G_c. \tag{23}$$

Differential Unbalance with In-Phase Feedback

The differential unbalance with in-phase feedback, G_u', is obtained from (10) in a similar manner:

$$G_u' = [(\mu-\gamma)(e_0-e_b)-(\mu'-\gamma')(e_0+e_b)]/2e_0$$
$$= \tfrac{1}{2}(\mu-\mu'-\gamma+\gamma')-\tfrac{1}{2}(\mu+\mu'-\gamma-\gamma')e_b/e_0 \tag{24}$$
$$= G_u-G_c e_b/e_0$$
$$= G_u-G_c[\beta(\mu+\gamma')-\beta'(\mu'+\gamma)] \\ /[1+\beta(\mu-\gamma')+\beta'(\mu'-\gamma)]. \tag{25}$$

If $\beta=\beta'$, this reduces to

$$G_u' = G_u-2\beta G_c G_u/[1+2\beta G_c]. \tag{26}$$

If $\beta G_c\gg 1$, this becomes

$$G_u' = 0$$

and the output is balanced.

4. Discussion of the Feedback Equations

The general equations for in-phase gain and inversion gain with feedback, (16) and (18), show that G_c' and G_i' may be reduced to a low value by sufficient feedback, even though the amplifier and feedback circuit both be nonsymmetrical ($\mu\neq\mu'$; $\gamma\neq\gamma'$; $\beta\neq\beta'$). This is of great importance in the design of differential amplifiers, as it allows excellent input balance to be maintained with components of commercial tolerance. For example, in some bioelectric recording it is necessary to keep the inversion gain less than one-thousandth the differential gain. This can be achieved even though the individual tubes, resistors, etc., differ by ten or twenty per cent.

Referring to (21) and (25) for G_0' and G_u', however, it is seen that the terms in β and β' appear as a difference. Thus, an inequality between β and β' will affect the differential gain and the output balance.

Another possible effect of having β and β' unequal is to make the amplifier unstable. Referring to (16), in an unsymmetrical amplifier γ' could be, for example, greater than μ. Then, if β were large and β' small, the denominator could become zero at some frequency, and the amplifier could oscillate. However, if $\beta=\beta'$ (17) shows that the expected phase relationships hold, the amplifier will be stable. A similar analysis applies to the other gain factors. Thus it is necessary that a satisfactory degree of balance be held in the feedback circuit to insure stability.

5. Characteristics of Ideal Feedback Amplifier

If the amplifier of Fig. 1 has a very large amount of in-phase feedback with $\beta=\beta'$, $G_c=G_i=G_u=0$. That is,

$$\mu+\mu'-\gamma-\gamma' = 0$$
$$\mu-\mu'+\gamma-\gamma' = 0$$
$$\mu-\mu'-\gamma+\gamma' = 0.$$

Solving simultaneously,

$$\mu = \mu' = \gamma = \gamma'.$$

If a signal is applied to the 1, 2 terminals, by (1a) and (1c), $e_2=-e_2'$, and the amplifier may be used as a phase inverter.

If a signal e_1 is applied to the 1, 2 terminals, and e_1' to the 3, 2 terminals, and the output is taken from the 4, 5 terminals, by (2) the output is proportional to e_1-e_1'. Thus the amplifier acts as a differential-input amplifier and may be followed by a single-ended amplifier. In the latter example, an equal and opposite output

signal also appears at the 6, 5 terminals. The amplifier, therefore, acts as a differential amplifier with balanced output.

6. Illustrative Examples—Conventional Amplifiers

Noncross-Coupled Push-Pull Amplifier

In the amplifier of Fig. 2, $\gamma=\gamma'=0$ as shown above. Due to variation in components, the amplifier will seldom be completely symmetrical, so μ is rarely exactly equal to μ'. The differential gain is then, by (5), the average of the gains of the two sides:

$$G_0 = \tfrac{1}{2}(\mu + \mu'),$$

and the in-phase gain is, by (7), equal to the differential gain:

$$G_c = \tfrac{1}{2}(\mu + \mu').$$

The inversion gain is, by (9),

$$G_i = \mu - \mu'$$

or just the difference in the gains of the two sides; and by (11), the differential unbalance is

$$G_u = \tfrac{1}{2}(\mu - \mu').$$

In a multistage amplifier μ and μ' may differ easily by 50 per cent, so that G_i becomes of the same order as G_0. An amplifier, as shown in Fig. 2, is thus entirely unsuited for differential use where there is any in-phase signal, or where the output must be balanced.

Phase Inverters

The familiar two-tube phase-inverter circuit (Fig. 4) may be considered as a push-pull amplifier in which $\mu'=\gamma'=0$, since the number 3 terminal is not connected.

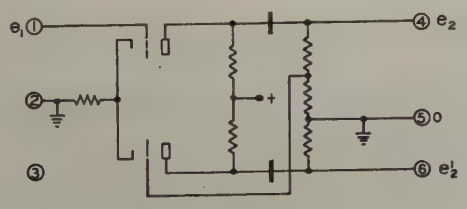

Fig. 4—Conventional phase inverter.

But balanced operation ($e_2=-e_2'$) is obtained, by (2) and (3), when $\mu=\gamma$. By (7), this requires that the in-phase gain $G_c=0$. By (9), the inversion gain is

$$G_i = \mu + \gamma = 2\mu.$$

This illustrates that balanced operation results if the in-phase gain is zero and the amplifier operates by virtue of the inversion gain. G_c is made zero by adjusting the tap on the grid resistor and balance is assisted by the in-phase feedback produced by the unby-passed cathode resistor.

7. Illustrative Examples—In-Phase Feedback

In applying in-phase feedback, it is essential that the feedback be effectively introduced in series with the common input lead, as shown in Fig. 3. Otherwise, inversion gain occurring before the point of introduction of feedback will not be cancelled. Thus, feedback introduced in the second stage of an amplifier loses most of its value.[3]

To insure that the feedback will be effective over the full response range of low-frequency amplifiers, it is desirable to employ only resistors in the feedback mesh. Both of these requirements have been met in the amplifiers described below.

One of the simplest methods of obtaining in-phase feedback is to employ a large cathode resistor in the first stage,[4] as shown in Fig. 5. Here, $\beta=R_k/R_{P1}$; $\beta'=R_k/R_P$.

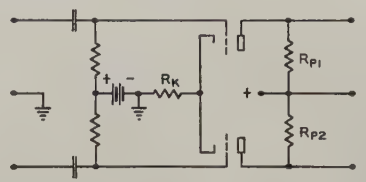

Fig. 5—In-phase feedback from cathode resistor.

With no cathode resistor ($\gamma=\gamma'=0$), $G_c=\frac{1}{2}(\mu+\mu')$. Thus $G_c'=\frac{1}{2}(\mu+\mu')/(1+\mu R_k/R_{P1}+\mu' R_k/R_{P2})$. A typical electroencephalograph amplifier had G_c reduced from 60 to 2 by use of a 60,000-ohm cathode resistor.

Amplified in-phase feedback is used in the vibration amplifier[5] shown in Fig. 6. The input signal is applied to one input grid, and conventional inverse feedback to the other. The in-phase feedback insures symmetrical operation, and the well-known advantages of push-pull amplifiers are obtained.

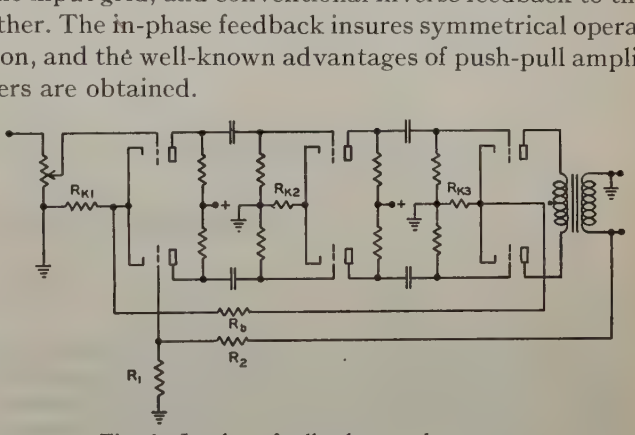

Fig. 6—In-phase feedback over three stages.

The balanced output transformer has low reactance to in-phase signals, and R_{k3} is effectively the load for such signals. The signal across R_{k3} is fed back to the first cathode through R_b. Then $\beta=R_{k1}/2R_b$, and $G_c'=G_c/(1+G_cR_{k1}/R_b)$. G_c was reduced from 200 to 18 with a moderate amount of feedback. Unbalance in the output transformer will make $\beta\neq\beta'$, and the amplifier may oscillate.

[3] Paul Traugott, "Electroencelographic design," *Electronics*, vol. 16, p. 132; August, 1943; and W. M. Rogers and H. O. Parrack, "Electronic apparatus for recording and measuring electrical potentials in nerve and muscle," Proc. I.R.E., vol. 32, p. 738; December, 1944; show in-phase feedback in the second stage only.

[4] S. N. Trevino and Franklin Offner, "An A.C. operated D.C. amplifier with large current output," *Rev. Sci. Instr.*, vol. 11, p. 412; December, 1940.

[5] Offner Electronics Type 134.

The feedback obtained in the circuit of Fig. 5 can be increased also by passing the screen current from the following stage through the cathode resistor (Fig. 7). It allows amplified in-phase feedback with only two stages, and improves the feedback ratio by about four times.

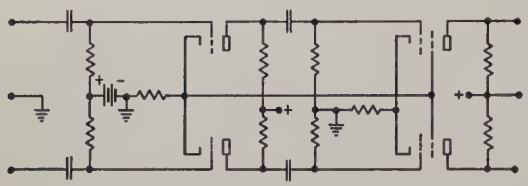

Fig. 7—In-phase feedback using screen current.

Another circuit[6] for amplified in-phase feedback over two stages is shown in Fig. 8. As the source is returned to the second cathode, either the source or power supply must be ungrounded. Therefore, its use in bioelectric work is limited.

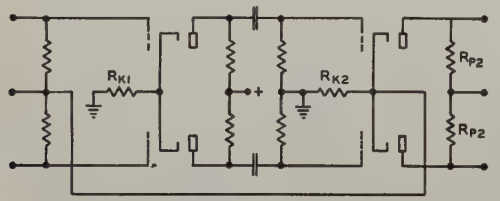

Fig. 8—In-phase feedback over two stages.

In-phase feedback in the above circuits is from indirectly heated cathodes. A portable vibration amplifier with filamentary tubes uses the circuit of Fig. 9. The in-phase feedback is produced by the alternating-current component of the plate current flowing through output-stage filaments. The potential produced is between the first stage filaments and ground, providing in-phase feedback.

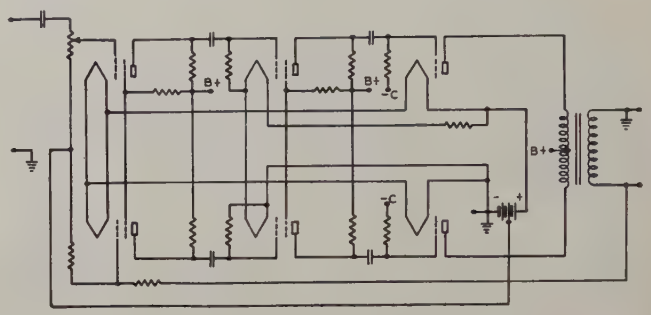

Fig. 9—In-phase feedback using filament tubes.

8. Conclusions

The addition of in-phase feedback gives push-pull amplifiers several desirable characteristics. The use of such amplifiers for special purposes is almost essential. For more conventional applications, where a single ended amplifier would usually be used, the improved performance and simplified design of the push-pull amplifier will frequently make its use desirable. Tubes such as the 12SC7, 12SL7GT, and 12L8GT require the us of but one tube per stage. Thus, a push-pull amplifier will frequently have a smaller total volume of components than a single-ended, and will have superior performance.

[6] Franklin Offner, "Push-pull resistance coupled amplifiers," *Rev. Sci. Instr.*, vol. 8, p. 20; January, 1937.

Test Equipment and Techniques for Airborne-Radar Field Maintenance*

E. A. BLASI†, senior member, i.r.e., and GERALD C. SCHUTZ†, member, i.r.e.

***Summary*—The scope of this paper covers the various testing methods, techniques, and equipment that are used for the field maintenance of airborne-radar systems. Techniques used in the measurement of frequency, power, and receiver sensitivity are outlined, as well as measurements of performance characteristics peculiar to airborne-radar equipment. The specially designed instruments required for field maintenance and the unique procedures devised to accomplish the measurement of radar performance characteristics for optimum radar performance are described. Special emphasis is directed to the application of special test equipment, such as echo boxes, directional couplers, and signal generators, for maintenance of microwave radar equipment.**

I. Statement of the Problem

A CONVENTIONAL airborne-radar system consists of an antenna, transmitter, receiver, indicator, modulator, and power supply. To determine whether such a system is not only functioning properly but in most cases at optimum performance, it is necessary to perform the following tests:

(1) Over-all system performance
(2) Transmitter frequency and power output
(3) Receiver sensitivity and local-oscillator frequency and power output
(4) Standing-wave ratio of the transmission line
(5) Frequency pulling of the magnetron
(6) Transmit-receive recovery time and receiver bandwidth
(7) Spectrum analysis of a transmitted pulse
(8) Pulse amplitude, time, and time-delay measurements
(9) Range and rate calibration.

It is evident from the above list that new techniques had to be devised and new instruments developed to make such techniques possible. Too often, and this cannot be too greatly stressed, the problem has been to design field-type instruments which not only possessed intrinsic electrical characteristic comparable

* Decimal classification: R537.4. Original manuscript received by the Institute, January 18, 1946; revised manuscript received, April 3, 1946. Presented, 1946 Winter Technical Meeting New York, N. Y., January 25, 1946.

† Aircraft Radiation Laboratory, Wright Field, Dayton, Ohio.

to instruments meeting stringent laboratory requirements but also the design had to incorporate the rigid requirements encountered under rugged field conditions. The designers were always faced with the problem of simplifying complex testing procedures and reducing the number of operating steps to an absolute minimum.

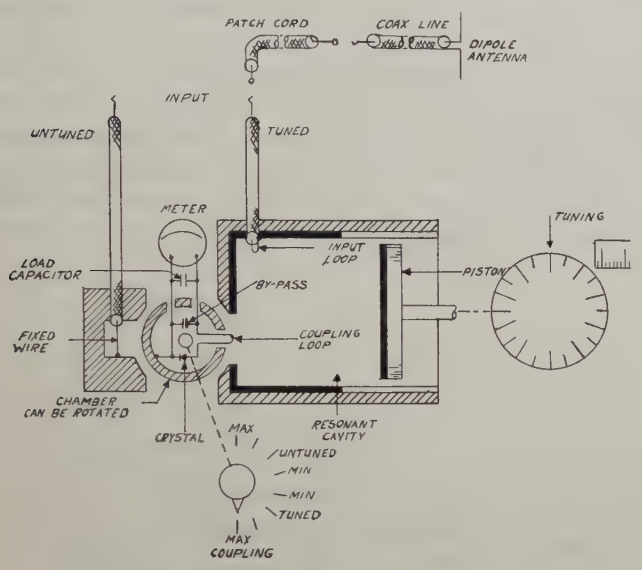

Fig. 1—Echo-box functional schematic diagram.

At the initiation of the microwave radar program, the only types of test sets available were those designed for production testing slightly modified for field use. Much of the test equipment was bulky and heavy. As soon as these test sets were introduced into the theaters of operation, the following disadvantages evolved:

(1) There were no trucks available to field maintenance personnel with which to haul around heavy test gear.

(2) Maintenance often had to be done under blackout conditions.

(3) The airplanes in the theaters of operation had to be camouflaged and kept well dispersed.

(4) Radar system in airplanes (including the B-29 Superfortress) were invariably installed in inaccessible locations.

In view of these disadvantages, an intensive design and development program was initiated. In the first place, the testing procedure for airborne radar systems was divided into two categories: (1) preflight or squadron testing, and (2) maintenance or depot testing. For preflight testing, light-weight and preferably passive-type instruments were developed and furnished in small packaged units. The heavier and bulkier instruments which were primarily intended for depot bench testing were designed to be as small and lightweight as possible, so that when necessary they could be easily transported by field maintenance personnel to airplane installations. The size, weight, and form factor of each test set was given careful consideration so that the instrument could be fitted into inaccessible airplane locations. The test points of the radar systems were standardized to facilitate field measurements and testing.

II. The Test Equipments

The desirable types of test sets for squadron use are those of the passive type; that is, those not requiring any power, either alternating-current or battery. However, this was not at all times possible. Of course, the primary requirement was that the squadron test sets be lightweight and small. Inasmuch as the process of elimination was usually followed in shooting trouble, the following order of tests was considered desirable:

(a) Over-all system performance.
(b) Transmitter power output, frequency, and spectrum analysis.
(c) Frequency and power output of the receiver local oscillator.

The over-all performance of a radar system is usually determined by an echo box. This device is a passive-type instrument and consists of a high-Q cavity, rectifying-crystal unit, tuning mechanism, and an indicating meter. (See Fig. 1.) The Q of the cavity usually ranges between 40,000 and 250,000, depending on the frequency spectrum to be covered. The cavity must be free of all spurious modes and reasonably flat in ringtime and through-transmission characteristics over the frequency band. A piston is moved in and out of the cavity, causing the cavity to be tuned over the frequency spectrum. The frequency dial is sufficiently geared down to allow spectrum analysis of radio-frequency pulse. The cavity is started into oscillation by means of the transmitted pulse, with oscillations building up as shown in Fig. 2. The oscillations die out

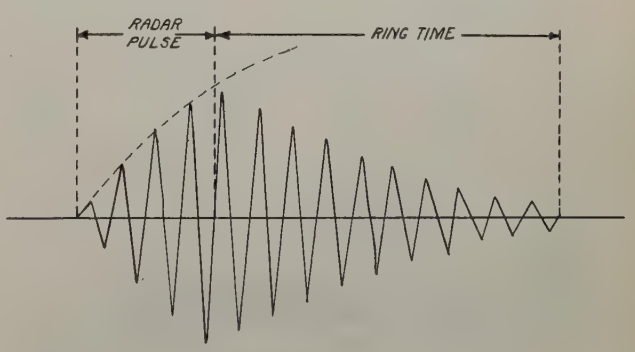

Fig. 2—Relation of radar pulse and ringtime.

gradually after the radar pulse has ended. During this interval, part of the stored energy is dissipated in the cavity and part is reradiated from the dipole or into the directional coupler. Some of this reradiated energy is passed into the radar antenna and then to the receiver. This causes a trace to form on the indicator of the radar system. During this period the cavity is said to be ringing. The ringtime is measured from the end of the radar transmitter pulse to the end of the signal reradiated from the cavity. The reflected signal is considered ended where the amplitude disappears into the

noise background. Therefore, it is apparent that the ringtime is dependent upon the transmitter power and the level of the noise in the receiver.

The echo box is an ideal passive-type instrument for squadron use. However, it has limitations in that the decibels per microsecond, when reading the ringtime on a radar scope, are rather large. In other words, the

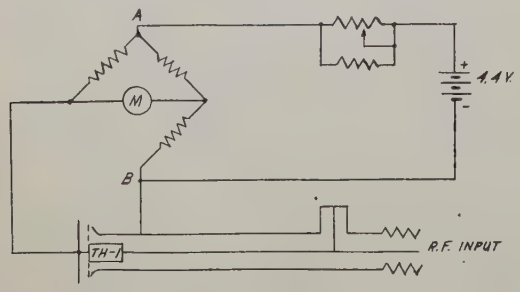

Fig. 3—Simplified thermistor-bridge circuit.

trace on the radar scope will have to be read to a tenth of a mile or better. A difference of a tenth of a mile in ringtime is equal to a difference of about 4 decibels in over-all performance of a radar system, which is about 26 per cent difference in range. Another limitation is a production factor. Echo boxes require very close machining tolerances and involve numerous other production problems which tax the production engineers, especially when it is attempted to construct all the boxes on a production run within very close limits of performance.

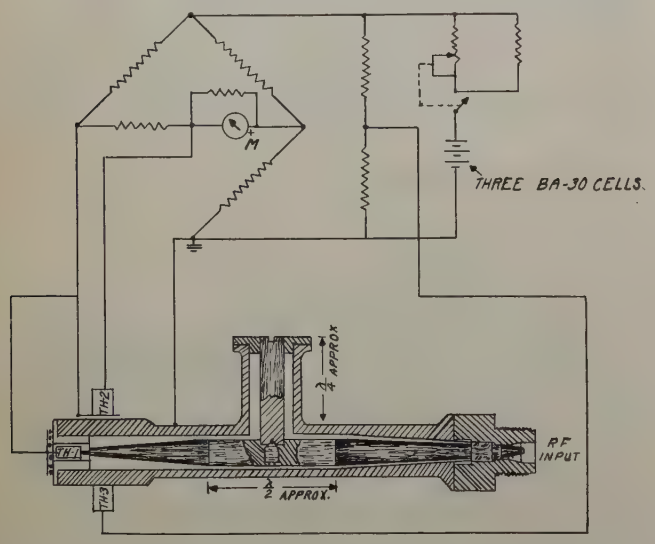

Fig. 4—Temperature-compensated thermistor bridge circuit.

The power output of a radar system is usually measured by means of a thremistor-type power-meter bridge circuit. A thermistor is a device which changes its resistive properties with changes in temperature. It has a negative resistance versus temperature characteristic. The thermistor is placed in a radio-frequency chamber, and at the same time, forms one leg of the bridge circuit. The bridge is balanced by means of direct-current power. When radio-frequency energy is inserted in the chamber it heats up the thermistor, which in turn causes the bridge to unbalance. Calibrated radio-frequency attenuation, in the form of lossy cables or resistive-material insertions, is used for extending the range of the thermistor power meter. Inasmuch as the bridge is influenced by ambient-temperature effects on the thermistor, the instrument has been designed with temperature compensation. Temperature compensation is usually accomplished by means of one or two additional thermistors placed in the circuit to compensate for bridge sensitivity and zero drift. Fig. 3 shows a simplified thermistor-bridge circuit, while Fig. 4 shows a temperature-compensated thermistor bridge circuit. The limitation of such a device is that it is not a passive-type instrument. That is, some

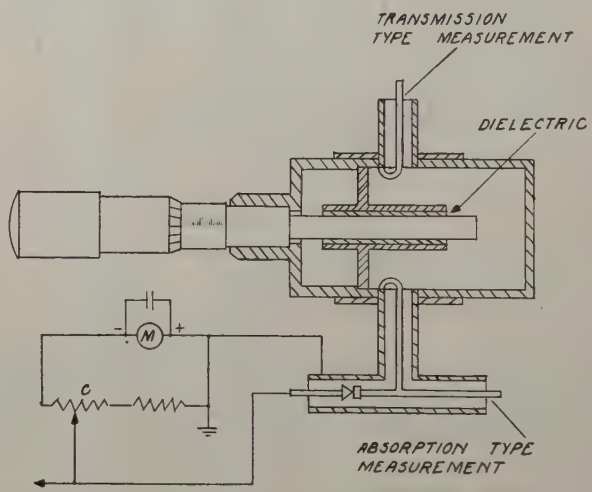

Fig. 5—Frequency-meter schematic.

form of direct-current power, either battery or otherwise, must be furnished in order to operate the bridge.

Frequency meters used in measuring either transmitter or local-oscillator frequency are either of the coaxial or cavity type. Most of the instruments operate in the Te_{01} mode and, depending on the Q required, can be designed either with one segment or with several segments each a quarter wave in length. The design can be either of the transmission type or absorption type. The absorption type is generally more sensitive than the transmission type, as more energy is absorbed in the cavity when it passes through a transmission-type frequency meter. A plunger moves in and out of the cavity, effecting the tuning of the instrument. The design must be such that the instrument is free of spurious modes. Frequency meters can be designed to be temperature-compensated. However, the calibration is affected not only by expansion and contraction of the metal cavity, but also by the effect of temperature and humidity on the dielectric (air). The mechanical drives are of the micrometer type, and take-up must be used for resetting accuracies. The absolute accuracy of an average field-type instrument is ± 3 megacycles at frequencies from 3000 to 10,000 megacycles

and only on certain frequencies for radar beacon purposes, it is made better than ±3 megacycles. The frequency-meter dial can either be made to be direct-reading, or a calibration chart can be furnished with each instrument. Fig. 5 shows a typical field-type frequency meter.

Before proceeding to describe some of the other test sets, it is desirable at this point to discuss the directional coupler. This device is one of the best means devised for making measurements in a radar system. It permits the measurement of power flowing in either direction in a transmission line and also provides a calibrated means of coupling in or out of a radar transmission line.

Fig. 6 illustrates a wave-guide directional coupler in its simplest form. The unit is inserted as a section of

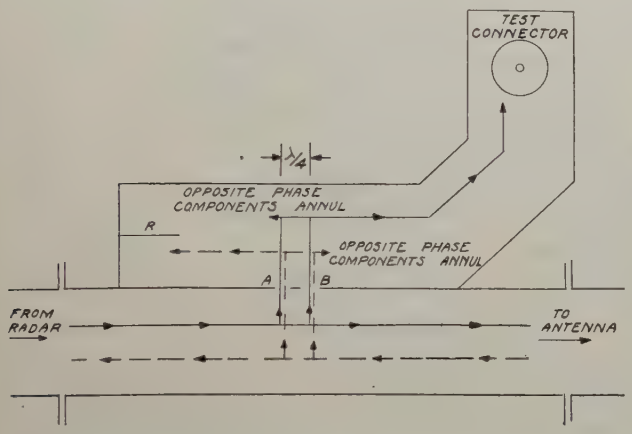

Fig. 6—Showing operation of directional coupler.

the radar transmission line. The auxiliary wave-guide section is permanently fastened and made a part of the inserted wave-guide section. The auxiliary guide is coupled to the main transmission line through two small holes, *A* and *B* which are one-fourth wavelength apart. The degree of coupling or coupling loss is controlled by the sizes of the two small holes. Inasmuch as there are two holes spaced one-fourth wavelength apart, the coupler attains directional properties. This can best be described if it is considered that a direct wave, represented by the solid line, is traveling from the radar to the antenna. Small and equal amounts of energy enter the auxiliary guide through holes *A* and *B*. The energy will divide itself through each hole and travel in both directions. The energy traveling towards the test connector from the two holes will travel over the same distance, and therefore will add at the test jack. On the other hand, the energy passing through hole *B* and in the direction of the termination will have traveled one-half wavelength more than the energy passing through hole *A*. The two components, therefore, will be opposite in phase and will cancel.

In the case of the reflected wave, the two components traveling towards *R* will add, and the energy is dissipated in the absorbing material. The components traveling towards the test jack will be opposite in phase and therefore cancel. The directional coupler of Fig. 6 can be completely reversed with respect to the position of the antenna and the radar, and it would then be possible to measure reflected power instead of direct power. Some radar systems have been equipped with bidirectional couplers. A bidirectional coupler is a section of transmission line which has two auxiliary guides on opposite sides of the transmission line. The auxiliary guides are such that one measures direct power while the other measures reflected power. This is convenient for making standing-wave measurements in the transmission line. The test jack on the directional coupler is also used for applying a test signal from a signal generator to the radar receiver.

The test sets described above constitute a good working list of test equipment items generally used for squadron field radar maintenance. The depot-type instruments not only perform the tests that are accomplished at the airplane squadrons but in addition perform tests that complete the measurement of radar systems at repair deposits. Below is an outline of tests performed at a depot:

(a) Over-all system performance.
(b) Transmitter power output, frequency, spectrum analysis, and frequency pulling.
(c) Receiver sensitivity, frequency and power output of local oscillator, bandwidth, and recovery time.
(d) Measurement of pulse amplitude, pulse width, time delay, range calibration, and range-rate calibration.

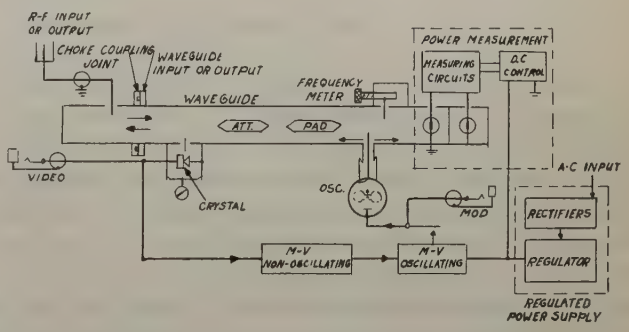

Fig. 7—Signal-generator functional block diagram.

A signal generator is used to measure receiver sensitivity. Microwave signal generators incorporate, as an integral part, a frequency meter and power meter similar to those already described. Fig. 7 shows a functional block diagram of a typical microwave signal generator. In addition to the frequency and power-measuring circuits, it will be noted that there is included super-high-frequency oscillator, multivibrator circuits, regulated power supply, attenuator pad, calibrated attenuator, and rectifying-crystal circuit. In measuring transmitter frequency and power, the energy is fed into the radio-frequency jack. A 35-decibel attenuator pad is switched out, and only the calibrated

attenuator is used in conjunction with the power meter. The power meter is set to a level of 1 milliwatt and the power level is read in decibels above 1 milliwatt (DBM) on the calibrated attenuator. The reason for the attenuator pad is that normally less than 35 decibels above 1 milliwatt is required for measuring transmitter power levels encountered in airborne radar systems; and more than −35 decibels below 1 milliwatt is required for making receiver sensitivity measurements. For frequency measurements, the frequency-meter dial is tuned until a dip is indicated in the power level indicating meter.

In making measurements at test-bench setups, it is usually handy to have a suitable load for terminating the radio-frequency section of a radar system. A radio-frequency load provides an excellent and well-matched termination. Also, it prevents spreading interfering radio-frequency radiation, which is objectional wherever there are more than one test-bench radar setups in a repair depot. Then, too, because of security reasons, precautionary measures must be taken in order not to spray too much radiation at bases of operation. The radio-frequency load is a relatively simple device, consisting of a section of wave guide packed with absorb-

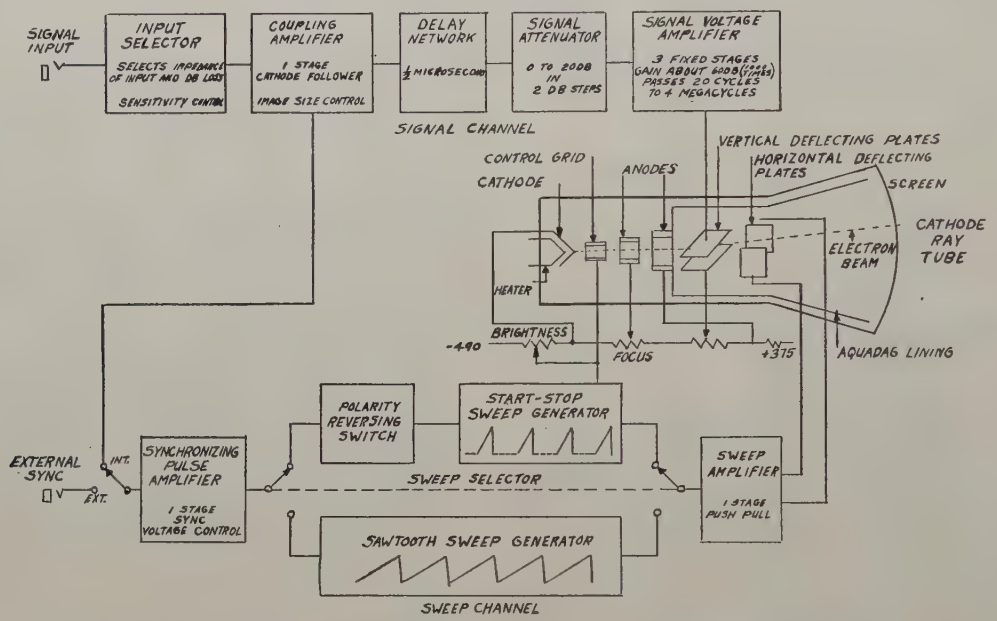

Fig. 8—Block diagram showing function and relation of oscilloscope components.

In making receiver sensitivity measurements, the super-high-frequency oscillator is turned on and set at continuous-wave operation. The super-high-frequency oscillator probe is coupled into the wave guide until the power-measuring level reads 1 milliwatt. Actually, the super-high-frequency oscillator is delivering 2 milliwatts, as the power entering the wave guide divides evenly in both directions: 1 milliwatt to the power-measuring thermistor and 1 milliwatt to the radio-frequency output jack before passing the pad and the attenuator. The frequency of the super-high-frequency oscillator, of course, can be set by the frequency meter. After these preliminary adjustments, the super-high-frequency oscillator is switched either to pulsed or frequency-modulated operation. There are several ways in which the signal generator can be pulsed and, for this reason, an external modulation jack is furnished on the test set. For frequency-modulation operation a sawtooth wave is used for modulating the signal generator. This causes a signal to sweep across the bandwidth response of the radar receiver. The crystal circuit, along the test-set wave guide, serves a useful purpose in eliminating the necessity for a synchronizing cable connection between the radar system and the test set.

ing material. Sufficient radiating fins are attached for dissipating heat. The radio-frequency absorbing material is so packed as to render the radar transmission line with a good termination.

In radar maintenance work an oscilloscope with good bandwidth characteristics is extremely important. The instrument must incorporate start-stop sweeps and be fast enough to view extremely short pulses. Fig. 8 illustrates a block diagram of an oscilloscope used in field-maintenance radar work. It will be noted that provision has been made so that the sweep circuits will trigger off on input video signals. The signal-channel attenuator has been calibrated so that pulse voltages can be measured over a range of better than 80 decibels. Provision is also made on such an oscilloscope for connecting a pulse voltage directly to one of the vertical plates. Accurate timing pips can also be connected directly to the grid of the cathode-ray tube. The input to the vertical signal channel can be made either high or low impedance.

The ½-microsecond delay network is designed to delay the signal pulse and move it into the visible portion of the sweep on the cathode-ray tube. The delay network provides another feature when improperly

terminated. The mismatch in impedance causes a sharp change in voltage to be reflected at the ends of the delay network. Successive reflections recur at 1 microsecond intervals owing to the round-trip travel time in the network. These reflections serve as timing impulses up to about 10 microseconds. In this manner, the fast sweep on the oscilloscope can be calibrated.

In measuring large-amplitude pulse voltages, a voltage divider is used. This device has step-down ratios of 10:1 and 100:1. Fig. 9 shows a schematic diagram,

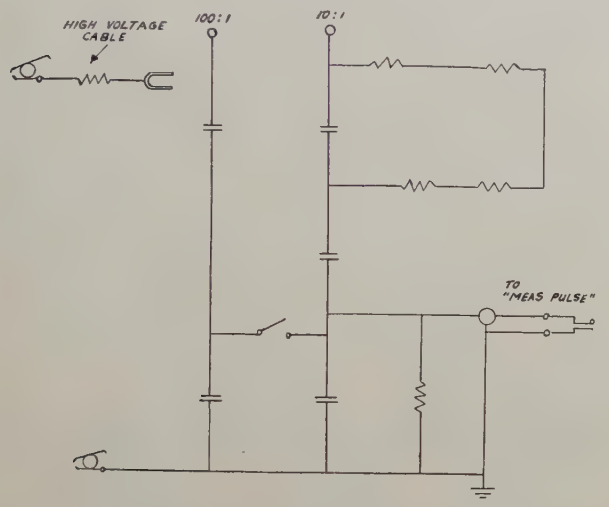

Fig. 9—Schematic diagram of voltage divider.

the circuits of which are simple combinations of series capacitors connected as a voltage divider. The resistors are placed across the output as bleeders to prevent high voltages from being built up. The resistor in the clip end of the high-voltage input cable is used to damp out parasitic resonance effects.

For range and range-rate calibration measurements, a precision range calibrator is used. This device is crystal-controlled and is accurate to 1/10 of 1 per cent. The output of this device is a continuous string of marker pulses accurately spaced 1500 feet apart. Simultaneously, a synchronizing pulse is furnished at pulse repetition rates usually encountered in radar bombing and

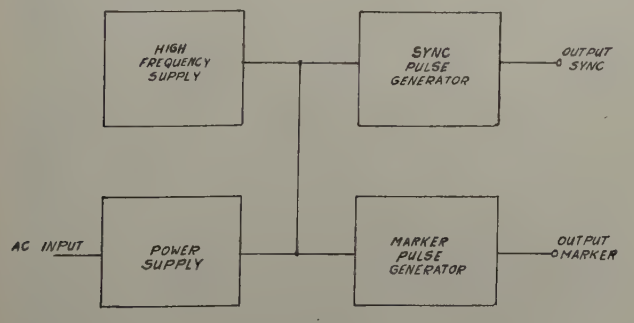

Fig. 10—Range calibrator—block diagram.

gun-laying systems. The marker and synchronizing pulses are continuously phaseable by means of a sine-wave phase shifter. Fig. 10 shows a simple block diagram of the range calibrator, and Fig. 11 shows a simplified schematic diagram of the phase shifter. The phase shifter requires a special continuously variable potentiometer. A 1/10-second-timer stop watch is furnished with each calibrator for range-rate measurements.

The list of test equipment items described and outlined above is not by far the total number of different types of field-maintenance instruments developed during the course of the war. However, the more significant items have been discussed, those which played the most important role in the testing and maintenance of airborne radar systems.

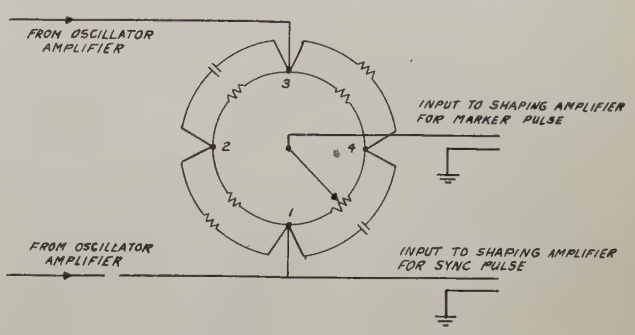

Fig. 11—Phase shifter—schematic diagram.

III. Radar Systems Testing Techniques

The requirements for frequency determination in microwave radar are relatively stringent. It is necessary in many cases to determine frequency accurately to one part in approximately ten thousand. However, this is an objective which has merely been approached in field-type frequency meters. In actual practice it is possible to obtain accuracies of three to five parts in ten thousand under ideal conditions with the type of field instruments described previously in this paper.

The primary use of the frequency meter is to adjust the local oscillator of the radar set to a frequency removed from the transmitting frequency by an amount equal to the intermediate frequency of the radar receiver. Since the bandwidth of the receiver varies between 0.03 and 2.00 per cent of the transmitter frequency, depending upon the particular radar set, it is extremely important to be able to adjust the local oscillator accurately.

On those radar sets which employ a second local oscillator to utilize the receiver for beacon operation, it is necessary to adjust this beacon local oscillator to a frequency removed from the beacon frequency by the intermediate frequency of the particular radar set. Since the absolute value of the beacon frequency is held to two parts in ten thousand and the bandwidth of the receiver is the same as before, the importance of making accurate frequency measurements reasserts itself.

It is necessary in some of the gun-directing radars, operating at approximately 12 centimeters, to stagger the operating frequencies in order to eliminate the

interference that would occur if all of the airplanes in one squadron had gun-directing systems operating at the same frequency. However, the accuracy requirements for fixing the operating frequency of these systems with a frequency meter are not as stringent as those previously mentioned, being in the neighborhood of four parts per thousand. It is interesting to note here that the maximum number of airplanes equipped with automatic gun-directing radars which can be flown effectively in any one formation is dependent, among other factors, upon the accuracy of the frequency meter used to stagger the operating frequencies.

There have been assigned some very specific frequency bands for the operation of different types of radar sets. It is therefore necessary to utilize a frequency meter to ascertain whether or not the radar transmitter under test is operating within the band assigned to it. On systems using a fixed-tuned oscillator, such as a magnetron, it is necessary to replace the tube if it is found to be operating out of the band. On the tunable types it is a simple matter to readjust the frequency.

While, from an interference standpoint, it is not too important in most cases to remain inside the allocated band, it is very important with respect to system efficiency to do so, since most of the radio-frequency components have a band-pass characteristic which is limited very nearly to the allocated frequency band. The accuracy requirement for this type of measurement is relatively low, being in the neighborhood of one half of one per cent.

A radar-type frequency meter, in order to be able to detect local-oscillator power, must be able to give a full-scale deflection for at least 1 milliwatt. It is usually necessary to couple the instrument very loosely from the system for a transmitter frequency measurement. Determination of the local oscillator frequency usually can be accomplished by removing from its holder the rectifying crystal which serves as the first detector, and inserting a small probe in its place to sample the energy there.

It may be noted here that the required accuracy for the adjustment of the frequency of the local oscillators, namely 0.01 per cent, cannot be met with existing frequency meters, which at best are no better than 0.03 per cent. It is, therefore, necessary to use the frequency meter to obtain a rough adjustment and then make the final adjustment using either a true or a simulated signal. In adjusting the frequency of the simulated signal from a signal generator to that of the transmitter, a high degree of accuracy can be obtained by adjusting the frequency meter to the frequency of the transmitter and, then leaving this setting on the meter fixed, adjusting the frequency of the signal source to that of the meter. Thus, the only error involved will be that due to observation on the part of the operator.

The most satisfactory method for coupling a power meter into the transmission line of a system has been through the use of a directional coupler (see Fig. 12). In practice, the coupling loss of this device varies from 20 to 35 decibels, depending upon the system, and is held to an over-all accuracy of plus or minus 0.5 decibel, this variation mainly being a function of the frequency over the operating band.

The milliwatt is a convenient reference level that has been used as a basis for both power and receiver-sensitivity measurements. Thus, power levels are expressed as so many decibels based on a milliwatt. In practice, a power meter is usually connected to the system through a directional coupler and a section of flexible, coaxial cable or wave guide. Both the directional coupler and the cable are calibrated at the factory and the amount of attenuation marked thereon in decibels. To make a power measurement, the variable attenuator on the power meter is then adjusted until a power level of 1 milliwatt is indicated, and the total attenuation, including the reading of the variable attenuator, the cable, and the directional coupler, is then

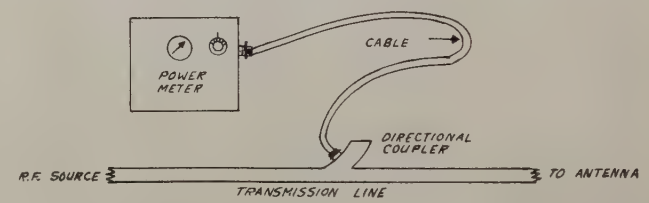

Fig. 12—Showing method for connecting microwave power meter to radar system.

the number of decibels above 1 milliwatt. On the direct-reading type of power meters, fixed attenuator pads are substituted for the variable, and the power level expressed in decibels above 1 milliwatt is indicated directly on the meter of the instrument.

The most favorable accuracy figure that has been obtained for the power measuring system just described is approximately ±0.75 decibel. Since the total error is a function of several independent errors that bear no relation to each other, either in magnitude or direction, it is not possible to evaluate the exact amount of error that will occur in all cases. However, the maximum error can be calculated if it is assumed that all of the individual errors occur in the same direction and are at their maximum value. Then, by using a probability law, it can be shown that in 93 per cent of all cases the probable error will be less than 50 per cent of the total error. This is the figure which has been used for indicating the probable accuracy obtainable on any measuring system employed in servicing airborne-radar systems. An example of this type of calculation for the power-measuring system described is as follows:

Maximum allowable error in power meter	±0.5 decibel
Maximum allowable error in directional coupler	±0.5 decibel
Maximum allowable error in cable	±0.5 decibel
Maximum allowable total error	±1.5 decibels

Thus it can be seen that the probable error for 93 per cent of all cases is ±0.75 decibel. This figure does not allow for the error due to the aging of cables.

Receiver sensitivity measurements have proved to be

one of the most difficult of all field tests. The probable reason for this difficulty has been the necessity for depending upon the operator's skill and judgment in any test procedure that could be evolved.

As stated previously, the milliwatt has been adapted as the standard reference level for this type of measurement, the criterion being the power level expressed in decibels above 1 milliwatt necessary at the input of the receiver to obtain a minimum discernible signal above the noise on an A-type oscilloscope connected to the output. It has been found that a figure of −90 decibels below 1 milliwatt would indicate a fairly satisfactory receiver in a typical 5-megacycle-bandwidth airborne-radar system.

Many attempts were made to evolve a testing procedure that would be applicable for field use and still

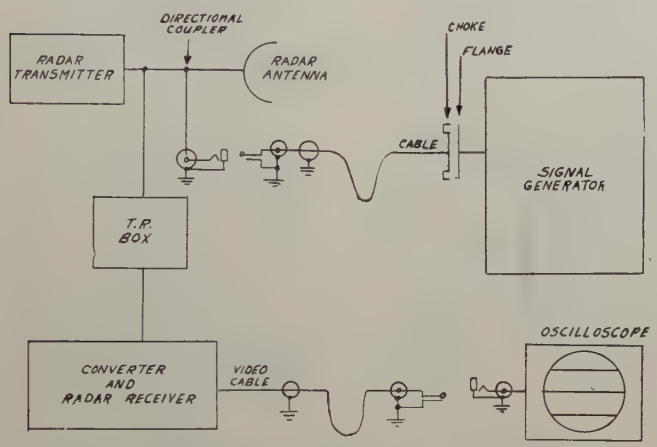

Fig. 13—Connections for making receiver sensitivity test.

give consistent results. The procedure finally accepted, while not being completely satisfactory, is indicated by the block diagram in Fig. 13 and consists of the following:

The signal generator is connected to the system through a cable and a directional coupler, and the signal generator is adjusted to give a frequency-modulated signal of approximately ±10 megacycles about the frequency of the transmitter. The peak energy level of the signal is established at 1 milliwatt, and provisions are made in the instrument for synchronizing the sweep of the frequency-modulated signal with the transmitted pulse from the radar system. A fast-sweep oscilloscope, such as a synchroscope, is connected to the video output of the receiver, and its sweep is also synchronized with the transmitted pulse. The receiver is then manually tuned to the transmitter frequency and its gain adjusted to obtain a deflection from the noise on the oscilloscope which is approximately 25 per cent of its saturation value. The signal will appear on the screen of the scope as a series of pulses, the shape of which is a function of the band-pass characteristic of the receiver and the time duration of which is a function of the time required for the frequency of the signal to vary over its ±10-megacycle range. Fig. 14 illustrates a train of responses. Provision is usually made in the signal generator to vary the phase of the signal, i.e., the time duration between the start of the transmitter pulse and the start of the signal, so that the signal can be phased beyond the recovery time of the receiving system.

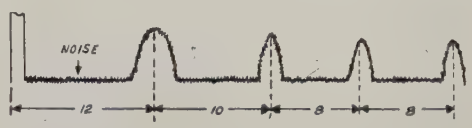

Fig. 14—Receiver-response characteristics, class-A oscilloscope presentation.

The calibrated variable attenuators on the signal generator are then increased, at the same time that the phase control is manipulated to vary the position of the signal about a given point, until the signal is just barely visible in the noise on the oscilloscope. The attenuator values are then noted, and the total attenuation is determined by the addition of the different losses in the measuring system. The resultant figure is an indication of the receiver sensitivity expressed in decibels below 1 milliwatt for a minimum discernible signal. An example of a typical receiver sensitivity measurement is as follows:

Signal-generator attenuator reading	63.5 decibels below 1 milliwatt
Cable	2.8 decibels
Directional coupler	25.2 decibels
Total	91.5 decibels below 1 milliwatt

This total indicates that the sensitivity of the receiver is such that it is necessary that a signal intensity of −91.5 decibels below 1 milliwatt be available at the input to the receiver in order that a minimum discernible signal occur at the output.

The automatic-frequency-control operation can be checked very simply at this point by increasing the signal generator output until the signal is about twice the noise amplitude. After it is ascertained that the receiver is manually tuned so that it is at an optimum sensitivity and bandwidth point, the receiver is then switched to automatic-frequency-control operation. If the image on the oscilloscope remains stationary, the automatic-frequency-control circuit is adjusted satisfactorily. However, if the signal changes in phase or amplitude, the circuit is adjusted for some frequency other than optimum, and can easily be readjusted at this point to obtain the required performance characteristics.

The errors which occur in this type of measurement are relatively large, primarily because of the fact that the basis of measurement depends upon the vision and judgment of the operator in determining at what point the signal is just "barely visible." It has been found that readings between two skilled operators may vary as much as 3 decibels and at best are seldom better than 1 decibel from absolute agreement on the same radar system and using the same instrument.

A second source of error exists in the signal generator which, because of its complexity, is relatively less accurate than the power meter. An optimistic figure for

the probable accuracy of the signal generator and its associated connecting cable is ±2.0 decibels, disregarding the aging effect in the cable.

It may be concluded, therefore, that the best probable agreement between receiver sensitivity measurements made on the same microwave radar set will not be much better than ±3.0 decibels. Of course, it is true that, under laboratory conditions and using special laboratory test equipment, this accuracy figure can be greatly improved. However, the complexity and size of the equipment necessary, together with the complexity of the procedures involved, prohibit application for field use.

An attempt was made to divide this over-all receiver test into a converter, radio-frequency, and video test, respectively. It was found that, in order to simplify the

Fig. 15—Receiver-recovery characteristics, class-A oscilloscope pattern.

testing procedure for this type of tests, it was necessary to add a number of test-point jacks which necessitated an undesirable increase in size and weight of the basic radar equipment.

A very simple test of the recovery time of the receiving system can be made with the previously indicated setup for receiver sensitivity. The signal generator is adjusted for pulsed operation at the transmitter frequency, and its signal is adjusted to obtain about a 3 to 1 ratio between signal and noise. If the signal generator is unsynchronized from the radar set by an appropriate control on its panel, a pattern will appear on the oscilloscope, as shown in Fig. 15 due to a combination of the unsynchronous pattern, and the recovery time of the system.

It was planned that the new lightweight equipment would be used primarily at the airplane for making tests in determining what component of the system (i.e. transmitter, receiver, indicator, synchronizer, etc.) was in need of maintenance, and, if a simple adjustment could not testify the trouble, the faulty component was to be removed to the radar shack where it would be thoroughly "gone over." Reports of extremely adverse operating conditions, however, indicated the need for a very simple and lightweight instrument that could be used to indicate the over-all performance condition of a radar system. This instrument could then check the operation of a system before a flight to ascertain its condition.

The echo box seemed to fit this requirement most favorably, and it was found to be one of the most useful of all of the instruments designed to be used at the airplane.

To use the echo box for an over-all test, it is connected to the system through a cable and directional coupler in the transmission line. The instrument is then tuned to the frequency of the transmitter by observing a peak in the transmission-current indicator on the box. The receiver is then manually tuned to the signal from the echo box, and the resulting ringtime is observed on the radar indicator and determined accurately as to its duration by a range marker or gate if the radar system is so equipped. Fig. 16 shows ringtime patterns of three types of indicator presentations. It will be noted that the flat top on the class-A presentation of the transmitted pulse is due to receiver satura-

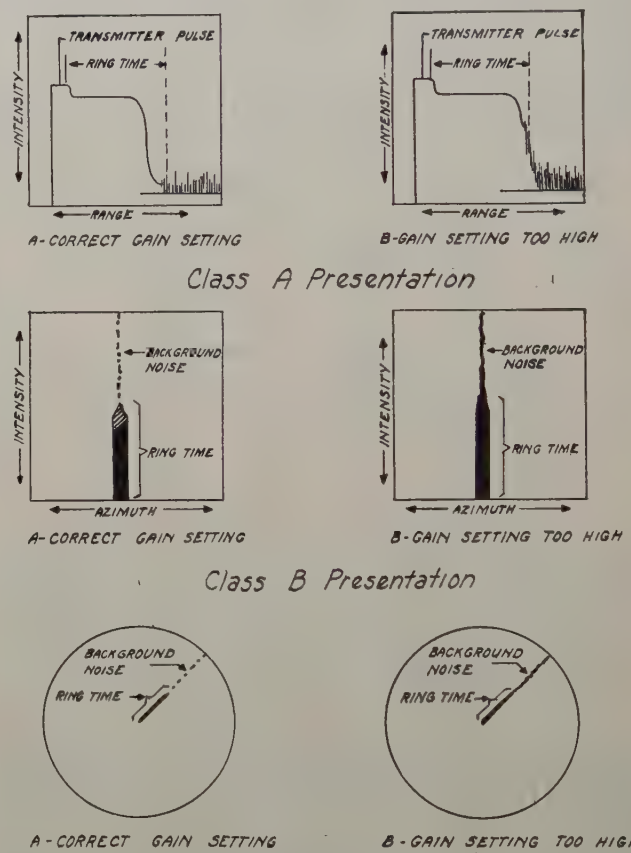

Fig. 16—Ringtime patterns.

tion on relatively strong signal levels. The indicated trace then slopes downward into the noise, more commonly known in radar terminology as "grass."

This instrument is also capable of making numerous other tests such as determination of the frequency spectrum of the transmitted pulse, determination of frequency pulling of the oscillator due to defective rotary joints in the transmission line, and adjustment of the transmit-receive and antitransmit-receive components. For spectrum analysis the echo box is tuned to the transmitter frequency and simultaneous readings are taken of the transmission current in the echo box and indicated frequency for small intervals about the frequency of the transmitter. Fig. 17 shows a spectrum pattern as determined by an echo box. Frequency-pulling measurement, made possible by the high Q, is determined by tuning the echo box to the transmitter and then rotating the antenna or manipulating the suspected part of

the transmission line until a decrease in ringtime is noted. Then, by retuning the echo box to obtain the initial ringtime, the amount of pulling is indicated by the extent of the frequency retuning required.

This instrument is also very convenient for adjusting the transmit-receive and antitransmit-receive cavities. Since the ringtime is a function of both transmitter power and receiver sensitivity, it is possible to obtain an optimum setting from an over-all performance standpoint by merely adjusting the transmit-receive

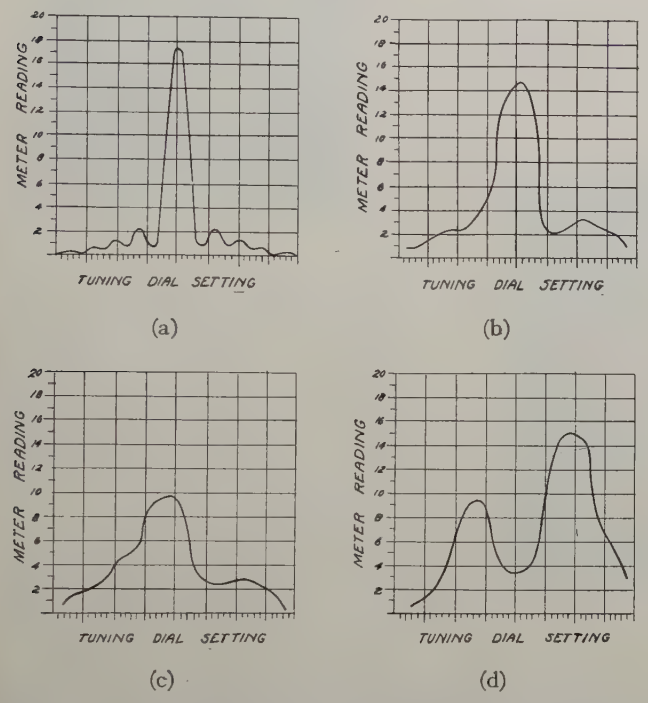

Fig. 17—Spectrum analysis. (a) Good spectrum; (b) fair spectrum; (c) poor spectrum; (d) poor spectrum.

cavity for maximum ringtime. Fig. 18 illustrates the method by which such an instrument can be used to detect slow recovery time in a radar receiver. Fig. 19 illustrates a method of detecting magnetron double-moding in the transmitter.

There have been many divergent opinions on the relative merits of making a standing-wave test on the transmission line of a microwave radar system. No attempt will be made to justify any of these opinions in this paper; instead, a summary of the different methods used will be presented. Probably the simplest method for determining if there are serious reflections in a relatively high-powered radar set (40 watts average power) is to place the bare hand on the metal coaxial line or wave guide. If the temperature of this line is above ambient, it is fairly certain that reflections exist in the line. In contrast to this method is the common slotted-line test using a traveling probe and crystal detector which will only give accuracies of approximately ± 10 per cent unless extreme care is taken in the design and fabrication of the instrument.

The bidirectional-coupler method is probably the simplest and can be made the most accurate of any type of standing-wave detector. This method utilizes two directional couplers in the transmission line, placed in opposition to each other so that one samples only the direct energy (energy directed towards the antenna)

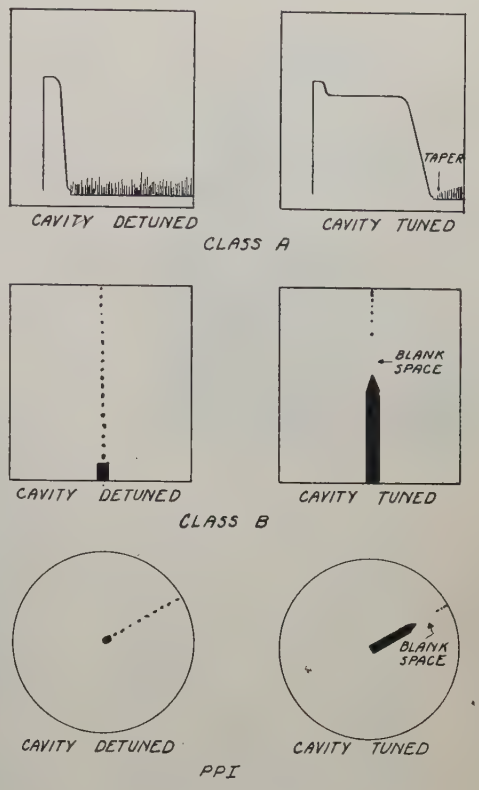

Fig. 18—Patterns from slow receiver recovery.

and the other samples only the reflected energy. A comparison of the two values will given an answer that can be converted directly into a standing-wave ratio. The

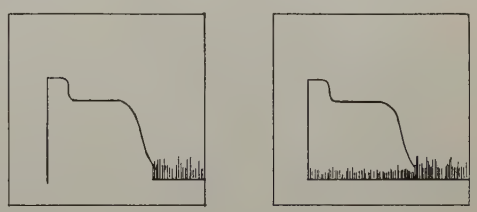

Fig. 19—Multiple-moding trace. (a) Normal moding; (b) multiple moding.

usual type of directional coupler which is designed specifically for transmitter and receiver tests does not have the necessary directivity (back-to-front ratio) and therefore will give errors as high as 20 per cent in making standing-wave tests. However, a pair of directional couplers can be designed that will give accuracies of ± 5 per cent in making these measurements.

On some of the precision-bombing radar sets, it is necessary to make allowance for the delay of the signal as it is amplified by the receiver circuits in order to adjust the range circuits accurately. It is required that this delay be determined with an objective accuracy of something better than ± 0.05 microsecond, and it has to be determined at the airplane in order to obtain the required accuracy. One of the most straightforward

methods for doing this is to locate a natural or artificial radar target, such as a water tower, smoke stack, or corner reflector, somewhere within a radius of 3 to 5 miles from a convenient parking place for the airplane on an airfield. Surveyors' instruments are then used to determine the exact distance between this target and the parking place for the airplane. The particular target is then located on the radar indicator, and its range circuit is adjusted so that it agrees with the range determined by the surveyors' instruments. This method will give an accuracy of approximately ± 0.1 microsecond. Among the many disadvantages of this method are difficulty in locating a satisfactory target and the necessity for exactly positioning the aircraft whenever adjustment is required. On those airfields upon which many planes are parked, it is almost impossible to provide sufficient parking places aligned with the necessary calibrated target in order to do the calibrating job on all of the planes in a reasonable length of time.

An alternate method for performing this function utilizes the leakage of the transmitted pulse through the transmit-receive cavity. The output of the video amplifier is connected to one vertical plate of an oscilloscope with an extremely fast sweep (one and one half inches per microsecond) and the output of the pulser which synchronizes the sweep and range circuits is connected to the other vertical plate. The resultant wave form observed on the oscilloscope will be a composite of the output from the two units, and if the sweep of the oscilloscope is initiated by the same pulse that initiates the transmitted pulse, the video output will contain the transmitted pulse delayed by an amount introduced by the receiving system. The range-synchronizing pulser delay is then adjusted until the edge of this pulse coincides with the leading edge of the transmitted pulse *as observed*. This procedure can result in accuracies of ± 0.15 microsecond.

The precision range calibrator is utilized for adjusting the absolute value of the range markers and tracking rates in precision-bombing radar sets. In this procedure the range unit of the system is synchronized from the calibrator and the marker output of the calibrator is introduced into the video channel of the receiver and indicator. The first marker from the calibrator is adjusted to coincide with the transmitted pulse by means of the phasing control on the calibrator. An artificial bombing problem is then inserted into the computor of the system, and the position of the release marked "pulse" is adjusted to coincide with the correct marker pulse. The tracking-rate circuits are checked by inserting an artificial tracking pulse to intercept a given number of marker pulses. A stop watch is provided on the calibrator for that purpose.

A rather large number of those who have been involved in the radar program have been under the impression that the best way to maintain a radar set at its optimum operating efficiency was to select a natural target a reasonable distance from the location of the radar and to use the reception from that target as a criterion of the performance of the system. It is believed that a rebuttal of that argument would be a fitting conclusion for this paper.

The use of standard echo from a permanent target is probably the simplest method for checking a radar set, and because of this fact it became one of the most popular. However, it can be proved that the strength of the returning signal is far from constant and varies considerably with different atmospheric conditions, frequency of the radar, and slight movements of the target or radar.

A target never reflects energy from a single point. The resultant reflection is a composite of all of the small reflections from each of the variously oriented surfaces and corners of the target. Since the distance between the radar and these various reflecting surfaces is different for each surface, a slight change in position as small as $\frac{1}{2}$ inch between the radar and target will change the phase relationships between them and can result in changes of signal strength amounting to 10 to 20 decibels. For this same reason the target is also frequency sensitive, and a drift of only a few megacycles can give the same amount of variation. Thus, a slight variation in either the frequency of the radar transmitter or the range of the target enormously increases or decreases the signal strength from the kinds of targets ordinarily considered as standard.

Probably the most variable factor influencing echo strength is atmospheric conditions. On the average, temperature and humidity gradients in the atmosphere are such as to bend the radar radiation earthward and to permit observation of targets slightly beyond the optical horizon. However, these variations are extremely variable since they depend upon a changing meteorological picture. At times the radiation pattern is bent strongly upward and thus rapidly dissipated. Signals are then weak, and the maximum radar range is short. At other times the pattern is bent downwards, and a duct is formed between the earth's surface and the refracting layer of atmosphere. Radiation is then propagated in what may be thought of as a two-dimensional wave guide, and in these instances, the range at which targets may be detected increases enormously.

It can be reasoned, therefore, that a combination of target variation and atmospheric variation will prohibit the use of any one target or group of targets as a criterion for the performance of a radar system.

Acknowledgment

The field-type instruments, equipments, and measuring techniques described in this paper are the result of the work of many individuals working in both government-sponsored and private laboratories during the recent war years. It is rather difficult to give individual credit, as much credit is due. However, it is fitting to say that the advancement of the science of microwave measurements owes much to many who, in a concerted effort, have rendered to us the instruments and techniques outlined in this article.

Contributors to Waves and Electrons Section

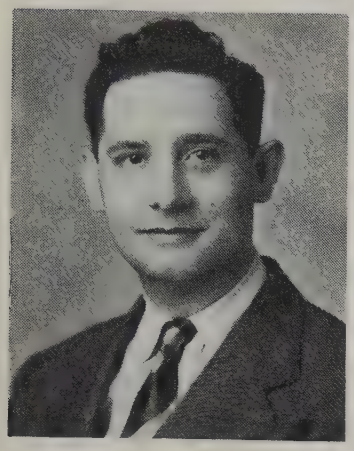

E. A. Blasi

E. A. Blasi (A'36–SM'46) was born at New Rochelle, New York, in 1913. He received the B.S. degree in electrical engineering from New York University in 1934. From 1934 to 1940 he was engaged in radio receiver design with the Radio Receptor Company and the General Electric Company. From 1940 to 1942 he was a test engineer in power-distribution networks with the Westchester Lighting Company. He joined the Radar Laboratory at Wright Field in 1942 and was commissioned in the United States Army in the fall of the same year. During his stay in the Army, he was assigned to the Radar Laboratory and was in charge of the research and development of microwave test equipment for airborne radar bombing, gun-laying, and search systems. Recently he has been appointed chief of the detail design unit, Aircraft Radiation Laboratory, Wright Field, Dayton, Ohio.

❖

John E. Gorham (A'42-M'46) was born on November 11, 1911 at Moline, Illinois. He received the B.S. and M.S. degrees in physics at Iowa State College in 1933 and 1934, respectively, and the Ph.D. degree in physics from Columbia University in 1938. While at Columbia he was a teaching assistant, and a postdoctorate research assistant for one year.

In 1939 he was associated with the Belmont Radio Company as production test-equipment engineer, and in early 1940 with the Continental X-Ray Corporation as electrical design engineer. Since 1940 Dr. Gorham has been associated with the Signal Corps Engineering Laboratories, and at various times has been engineer in charge of radar transmitter and modulator development and vacuum-tube development. At present he is chief of the Thermionics Branch, Evans Signal Laboratory. He was recently awarded the War Department Medal for Exceptional Civilian Service.

Dr. Gorham is a member of the American Physical Society, Sigma Xi, Phi Kappa Phi, and Pi Mu Epsilon.

John E. Gorham

❖

Franklin F. Offner

Franklin F. Offner (A'36–SM'46) was born at Chicago, Illinois, on April 8, 1911. He received his B. Chem. degree from Cornell University in 1933; his M.S. degree from California Institute of Technology in 1934; and his Ph.D. in biophysics from the University of Chicago in 1938. From 1935 to 1938, he was research assistant at the University of Chicago. From 1939 to the present date he has been president and chief engineer of Offner Electronics Inc. He is a member of Sigma Xi.

❖

Joseph M. Pettit (S'39–A'40–M'45–SM '46) was born on July 15, 1916, at Rochester, Minnesota. He received the B.S. degree in 1938 from the University of California, the degree of engineer in 1940 from Stanford University, and the Ph.D. degree in 1942 from the same institution. From 1938 to 1940 Dr. Pettit was teaching and research assistant in electrical engineering at Stanford University. From 1940 to 1942 he was instructor in electrical engineering at the University of California, and at the same time was a research associate in electrical engineering at Stanford University, in charge of a project under the National Defense Research Committee.

For the period 1942 through 1945, Dr. Pettit was on the staff of the Radio Research Laboratory, which operated under Harvard University in co-operation with the Office of Scientific Research and Development. He served progressively as receiver development engineer, group leader, and assistant executive engineer. During 1944, Dr. Pettit served in India and China as a technical observer

Joseph M. Pettit

with the Twentieth Air Force, and in 1945 he was in England as associate technical director of ABL-15, a laboratory associated with the Radio Research Laboratory. In 1945, he became supervising engineer at Airborne Instruments Laboratory, Inc., Mineola, N. Y., in charge of receiver development. In 1947 he returned to Stamford University as acting associate professor.

Dr. Pettit is a member of the American Institute of Electrical Engineers, Sigma Xi, Tau Beta Pi, and Eta Kappa Nu.

❖

Gerald C. Schutz (M'46) was born on September 15, 1917, at Chicago, Illinois. He attended evening sessions at the Armour Institute of Technology and completed his undergraduate work at the University of Illinois, receiving the B.S. degree in electrical engineering in February, 1942.

Mr. Schutz has been associated with the Aircraft Radio Laboratory at Wright Field since February of 1942, serving first as a design engineer on radar transmitters and later as the assistant chief of the radar test equipment unit. He is now chief of the electronics application unit of the Aircraft Radiation Laboratory, Wright Field, Dayton, Ohio.

Mr. Schutz is a member of Tau Beta Pi

❖

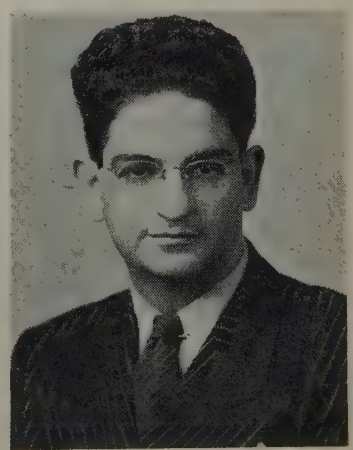

Gerald C. Schutz

Abstracts and References

Prepared by the National Physical Laboratory, Teddington, England, Published by Arrangement with the Department of Scientific and Industrial Research, England, and *Wireless Engineer*, London, England.

NOTE: The Institute of Radio Engineers does not have available copies of the publications mentioned in these pages, nor does it have reprints of the articles abstracted. Correspondence regarding these articles and requests for their procurement should be addressed to the individual publications and not to the I.R.E.

The number at the upper left of each Abstract is its Universal Decimal Classification number and is not to be confused with the Decimal Classification used by the United States National Bureau of Standards. The number in heavy type at the top right is the serial number of the Abstract.

The Annual Index to these Abstracts and References, covering those published from January, 1946, through December, 1946, may be obtained for 2s. 8d., postage included, from the Wireless Engineer, Dorset House, Stamford St., London S. E., England.

ACOUSTICS AND AUDIO FREQUENCIES

534 327

Problems of Modern Acoustics. Noise and Vibration—P. Chevasse. (*Onde Élec.*, vol. 26, pp. 274–287; July, 1946.) A review of the subject covering architectural, physiological, and musical acoustics; electroacoustics and supersonics. The definition of intensity, in accordance with the Weber-Fechner law, leads to the units decibel, phon, son, pal, and vibor based on the frequency curves of equal aural or tactile sensation. Apparatus which gives an objective indication of sound level has been constructed using microphones and an amplifier with a frequency weighting circuit corresponding to the response of the ear.

534.212:534.321.9 328

The Directional Characteristics for [Supersonic Radiation] of a Free-Edge Disk Mounted in a Flat Baffle or in a Parabolic Horn—F. H. Slaymaker, W. F. Meeker, and L. L. Merrill. (*Jour. Acous. Soc. Amer.*, vol. 18, pp. 355–370; October, 1946.) Full paper, summary of which was noted in 3512 of January.

534.231 329

Ray Computation for Non-Uniform Fields—J. S. Saby and W. L. Nyborg. (*Jour. Acous. Soc. Amer.*, vol. 18, pp. 316–322; October, 1946.) A formula is derived which simplifies computation and ray tracing. The method is particularly useful in the study of the propagation of supersonic waves in the atmosphere.

534.24:551.510.52 330

Reflection of Sound Signals in the Troposphere—G. W. Gilman, H. B. Coxhead, and F. H. Willis. (*Jour. Acous. Soc. Amer.*, vol. 18, pp. 274–283; October, 1946.) Attempts have been made to detect nonhomogeneities in the first few hundred feet of the atmosphere by vertical propagation of sound waves with a low-power set which has been named the sodar. Periods of strong temperature inversion, strong sodar displays, and strong microwave fading tended to coincide, but it is significant that sound echoes were often very strong when there was no meteorological reason to expect them. The sodar seems to have confirmed the existence of nonhomogeneities which it would be difficult or impossible to observe by conventional methods.

534.321.9:621.395.613.5 331

An Ultrasonic Condenser Microphone—T. H. Bonn. (*Jour. Acous. Soc. Amer.*, vol. 18, pp. 496–502; October, 1946.) The microphone has over-all diameter 0.875 inch, special electrode design, and essentially constant free-field calibration of 51 decibels below 1 volt per dyne per square centimeter up to 32 kilocycles.

534.322.1 332

Analyses of the Tones of a Few Wind Instruments—F. A. Saunders. (*Jour. Acous. Soc. Amer.*, vol. 18, pp. 395–401; October, 1946.) Charts are given for clarinet, oboe, English horn, French horn, and flute, covering the whole range of each instrument.

534.612:621.396.611.21 333

A New Sound Measurement System—F. Massa. (*Communications*, vol. 26, pp. 16–17, 50; October, 1946.) Determines the absolute magnitude of sound pressures with a minimum of disturbance to free-field conditions, or conditions inside small enclosures, by means of a new design of calibrated piezoelectric substandard microphone.

534.612.4(23.03):621.395.613.5 334

On the Absolute Pressure Calibration of Condenser Microphones by the Reciprocity Method—A. L. Dimattia and F. M. Wiener. (*Jour. Acous. Soc. Amer.*, vol. 18, pp. 341–344; October, 1946.) Calibration details are given for temperatures from −25 to +40 degrees centigrade and pressures corresponding to altitudes up to 40,000 feet. The estimated accuracy is ±0.2 decibel.

534.78 335

On the Intelligibility of Bands of Speech in Noise—J. P. Egan and F. M. Wiener. (*Jour. Acous. Soc. Amer.*, vol. 18, pp. 435–441; October, 1946.) Tests were conducted with several communication systems of different bandwidth, under different conditions of masking noise, and the acoustic gain of the system expressed relative to the transmission of speech through 1 meter of air. For each system a relation between syllable articulation and level of received speech was obtained.

534.78 336

Speech Clippers for More Effective Modulation—J. W. Smith and N. H. Hale. (*Communications*, vol. 26, pp. 20–22, 25; October, 1946.) Peak-limiting methods in transmitters give high-average modulation, and improve intelligibility when static interferes with reception or frequency channels are congested. The advantages rise in proportion to the interference. The method also prevents over-modulation and, with a filter, provides a clean, sharp signal with no splatter. The carrier is fully used.

534.78 337

The Masking of Speech by Sine Waves, Square Waves, and Regular and Modulated Pulses—S. S. Stevens, J. Miller, and I. Truscott. (*Jour. Acous. Soc. Amer.*, vol. 18, pp. 418–424; October, 1946.) Optimum masking is produced when the fundamental frequency of the interfering signal lies in the range 100 to 500 cycles, the exact position depending on its other characteristics. Full paper, summary of which was noted in 3527 of January.

534.78:621.396.813 338

Effects of Amplitude Distortion upon the Intelligibility of Speech—J. C. R. Licklider. (*Jour. Acous. Soc. Amer.*, vol. 18, pp. 429–434; October, 1946.) The reduction in intelligibility depends on the type of distortion, but with peak clipping (symmetrical and asymmetrical) the reduction is almost zero. Appreciable center clipping or linear rectification has a serious effect. Tests under aircraft-noise conditions are described; and the improvement in radio communication prvoided by the noise limiting action of an audio clipping circuit is discussed. Full paper, summary of which was noted in 3524 of January.

534.781:371.3 339

Training for Voice Communication—J. W. Black and H. M. Mason. (*Jour. Acous. Soc. Amer.*, vol. 18 pp. 441–445; October, 1946.) Speech training program for telephone or radio communication in the United States Army Air Force.

534.833.082.4 340

The Measurement of Acoustic Absorption by the Stationary Wave Method—G. Sacerdote. (*Alta Frequenza*, vol. 15, pp. 68–76; June, 1946. With English, French and German summaries.) A theoretical analysis.

534.833.1 341

Absorption of Sound by Coated Porous Rubber Wallcovering Layers—C. W. Kosten. (*Jour. Acous. Soc. Amer.*, vol. 18, pp. 457–471; October, 1946.)

534.843 342

The Effect of Non-Uniform Wall Distributions of Absorbing Material on the Acoustics of Rooms—H. Feshbach and C. M. Harris. (*Jour. Acous. Soc. Amer.*, vol. 18, pp. 472–487; October, 1946.)

534.846.3 343

Acoustical Correction by Sound Diffusion—F. L. Bishop. (*Communications*, vol. 26, pp. 36–37; October, 1946.) Hemispherical sound

diffusers 12 to 36 inches in diameter were arranged in random pattern on one wall of a studio to improve its acoustical properties.

534.862 344
A Simplified Recording Transmission System [to Operate from a Microphone and into a Sound Recording Modulator]—F. L. Hopper and R. C. Moody. (*Jour. Soc. Mot. Pic. Eng.*, vol. 47, pp. 132–141; August, 1946.) Requirements were: light weight; parts easily accessible; high reliability; and low-power consumption. The instrument described has a transmission system (whose output is limited by a discharge tube), an amplifier and a noise-reduction system. Several components are marked with normal operating voltages for ease in detecting faults. Circuit diagrams are given of the amplifier and power-supply unit, together with noise-reduction-performance graphs.

621.395.61:621.385.82.029.3 345
[The Development of] a High Power Thermionic Cell using Positive Ion Emission and Operating in a Gaseous Medium—Klein. (*See* 602.)

621.395.613:621.385 346
"Vibrotron" Tube—Radio Corporation of America. (*See* 585.)

621.395.623.6 347
Development of Midget Earphones for Military Use—H. A. Pearson, A. B. Mundel, R. W. Carlisle, W. F. Knauert, and M. E. Zaret. (*Jour. Acous. Soc. Amer.*, vol. 18, pp. 348–354; October, 1946.) Full paper, summary of which was noted in 3534 of January.

621.395.625.2 348
Lateral Disc Recording at the Naval Research Laboratory—A. T. Campbell. (*Communications*, vol. 26, pp. 11–15, 50; September, 1946.) Description of Naval Research Laboratory sound-recording system facilities, of the types of record produced, and of modifications to commercial equipment used in the system. Response curves over the frequency range 50 to 10,000 cycles illustrate the performance of different types of pickup. Further improvements are expected from the use of a newly designed moving-coil pickup of which brief details are given.

621.396.33.029.3.083.7:656.2 349
Train Position Indicator—Dahl. (*See* 535.)

621.396.645.029.3 350
Modern Studio and Portable Speech Input Equipment—L. G. Killian, P. L. Tourney, and J. W. Hooper. (*Radio*, vol. 30, pp. 14–17, 31; September, 1946.) Technical details for a studio console and a three-channel remote amplifier.

AERIALS AND TRANSMISSION LINES

621.315.211.2:679.5 351
Developments in Solid Dielectric R.F Transmission Lines—R. C. Graham. (*Radio News*, vol. 36, pp. 46–48, 157; October, 1946.) A brief account of the use of polythene in various types of high-frequency cable.

621.315.211.9.052.63:621.396.44 352
Carrier-Current Communication on Air and Paper Insulated Cables—F. Lucantonio. (*Alta Frequenza*, vol. 15, pp. 77–110; June, 1946. With English, French, and German summaries.) An appreciation of the future importance of this system, using pair and quad lines, for long distance communication, and a discussion of the primary and derived characteristics—impedance, attenuation, cross-talk, and distortion, with numerical data.

621.392 353
Waves Guides—M. H. L. Pryce. (*Jour. I. E. E.* (London), part I, vol. 93, pp. 459–460; October, 1946 [summary] and part IIIA, vol. 93, pp. 33–39 [full version]; 1946.) The early development of wave guides is surveyed. Only when 10 centimeter waves were developed was the size of wave guides sufficiently convenient to encourage their development. Early guides had high losses. Wave guides became more important when 100-kilowatt magnetrons were developed, as they have low attenuation and are less liable to breakdown by sparking than concentric feeders. It is undesirable that a wave guide should propagate more than one mode, so that a rectangular guide with one side above the critical dimension for the H_{10} mode ($\lambda_0/2$) but less than the critical dimension for the H_{20} mode (λ_0), and the other side below the critical dimension for the H_{01} mode ($\lambda_0/2$) is preferred. The wave guide must be matched to the media or units which precede and follow it. The use of wave guides involves a number of auxiliary components such as couplings, bends, corners, branches, switches, rotating joints, etc., whose design involves specialized techniques.

621.392:621.396.11 354
Some Questions Connected with the Excitation and Propagation of Electromagnetic Waves in Tubes—Mandelstam. (*See* 506.)

621.392:621.396.67 355
Dielectric [Rod and Tubular] Aerials—(*Onde Élec.*, vol. 26, pp. 387–390; October, 1946.) A review of unpublished German work mainly of an empirical nature by Zinke and Mallach. The polar diagrams of both rod and tubular type aerials are considered in relation to the aerial dimensions and permittivity of the material concerned. For tubes maximum values of 68 and 0.8 wavelengths are suggested for the length and diameter respectively; the upper limit to the wall thickness is set by the need for adequate side- and back-lobe suppression. Similar considerations result in an optimum range for the diameter of a rod aerial. An example of a tapered rod aerial is briefly discussed. Finally, it is suggested that a given dielectric aerial will behave satisfactorily over a frequency range of approximately 2 to 1.

621.396.67:537.122:538.3 356
Complete Calculation of the Radiation of a Linear Sinusoidal Oscillator—É. Durand. (*Compt. Rend. Acad. Sci.* (Paris), vol. 222, pp. 68–70; January 2, 1946.) From formulas developed previously (see 392 and 393 below) it is shown that in the radiation field of an electric charge oscillating sinusoidally along a straight line, all the harmonics of the fundamental frequency are present, the amplitudes involving Bessel functions. Potential formulas are derived from which the fields can be easily deduced. With two oscillating charges of opposite sign always occupying symmetrical positions with respect to the origin, only the odd harmonics are found.

621.396.67:621.315.62 357
Dipole Reflector Insulation—J. A. Saxton and L. J. Ford. (*Wireless Eng.*, vol. 23, pp. 325–327; December, 1946.) "The effects of various insulators, used to support the ends of the parasitic aerial, were determined by measurements of the front-to-back signal ratio of a receiving-aerial system consisting of a half-wavelength dipole and a single parasitic reflector, at a wavelength of six meters. The particular insulators used in this investigation resulted in the effective length of the reflector being increased by about 20 per cent."

621.396.67:621.396.9 358
Aerials for Radar Equipment—J. A. Ratcliffe. (*Jour. I. E. E.* (London), part I, vol. 93, pp. 458–459 [summary]; October, 1946 and part IIIA, vol. 93, pp. 22–33 [full version]; 1946.) For flood-lighting at wavelengths greater than about 3 meters, an elevated horizontal dipole was usually used as a transmitter, and an elevated crossed pair of dipoles as receiver. Bearing was obtained by comparing the electromotive forces in the two receiving dipoles with a rotating goniometer coil. Elevation was determined by comparing signals in aerials at different heights. Broadside arrays with arrangements for swinging the beam rapidly by electrical means from side to side were also used to determine bearing. The satisfactory use of a common aerial for transmission and reception was one of the major achievements in radar development. An important and fundamental theorem shows that the space distribution diagram of an aerial is given by the Fourier analysis of the distribution of radiating sources over the aerial. At centimeter wavelengths, pencil beams narrow in elevation and azimuth, or fan beams narrow in one plane only (usually azimuth) become possible. Fan beams rotated about a vertical axis were extensively used for searching.

Pencil beams have usually been produced by a small radiating source situated near the focus of a parabolic mirror, with reflector and/or director elements to ensure that radiation from the source is predominantly towards the mirror.

Fan-shaped beams were produced by distorting a parabolic mirror in one section; a method originated by Chu is available for calculating the mirror shape for any required secondary-radiation pattern. Fan-shaped beams could also be produced by combining a long linear array with a specially shaped cylindrical mirror. The linear array provided a broadside of aerials which must be fed in phase. For this purpose they were coupled to a wave guide and spaced one guide-wavelength apart. A second set of aerials was placed at points midway between the first set and fed in the opposite phase to strengthen the required beam at the expense of an unwanted side beam. A slight adjustment of position is also required to avoid a highly frequency-sensitive effect due to reflections at coupling points.

621.392 359
Wave Guides [Book Review]—H. R. L. Lamont. Methuen, London, 96 pp., 6s. 3d (in Australia). (*Proc. I.R.E.* (Australia), vol. 7, p. 31; October, 1946.)

CIRCUITS AND CIRCUIT ELEMENTS

621.314.6 360
Nonlinear Commutating Reactors for Rectifiers—A. Schmidt, Jr. (*Trans. A.I.E.E.* (*Elec. Eng.*, October, 1946), vol. 65, pp. 654–656; October, 1946.) A commutating reactor is used to "drag out" the anode current, i.e., to maintain it at a low value for a sufficient period just before the end of commutation, in order, substantially to reduce residual ionization and the probability of arc back.

621.314.671 361
Circuit Cushioning of Gas-Filled Grid-Controlled Rectifiers—D. V. Edwards and E. K. Smith. (*Trans. A.I.E.E.* (*Elec. Eng.*, October, 1946), vol. 65, pp. 640–643; October, 1946.) A small resistance and capacitance connected in series between the cathode and anode delays the rise of initial inverse voltage by a few microseconds, and, therefore, increases the life of the rectifier.

621.316.313.025 362
A New Design for the A.C. Network Analyzer—J. D. Ryder and W. B. Boast (*Trans. A.I.E.E.* (*Elec. Eng.*, October, 1946), vol. 65, pp. 674–680; October, 1946.) A general description is given of the analyser, which operates at 10,000 cycles using standard radio components. The cost is, therefore, much less than for previous types operating at 400 to 500 cycles. See also 31 of February (Myers and Schultz).

621.316.726.078.3:531.3 363

On the Theory of Frequency Stabilization—S. M. Rytoff, A. M. Prokhoroff, and M. E. Zhabotinski. (*Zh. Eksp. Teor. Fiz.*, vol. 15, pp. 557–571; 1945. In Russian.) In all investigations so far published on the operation of a tube oscillator containing a stabilizing element, simplifying assumptions are made regarding the linearity of the system under consideration. There are strong reasons to believe that good results can be obtained by using rigorous methods based on the Poincaré-Lyapunoff theory, although this is only applicable to slightly nonlinear systems, i.e., to systems with a small parameter μ determining the deviation of the system from linearity.

Accordingly, the operation of a pull-in system consisting of a tube oscillator inductively coupled to an LCR circuit (Fig. 1) is discussed from the standpoint of the theory. The properties of the LCR circuit necessary for it to act as a "quartz" stabilizer are determined and a definition of stability is given.

The operation of pull-in crystal-controlled oscillators with a capacitive coupling (Fig. 3, bottom) and of Pierce's oscillator (Fig. 3, top) is then considered, and equations (11) and (17) are derived for the two systems, respectively; an analysis of the first system only is given. A periodic solution of equations (17) is found and its stability investigated. Formulas (24) and (26) determining the variation of the amplitude and of the frequency, respectively, are derived, and it is shown that in the absence of anode reaction and grid current the stabilization makes the frequency of oscillations independent of the tube parameters apart from second order effects. A numerical example of the calculation of the oscillation frequency is added. See also 377 below.

621.317.373 364

Phase Detectors: Some Theoretical and Practical Aspects—Farren. (*See* 474.)

621.318.3/.4].042:621.396 365

Coils, Cores, and Magnets: Part 1. — Magnetic Design Factors of Modern Radio Components—H. W. Schendel. (*Radio Craft*, vol. 18, pp. 30–31, 47; October, 1946.)

621.318.4:538.12 366

Effective Impedance of a Sphere in a Magnetic Field—T. S. E. Thomas. (*Wireless Eng.*, vol. 23, pp. 322–324; December, 1946.) "A conducting sphere in a uniform magnetic field may be regarded as being equivalent to a single-turn coil of the same diameter. Formulas are given for (a) the equivalent resistance and inductance of the coil. (b) the change in inductance and resistance of a solenoid when a sphere is placed at its center, (c) the heat dissipated in a sphere in a uniform alternating magnetic field."

621.318.4.011.3 367

Calculating the Inductance of Universal-Wound Coils—A. W. Simon. (*Radio*, vol. 30, pp. 18, 31; September, 1946.) It is required to find the number of turns to produce a given inductance. For universal-wound coils this can be done by a method based on 1464 of 1945 (Simon).

621.392:621.396.645.029.64 368

Circuits for Use with Triode Amplifiers and Oscillators Operating at U.H.F.—G. Lehmann. (*Onde Élec.*, vol. 26, pp. 357–366; October, 1946.) A general paper in which the desirable electrical features of cavities and coaxial line derivatives are analyzed. The design principles for the triode tube itself were discussed in an earlier paper (3821 of January). In the amplifier application the effects of the Q and impedance of the cavities on operation are considered, neglecting the effect of intercavity coupling via the grid screen. It is concluded that these circuit parameters should be high in the case of the anode (output) circuit, and low for the cathode (input) circuit. Possible ways of neutralizing the tube are considered in relation to the design of power amplifiers; experimental arrangements are outlined for achieving neutralization empirically. The circuit conditions necessary to ensure satisfactory operation of ultra-high-frequency triode oscillators are considered. It is established that, for maximum energy dissipation at a fixed frequency in a given load, four independent adjustments are necessary and sufficient. One of these determines the operating frequency, the second, the impedance match of the load; the third and fourth fix the real and imaginary components of the transfer impedance from the anode to the cathode cavity. Means of making these adjustments in practice are discussed; the common use of an internal capacitive-type coupling between the cavities is criticised. Finally the power output possibilities of triodes in the wavelength range 10 to 300 centimeters are summarized.

621.392.051 369

Conditions for Transfer of Maximum Power—H. E. Ellithorn. (*Communications*, vol. 26, pp. 26–28, 35; October, 1946.)

621.392.51:534.1 370

Violation of the Reciprocity Theorem in Linear Passive Electromechanical Systems—E. M. McMillan. (*Jour. Acous. Soc. Amer.*, vol. 18, pp. 344–347; October, 1946.) It is shown by an energy argument that the theorem of reciprocity is satisfied by crystal or electrostatic transducers in both magnitude and sign, but in the case of magnetic or electrodynamic transducers it is satisfied only in magnitude. By combining these two types, systems can be constructed that violate reciprocity in magnitude.

621.394/.397].645.34 371

Radio Design Work Sheet No. 53: Graphics of Negative Feedback in Cascade—(*Radio*, vol. 30, pp. 17–18; October, 1946.)

621.394/.397].645.34 372

How Negative Feedback Operates—C. A. A. Wass. (*P. O. Elec. Eng. Jour.*, vol. 39, pp. 114–116; Ocotber, 1946.) Demonstration by numerical and pictorial examples of the way in which negative feedback improves amplifier performance.

621.395.645 373

Three-Channel Amplifier: a 15-W Unit with Individual Control of Each Channel—M. Contassot. (*Toute la Radio*, vol. 13, pp. 36–37; January, 1946.) A French version of 2845 of 1946.

621.395.661 374

Mica Capacitors for Carrier Telephone Systems—A. J. Christopher and J. A. Kater. (*Trans. A.I.E.E.* (*Elec. Eng.*, October, 1946), vol. 65, pp. 670–674; October, 1946.) Silvered mica capacitors are superior to the previous dry-stack type, because of their relatively simple unit construction and ease of adjustment to the very close capacitance tolerance required. Construction details and performance characteristics are given.

621.396.61:538.56:535.23 375

The Radiation Through an Aperture in a Resonator—L. Mandelstam. (*Zh. Eksp. Teor. Fiz.*, vol. 15, pp. 471–473; 1945. In Russian.) An electromagnetic field is set up inside an ideal hollow conductor with infinitely thin walls and a circular aperture whose diameter is small compared to the wavelength. The radiation through the aperture is determined by a method similar to that used by Rayleigh for diffraction at a small aperture.

The following two auxiliary problems are solved first: (a) given a flat capacitor with two infinite plates A and B at an infinite distance apart, and that plate B is infinitely thin and has a circular aperture in it, determine the additional field due to this aperture; and (b) given two ideally conducting infinitely thin plates A and B at an infinite distance apart, such that a current flows in plate A and, in the opposite direction, in plate B, and that a circular aperture is made in plate B, determine the distribution of the magnetic field.

For the main problem, it is assumed that the tangential component of the field at the point where the aperture is to be made is H_0. It is shown that the field set up by the aperture at a great distance is that of a magnetic dipole with a moment $2a^3H_0/3\pi$ where a is the radius of the aperture. Similarly, if E_1 is the normal component of the electric field at the point where the aperture is to be made, the field due to the aperture is that of an electric dipole with a moment $a^3 E_0/3\pi$.

621.396.611 376

Electromagnetic Cavities—J. Bernier. (*Onde Élect.*, vol. 26, pp. 305–317; August–September, 1946.) A mathematical paper. The natural modes of oscillation of cavities having infinitely conducting walls are first considered, particular attention being paid to resonators having mathematically convenient forms. An expression for the perturbation of the natural frequency of the resonator due to a small change in its shape is derived by two methods. The damping and frequency shift introduced by assigning a finite conductivity to the walls are determined. The fact that practical resonators have Q values lower than the theoretical is attributed either to oxidation or to the nature of the top few microns of the cavity walls. Finally, the behavior of cavities under conditions of forced oscillation is examined, and the nature of "lumped value" equivalent circuits discussed.

621.396.611:531.3 377

On a Special Case of Systems with Two Degrees of Freedom—M. E. Zhabotinski. (*Zh. Eksp. Teor. Fiz.*, vol. 15, pp. 573–585; 1945. In Russian.) If approximate methods are used for examining systems with two degrees of freedom, system equations are derived with small terms of the same (first) order of smallness as the small parameter μ. If, however, exact methods based on the Poincaré-Lyapuno theory are applied, terms of higher orders of smallness may appear in the equations. In the present paper an analysis is made of the case when terms of any arbitrary orders may appear together with terms of the first order. Methods are indicated for finding a periodic solution of the system equations (1) for different cases, for example, when the system is operated with or without a stabilizing element. and conditions of stability are derived. It is shown that the calculations involved in the use of the exact methods are no more complicated than in the case of an equation with terms of the first order of smallness only. See also 363 above.

621.396.611:621.317.79.029.64 378

High Q Resonant Cavities for Microwave Testing—I. G. Wilson, C. W. Schramm, and J. P. Kinzer. (*Bell Sys. Tech. Jour.*, vol. 25, pp. 408–434; July, 1946.) An engineering approach to the design of tunable cylindrical cavities resonant in the $TE01n$ mode which gives the maximum Q in a given volume. The dimensions, to give as few unwanted modes as possible, may be determined from charts. The suppression of the unwanted modes, particularly the $TM11n$ mode which has the same frequency as the required mode, is discussed. Methods of coupling a $TE10$ wave guide to the

cavity are given in tabular form. As a practical example an outline electrocoil design for an echo box is described and the mechanical requirements outlined. The uses of such a box for radar testing are indicated.

621.396.611.018.41 379
Theory and Measurements of the Natural Frequencies of Various Kinds of Resonant Cavities [Thesis]—J. J. Verschuur. Drukkerij Waltman (A. J. Mulder), Delft, 1946. A mathematical and experimental investigation of the natural frequencies of symmetrical and asymmetrical cavity resonators, with particular reference to symmetrical "re-entrant" types (i.e., the space between two concentric cylinders). A method of analysis in terms of an equivalent circuit has proved to be much simpler than previous analyses, and has given theoretical values of resonant frequency within 5 per cent of measured values. The measurements were made over the range 35 to 200 centimeters. A long summary in English is given (pp. 114–115) and a bibliography of 58 items is appended.

621.396.611.1 380
Mathematical Treatment of n Directly Coupled H.F. Oscillatory Circuits—H. Behling. (*Funktech. Mh.*, pp. 75–80; May, 1940.) A general method is developed for obtaining the selectivity curve of any number n of directly coupled circuits and this is applied specially to the case of $n=4$. Selectivity and amplification formulas are then given for $n=2$, 3, 6. The selectivity curves for $n=2$, 4, 6 present marked similarities, as also do those for $n=3$ and 5. Numerical calculations are given for a 4-circuit filter.

621.396.611.21:537.228.1:534.13 381
General Dynamical Considerations Applied to Piezoelectric Oscillations of a Crystal in an Electrical Circuit—W. F. G. Swann. (*Jour. Frank. Inst.*, vol. 242, pp. 167–195; September, 1946.) A mathematical paper dealing with forced and free oscillations in an X-cut crystal. Electrical and mechanical damping effects are taken into account, but for certain solutions of practical interest, internal mechanical damping is neglected. An expression is developed for the mechanical displacement at the two ends of the crystal under resonant conditions. When the frequency of the applied electromotive force is equal to the lowest natural frequency of the crystal (or to an odd harmonic thereof) the displacements at the two ends are equal, even when the media surrounding the two ends of the crystal are different. See also 3244 of 1946 (Ekstein).

621.396.615.1 382
Response of Oscillator to External E.M.F.—D. G. Tucker: R. E. Burgess. (*Wireless Engr.*, vol. 23, pp. 341–342; December, 1946.) Correspondence on 3216 of 1946. Tucker suggests that "it is not possible to consider the effective 'half-power' bandwidth of the system, nor to express it in terms of a linear tuned circuit." Burgess in reply amplifies his treatment and reasserts its validity for the conditions he specified.

621.396.62 383
Design and Application of Squelch Circuits—Delanoy. (*See* 519.)

621.396.62 384
Notes on the Design of Squelch Circuits—Delanoy. (*See* 520.)

621.396.645.014.332 385
Class-B Amplifiers—A. S. G. Gladwin. (*Wireless Eng.*, vol. 23, p. 343; December, 1946.) Extension of the method of 3563 of January (Sturley) to the case when the grid excitation is of arbitrary waveform.

621.396.645.211 386
Improved Analysis of the RC Amplifier—J. Roorda, Jr. (*Radio*, vol. 30, pp. 15–16; October, 1946.) New design formulas are developed rigorously, whereby analysis of resistance-coupled amplifier performance is simplified, and an equivalent circuit holding at all frequencies of the amplifier is obtained. A numerical example is given.

621.397.621 387
Deflector Coil Coupling—Cocking. (*See* 558.)

GENERAL PHYSICS

530.13:530.12 388
A Relativistic Misconception—C. R. Eddy. (*Science*, vol. 104, pp. 303–304; September 27, 1946.) "The idea that matter and energy are interconvertible is due to a misunderstanding of Einstein's equation $E=mc^2$. . . . In calculating the kinetic energy released or consumed by nuclear reactions from the formula $E=(\Delta m)c^2$, the rest masses and not the actual masses must be used in computing Δm." The total actual mass of the system is invariant.

530.145.63 389
On Dirac's Theory of Quantum Electrodynamics: the Interaction of an Electron and a Radiation Field—C. J. Eliezer. (*Proc. Roy. Soc. A*, vol. 187, pp. 197–219; October 22, 1946.)

531.18:531.15 390
Is Rotation Relative, or Absolute?—B. A. Hunn and D. A. Bell. (*Wireless Eng.*, vol. 23, pp. 342–343; December, 1946.) Correspondence on 3564 of January. (G. W. O. H.)

532.13:537.29 391
The Effect of an Electric Field on the Viscosity of Liquids—E. N. da C. Andrade and C. Dodd. (*Proc. Roy. Soc. A*, vol. 187, pp. 296–337; November 5, 1946.) A description of apparatus for measuring this effect, in which the liquid runs in a narrow channel between plane-metal boundaries which can be used as electrodes.

Measurements on polar and nonpolar liquids are described and the observations are explained theoretically.

537.122:538.3 392
Calculation of the Field Due to a Moving Electric Charge—E. Durand. (*Compt. Rend. Acad. Sci.* (Paris), vol. 219, pp. 510–513; November 20, 1944.) It is shown that the method of calculation given by R. Reulos (4374 of 1937, *Cah. Phys.* (Paris), pp. 1–14, 1941), which seems to differ essentially from the classical treatment, is in reality completely equivalent to it. See also 393 below and 356 above.

537.122:538.3 393
Calculation of the Field Due to a Moving Electric Charge—É. Durand. (*Compt. Rend. Acad. Sci.* (Paris), vol. 219, pp. 584–587; December, 1944.) The potential formulas previously given (see 392 above) are applied to the case where the trajectory remains within a spatially limited domain, the potentials being calculated outside this domain. A formula is derived for the radiation of the particle. Simplified potential formulas are given for small distances from the domain. For two charges symmetrical with respect to the origin the formulas yield the classical results for the dipolar oscillator.

537.291 394
Volt-Ampere Characteristics for the Flow of Ions or Electrons between Concentric Cylinders in Gases at Atmospheric Pressure—C. W. Rice. (*Phys. Rev.*, vol. 70, pp. 228–229; August 1–15, 1946.)

537.533.73 395
Refraction Effects in Electron Diffraction—J. M. Cowley and A. L. G. Rees. (*Nature* (London), vol. 158, pp. 550–551; October 19, 1946.) Study of diffraction patterns of magnesium and cadmium oxide smokes with the R.C.A.-type electron microscope. Results are explained in terms of variations of inner potential. See also 3697 of 1945 (Sturkey and Frevel).

538.3 396
Stresses in Magnetic and Electric Fields—G. W. O. H. (*Wireless Eng.*, vol. 23, pp. 319–321; December, 1946.) A critical theoretical discussion setting forth the discrepancies between the results arrived at by various workers.

538.566 397
The Group Velocity in a Crystal Lattice—L. Mandelstam. (*Zh. Eksp. Teor. Fiz.*, vol. 15, no. 9, pp. 475–478; 1945. In Russian.) The group and phase velocities of waves propagated in a continuous medium have the same direction, and the group velocity is in this case said to be positive. There are however, real media in which the velocities have opposite directions, i.e., the group velocity is negative. An analysis is made of the propagation of waves in a crystal lattice and it is shown that the group velocity $d\omega/dk$ is in this case negative (ω is the frequency and k the wave number). It is also shown that the velocity W of the propagation of energy, as defined by Rayleigh, is in this case equal to the group velocity. It is pointed out that the crystal lattice is a limiting case of a continuous medium with a periodically variable parameter, such as density, dielectric constant, etc. As an example the propagation of waves in the direction x, in a medium the properties of which vary only with x is briefly considered.

539.185 398
Two Kinds of Neutrons?—J. DeMent. (*Science*, vol. 104, p. 303; September 27, 1946.) The usual neutron breaks down into a proton with the emission of a β particle. Theory appears to require a second kind which would break down into a negative proton with the emission of a positive electron.

548.0:546.74:538 399
Magnetic Studies on Nickel Ions in Crystals—A. Mookherji. (*Indian Jour. Phys.*, vol. 20, pp. 9–20; February, 1946.)

GEOPHYSICAL AND EXTRATERRESTRIAL PHENOMENA

522.23:523.755 400
Scientists Explore Sun—M. G. Morrow. (*Sci. News Let.*, Washington, vol. 50, pp. 170–171; September 14, 1946.) Describes the use of a coronagraph at the High Altitude Observatory at Climax to observe continuously the solar corona.

523.165 401
An Observed Abnormal Increase in Cosmic-Ray Intensity at Lahore—H. R. Sarna and O. P. Sharma. (*Nature* (London), vol. 158, p. 550; October, 1946.) A threefold increase in directional total intensity of cosmic radiation was observed during the period July 31, to August 3, 1946.

523.7+523.854]:621.396.11 402
Extra-Tropospheric Influences on Ultra-Short-Wave Propagation—E. V. Appleton. (*Jour. I.E.E.* (London), part IIIA, vol. 93, no. 1, pp. 110–113; 1946.) The effect of the ionosphere and of radio noise of extraterrestrial origin is considered. Transient echoes from temporarily ionized scattering centers at about the level of the E layer are probably the ionization trails of meteorites. The scattering coefficient L (defined in Scott's paper 510 below) is about 100 meters at 9 megacycles, and very roughly L varies as $1/f^n$ where f is the frequency and

n is about 2. Early experimental evidence of long-distance scatter with a delay time of 15 to 25 milliseconds is now believed to be caused by waves which have been reflected by the F layer, scattered back, and then reflected again by the F layer. The limiting frequency for such scattering may be taken as 3.5 times the vertical-incidence F_2-layer critical frequency for the midpoint of the trajectory. Account must be taken of the general world morphology of F_2-layer ionization.

Galactic radio noise has been studied among others by Hey, Parsons, and Phillips (see 3599 of January and back reference) while L. A. Moxon and J. M. C. Scott have found that galactic noise power varies roughly as the square of the wavelength for frequencies above about 20 megacycles.

Solar radio noise in excess of the expected black-body intensity by a factor as great as 10^5 or 10^6 on meter wavelengths, and connected with sunspot activity, has frequently been reported recently, as in 403 below. Such noise is not appreciable at centimeter wavelengths. It is sometimes convenient to express results in terms of the "equivalent black-body temperature" of the noise source. The pioneer work in this field was done by Burgess (see 438 of 1942 and back references).

523.72:621.396.822 403

Noise During Radio Fade-Out—O. P. Ferrell. (*Terr. Magn. Atmo. Elec.*, vol. 51, p. 449; September, 1946.) A survey of observations of solar noise discussed more fully in 402 above.

523.72:621.396.822.029.62 404

Conditions of Escape of Radio-Frequency Energy from the Sun and the Stars—M. N. Saha. (*Nature* (London), vol. 158, p. 549; October 19, 1946.) The minimum frequency of electromagnetic waves that can escape from various layers of the sun, and from sunspots, is calculated from Appleton's magneto-ionic theory. It is concluded that the ordinary wave cannot escape, and that the larger sunspots are most favorable for the escape of extraordinary waves in the frequency range 10 to 200 megacycles; therefore, radio waves reaching the earth should be circularly polarized.

523.72:621.396.822.029.62 405

Abnormal Solar Radiation on 75 Megacycles—S. E. Williams and P. Hands. (*Nature* (London), vol. 158, p. 511; October 12, 1946.) Observations on the nature of solar radiation on 75 megacycles were made during periods of sunspot activity in July and August, 1946. The radiation can be roughly divided into two components, one slowly variable, and the other abruptly variable, and showing correlation with visual solar observations. Correlation between solar noise and prominence activity seems probable. Short abstract only. See also 406.

523.72:621.396.822.029.62 406

Abnormal Solar Radiation on 72 Megacycles—A. C. B. Lovell and C. J. Banwell. (*Nature* (London), vol. 158, pp. 517–518; October 12, 1946.) Experimental data on a frequency of 72.6 megacycles obtained during July and August, 1946, confirm that solar radiation on radio frequencies can be as much as 10^8 times the black body value; this appears to be associated with solar flares. See also 405 above, 86 of February, and back references.

523.78:551.510.535 407

Effects on the Ionosphere at Huancayo, Peru, of the Solar Eclipse, January 25, 1944—Ledig, Jones, Giesecke, and Chernosky. (*See* 503.)

523.78:551.510.535 408

Eclipse-Effects in F_2-Layer of the Ionosphere—Wells and Shapley. (*See* 502.)

538.566.3+621.396.812 409

Observations on the Interaction of Waves in the Ionosphere, in Relation to the Gyrofrequency—Cutolo, Carlevaro, and Gherghi. (*See* 513.)

538.71 410

The Development and Applications of Airborne Magnetometers in the U.S.S.R.—A. A. Logachev. (*Geophys.*, vol. 11, pp. 135–147; April, 1946.) Translation of three papers describing the pioneer work by the Russians in magnetic exploration with airborne equipment.

550.38(091) 411

Chapters in the History of Terrestrial Magnetism—A. C. Mitchell. (*Terr. Magn. Atmo. Elec.*, vol. 51, pp. 323–351; September, 1946.)

550.385:525.241 412

The Mean Field of Disturbance of Polar Geomagnetic Storms—L. Harang. (*Terr. Magn. Atmo. Elec.*, vol. 51, pp. 353–380; September, 1946.)

551.501.7 413

Measurements of Refractive Index Gradient—F. L. Westwater. (*Jour. I.E.E.* (London), part IIIA, vol. 93, no. 1, pp. 100–101; 1946.) Three yachts were equipped to take temperature and humidity observations in the first 200 feet in connection with the Cardigan Bay experiments described in 518 below. Pairs of dry and wet copper-constant thermocouples fitted in double radiation shields were mounted on the masts at heights of 25, 40, and 50 feet, and on 10-foot booms projecting over the ship's side at heights of 5, 10, and 15 feet, respectively. For temperature readings, each dry thermocouple was compared electrically with a standard thermocouple; for humidity readings, with its corresponding wet thermocouple. Readings were taken at half-hourly intervals. Sea temperature was also measured by means of a thermocouple, and checked by direct reading from sea water in a bucket. Similar thermocouples were also fitted to a barrage balloon, readings being taken at 50-foot intervals up to 200 feet. The measurements reveal very complex conditions. Sharp discontinuities are common. Similar measurements on a barrage balloon at Cardington revealed a very sharp temperature discontinuity occurring across a subsidence inversion.

551.510.53 414

The Basic Reactions in the Upper Atmosphere: Part 1—D. R. Bates and H. S. W. Massey. (*Proc. Roy. Soc. A*, vol. 187, pp. 261–296; November 5, 1946.) "The properties of the upper atmosphere and in particular of the ionosphere and of the night-sky emission are outlined. The fundamental processes that might be involved are discussed. Various suggestions regarding the production of the layers are considered in detail, and the main difficulties indicated. The theory of the equilibrium of the layers is built up and the outstanding problem of explaining the rate of disappearance of electrons is emphasized. Current views on the origin of the night-sky light are studied critically and serious discrepancies are shown to exist. Other possibilities are examined." An extensive bibliography is appended.

551.510.535 415

On Diffusion in the Ionosphere—V. C. A. Ferraro. (*Terr. Magn. Atmo. Elec.*, vol. 51, pp. 427–431; September, 1946.) "It is shown that Jaeger's discussion of diffusion in the ionosphere [598 of 1946] is applicable only to regions of the F_2 layer 100 km or more above the level of maximum ion-production. Further reasons are given for the conclusion reached in an earlier paper [3785 of 1945] that, though diffusion in the F_2 layer may not be negligible (as in the case of the E and F_1 regions), its effect is likely to be small. The air-density in the F_2 layer at the level of maximum electron-density is then unlikely to be much less than 10^{10} mol per cc."

551.510.535 416

The Mechanism of Ionospheric Ionization—R. v. d. R. Woolley. (*Proc. Roy. Soc. A*, vol. 187, pp. 102–114; October 8, 1946.) "The available mechanisms for the production of electrons in the three regions of the ionsophere are discussed with special reference to the question whether it is possible to account for the observed electron densities without supposing that the sun emits far more energy in the remote ultraviolet spectrum than would be emitted by a black body at 6000 degrees. The contributions to electron densities made by metastable states of atoms and molecules are examined. It is concluded that the observed electron densities may be accounted for without requiring high solar energy in the ultraviolet if the effective recombination coefficient in the F_2 region is 10^{-11}. The F_2 region is attributed to the ionization of atomic oxygen, and the E region to the ionization of molecular oxygen. The electrons forming the F_1 region are supposed to be provided by metastable N_2 or by NO."

551.594.51 417

The Auroral Luminosity-Curve—L. Harang. (*Terr. Magn. Atmo. Elec.*, vol. 51, pp. 381–400; September, 1946.) The auroral luminosity curve is calculated theoretically as a function of height for cathode rays penetrating the ionosphere rectilinearly. Estimates are made of cathode-ray velocities for observed aurorae, and the heights of abnormal-E reflections and of the absorbing layer are discussed.

621.396.812.029.64 418

Elements of Radio Meteorology: How Weather and Climate Cause Unorthodox Radar Vision Beyond the Geometrical Horizon—Booker. (*See* 516.)

621.396.812.029.64 419

The Attenuation of Centimetre Radio Waves and the Echo Intensities, Resulting from Atmospheric Phenomena—Ryde. (*See* 515.)

551.510.535(02) 420

Contribution à l'Étude de la Structure de l'Ionosphère. (Mémoires de l'Institut Royal Météorologique de Belgique, Vol. 19) [Book Review]—M. Nicolet. Institut Royal Météorologique de Belgique, Brussels, 1945, 162 pp. (*Observatory*, vol. 66, pp. 345–346; October, 1946.)

LOCATION AND AIDS TO NAVIGATION

621.396:629.13 421

Aviation Radio Equipment—(*Wireless World*, vol. 52, pp. 366–368; November, 1946.) The main types of radio equipment shown at the exhibition of the Society of British Aircraft Constructors, were: general purpose communication sets, very-high-frequency apparatus, radio aids to navigation, airborne power supply units, and electronic equipment for balancing gyroscope rotors and flaw detection.

621.396.9 422

I.E.E. Radiolocation Convention, March, 1946—(*See* 622.)

621.396.9:623.451:551.46 423

Properties of Radar Echoes from Shell Splashes—H. Goldstein. (*Phys. Rev.*, vol. 70, pp. 232–233; August 1–15, 1946.) Scattering from spray drops has been suggested as the explanation of sea echo on microwave radar. Experiments on echoes from shell splashes are described which provide further evidence that

this is not the case. Wavelengths of 9.2, 3.2, and 1.25 centimeters were used and a high-speed photographic technique employed to compare the echo intensities; simultaneous motion pictures of the splashes were also taken with a cine-theodolite.

The effective cross section of the splash at any instant could be calculated, and a detailed comparison of the results on 9.2 and 1.25 centimeters was made. The cross section was initially greater on 9.2 centimeters, but as the splash changed to spray this condition was reversed, and the 1.25 centimeter echo was still appreciable after the other had disappeared. The ratio of the cross sections for very fine drops is given by the Rayleigh λ^{-4} law as +35 decibels, whereas the maximum value measured was about +20 decibels. This is still much greater than the +8 decibels observed for sea echo, which, therefore, cannot arise from small drops of spray.

621.396.9(52) 424

Short Survey of Japanese Radar. Parts 1 and 2—R. I. Wilkinson. (*Elec. Eng.*, vol. 65, pp. 370–377, and 455–463; August–September and October, 1946.) A report based on a study made immediately after the fall of Japan by the United States Army, which was particularly useful because of the obvious willingness of the Japanese to volunteer technical information. Army and navy radar are discussed, together with general problems concerning the manufacture and operation of radar equipment.

621.396.932 425

The SL Radar—N. I. Hall. (*Bell Lab. Rec.*, vol. 24, pp. 353–357; October, 1946.) A brief descriptive account of a shipborne 10-centimeter radar system with plan-position-indicator display, designed in 1942 for submarine detection.

621.396.933 426

Air Navigation: Survey of Radio Aids to Civil Aviation—M. G. Scroggie. (*Wireless World*, vol. 52, pp. 352–356; November, 1946.) The principal types of navigational aid available at present are briefly discussed. The main immediate need is for world-wide standardization and co-ordination of these equipments to reduce the number that aircraft must carry. Attempts are also being made to replace cathode-ray-tube displays developed during the war by meters which give the pilot a direct reading of the information he requires.

621.396.933.4 427

Anti-Collision Radio—H. W. Secor and E. Leslie. (*Radio Craft*, vol. 18, pp. 17, 75; October, 1946.)

621.396.933(02) 428

Demonstrations of Radio Aids to Civil Aviation [Book Review]—H. M. Stationery Office, London, 80 pp., 5s. (*Wireless Eng.*, vol. 23, p. 298; November, 1946.) Descriptions of equipments shown to delegates of the Provisional International Civil Airways Organization.

MATERIALS AND SUBSIDIARY TECHNIQUES

533.275.083 429

Measuring Humidity in Air and Gases by the Dew-Point Method—R. Czepek. (*Arch. Tech. Messen*, no. 108, pp. T85–86; August, 1940.) A review of the principles, and brief description of seven practical methods.

533.5:621.3.032.53 430

Stresses in Cylindrical Glass-Metal Seals with Glass Inside—A. W. Hull. (*Jour. Appl. Phys.*, vol. 17, pp. 685–687; August, 1946.) The stresses in the glass are shown to be all of the same sign and, thus, a moderate mismatch is allowable when the thermal expansion of the metal is greater than that of the glass. The theory is given in an earlier article: Glass to Metal Seals, by A. W. Hull and E. E. Burger (*Physics*, vol. 5, pp. 387 ff; 1934.) See also 431 below.

533.5:621.3.032.53 431

Theory and Practice of Glass-Metal Seals: Part 4—J. A. Monack. (*Glass Ind.*, vol. 27, pp. 556–559, 582; November, 1946.) For previous parts see 119 of February. See also 430 above.

535.37 432

Fluorescence Fatigue—T. Alper. (*Nature* (London), vol. 158, p. 451; September 28, 1946.)

537.533.8 433

The Change in Conductivity of Aluminum Oxide when it is Bombarded by Electrons—I. F. Kvartskhava. (*Bull. Acad. Sci.* (URSS), sér. phys., vol. 8, no. 6, p. 373; 1944. In Russian.) Summary of a report. In studying secondary electron emission is it important to observe the excitation of electrons in the emitter by primary electrons. Certain experimental difficulties are obviated by the use of aluminum oxide emitters. In experimenting with these it was found that with gradients of the order of 10^6 volts per centimeter a process takes place in the emitter causing an increase in the dark conductivity and a decrease in the excitation of the electrons.

539.23:669 434

Identification of Electroplated Coatings—(*Materials and Methods*, vol. 24, p. 673; September, 1946.) Table of simple identification tests involving scratching, spot tests with concentrated HNO_3 and HCl, and other chemical tests.

539.234 435

Structure of Catalytic Metal Films—D. D. Eley. (*Nature* (London), vol. 158, p. 449; September 28, 1946.) When certain metals evaporate on to the walls of a glass tube, films are formed whose actual area is several times their apparent area. This is best explained by assuming such films to be microcrystalline.

546.287 436

Silicones: Food for Imagination—R. R. McGregor. (*Jour. Frank. Inst.*, vol. 242, pp. 93–102; August, 1946.) Address to a joint meeting of the Franklin Institute and the Philadelphia Science Teachers Association.

620.191.33:669.3 437

Microfissures—"Recorder II" (*Metal Ind.* (London), vol. 69, p. 347; October 25, 1946.) Fine cracks otherwise invisible in impure copper or copper alloy specimens can be detected microscopically if the specimens are electrolytically polished and immersed in a special ammonium sulphide reagent.

620.193.8(213) 438

The Deterioration of Materiel in the Tropics—W. G. Hutchinson. (*Sci. Mon.*, vol. 63, pp. 165–177; September, 1946.) A brief résumé of the ways in which different classes of materiel are affected. Some possible measures of control are indicated.

621.315.211.2:679.5 439

Developments in Solid Dielectric R.F. Transmission Lines—Graham. (*See* 351.)

621.315.6:621.39 440

Dielectrics for Telecommunication Purposes—W. Jackson. (*Engineering* (London), vol. 162, pp. 427–428; November, 1946.) Another account of part 2 of 314 of Febuary.

621.315.61.015.5:547 441

Determination of the Flashpoint of Organic Insulating Materials—M. Zürcher. (*Schweiz. Arch. Angew. Wiss. Tech.*, vol. 11, pp. 94–96; March, 1945.) Powdered materials in tubular containers are inserted in holes in a copper block preheated to a known temperature. Any gases given off are collected and tested for combustibility. The sensitivity of the apparatus and the effect of grain size are discussed and results given graphically for certain materials.

621.315.612.2:551.547 442

Investigation of Porcelain Insulators at High Altitudes—C. V. Fields and C. L. Cadwell. (*Trans. A.I.E.E.* (*Elec. Eng.*, October, 1946), vol. 65, pp. 656–660; October, 1946.) Flashover voltages are given for alternating and direct current for porcelain bushings. Tests were made at both normal and reduced pressure. Solid insulation should be used to obtain the benefit of its puncture strength rather than its flashover under extreme conditions.

621.315.615.2 443

The Influence of the Concentration and Mobility of Ions on Dielectric Loss of Insulating Oils—B. P. Kang. (*Trans. A.I.E.E.* (*Elec. Eng.*, July, 1946), vol. 65, pp. 403–407; July, 1946.) The relationships between the amount of impurities, the viscosity, and the dielectric loss in insulating oils are investigated.

621.315.617.3 444

Insulating Varnishes and Compounds—N. Bromberger. (*Proc. I.R.E.* (Australia), vol. 7, pp. 4–12; October, 1946. Discussion, pp. 12–14.) The selection and characteristics of both natural and synthetic materials are outlined, and details are given of the processes involved in the manufacture of varnishes and compounds. Their application and methods of production control are also discussed.

621.318.22/.23 445

Modern Hard Magnetic Materials—K. Hoselitz. (*Metal Treatment*, vol. 13, pp. 213–222; Autumn, 1946.) Reprint of 2607 of 1946.

621.319.7:621.385 446

Plotting Electrostatic Fields—G. Silva. (*Alta Frequenza*, vol. 15, pp. 117–118; June, 1946.) Comment on 3322 of 1946 (Pinciroli and Panetti).

621.357.1:666.1:621.314.67 447

Electrolysis Phenomena in Soft-Glass Stems of Rectifier Tubes—J. Gallup. (*Jour. Amer. Ceram. Soc.*, vol. 29, pp. 277–281; October 1, 1946.) The longitudinal cracks and black deposits which form along leads during the life of rectifier tubes were found to be due to electrolysis in the soft glass stems. Rupture was caused by glass bombardment by reverse emission from the rectifier anode. This theory is supported by mass spectrometer analysis of the gas produced. Associated electrolysis phenomena are also described.

621.357.7:669.3 448

Copper Plating—C. Struyk and A. E. Carlson. (*Metal Ind.*, (London), vol. 69, pp. 348–352; October 25, 1946.) Description of the advantages of using copper fluoborate solutions with high-limiting current densities for the electrodeposition of copper, instead of the ordinary copper sulphate solutions.

621.791.353 449

Soft Soldering—"Recorder II" (*Metal Ind.* (London), vol. 69, p. 476; December 6, 1946.) Survey of progress of investigations into the problem of "solderability."

666.1:62 450

Modern Developments in Glasses for Technical Purposes—W. E. S. Turner. (*Endeavour*, vol. 4, pp. 3–16; January, 1945.) Recent discoveries of chemical, thermal, and mechanical properties are described and the use of glass in combination with metals and as fibre is discussed.

666.1.032 451
Scientific Glass Blowing and Laboratory Techniques—W. E. Barr and V. J. Anhorn. (*Instruments*, vol. 19, pp. 14–32; January, 1946.) To be continued.

666.11 452
Dielectric Properties of Glasses at Ultra-High Frequencies and Their Relation to Composition—L. Navias and R. L. Green. (*Jour. Amer. Ceram. Soc.*, vol. 29, pp. 267–276; October 1, 1946.) The dielectric constants and dielectric losses of 104 kinds of glass were measured at 3000 and 10,000 megacycles by the resonant cavity method. SiO_2 and B_2O_3 glasses are relatively transparent at these frequencies. Alkali ions in glasses give high losses increasing with the number of ions. Glasses containing a combination of alkalis show lower losses than the equivalent compositions with only one alkali. Divalent ions contribute less to losses than alkalis.

666.3:539.4 453
Stress-Strain Relations in Ceramic Materials—M. Lassettre and J. O. Everhart. (*Jour. Amer. Ceram. Soc.*, vol. 29, pp. 261–266; September 1, 1946.)

678.77 454
Some Recent Contributions to Synthetic Rubber Research—C. S. Fuller. (*Bell. Sys. Tech. Jour.*, vol. 25, pp. 351–384; July, 1946.)

679.5 455
Annealing of Styrene and Related Resins—J. Bailey. (*Mod. Plast.*, vol. 24, pp. 127–131; October, 1946.) Failure of parts caused by thermal and mechanical strains can be overcome by the use of appropriate annealing processes.

679.5 456
Manufacture of Laminates in Germany—(*Mod. Plast.*, vol. 24, pp. 147–149, 210; October, 1946.) Translation based on a production manual of Dynamit A.-G. Troisdorf, a subsidiary firm of I. G. Farbenindustrie A.-G.

679.5:62 457
Plastic Laminates—as Engineering Materials—K. Rose. (*Materials and Methods*, vol. 24, pp. 653–664; September, 1946.) Comprehensive article dealing with the industrial aspect of these materials, with their light weight, high dielectric strength, low water absorption, and resistance to attack by chemicals. They can be supplied in sheets, rods and tubes, and other forms. The production of high-pressure, low-pressure and composite laminates is described, with their particular industrial uses, and details concerning the machining of these materials.

679.5:669 458
Metal Test Specimens Mounted in Urea—(*Mod. Plast.*, vol. 24, p. 121; October, 1946.) Metal specimens must be mounted for certain microscope tests. Moulded Plaskon is an economical mounting material which is easy to use and can be colored.

778.534.8 459
A System for Rapid Production of Photographic Records—F. M. Brown, L. L. Blackmer, and C. J. Kunz. (*Jour. Frank. Inst.*, vol. 242, pp. 203–212; September, 1946.) Equipment for automatic exposure, processing and projection of 16-millimeter film is described. The final image is completely processed in 15 seconds on Eastman fine grain release positive film type 5302.

MATHEMATICS

517.942 460
Mathieu Functions and Their Classification—N. W. McLachlan. (*Jour. Math. Phys.*, vol. 25, pp. 209–240; October, 1946.)

518.5 461
The Automatic Sequence Controlled Calculator: Parts 1 and 2—H. H. Aiken and G. M. Hopper. (*Elec. Eng.*, vol. 65, pp. 384–391 and 449–454; August–September, and October, 1946.) See also 468 below.

518.5 462
The ENIAC, an Electronic Computing Machine—D. R. Hartree. (*Nature* (London), vol. 158, pp. 500–506; October 12, 1946.) General description with examples of operations.

518.61 463
An Escalotor Process for the Solution of Linear Simultaneous Equations—J. Morris. (*Phil. Mag.*, vol. 37, pp. 106–120; February, 1946.) The Escalator process, originally devised for the solution of Lagrangian frequency equations in connection with aircraft vibration problems (see 1636 of 1945) is adapted to the solution of linear simultaneous equations, particularly those which are "ill-conditioned" and difficult to solve by other methods. Each of the variables involved is introduced in turn by definite selfcontained stages, at each of which powerful checks are available to assess, and if necessary to adjust, accuracy. A numerical example is fully explained.

The Escalator method has a very wide application to vibration problems because it enables the various parts of a complicated system to be considered separately. It has also an application to networks and transients, but further work is necessary to make this fully effective. A comprehensive account of the method will be published in book form shortly.

519.2:518.4 464
Graphical Solutions of Statistical Problems—F. Levi. (*Engineer* (London), vol. 182, pp. 338–340 and 362–364; October 18–25, 1946.) Discusses the applications of "probability graph paper."

519.28:621.3 465
A New Approach to Probability Problems in Electrical Engineering—H. A. Adler and K. W. Miller. (*Trans. A.I.E.E.* (*Elec. Eng.*, October, 1946), vol. 65, pp. 630–632; October, 1946.)

531.3:621.396.611 466
On a Special Case of Systems with Two Degrees of Freedom—Zhabotinski. (*See* 377.)

51(02) 467
The Common Sense of the Exact Sciences [Book Review]—W. K. Clifford. A. A. Knopf, New York, 249 pp., $4.00. (*Sci. Mon.*, vol. 63, p. 242; September, 1946.) "Mathematics made easy."

518.5 468
A Manual of Operation for the Automatic Sequence Controlled Calculator—(Annals of the Computation Laboratory of Harvard University, Vol. 1) [Book Review]—Staff of the Computation Laboratory. Harvard Univ. Press, Cambridge, Mass.; Oxford Univ. Press, London, 561 pp., $10.00. (*Nature* (London), vol. 158, pp. 567–568; October 26, 1946.) The machine described can be regarded as a modern version of Babbage's difference engine, and "is largely composed of standard Hollerith counters, but with a superimposed and specially designed tape-sequence control for directing the operations of the machine." See also 461 above.

518.61 469
Relaxation Methods in Theoretical Physics [Book Review]—R. V. Southwell. Clarendon Press, Oxford, 248 pp., 20s. (*Electrician*, vol. 137, p. 1137; October 25, 1946.) It is claimed that any problem that can be formulated can be solved arithmetically. See also 463 above.

MEASUREMENTS AND TEST GEAR

621.317.2:656.2 470
Mobile Electrical Measurements Laboratories for the German State Railways—E. W. Curtius. (*Arch. Tech. Messen*, no. 108, pp. T93–94; August, 1940.) Choice of test gear and of methods of measurement is limited mainly by the essential requirement of robust equipment that can withstand the severe vibrations encountered in railway rolling-stock.

621.317.32:537.221 471
Measurement of Surface Potential or Contact Potential Differences—A. A. Frost. (*Rev. Sci. Instr.*, vol. 17, pp. 266–268; July, 1946.) The term surface potential is preferable when surface effects are being studied. Such potentials may conveniently be measured by forming the two surfaces into a capacitor whose charge is neutralized by an opposing potential supplied by a *pH* meter. See also 1282 of 1946 (Meyerhof and Miller).

621.317.32.027.3 472
High-Voltage Measurement—F. M. Bruce. (*Elec. Rev.* (London), vol. 139, p. 838; November 22, 1946.) Summary of two Institution of Electrical Engineers papers, one discussing factors in the design of an ellipsoid voltmeter, and the other describing spark gap calibration.

621.317.35:621.396.611.1.015.3 473
Evaluation of Circuit Constants from Oscillograms—L. S. Foltz. (*Elec. Eng.*, vol. 65, pp. 490–492; October, 1946.) Formulas are derived and applied to typical oscillograms of transients in series circuits, and it is shown that the results, (values of the resistance, capacitance and inductance present) have an accuracy which makes the formulas and the method useful.

621.317.373 474
Phase Detectors: Some Theoretical and Practical Aspects—L. I. Farren. (*Wireless Eng.*, vol. 23, pp. 330–340; December, 1946.) Fundamental methods were described by Levy (2323 of 1940). In the present paper, a detailed analysis shows that simple push-pull detectors are more efficient than the balanced type. Simple push-pull detectors with sinusoidal input voltages have good sensitivity, but a sinusoidal relationship between the output and the phase-difference of the input voltages; this relationship is more nearly linear in the square-wave case, but sensitivity is less.

621.317.39.029.6:536.33 475
The Measurement of Thermal Radiation at Microwave Frequencies—R. H. Dicke. (*Rev. Sci. Instr.*, vol. 17, pp. 268–275; July, 1946.) The connection between "Johnson noise" and black-body radiation is discussed, using a simple thermodynamic model. A suitable microwave-receiver assembly with a wide-band intermediate-frequency amplifier is described in which the effect of radio noise generated in the apparatus is eliminated.

The experimentally measured root-mean-square fluctuation of the output meter of such a microwave radiometer is 0.4 degree centigrade, compared with a theoretical value of 0.46 degree centigrade.

The method of calibrating, using a variable temperature resistive load, is described. See also 219 of February (Kyhl, Dicke, and Beringer).

621.317.728 476
Measurement of R.M.S. Voltage using a Sphere Gap—W. Raske. (*Arch. Tech. Messen*, no. 106, p. T42; April, 1940.) Methods of adapting a sphere gap, used for peak voltage measurement, to find the root-mean-square value. Calibration and errors are discussed.

621.317.75 477
Frequency Spectrum Analysis: Principles and Applications—E. Aisberg. (*Toute la Radio*, vol. 12, pp. 9–12; December, 1945.) An account of the construction and operation of an analyzer suitable for studying the frequency characteristics of the various circuits in radio receivers.

621.317.79.029.64 478
Techniques and Facilities for Microwave Radar Testing—E. I. Green, H. J. Fisher, and J. G. Ferguson. (*Bell. Sys. Tech. Jour.*, vol. 25, pp. 435–482; July, 1946.) Reprint of 2645 of 1946.

621.317.79.029.64:621.396.611 479
High Q Resonant Cavities for Microwave Testing—Wilson, Schramm, and Kinzer. (*See* 378.)

621.318.572 480
Counting Rate and Frequency Meter—E. Lorenz, J. Weikel, and S. G. Norton. (*Rev. Sci. Instr.*, vol. 17, pp. 276–279; July, 1946.) A counting rate and frequency meter consists essentially of an apparatus for bringing signals of different amplitudes and waveforms to a uniform unidirectional size and measuring their rate of arrival. The instrument described has a resolving power of 10^{-6} seconds for evenly spaced pulses and consists of a thyratron whose rate of striking is controlled by the input pulses, while the duration of the arc at each discharge is fixed by a resistance-capacitance circuit. The resulting anode current is thus proportional to the frequency of the input pulses.

621.319.4:621.317 481
The Characteristics and Errors of Capacitors used for Measurement Purposes—C. G. Garton. (*Jour. I.E.E.* (London), part II, vol. 93, pp. 398–408; October, 1946. Discussion pp. 408–414.) Causes of variation of capacitance and loss angle are discussed with relation to time, humidity, temperature, frequency, voltage, screening, and the properties of materials used in capacitor construction. When a guard ring is used to measure the capacitance and loss angle of a plane sample of dielectric, errors in loss angle due to surface conductivity are small only if $g \ll t$, $g \ll R$, or $r > 10^{-17}/Rf$ where $2g$ is the guard ring gap, t is the thickness of the sample, R is the radius of the main electrode, and f is the frequency. These conditions are difficult to realize in practice, and if none of them is satisfied, spurious loss angles up to 10^{-2} may occur in specially unfavorable cases.

621.396.611.21.012.8:537.228.1 482
Methods of Measuring the Constants of the Equivalent Network of a Piezoelectric Crystal: Quartz Meter—Jacquinot, Dumesnil, and Boughon. (*Onde Élec.*, vol. 26, pp. 259–273; July, 1946.) The equivalent circuit has components L, C, and R in series with C_p in shunt. The natural frequency and bandwidth give the magnification Q. The time constant $\tau = 2L/R$ is determined by observing the decay of free oscillations in the crystal when the excitation is removed and a fluxmeter integrator gives direct indication of τ. The bandwidth is measured as the difference of the quadrantal frequencies at which phase displacements of ± 45 degrees are obtained relative to the resonant frequency and cathode-ray-oscilloscope indication is used. The dynamic resistance is determined by comparison with a known resistance (using cathode-ray-oscilloscope indication). The various methods of measurement are combined in a single instrument (a universal Quartz meter) for use between 50 kilocycles and 10 megacycles.

OTHER APPLICATIONS OF RADIO AND ELECTRONICS

536.48 483
On the Possible Use of Brownian Motion for Low Temperature Thermometry—A. W. Lawson and E. A. Long. (*Phys. Rev.*, vol. 70, pp. 220–221; August 1–15, 1946.) Thermal noise in a high resistance is only suitable for measuring temperatures down to about 0.01 degree Kelvin and requires an amplifier of very narrow pass band; the resistance, necessarily of a semiconductor, will have an exponential temperature coefficient which introduces difficulties.

Alternatively by measuring the thermal noise voltage of a quartz resonator (after calibration at the boiling point of helium) temperatures as low as 0.0001 degree Kelvin should be measurable. The main experimental difficulty is to establish thermal contact between the resonator and its surroundings without reducing its Q.

539.16.08 484
Design of Beta-Ray and Gamma-Ray Geiger-Müller Counters—W. Good, A. Kip, and S. Brown. (*Rev. Sci. Instr.*, vol. 17, pp. 262–265; July, 1946.)

539.16.08:57 485
An Electronic Method of Tracing the Movements of Beetles in the Fields—G. A. R. Tomes and M. V. Brian. (*Nature* (London), vol. 158, p. 551; October 19, 1946.) A beetle is made to carry 5 micrograms of radium sulphate; its position is then detected with a special form of Geiger-Müller tube.

615.84 486
Crystal-Controlled Diathermy—R. L. Norton. (*Electronics*, vol. 19, pp. 113–115; October, 1946.) Description of a 500-watt unit operating at about 27 megacycles, crystal frequency being a quarter of carrier frequency. An air-cooled tetrode is used in the output stage to which the load is connected by means of leads 4 feet in length. Provision is made for tuning the load: a lamp, loosely coupled to the output leads, is used as an indicator.

621.316.9:621.38 487
Electronic Devices in Power Supply—"Kilovar." (*Overseas Eng.*, vol. 20, pp. 155–157; December, 1946.) A general account of the protection of large high voltage power supply networks by electronic devices, and their use in telemetering, fault location, etc.

621.318.572 488
Electronic Relay—G.G.C. Development Co. (*Jour. Sci. Instr.*, vol. 23, p. 247; October, 1946.) When the control contact is open the anode and grid of a tube are fed with alternating current in antiphase. Closure of this contact earths the grid and causes anode current to flow thus operating the relay. The maximum current through this contact is 15 microamperes.

621.318.572:623.451 489
A Paper Screen Signaling Missile Passage in Ballistics—H. Lamport and M. G. Schorr. (*Rev. Sci. Instr.*, vol. 17, p. 280; July, 1946.)

621.365.036.65 490
A Simple Automatic Furnace Temperature Control—E. L. Yates. (*Jour. Sci. Instr.*, vol. 23, pp. 229–231; October, 1946.) By using a platinum resistance thermometer in an alternating-current bridge, furnace temperature can be automatically controlled to within ± 0.5 degrees centigrade at all temperatures between 0 degree and 1000 degrees centigrade.

621.365.92:677 491
Radio Heating in Textile Industry—C. N. Batsel. (*Radio News*, vol. 36, pp. 44–45, 82; October, 1946.) High frequency heating is used for processing cotton, rayon, nylon, and wool, mainly for drying and setting the twist. A method has also been developed for curing the resin in impregnated fabrics.

621.38:62 492
Electronics: Their Scope in Heavy Engineering—W. G. Thompson. (*G. E. C. Jour.*, vol. 14, pp. 59–72; August, 1946.) A survey of various types of electronic equipment, and their application to research, testing, manufacture, power control, and safety in heavy engineering.

621.38.001.8:621.9 493
Electronics and Precision Grinding Machines—(*Engineer* (London), vol. 182, pp. 300–301; October 4, 1946.)

621.384:538.691 494
The Stability of Electron Orbits in the Synchrotron—N. H. Frank. (*Phys. Rev.*, vol. 70, pp. 177–183; August 1–15, 1946.) The motion of an electron in an axially symmetric magnetic field under the action of an external torque due to a radio-frequency field is analyzed and the oscillations about the equilibrium orbit investigated. The transition from betatron to synchrotron motion is examined and the condition restablished for the "locking in" of the electrons to synchronous driving by the radio-frequency field. Stable synchrotron operation is shown to be quite practicable. See also 3440 of 1946 (Denison and Berlin).

621.384.032.21 495
R.F. Heating Cyclotron Filaments—A. E. Hayes, Jr. (*Phys. Rev.*, vol. 70, pp. 220; August 1–15, 1946.) The radio-frequency generator which feeds the filament of a cyclotron is usually remote (for ease of adjustment) and so requires a long transmission line between the oscillator and the ion source. The advantage of using a mean oscillator frequency which makes the line one quarter wavelength long are explained.

621.385.833+537.533.72 496
The Electron Microscope—G. Dupouy. (*Metal Treatment*, vol. 13, pp. 153–168, 205; Autumn, 1946.) Description of its theory, construction, and operation, and some of the results obtained by its application to the study of metals.

621.396.998:629.135 497
Drones — Prelude to "Push-Button" Warfare?—O. Read. (*Radio News*, vol. 36, pp. 25–29, 104; October, 1946.) A brief account of the use of automatically controlled aircraft for taking observations during atom-bomb tests. The aircraft were controlled by radio from piloted aircraft.

621.397.26:343.977.33 498
Transmission of Finger-Prints by Radio—(*Nature* (London), vol. 158, pp. 525–526; October 12, 1946.) Note of some recent applications of facsimile to police work described in a pamphlet by F. R. Cherrill.

771.448.1 499
Photographic Use of Electrical Discharge Flashtubes—H. E. Edgerton. (*Jour. Opt. Soc. Amer.*, vol. 36, pp. 390–399; July, 1946.)

PROPAGATION OF WAVES

538.566 500
The Group Velocity in a Crystal Lattice—Mandelstam. (*See* 397.)

551.501.7 501
Measurements of Refractive Index Gradient—Westwater. (See 413.)

551.510.535:523.78 502
Eclipse-Effects in F_2-Layer of the Ionosphere—H. W. Wells and A. H. Shapley. (*Terr. Magn. Atmo. Elec.*, vol. 51, pp. 401–409; September, 1946.) A study of ionospheric observations at College, Watheroo, and Huancayo during the partial solar eclipses of February and August, 1943, and January, 1944. F_2-

layer ionization was in all cases subnormal before and after the eclipse, indicating that radiations from beyond the limb of the sun may contribute to the ionization of the region. Estimated values of the recombination coefficient for the F_2 layer for these eclipses lie between 10^{-9} and 2×10^{-10}. At Huancayo during the 1944 eclipse the F_2 layer rose to great heights at a rate of about 200 kilometers per hour, and a new F-region stratification developed at normal heights. See also 503 below.

551.510.535:523.78 503

Effects on the Ionosphere at Huancayo, Peru, of the Solar Eclipse, January 25, 1944—P. G. Ledig, M. W. Jones, A. A. Giesecke, and E. J. Chernosky. (*Terr. Magn. Atmo. Elec.*, vol. 51, pp. 411–418; September, 1946.) A detailed account of the results for the E, F_1 and F_2 layers is given, together with simultaneous signal intensities observed on a 15-megacycle transmission over a distance of 3500 miles. Minima in ion density were recorded for the E and F_1 layers near the time of maximum eclipse, with a delayed effect in the case of the F_2 layer. An effect on F_2-layer ion density possibly due to a corpuscular eclipse is also described. See also 502 above.

551.594.51 504

The Auroral Luminosity-Curve—Harang. (*See* 417.)

621.396.11:523[.7+.854 505

Extra-Tropospheric Influences on Ultra-Short-Wave Propagation—Appleton. (*See* 402.)

621.396.11:621.392 506

Some Questions Connected with the Excitation and Propagation of Electromagnetic Waves in Tubes—L. Mandelstam. (*Zh. Eksp. Teor. Fiz.*, vol. 15, no. 9, pp. 461–470; 1945. In Russian.) A new analytical method is proposed. The excitation of electromagnetic waves in free space is considered first. It is assumed that in the plane $z=0$ there is a double layer of electric charges, i.e., a plane layer of dipoles with their axes parallel to the z axis. A formula (1) is quoted determining the z-component Π of the Hertz vector, and is transformed into formula (4). The latter formula is applied to the case of a linear belt of dipoles of radius r and constant linear dipole density m. A formula (5) determining Π for this case is derived. If the belt is reduced to a point the well known Sommerfeld integral is obtained.

A circular tube of infinite length and with ideally conducting walls is then considered. The exciter is assumed to be a plane double electric layer, i.e., a layer of electric moments lying in the plane $z=0$ and directed along the z axis of the tube. A formula (11) determining Π for this case is derived together with formula (15) for the case of a point dipole on the axis of the tube. Methods for determining E and H from these formulas are indicated. Formula (15) is analyzed, and various peculiarities are pointed out. The excitation by a point dipole displaced from the z axis is also considered.

The case of "magnetic" excitation of waves in tubes is discussed next. This type of excitation (can be achieved by introducing into the tube in the plane $z=0$ a loop carrying current and having a figure-of-eight or more complicated shape. Methods for determining the "magnetic" Hertz vector Π^* for this case, as well as E and H, are suggested.

The attenuation of the waves in tubes due to losses in the walls is considered and relationships between the various quantities involved are established.

Finally, it is shown that the problem considered can be reduced to the same boundary conditions as those of a vibrating diaphragm. It is, therefore, possible to make use of Courant's theorems for obtaining additional information such as the effect of varying the shape of the tube cross section or introducing a conductor along the axis of the tube.

621.396.11.029.64 507

Perturbation Theory of the Normal Modes for an Expontial *M*-Curve in Non-Standard Propagation of Microwaves—C. L. Pekeris. (*Jour. Appl. Phys.*, vol. 17, pp. 678–684; August, 1946.) The region beyond the horizon is mainly considered, for cases in which the deviation of the M-curve from the standard is an exponential function of the height expressed in natural units. (M denotes modified refractive index.) Within its region of convergence the theory is applicable to the most general type of M-curve, including elevated ducts. "The region of practical convergence ranges from highly substandard conditions down to cases where the decrement is a fraction of the standard value." The procedure is to express the height-gain function of any mode in the nonstandard case as a linear combination of the height-gain functions of all the modes in the standard case. The success of this depends on being able to evaluate quantities $\beta_{nm}(\lambda)$ which can be expressed as infinite integrals involving products of the height gain functions of the standard case.

621.396.65 508

Hertzian Cable [Radio Links in Multichannel Telephony Circuits]—Clavier and Phélizon. (*See* 540.)

621.396.81.029.6:551.43 509

An Experimental Investigation on the Propagation of Radio Waves over Bare Ridges in the Wavelength Range 10 cm. to 10 m. (Frequencies 30 to 3000 Mc.)—J. S. McPetrie and L. H. Ford. (*Jour. I.E.E.* (London), part IIIA, vol. 93, no. 1, pp. 108–109; 1946.) For horizontally polarized transmission over an approximately cylindrical hill of radius 11,000 feet, experimental results are in good agreement with the rate of attenuation calculated by Domb and Pryce (assuming a ground reflection coefficient of -1) at wavelengths 9.2, 25, and 56 centimeters.

For a cylindrical ridge of radius 1250 feet, wavelength 2.25 meters, horizontal polarization gives results agreeing with the calculations of Domb and Pryce for a sphere of 1250 feet radius, but vertical polarization shows a lower rate of attenuation, and signal strength less out of the shadow and greater in the shadow. Experiments were also made at 9.2, 25, 56 centimeters and 11.15 meters; at 11.15 meters attenuation was less with vertical than with horizontal polarization, otherwise results were the same on the two polarizations. Summary of an Institute of Electrical Engineers Radiolocation Convention paper.

621.396.81.029.63/.64 510

Theoretical Estimation of Field Strength—J. M. C. Scott. (*Jour. I.E.E.* (London), part IIIA, vol. 93, no. 1, pp. 104–105; 1946.) The reflecting power of a target for decimeter or centimeter waves can be satisfactorily expressed in terms of a "linear scattering constant" L which is roughly 2 to 4 meter for the head-on aspect and 1 meter for other aspects; received power is proportional to transmitted power$\times L^2\lambda^2$.

Ray-theory interference patterns obtained by geometrical optics are satisfactory at short ranges or great heights. For long ranges and low heights, wave theory must be used, especially when some of the power emitted by the transmitter becomes trapped in an atmospheric layer. This effect can set in below a certain wavelength depending on the meteorological situation. According to the wave theory there is an infinite series of characteristic waves (for "normal modes") of which, for any particular meteorological situation, some may travel horizontally with little attenuation while the rest are rapidly attenuated. The attenuation constants and height gains can be calculated numerically from the wave equation; tables for various types of atmospheric model are available.

If the wavelength is small compared to that for energy trapping, ray tracing methods can be used; the rays in a heterogeneous atmosphere with a nonlinear structure form a series of envelopes or caustic curves. Calculations are laborious.

Calculations have also recently been made of the reflection coefficient of an elevated inversion layer at oblique incidence.

621.396.81.029.64:551.43 511

Some Experiments on the Propagation over Land of Radiation of 9.2 cm Wavelength, Especially on the Effect of Obstacles—J. S. McPetrie and L. H. Ford. (*Jour. I.E.E.* (London), part IIIA, vol. 93, no. 1, pp. 107–108, 1946.) A signal of known power was transmitted, and the received signal strength measured with a calibrated receiver. Short range results on a level site (up to 1 kilometer) agreed with the inverse square law and a ground reflection coefficient of -1, but this was not true for an undulating site. It was found that a large tree should be regarded as an opaque body. A dense screen of leafless trees was comparable to a solid obstacle over which Fresnel diffraction took place. Screens of trees in full leaf, even only two or three trees thick, formed an opaque obstacle. Most buildings must be regarded as opaque, diffracting objects. Summary of an Institution of Electrical Engineers Radiolocation Convention paper.

621.396.81.029.64 512

A Study of Some of the Factors Influencing Microwave Propagation—B. J. Starnecki. (*Jour. I.E.E.* (London), part IIIA, vol. 93, no. 1, pp. 106–107; 1946.) An analysis of the experimental results described in Megaw's paper (518 below). For a slightly nonoptical link propagation can be regarded as normal. On the other hand, for a 60-mile link 2.3 times optical range, signal levels are mainly much higher than can be expected from refraction-diffraction formulas. Only in about 15 per cent of the cases was there clear meteorological evidence of the formation of a radio duct of width greater than 50 feet, but comparison of simultaneous signal levels on 3 and 9 centimeters suggested that between 50 per cent and 70 per cent of the results on this link were due to ducts with heights between 20 and 40 feet, the remainder being due to normal propagation. The signal level was above "free space" level for about 20 per cent of the whole 5-month period. When the receiver was replaced by one at 20 feet, the results still agreed well with those expected for duct widths between 20 and 40 feet. For the 200-mile link, 70 per cent of the observed signal levels can only be explained by the presence of ducts. Summary of an Institution of Electrical Engineers Radiolocation Convention paper.

621.396.812+538.566.3 513

Observations on the Interaction of Waves in the Ionosphere, in Relation to the Gyrofrequency—M. Cutolo, M. Carlevaro, and M. Gherghi. (*Alta Frequenza*, vol. 15, pp. 111–117; June, 1946.) A description of experiments carried out in Italy in 1946 on the Luxemburg (cross-modulation) effect. Observations on a number of stations, one of which was varied in frequency, confirmed V. A. Bailey's theoretical prediction that the degree of cross modulation is greatly increased if the frequency of the disturbing station is in the neighborhood of the gyrofrequency. See 2437 of 1937 and back references.

621.396.812+621.396.11 514

The Importance of Theory in the Development and Understanding of Radar Propaga-

tion—T. L. Eckersley. (*Jour. I.E.E.* (London), part IIIA, vol. 93, no. 1, pp. 103–104; 1946.) The phase integral theory was originally applied to the problem of diffraction round an imperfectly conducting earth, and was later extended to include the effect of atmospheric refraction in a particularly easy and significant way. Ray methods are essentially inaccurate and must be replaced by correct wave theory. To use refraction in radar work a more thoroughly satisfactory meteorological theory is required than yet exists. Sudden discontinuities of refractive index at considerable heights, due for example to subsidence inversions could cause long-distance propagation by the internal reflection of characteristic waves. The radio problem is perfectly definite if the radio refractive index is known everywhere as a function of height, though the solution may be difficult in practice.

Carefully controlled experiment could help to decide the physical basis of theories for problems as yet imperfectly understood, such as turbulence and attenuation due to scattering.

621.396.812.029.64 515

The Attenuation of Centimetre Radio Waves and the Echo Intensities Resulting from Atmospheric Phenomena—J. W. Ryde. (*Jour. I.E.E.*, (London), part IIIA, vol. 93, no. 1, pp. 101–103; 1946.) The effects to be considered are quite negligible for wavelengths above the centimeter band, but, in general, increase rapidly as wavelength decreases. Of atmospheric gases, oxygen produces an attenuation between 0.01 and 0.02 decibel per kilometer throughout the centimeter band, while water produces a very small attenuation at 10 centimeters rising to about 0.2 decibel per kilometer near 1 centimeter; other gases can be neglected.

For fogs and fine droplet clouds, attenuation depends only on the total mass of liquid per unit volume; a table gives attenuation approximately in terms of visual range in such clouds.

For rain, average attenuation in decibels per kilometer is approximately proportional to precipitation rate in the centimeter band: the constant of proportionality depends upon temperature and wavelength.

The attenuation produced by hail is small compared to that for rain except for wavelengths near 1 centimeter.

Echo intensities from atmospheric fogs and fine droplet clouds are very weak: even moderate rain, however, can produce an echo intensity (for which a formula is given) comparable with that from an aircraft.

621.396.812.029.64 516

Elements of Radio Meteorology: How Weather and Climate Cause Unorthodox Radar Vision beyond the Geometrical Horizon—H. G. Booker. (*Jour. I.E.E.* (London), part I, vol. 93, pp. 460–462; October, 1946; [summary] and part IIIA, vol. 93, pp. 69–78; 1946. [full version].) Radar receivers are frequently able to see round the curved surface of the earth owing to radio refraction in the lower atmosphere. The phenomenon is most marked when both radar equipment and target are close to the earth. In its simplest form it involves an atmospheric wave guide, or radio duct, close to the earth's surface; within the duct the curvature of a radio ray emanating horizontally from a transmitter would exceed that of the earth. The longer the wavelength, the greater must be the width of this radio duct for efficient guiding to take place. In the British Isles, a typical duct involving important conditions of super refraction would be one extending from the earth's surface up to 100 feet. This can be an efficient wave guide for centimeter wavelengths, but at meter wavelengths it would merely produce an abnormal reduction of horizontal attenuation beyond the horizon. In other parts of the world, such as India during the hot season, duct widths or 1000 feet or more can occur; a case is cited of a 1½-meter radar near Bombay which had at various times seen different points on the Arabian coastline up to 1500 miles away.

The most important meteorological conditions for super refraction are that the upper air, at a height of a few thousand feet, should be exceptionally warm and dry in comparison with the earth's surface; the associated unusual gradients of temperature and humidity are the cause of downward super refraction. In order to allow for the normal drop of temperature and humidity with height in a well-mixed air mass, it is advisable to use "potential temperature" and "specific humidity" as the fundamental parameters. Stormy and turbulent conditions, and bad weather in general, produce a well-mixed air mass near the ground with little vertical change of potential temperature or specific humidity and, therefore, with orthodox propagation. Super refraction occurs when upper-air potential temperature exceeds appreciably that at the surface, while upper-air specific humidity falls short of that of the surface. This is essentially a fine-weather phenomenon, and, therefore, tends to be most intense in tropical (but not equatorial) climates, inland at night in fine, warm weather, and when warm, dry air over land drifts out over relatively cool sea. At present only qualitative forecasting of super refraction is possible.

621.396.812.029.64 517

A Preliminary Investigation of Radio Transmission Conditions over Land and on Centimetre Wavelengths—R. L. Smith-Rose. (*Jour. I.E.E.* (London), part IIIA, vol. 93, no. 1, pp. 98–100; 1946.) A study of the radio-meteorological aspects of the experiments described in Megaw's paper (518 below). In overland transmission along a 38-mile path, mean hourly intensity was sometimes steady to within 1 or 2 decibels all day, while on other occasions there was a marked diurnal variation from a minimum in the early morning to a peak near midnight, associated with fine, clear nights. If fog occurred, the signal strength would drop to a well-marked minimum, and rise to the normal daily value when the fog cleared. For radio communication links at centimeter wavelengths on an over-sea non-optical path, it is advantageous to place the stations as high as practicable if the maximum reliability of service is required.

During good weather, signal level is usually high and somewhat variable; low signal corresponds to poor visibility; a decrease followed by an increase is associated with the passage of a front. Special meteorological observations by aircraft between 50 and 1500 feet were made, from which could be calculated the radio signal strength to be expected; the agreement with the observed values is very good (Fig. 3).

621.396.812.029.64 518

Experimental Studies of the Propagation of Very Short Radio Waves—E. C. S. Megaw. (*Jour. I.E.E.* (London), part I, vol. 93, pp. 462–463; October, 1946 [summary]; and part IIIA, vol. 93, pp. 79–97; 1946; [full version].) "The main experimental program described consisted of measurements of 3-centimeter, 9-centimeter and 3½-meter waves over sea paths 57 and 200 miles long; and of 9-centimeter waves over a single 38-mile land path. The measurements were continuous over some of these paths for periods between two and three years; and, particularly as regard detailed correlation with meteorological measurements, the work is still in progress."

From preliminary studies it is concluded that for optical paths (up to about 20 miles) over sea the observed field differs little from that calculated from a standard atmosphere; over longer paths with correspondingly greater heights, variability increases; over very long optical paths variability increases still further: fades of 30 decibels lasting a few minutes are not uncommon while fades of 10 decibels lasting an hour may occur in fine weather. Atmospheric absorption is unimportant at 9 centimeters over a path of 100 miles. Short-period fading on 9.2 centimeters is quite different from that on 10.0 centimeters though general trends are similar.

For optical paths over land up to 50 miles, results are similar to those for sea except for unexpectedly low, steady levels over some short paths, possibly due to interference. Variations are greatest at night. For nonoptical paths over sea, the minimum signal level (when measurable) was usually close to that calculated for a standard atmosphere; the maximum approaches but rarely exceeds the level corresponding to free-space propagation. In anticyclonic weather with the wind mainly offshore, there tends to be a diurnal maximum in the afternoon and evening, and a minimum in the early morning. For nonoptical paths over land results are similar to those for sea but less definite owing to geometrical uncertainties concerning the path. High diurnal levels occur during radiation-inversion nights, but overcast skies or wind suppress this variation.

Change of polarization had little effect; changes in bearing exceeding the measurement accuracy of about 1 degree were hardly ever observed. See also 517 above.

RECEPTION

621.396.62 519

Design and Application of Squelch Circuits—F. Delanoy. (*Radio*, vol. 30, pp. 11–13, 30; September, 1946.) Two main classes of squelch circuits are considered, namely, that in which a control voltage related to the amplitude of the input carrier immobilizes the receiver via an electromagnetic relay, and that in which the action is fully electronic. Examples from each class are briefly described. See also 520 below.

621.396.62 520

Notes on the Design of Squelch Circuits—F. Delanoy. (*Radio*, vol. 30, pp. 12–14; October, 1946.) Descriptions of various interchannel noise-suppression circuits for frequency-modulation receivers, including blocked audio-frequency circuits, reflected-impedance squelch circuits, and squelch oscillators. The severe distortion due to signal levels, which partially operate the squelch tube but do not suppress reception completely, can be overcome by using an adjustable threshold control, or a squelch disabling switch. See also 519 above.

621.396.62:621.317.755 521

Panadaptor—Panoramic Radio Corporation. (*Rev. Sci. Instr.*, vol. 17, p. 285; July, 1946.) An instrument for panoramic reception, which may be attached to communications receivers with intermediate-frequency of 450–470 kilocycles. The bandwidth is adjustable from 200 kilocycles down to zero. Many applications are indicated, including three-station communication, air-traffic control when an aircraft transmitter is off frequency, detection of frequency shift, and study of signal characteristic.

621.396.621 522

Designing the Postwar Receiver—B. Halligan and C. Read. (*Radio News*, vol. 36, pp. 50–51, 110; October, 1946.) The receiver described provides amplitude modulation or continuous-wave reception from 540 kilocycles to 110 megacycles and frequency-modulation reception from 27 to 110 megacycles. This wide coverage is obtained by the use of a new radio-frequency "split-stator" circuit. Other features of the receiver circuit are described briefly.

621.396.621.029.62 523
Super-Regenerative 2 Meter Receiver—J. A. Kirk. (*Radio News*, vol. 36, pp. 30–31, 108; October, 1946.) General remarks on the performance of superregenerative receivers and details of a suitable circuit for such a receiver operating at very-high-frequency.

621.396.621.54 524
Zero Tracking Error in Superheterodynes—A. Bloch. (*Wireless Eng.*, vol. 23, pp. 328–329; December, 1946.) Describes a pair of LC circuits which give zero tracking error over the entire tuning range. This is obtained by simultaneous variation of L/C such that the ratio LC remains constant. A first-order deviation from this constant ratio leads only to second-order tracking errors. The treatment is theoretical, but the principle has been successfully applied in a practical case.

621.396.813:534.78 525
Effects of Amplitude Distortion upon the Intelligibility of Speech—Licklider. (*See* 338.)

621.396.822:621.385.032.21 526
Radio Design Worksheet No. 52: A. C. Filament Noise—(*Radio*, vol. 30, p. 20; September, 1946.) The nature of the interfering voltages introduced into the anode current of a directly heated tube operated with an alternating-current filament supply is considered.

STATIONS AND COMMUNICATION SYSTEMS

621.394/.396[.7.029.58 527
Radio Stations near Toulouse—C. Cardot and M. Bergeron. (*Onde Élect.*, vol. 26, pp. 318–330; August–September, 1946.) Describes a system of radio stations planned as a Government communication headquarters and partially constructed despite the German occupation, operating in the wave-length range 13 to 60 meters.

621.394.441 528
Performance Characteristics of Various Carrier Telegraph Methods—T. A. Jones and K. W. Pfleger. (*Bell Sys. Tech. Jour.*, vol. 25, pp. 483–531; July, 1946.) On-off, single sideband, and one- and two-source frequency shift methods were considered to determine their relative advantages from the standpoints of signal speed, sensitivity to level change, carrier-frequency drift, interchannel interference, and line noise. For stable, quiet circuits the on-off system is the most suitable, but the other systems may result in improvement under certain adverse conditions. Numerous graphical results are summarized in tabular form.

621.395/.396[.7 529
R.M.S. Queen Elizabeth—(*Wireless World*, vol. 52, pp. 357–358; November, 1946.) A general description of equipment carried, which includes: a ship-to-shore radio telephone system; lifeboat radio equipment; a low power system for communication between pilot and tugs when docking; Gee, loran, and other navigational aids; and a public address system.

621.395(7) 530
Telecommunications Developments—(*Electrician*, vol. 137, pp. 935–936; October 4, 1946.) Summary of a report on the visit of British Post Office Officials to North America. Recent developments here include a new automatic telephone system using the "cross bar" switch; equipment for use on coaxial cables; mobile telephones for motor cars; temporary splitting of trunk circuits; and an automatic (trunk-call) ticketing system. Experiments were in progress to develop telephones for communication between train driver and guard, and for shunting.

621.395.44 531
New Single Channel Carrier Frequency Telephone System for Open-Wire Lines—E. Eklund. (*Ericsson Rev.*, vol. 23, no. 3, pp. 259–266; 1946.) A new system ZAF11 has been developed replacing the older ZL400 (described in *Ericsson Rev.*, no. 2, 1936). The dimensions and weight of the new system are considerably reduced. The range is 700 kilometers without intermediate repeaters when using an open-wire circuit of copper wires 3 millimeters in diameter.

621.396:629.13 532
Aviation Radio Equipment—(*See* 421.)

621.396.004.67:629.135 533
Airline Radio Service—E. D. Padgett. (*Radio Craft*, vol. 18, pp. 20–21, 53; October, 1946.) A table of common faults, probable causes, and remedies is given, together with miscellaneous suggestions for preventive maintenance.

621.396.1:621.396.933.1/.4 534
International Conference on Air Routes over Europe and the Mediterranean (Paris, April–May, 1946)—Dalle. (*Onde Élect.*, vol. 26, pp. 299–300; July, 1946.) Among the subjects discussed were the provision of various aerodrome and ground facilities, and the allocation of frequencies for telecommunications, navigation systems, and distress signals.

621.396.33.029.3.083.7:656.2 535
Train Position Indicator—E. A. Dahl. (*Electronics*, vol. 19, pp. 122–124; October, 1946.) Outline description of an audio-frequency system in which the times of arrival of trains at chosen points and departures therefrom, are recorded on paper in a remote signal-box.

621.396.4:551.509 536
AACS Radioteletype Weather Transmission System—F. V. Long. (*Communications*, vol. 26, pp. 16, 55; September, 1946.) The frequency-shift system as used by the United States Army Air Force for transmission of weather reports is illustrated with the aid of block diagrams. Methods used during the first weather broadcasts by radioteletype, with intercept receiving installations at smaller airfields and the operational difficulties of simplex systems are described. An analysis is made of improved results obtained from full duplex operation.

621.396.41:621.398 537
Test Shows how Wire-Carrier and Beamed Radio Direct Signals and Train Operation—(*Telegr. Teleph. Age*, vol. 64, pp. 5–6, 30; October, 1946.) Demonstration of the application of existing wire-carrier and centimeter-wave multiplex communication circuits to the operation of signals and points of a railway system at very long ranges from a control signal box. Signals from the control box were sent by a roundabout route about 900 miles long to operate signals and points some 60 miles distant. The significance of the tests is briefly discussed.

621.396.44:621.315.211.9.052.63 538
Carrier-Current Communication on Air and Paper Insulated Cables—Lucantonio. (*See* 352.)

621.396.619 539
High Efficiency Modulating Method—J. Beckwith. (*Radio*, vol. 30, pp. 9–11, 32; October, 1946.) Amplitude modulation is achieved by shifting the phase of the carrier frequency at an audio-frequency rate and combining the phase-shifted carrier with the unmodulated carrier, producing a resultant varying in amplitude as the phase is shifted. The magnitude and spread of the phase-modulation side-bands (which accompany the amplitude-modulation side-bands in the radio ated signal), are not excessive by Federal Communications Commission regulations. Circuit diagrams are given for a 4.5-kilowatt transmitter.

621.396.65 540
Hertzian Cable [Radio Links in Multichannel Telephony Circuits]—A. G. Clavier and G. Phélizon. (*Onde Élect.*, vol. 26, pp. 331–334; August–September, 1946.) Discussion of the application of frequency-modulated centimeter-wave radio links to multichannel telephony circuits, followed by a general description of a twelve-channel link about 10 miles long between Paris and Montmorency (*See also* 3743 of January). In this circuit, transmission in one direction is horizontally polarized on a wavelength of 9 centimeters, with vertical polarization on 10 centimeters in the reverse sense. Separate horns having beam widths of the order of 10 degrees are used for transmission and reception. The radio link is designed for direct insertion in a carrier telephony circuit, the twelve speech channels occupying the frequency band 12 to 60 kilocycles. At the transmitter a velocity modulated oscillator developing about 30 watts of radio-frequency power is used. The speech-modulated carriers are used for frequency modulation of the oscillator which has a sensibly uniform characteristic for a frequency range of about 1 megacycle. Superheterodyne receivers having positive grid oscillators and diode mixers are used. Extensive application is made of negative feedback technique in transmitters and receivers to maintain linearity and stability of operation; the principles involved are discussed in some detail. The possible future development of radio links for transmission of wide-band intelligence is outlined; the attenuating effects of constituents of the atmosphere at centimeter wavelengths are briefly mentioned.

621.396.712.004.5 541
Preventive Maintenance for Broadcast Stations: Part 4—C. H. Singer. (*Communications*, vol. 26, pp. 36, 38; September, 1946.) A discussion of "seven basic preventive maintenance procedures . . . feel, inspect, tighten, clean, adjust, lubricate, and measure." For part 3 see 3423 of 1946.

621.396.712 542
Radio Stations [Book Notice]—Federal Communications Commission, 26 pp., $.10. (*U. S. Govt. Publ.*, no. 618, p. 777; July, 1946.) Standards of good engineering practice concerning frequency-modulation broadcast stations, revised to January 9, 1946.

SUBSIDIARY APPARATUS

621–526 543
Dimensionless Analysis of Servomechanisms by Electrical Analogy—S. W. Herwald and G. D. McCann. (*Trans. A.I.E.E.* (*Elec. Eng.*, October, 1946), vol. 65, pp. 636–639; October, 1946.)

621.314.6+621.319.4+621.383]:669.018 544
Light Alloys in Metal Rectifiers, Photocells and Condensers—Continuing the series in various issues of *Light Metals*. For previous parts see 3768 of January,

(vi) Vol. 7, pp. 565–566; December, 1944. Begins "a detailed consideration of the theory and practice of electrolytic capacitors."

(vii) Vol. 8, pp. 25–41; January, 1945. "An exhaustive discussion . . . on the theory, practice and operation of the electrolytic capacitor. In particular the properties of the aluminium-oxide film are considered."

(viii) Vol. 8, pp. 87–100; February, 1945. " . . . consideration is given to the theory and practice of the formation of electrolytes for

electrolytic capacitors, and to [their] design and production," with typical examples.

(ix) Vol. 8, pp. 193–202; April, 1945. "Discussion on the theory and practice of electrolytic capacitors."

(x) Vol. 8, pp. 246–254; May, 1945. Concludes (ix) and considers in detail fixed paper capacitors.

(xi) Vol. 8, pp. 292–304; June, 1945. Fixed paper capacitors, and the use of tin and aluminium foils, are discussed.

To be continued.

621.317.755.087.5 545

Recording of Transients—W. Nethercot. (*Elec. Times*, vol. 110, pp. 648–651; November 14, 1946.) For all except the highest writing speeds a sealed-off cathode-ray oscillograph with an accelerating voltage not less than 5 kilovolts and a blue-violet screen may be used. A camera with an *F*1.0, 2-inch-focus lens operating with an object versus image ratio of 4 or 5 to 1 and using a high-speed orthochromatic film is recommended. Thirteen prints with writing speeds up to 20,000 kilometers per second are shown.

621.318.42 546

Saturable Choke Controlled Rectifiers—H. S. Double. (*P.O. Elec. Eng., Jour.*, vol. 39, part 3, pp. 110–113; October, 1946.) Notes on the basic principles and capabilities of this form of control for direct-current power supplies

621.352.7 547

Miniature Dry Cell—(*Rev. Sci. Instr.*, vol. 17, pp. 286–287; July, 1946.) A dry cell having a high ratio of capacity to volume with long cell life has been developed for tropical use by P. R. Mallory and Co. Within its rating the cell has an ampere-hour capacity substantially independent of rate of discharge. Dimensions of cell are 1 inch in diameter and 5/8 inch high.

621.383 548

Various Papers on Electron Multipliers—(*See* 577–578.)

621.384 549

Various Papers on Electron Accelerators—(*See* 494–495.)

621.395.631.4 550

Recent Design of a Small Telephone Magneto—D. S. Smith. (*Canad. Jour. Res.*, vol. 24, pp. 406–408; September, 1946.) "An example is given of the product obtained by applying modern methods in permanent magnet design to the problem of constructing a hand-driven magneto of about flashlight battery size."

621.791.76 551

Miniature Spot-Welding Tools—R. W. Hallows. (*Wireless World*, vol. 52, pp. 373–374; November, 1946.) The tool, which is made by Siemens-Halske A.-G., is 10 inches long and 1 inch in diameter: the smaller model can be used for wire up to 0.8 millimeter diameter while the larger is for any joint whose surface area does not greatly exceed 10 square millimeters. Mains supply at 110 or 250 volts (50 cycles) can be used: the welding voltage does not exceed 35 volts.

TELEVISION AND PHOTOTELEGRAPHY

621.396.8:621.397.26 552

Television Link Tests in Southern California—P. B. Wright. (*Communications*, vol. 26, pp. 15, 55; October, 1946.) Report of experimental frequency-modulation television transmission and reception over 17.2-mile line-of-sight paths betwen Mt. Wilson (5700 feet) and Hollywood. In one case metallic lenses 5½ by 7½ feet with power gain about 35 decibels per lens were used; in the other, 57-inch parabolic reflector-type radiators, with gain 3 to 4 decibels less. Each lense gave an effective directed power of 1200 watts over that of an omnidirectional point source. This gives a sufficient margin even under severe fading conditions. The frequency-bands were 4416 to 4420 megacycles (reflectors) and 4376 to 4380 megacycles (lenses).

621.397.262 553

Approximate Method of Calculating Reflections in Television Transmission—D. A. Bell. (*Jour. I.E.E.* (London), part III, vol. 93, pp. 352–354; September, 1946.) An examination of the effects of "carrier frequency, size of reflecting obstacle, distance of reflecting obstacle from transmitter and from receiver, and degree of definition of the television picture, on the incidence of reflection troubles in television reception. The diffraction problem is treated by a simple mathematical approximation which has been previously used in optics."

621.397.5:532.62 554

Oil-Film Television—(*Radio Craft*, vol. 18, pp. 22–23; October, 1946.) An electron gun, modulated by incoming signals, scans 50 times a second the surface of a film of special liquid about 0.1 millimeters thick and deforms it in such a way that light from an arc lamp is allowed to pass on to a projection screen. The film rests on a glass plate, which is illuminated from below by focusing the arc lamp beam with mirrors and a lens. The deformation is increased by placing a charged electrode near the film and by charging the film uniformly with a second electron gun. The glass plate rotates uniformly, carrying the film, and provision is made for the film to be smoothed ready for further use.

621.397.6 555

U. S. Television Gear—(*Wireless World*, vol. 52, p. 380, November, 1946.) Description of an image orthicon camera developed by R.C.A. with a revolving lens turret, a device for rapid changing of lenses and a wide-band microwave relay link.

621.397.6 556

Surveying Recent Television Advances—R. B. Batcher. (*Elec. Ind.*, vol. 5, pp. 46–48, 106; October, 1946.) New cameras include the image-orthicon with a telephoto lens system while the iconoscope and the orthicon tubes have been improved. New tubes are now used in transmitters and receivers and relay systems involving airborne apparatus are being investigated. Mirror and lens systems are being used for large-screen projection and experiments with skiatrons are in progress. American television-frequency data are tabulated.

621.397.62 557

Rebuilding a Televiser—N. Chalfin. (*Radio Craft*, vol. 17, pp. 832, 881; September, 1946.) Describes methods of modernizing prewar television receivers; a circuit diagram indicates the changes necessary.

621.397.621 558

Deflector Coil Coupling—W. T. Cocking. (*Wireless World*, vol. 52, pp. 360–363; November, 1946.) A straightforward semigraphical method is described whereby curvature of tube characteristics may be used to compensate the nonlinear characteristics of the deflector coil to produce a linear saw-tooth output. A numerical example is fully discussed. See also 272 of February (Cocking).

621.397.74 559

Multi-Outlet T-V [Television]—(*Elec. Ind.*, vol. 5, p. 57; October, 1946.) Describes a system for providing a large number of television receivers with choice of program. The programs are received by suitable aerial systems and passed through single-tube amplifiers into a common concentric line. Attenuating pads at each receiver prevent mutual interference.

TRANSMISSION

621.396.61:621.396.619.018.41 560

Direct F.M. Transmitters: Part 9—N. Marchand. (*Communications*, vol. 26, pp. 26–29, 35; September, 1946.) Design principles are considered with the aid of block and circuit diagrams. Input capacitance, phase discriminator exciter, and pulse control exciter units are discussed. For part 8 see 3452 of 1946.

621.396.61:621.396.619.018.41 561

Mobile F.M. Transmitters: Part 10—N. Marchand. (*Communications*, vol. 26, p. 30; October, 1946.) The advantages of frequency-modulation are briefly stated and a 25- to 50-watt mobile transmitter on 30 to 44 megacycles is described. For earlier parts see 560 above and back references.

621.396.61:621.396.721 562

An Auxiliary Radio Transmitter for Broadcast Service—C. A. Cullinan. (*Proc. I.R.E.* (Australia), vol. 7, pp. 4–11; September, 1946. Discussion, pp. 11–12.) Designed and constructed with available war-time material, the circuit consists of a crystal-controlled oscillator, a single radio-frequency buffer stage, and a class-C amplifier with a class-B modulator (anode modulation). The carrier power was 125 to 150 watts, capable of 100 per cent modulation. The audio-frequency response was "within 0.5 decibels from 40 to 10,000 cycles and within 2 decibels down to 30 cycles." Distortion and noise were virtually nonexistent. A 56-foot vertical radiator was used, and the transmitter could be in operation in less than a minute.

621.396.61:621.396.97 563

Experimental 88 to 108-Mc 250-Watt F.M. Broadcast Transmitter—J. H. Martin. (*Communications*, vol. 26, pp. 22–24, 45; September, 1946.) Main features include the Armstrong phase-shift system modulator, with the center carrier frequency directly controlled by crystal for stability reasons. The complicated modulator system is explained fully. The power amplifier comprises 4-125A-type tetrodes, neutralized by tuning the screen inductance to earth by means of a split-stator capacitor.

621.396.61[(43)+(44)+(73)]"1939/45" 564

Transmitting Equipment of the French, German, and American Armies—R. Besson. (*Toute la Radio*, vol. 13, pp. 31–35; January, 1946.) An account of the special features of various types of equipment handled by a French technician between 1939 and 1945. The great tactical superiority of the frequency-modulation apparatus used by the Americans is stressed.

621.396.61.029.56/.58 565

Top-Band Two Transmitter—J. N. Walker. (*R.S.G.B. Bull.*, vol. 22, pp. 66–69, 75; November, 1946.) Description of a self-contained low-power transmitter for use on 1.8, 3.5, and also on 7.5 megacycles at somewhat reduced efficiency. Constructional details, a circuit diagram, and a list of components are given.

621.396.61.029.62 566

A 100-kW Portable Radar Transmitter—H. L. Lawrence. (*Communications*, vol. 26, pp. 30, 33; September, 1946.) The unit contains the radio-frequency power-oscillator modulator, high-voltage power supply, and a wavemeter for frequency measurement. Frequency range is 225 to 250 megacycles mean power output, 40 watts; pulse shape, half sine wave; pulse length, 1.6 microseconds; and recurrence frequency, 600 cycles. Primary power is obtained from a petrol driven generator. Special air cooled oscillator tubes 4C27, are used in a grounded plate circuit, and the frequency is controlled by a variable inductance in the grid circuit. The cathode is tuned by a parallel

wire transmission line, to which the antenna is directly coupled. "The radio-frequency oscillator is plate-modulated by a gas-discharge tube pulse-forming circuit."

621.396.619.018.41.029.6 567

Über Frequenzmodulatoren für Ultrahochfrequenz [Book Review]—G. Weber. Gebr. Leemann, Zürich, 95 pp., Swiss Fr. 9. (*Wireless Eng.*, vol. 23, p. 340; December, 1946.) "... deals with the difficulties of applying frequency modulation to transmitters working at frequencies of 100 to 600 megacycles."

VACUUM TUBES AND THERMIONICS

537.533.7 568

Electron-Optical Properties of Emission System—L. A. Artsimovich. (*Bull. Acad. Sci.* (U.R.S.S.), sér. phys., vol. 8, no. 6, pp. 313–329; 1944. In Russian.) Apparatus in which an electron-optical image of an object emitting slow electrons is obtained can be divided into three classes according to whether the image is (a) greatly magnified, e.g., in emission electron microscopes used for studying thermo- and photo-cathodes, (b) of approximately the same dimensions as the object, e.g., in devices used in television, or (c) reduced to a point, e.g., in the electron gun. A brief survey of each class is given. This is followed by a detailed mathematical analysis of the formation and focusing of electron beams by electrostatic methods. Equations are derived determining the trajectories of the electrons and approximate solutions indicated. Chromatic aberration, transverse as well as longitudinal, is calculated, and the plane of the optimum image found. The depth of focus, determining the accuracy of focusing, is examined. Further possible defects of electron-optical systems, such as spherical aberration, curvature of the image, and astigmatism, are also discussed. A technically ideal system would use purely electrostatic focusing, with two electrodes only. An analysis of its operation is given and possible applications are discussed.

537.533.7:621.383 569

The Electron-Optical Properties of the Magnetic Tube (Electron Multiplier) of Kubetski—C. R. Rik. (*Bull. Acad. Sci.* (U.R.S.S.) sér. phys., vol. 8, no. 6, pp. 366–369; 1944. In Russian.) A detailed investigation of the tube was carried out and in this paper a brief summary of the results obtained is given. The equipotential lines of the electric field and the electron trajectories in the region of the cathode are plotted. The absence of an accelerating field near the cathode and the lack of co-ordination between the fields result in a useless dispersion of a large number of photoelectrons. The curves of focusing in the longitudinal direction are shown. The variation in the size of the emitting rings (they become wider beginning from No. 12 ring) is not adjusted to the longitudinal gradient of the magnetic field with the result that further dispersion of electrons occurs. The electron trajectories near the anode are shown in Fig. 3. The diffusion of the magnetic field in this region obstructs the collection of electrons at the anode. The general conclusion reached is that electron-optical properties of the tube are rather poor, but that they could be improved by modifying the operating conditions and altering certain constructional details. See also 577 below (Kubetski).

537.533.8 570

On the Secondary Electron Emission from Solid Bodies—S. Y. Luk'yanoff. (*Bull. Acad. Sci.* (U.R.S.S.), sér. phys., vol. 8, no. 6, pp. 330–339; 1944.) In Russian.) A general theory of the phenomenon based on modern conceptions and experimental data is presented. The penetration of a primary electron into a solid body is discussed and processes determining the appearance and intensity of secondary emission are examined in detail. It is shown that the shape of the $(\sigma, E\rho)$ curve is determined mainly by the ionizing effect of the primary electron (proportional to the total loss of energy per unit length) in the layer from which secondary electrons are emitted. The possibility of an experimental verification of this statement is indicated and results obtained by other investigators are quoted. A table of the latest reliable data on secondary emission for various metals is given, whence it appears that σ_{max} is low for all metals and that there is no direct relationship between it and the work function. It is suggested that the variation of σ_{max} for various metals is determined by the effect of bound electrons in the metal, and by the number of atoms per unit volume. Finally, the secondary emission from semiconductors and dielectrics is examined. Although not every semiconductor or dielectric has a σ_{max} exceeding those for pure metals, materials with very high values of σ_{max} must necessarily be semiconductors or dielectrics. The reasons for this are suggested and experimental data for some of the materials are quoted. Reference is made to the possibility of increasing the secondary emission of a material with high resistance by electron bombardment which causes the appearance of surface charges on the material. This effect is utilized in various devices, such as electron multipliers, but the author is not inclined to regard it as important. An Abstract in English was noted in 2074 of 1946.

537.533.8 571

The Effect of Strong Electric Fields on the Secondary Electron Emission from Thin Dielectric Films—D. V. Zernoff. (*Bull. Acad. Sci.* (U.R.S.S.), sér. phys., vol. 8, no. 6, pp. 352–356; 1944. In Russian.) As a result of the action of an electron beam on a thin film of dielectric deposited on a metallic base, a strong field is built up in the film affecting in a number of ways the characteristics of the emitter. The effects of the field are enumerated and, in order to clarify the processes taking place in the film, a mathematical analysis is presented of the energy spectrum of the system metal-dielectric-vacuum (Fig. 1). Experiments carried out with the MgO and Al_2O_3-Cs_2O emitters are described, and the possibility of obtaining large secondary currents, especially in the form of short impulses, is indicated. An abstract in English was noted in 2075 of 1946.

537.533.8:621.385 572

Electronic Apparatus with Effective Emitters of Secondary Electrons—R. M. Aranovich. (*Bull. Acad. Sci.* (U.R.S.S.), sér. phys., vol. 8, no. 6, pp. 346–351; 1944. In Russian.) Emitters prepared by evaporating magnesium and other metals in dry oxygen are briefly discussed. The effects of various gases, of materials used for bases, of the velocity of primary electrons, of the conditions under which the evaporation of the metal is carried out, and of the manner in which the secondary voltage gradient is built up were investigated and experimental curves were plotted. Emitters with $\sigma = 80$ were produced and even with $\sigma = 100$–10,000, although in the last case inertia of secondary emission was observed. The breakdown of the emitters is discussed, and microphotographs showing their structure are included. An interpretation of the experimental results is offered. The operating data of a photocell and a tube with one stage of amplification are given. An abstract in English was noted in 2390 of 1946.

537.533.8:621.385.1.032.216 573

The Emission from an Oxide Cathode under the Application of an Impulse Voltage—A. M. Andrianoff. (*Bull. Acad. Sci.* (U.R.S.S.), sér. phys., vol. 8, no. 5, p. 290; 1944. In Russian.) A preliminary note on an experimental investigation in which it was found that if an impulse voltage at a frequency of 50 pulses per second is applied to the anode of a diode with an oxide cathode, the emission from the latter at the normal temperature of 850 to 900 degrees centigrade is enormously increased and reaches the value of 30 amperes per centimeter squared. An abstract in English was noted in 2076 of 1946.

621.314.653 574

Excitation, Control, and Cooling of Ignitron Tubes—C. C. Herskind and E. J. Remscheid. **Rectifier Capacity**—C. C. Herskind and H. C. Steiner. (*Trans. A.I.E.E.* (*Elec. Eng.* October, 1946), vol. 65, pp. 632–635 and 667–670; October, 1946.) The first paper describes the control, limitations, and operating requirements of mercury-arc tubes of the ignitron type, while the second paper deals with the load-time and volt-ampere characteristics of these tubes, the relations between these characteristics and the factors affecting them.

621.314.67:621.357.1:666.1 575

Electrolysis Phenomena in Soft-Glass Stems of Rectifier Tubes—Gallup. (*See* 447.)

621.319.7:621.385 576

Plotting Electrostatic Fields—Silva. (*See* 446.)

621.383 577

Some Conclusions Reached from the Use of Secondary Electron Multipliers—L. A. Kubetski. (*Bull. Acad. Sci.* (U.R.S.S.) sér. phys., vol. 8, no. 6, pp. 357–365; 1944. In Russian.) Since the first attempts by the author in 1934 to use secondary emission for the amplification of the primary electron current, a large amount of work both experimental and theoretical has been carried out. In the present paper the results achieved are systematized and further lines of development indicated. The specific requirements for electron multipliers are enumerated and reference is made to the type evolved by the author to meet these requirements. A logical basis for further search of suitable emitters is elaborated; those of the Cu-S-Cs type developed by the author are described. Criteria determining the quality of electron multipliers are established. The maximum amplification and the threshold of sensitivity of multipliers are also discussed. An abstract in English was noted in 2029 of 1946.

621.383 578

Electron Multipliers—E. G. Kormakova. (*Bull. Acad. Sci.* (U.R.S.S., sér. phys., vol. 8, no. 6, pp. 370–372; 1944. In Russian.) Since systems with a magnetic field are not convenient in use, only systems with an electrostatic field were considered. It was found that focusing was best achieved by means of grids. Accordingly, a multiplier with a cylindrical grid and using caesium oxide cathode and emitters was developed. Equipotential lines and lines of force are plotted by a graphical method of successive approximation. Various characteristics of the multiplier are shown and operating data given. An abstract in English was noted in 2028 of 1946.

621.385 579

On the Flow of High-Frequency Currents Through Electronic Apparatus—S. D. Gvozdover. (*Bull. Acad. Sci.* (U.R.S.S.), sér. phys., vol. 8, no. 5, pp. 267–274; 1944. In Russian.) It is not always possible, in designing high-frequency apparatus, to regard $\beta = \omega T_0$ as a small quantity where ω is the frequency and T_0 the traveling time determined by the constant voltages. Solutions for any value of θ can be obtained in all cases without much difficulty if the approximate solution derived by expansion in series are modified in accordance with La-

place's transformation. It is assumed that the electron stream passes between flat electrodes, and that the electron velocity is a single-valued function of the co-ordinates, i.e., that the electrons cannot overtake one another.

Equations (1–4) determining the movement of the electrons between the electrodes are given, and an approximate solution (14) is derived by expansion. Laplace's transformation is applied to this solution, and a modified formula (15) is derived which is more suitable for calculations. The results obtained are used in a discussion divided into the following sections: (a) the determination of the current in the external circuit, and of the power consumed; (b) the determination of the self-excitation regions in the case of a single-circuit klystron (monotron); (c) the determination of the dielectric constant of an electron gas; (d) an analysis of the rectification of high-frequency currents in a diode; and (e) the calculation of the amplitude of stationary oscillations in a monotron. An abstract in English was noted in 2389 of 1946.

621.385 580

The Role of Surface Charges in Electronic Apparatus—P. V. Timofeeff. (*Bull. Acad. Sci.* (U.R.S.S.), sér phys., vol. 8, no. 6, pp. 340–342; 1944. In Russian.) While the effects of space charges are widely used in electronic apparatus, little attention has been paid to the possibility of utilizing charge appearing on the surface of insulators inside the apparatus. Normally, these charges are formed as a result of secondary emission from the insulators, caused by electron bombardment. An insulator can thus be charged to a high positive potential and the following three possible applications of this effect are indicated: (a) an insulator mounted near the cathode and acquiring a high positive charge may produce a potential gradient sufficient for cold emission of electrons from the cathode; (b) the high secondary emission from caesium-oxide cathodes is probably due to the presence of dielectric particles in the cathodes, which may acquire positive charges (Fig. 1); this opens a possibility for a further increase in the secondary emission; and (c) positive charges also would assist photoemission from caesium-oxide cathodes which may be achieved by making this effect more pronounced. An abstract in English was noted in 2388 of 1946.

621.385 581

The Mechanism of the Operation of Kenotrons with Cold Cathodes—V. V. Sorokina. (*Bull. Acad. Sci.* (U.R.S.S.), sér. phys., vol. 8, no. 6, pp. 343–345; 1944. In Russian.) A brief description is given of a kenotron developed in Russia and consisting essentially of a nickel cylinder (the anode) in a cylindrical glass envelope on which a layer of caesium oxide (the cathode) is deposited. A characteristic of the kenotron is plotted and discussed. An abstract in English was noted in 2387 of 1946.

621.385:519.24 582

Analysis of Special Electronic-Tube Tests—J. H. Campbell and C. G. Donsbach. (*Trans. A.S.M.E.* vol. 68, pp. 481–486; July, 1946.) Illustrates the improvements in tube manufacturing technique which may be accomplished by controlled tests on tubes in the course of production, followed by statistical analysis of the results.

621.385:621.317.723 583

Improvements in the Stability of the FP-54 Electrometer Tube—J. M. Lafferty and K. H. Kingdon. (*Phys. Rev.*, vol. 69, p. 699; June 1–15, 1946.) Greater stability was obtained by increasing the action time from 8 to 40 minutes. Filament end shields also reduced rapid fluctuations. A special split tube using both oxide-coated and thoriated tungsten filaments was made which eliminated long-term drift in a bridge circuit and reduced rapid fluctuations tenfold. Summary of American Physical Society paper.

621.385:621.395.613 584

"Vibrotron" Tube—Radio Corporation of America (*Rev. Sci. Instr.*, vol. 17, p. 282; July, 1946.) A small electron tube for translation of mechanical motion into variable electron flow, which can be used in microphones. When used in a gramophone pickup it is claimed that the tube will perform up to the highest requirements of fidelity and sensitivity. The tube is a metal triode about 1 inch in length, and $\frac{1}{4}$ inch in diameter weighing 1/15 of an ounce.

621.385.029.63/.64 585

The Traveling Wave Valve—R. Kompfner. (*Wireless World*, vol. 52, pp. 369–372; November, 1946.) Amplification in transit-time tubes may be greatly increased if a field traveling at the speed of the electrons is used instead of a stationary electric field. By this means electron acceleration is obtained in both half cycles of the wave. Such a field can be produced if the signal travels along a helix of suitable dimensions. The presence of the electron beam also causes amplification in the wave itself; hence, the helix-electron-beam system is an amplifier. Experimental data on this type of tube are briefly mentioned, and future applications, including television and ultra-high-frequency transmissions, suggested.

621.385.029.63/.64] 586

Traveling Wave Tubes—M. A. Barton. (*Radio*, vol. 30, pp. 11–13, 32; August, 1946.) A simple description of the new centimeter-wave tube, in which an electron beam is transmitted along the axis of a long narrow helix, which acts as a wave guide with a low velocity of propagation. The tube gives high gain over a broad band in the region of 4000 megacycles. For another account see *Elect. World*, vol. 126, pp. 20–21; September 21, 1946.)

621.385.1 587

The Theory of a Reflex Klystron—S. Gvozdover. (*Zh. Eksp. Teor. Fiz.*, vol. 15, no. 9, pp. 521–531; 1945. In Russian.) The resonant frequencies of a reflex klystron are calculated as a function of its dimensions and the applied voltages. Graphs and formulas for computation are given.

621.385.1 588

The Maximum Efficiency of Reflex Oscillators—E. G. Linder and R. L. Sproull. (*Phys. Rev.*, vol. 69, p. 700; June 1–15, 1946.) A formula is given for maximum efficiency with optimum electron bunching and loading. Possible methods of increasing efficiency are investigated. Summary of American Physical Society paper.

621.385.12:621.396.822 589

Cold-Cathode Gas Tubes as Noise Generators—S. Ruthberg. (*Phys. Rev.*, vol. 70, p. 112; July 1–15, 1946.) A glow tube, a mercury arc with mercury-pool electrodes, and a corona discharge monode were examined. The glow tube gave spectra from .05 to 5 megacycles, and oscillations and noise were affected by a transverse magnetic field. See also 3267 of 1946 (Gallagher and Cobine). The mercury arc was not sufficiently stable for quantitative measurements, and the corona monode gave noise of a steep pulse character. Summary of an American Physical Society paper.

621.385.16 590

How the Magnetron Works—"Radionyme." (*Toute la Radio*, vol. 13, pp. 26–28; January, 1946.) The performance of three types is noted: (a) British, with 8 resonant cavities, 100-kilowatt peak power, 1-microsecond pulses, 600 pulses, wavelength 9 centimeters, 15-kilovolt anode voltage, 20-amperes anode current, magnetic field 1700 oersteds, and efficiency 30 per cent; (b) Russian, with 116 watts on continuous wave at wavelength 9 centimeters, and efficiency 22 per cent; and (c) German, with peak power 8 kilowatts and wavelength 1.75 centimeters.

621.385.8:538.6 591

Magnetically-Controlled Gas Discharge Tubes—R. E. B. Makinson, J. M. Somerville, K. R. Makinson and P. Thonemann. (*Jour. Appl. Phys.*, vol. 17, pp. 567–572; July, 1946.) In these tubes, a glow discharge is initiated by means of a magnetic field pulse. Ions from this discharge produce an arc spot on the pool of mercury through which the main current passes. A current pulse of 200 amperes of duration 1 to 10 microseconds can be used.

621.385.8.032.21:537.525.83 592

The Normal Cathode Fall for Molybdenum and Zirconium in the Rare Gases—T. Jurriaanse, F. M. Penning, and J. H. A. Moubis. (*Philips Res. Rep.*, vol. 1, pp. 225–238; April, 1946.) In gas discharge tubes with molybdenum or zirconium cathodes greater stability of the voltage maintaining the discharge has been obtained by sputtering the cathode material over the whole of the walls of the tube. The action of this metallic layer is thought to be partly due to absorption of gases released from the walls during the discharge and partly to its screening action which prevents the liberation of such gases.

621.385.82.029.3:621.395.61 593

[The Development of] a High-Power Thermionic Cell using Positive Ion Emission and Operating in a Gaseous Medium—M. S. Klein. (*Onde Élect.*, vol. 26, pp. 367–373; October, 1946.) The cell is small, cylindrical in shape and comprises an axial heater surrounded by a ceramic sheath on the outer surface of which finely divided platinum is deposited. This anode is surrounded by a silver cylindrical cathode; the interlectrode spacing is about 1 millimeter. Positive ion currents of the order of several tens of microamperes are produced at atmospheric pressure for a polarizing voltage of a few hundred volts. Since the current depends on pressure, the cell may be used as a microphone at audio and subaudio frequencies. Conversely, the cell may be used as a loudspeaker, since energy from the pulsating ion stream is lost to the air molecules. A 'triode' version of the cell is also described for the loudspeaker application. The pressure versus current characteristic for the diode is given.

621.385(075) 594

Elektronenröhren [Book Review]—A. Daeschler. Archimedes Verlag, Zürich, 1945, 104 pp., Swiss Fr. 6.80. (*Tech. Wet. Tijdschr.*, vol. 15, p. 50; April–May, 1946. In Flemish.) First of a series of textbooks on radio intended for the radio serviceman.

MISCELLANEOUS

001.8 595

Scientific Information Services—(*Nature* (London), vol. 158, pp. 353–356; September 14, 1946.) Editorial on the report of the Royal Society on needs of postwar research, with special reference to publication and scientific intelligence. It is estimated in the report that in physics and chemistry alone at least two thousand papers will now be released for publication but cannot be published without substantial assistance from Treasury funds.

00.189:621.396 596

The 7th General Assembly of the International Radio-Scientific Union—A. Haubert. (*Onde Élec.*, vol. 26, pp. 391–393; October, 1946.) Held in Paris, September 27, to October

5, 1946. Committees were set up on measurements, propagation (ionospheric and tropospheric), atmospherics and radiophysics.

535.65:001.4 597
International Names in Colorimetry—P. Moon and D. E. Spencer. (*Jour. Opt. Soc. Amer.*, vol. 36, pp. 427–428; July, 1946.) A study of internationality in the endings of scientific words shows that the following endings are ordinarily used with the same meanings in most of the languages of Europe and America: *-or* = a device, *-tion* = a process, *-ance* = a passive property of a device and *-ity* = a passive property of a substance." "Thus these endings may be regarded as international, and their use in the coining of new scientific terms should be encouraged.

6(43) 598
A Classified List of Industrialists' Reports on Germany [up to July 27, 1946]—CIOS, BIOS, FIAT, and JIOA. Obtainable from H.M. Stationery Office. Section *F* covers electrical engineering industry, including radio; Section *D* includes plastics; Section *G*, glass and ceramics; and Section *K*, metals.

620.193.8(213) 599
The Deterioration of Materiel in the Tropics—Hutchinson. (*See* 438.)

621.3:371.3 600
Post-Graduate Courses in Electrical Engineering, including Radio—(*Jour. I.E.E.* (London), part III, vol. 93, pp. 363–364; September, 1946.) Summary of Institution of Electrical Engineers Radio Section discussion led by W. Jackson and T. Greig on the "means by which qualified electrical engineers might acquire and sustain, an intimate knowledge of the particular branches of the subject in which their individual contributions [are] to be made." See also 2435 of 1946.

621.38/.39+331(07):621.3 601
Post War Development Report—(*Jour. Brit. Instn. Radio Eng.* vol. 4 pp. 135–161; October–December, 1944.) In part 1 the whole field of electronics is briefly surveyed, and the outstanding problems in each branch are mentioned. In part 2 the provision of staff for the development program, and their education and training, are discussed.

621.395(091) 602
A Critical Review of the History of the Controversy Concerning the Invention of the Telephone Examined in the Light of Contemporary Literature—C. Frachebourg. (*Tech. Mitt. Schweiz. Telegr.-Teleph Verw.*, vol. 24, pp. 36–42; February 1, 1946. In French.)

621.396.9 603
I.E.E. Radiolocation Convention, March, 1946—(*Jour. I.E.E.* (London), part I, vol. 93, October, 1946.) Summaries of the survey papers read at the convention are given. A bibliography of the remaining papers conconnected with the convention is also included; these papers together with fuller versions of the survey papers, are being published in *Jour. I.E.E.* (London), part IIIA, vol. 93, 1946, and will be abstracted in due course.

621.882.082.2 604
The Unification of Screw-Thread Practice—(*Engineering* (London), vol. 162, pp. 253–254: September 13, 1946.) Proposal for a modification of the standard Whitworth thread, to one of 60-degree angle with flat or rounded crests, and rounded roots.

621.38(02) 605
An Introduction to Electronics [Book Review]—R. G. Hudson. Macmillan, New York 93 pp., $3.00. (*Proc. I.R.E.* (Australia), vol. 7, p. 31; October, 1946.)

621.396 606
The Wireless Trader Books [Book Notice]—Iliffe and Sons, London, 1946, 160 pp., 10s. 6d. (*Electrician*, vol. 137, p. 185; July 19, 1946.)

621.396 607
Radio [Book Notice]—National Bureau of Standards, 87 pp. (*U. S. Govt. Publ.*, p. 730; July, 1946.) Revised classification of radio subjects, dated January 11, 1946.

621.396 608
Précis de Radio Électricité [Book Review]—E. Divoire. Éditions Desoer, Liège, 1945, 222 pp., 171 figs. (*Tech. Wet. Tijdschr.*, nos. 10–12, p. 114; October–December, 1945. In Flemish.) " . . . A survey of the theory and applications, addressed to engineers, scientists and university students, who wish to extend their knowledge to this new field. . . . "

621.396(075) 609
Experimental Radio [Book Review]—R. R. Ramsey. Ramsey Publishing Co., Bloomington, Indiana, fourth edition, 1937, 196 pp., $2.75. (*Proc. I.R.E.* (Australia), vol. 7, p. 29; September, 1946.) "Very little theory appears in the text, it being the aim of the author to make the student think for himself." A very practical and useful book, "which does not suffer as a result of the age of its subject matter."

621.396.029.6 610
Ultra-High-Frequency Radio Engineering [Book Review]—W. L. Emery. Macmillan, New York, 1944, 281 pp., $3.25. (*Proc. I.R.E.* (Australia), vol. 7, pp. 37–38; September, 1946.) " . . . The treatment is generally fairly simple and confined to basic principles."

New England Radio Engineering Meeting

On May 17, 1947, in Cambridge, Massachusetts, there will be an all-day New England Radio Engineering Meeting under the sponsorship of the North Atlantic Region of The Institute of Radio Engineers.

All persons interested in radio and electronic engineering are cordially invited to attend. There will be six technical sessions, none held concurrently, exhibits by the leading manufacturers in New England, a luncheon and a banquet with entertainment.

The entire program will be held at the Continental Hotel, Cambridge, Massachusetts. A complete program announcement will be made in April.

Your are cordially invited—May 17, 1947—Cambridge, Massachusetts.

❖

Georgia Radio Broadcast Engineering Institute

A Radio Broadcast Engineering Institute will be held in Atlanta, Georgia, April 14–18, 1947. The general chairman is Professor Martial A. Honnell (A'40), of the Georgia School of Technology, which is sponsoring the Institute in co-operation with the Georgia Association of Broadcasters and the Atlanta Section of The Institute of Radio Engineers. Plans are being made to have outstanding experts cover the latest developments in radio broadcasting and television. Space will be provided for manufacturers' exhibits, and an opportunity will be given to visit the studios and transmitters of Atlanta radio stations as well as the modern frequency-modulation transmitter at the Georgia School of Technology which is now operating on an experimental basis.

❖

Meetings and Conferences

❖

Delays May Occur—Please Wait!

It is intended that the Proceedings of the I.R.E. shall reach its readers approximately at the middle of the month of issue. However, present-day printing and transportation conditions are exceptionally difficult. Shortages of labor and materials give rise to corresponding delays. Accordingly, we request the patience of our Proceedings readers. We suggest further that, in cases of delay in delivery, no query be sent to the Institute unless the issue is at least several weeks late. If numerous premature statements of nondelivery of the Proceedings were received, the Institute's policy of immediately acknowledging all queries or complaints would lead to severe congestion of correspondence in the office of the Institute.

IRE-URSI Meeting

The annual joint meeting of the American Section, International Scientific Radio Union, and the Washington Section, Institute of Radio Engineers, will be held in Washington on Monday, Tuesday, and Wednesday, May 5, 6, and 7, in the Auditorium of the New Interior Department Building, C Street between 18th and 19th Streets, N.W. The program will, as usual, be devoted to the more fundamental and scientific aspects of radio and electronics. The program of titles and abstracts will be available in booklet form for distribution before the meeting. Correspondence should be addressed to the Institute office, or to Dr. Newbern Smith, Secretary, American Section, U.S.R.I., National Bureau of Standards, Washington 25, D. C.

❖

Chicago I.R.E. Conference

The second Chicago I.R.E. Conference will be held on Saturday, April 19, at Northwestern Technological Institute. There will be an all-day series of technical sessions and discussions on the practical side of electronic engineering, with emphasis on applied electronics. Outstanding engineers in the various fields will lead the discussions, which will be of vital interest to engineers in all branches of electronics. The Chicago Section of The Institute of Radio Engineers will sponsor the Conference.